

Aus dem Max von Pettenkofer-Institut für Hygiene
und Medizinische Mikrobiologie Lehrstuhl: Bakteriologie
der Ludwig-Maximilians-Universität München
Vormaliger Direktor: Prof. Dr. Dr. Jürgen Heesemann
Kommissarischer Vorstand: Prof. Dr. Rainer Haas

Thema der Dissertation:

**Establishment of a gnotobiotic mouse model to investigate the
mechanisms of colonization resistance against *Salmonella enterica*
serovar Typhimurium (*S. Tm*) and study of the protective role of the
intestinal mucus layer during *S. Tm* infection**

Dissertation zum Erwerb des Doktorgrades der
Naturwissenschaften an der Medizinischen Fakultät
der Ludwig-Maximilians-Universität München

vorgelegt von

Sandrine Brugiroux

aus Firminy, Frankreich

2016

Gedruckt mit Genehmigung der Medizinischen Fakultät
der Ludwig-Maximilians-Universität München

Berichterstatter: Prof. Dr. Bärbel Stecher

Mitberichterstatter: Prof. Dr. Heinrich Jung

Mitbetreuung durch den
promovierten Mitarbeiter:

Dekan: Prof. Dr. med. dent. Reinhard Hickel

Tag der mündlichen Prüfung: 10.10.2016

Eidesstattliche Erklärung

Ich, Sandrine Brugiroux, erkläre hiermit an Eides statt, dass ich die vorliegende Dissertation mit dem Thema:

“Establishment of a gnotobiotic mouse model to investigate the mechanisms of colonization resistance against *Salmonella enterica* serovar Typhimurium (*S. Tm*) and study of the protective role of the intestinal mucus layer during *S. Tm* infection”

selbständig verfasst, mich außer der angegebenen keiner weiteren Hilfsmittel bedient und alle Erkenntnisse, die aus dem Schrifttum ganz oder annähernd übernommen sind, als solche kenntlich gemacht und nach ihrer Herkunft unter Bezeichnung der Fundstelle einzeln nachgewiesen habe. Ich erkläre des Weiteren, dass die hier vorgelegte Dissertation nicht in gleicher oder in ähnlicher Form bei einer anderen Stelle zur Erlangung eines akademischen Grades eingereicht wurde.

Nîmes, 20.10.2016

Ort, Datum

Sandrine Brugiroux

Unterschrift

To all the mice sacrificed for science.

Table of contents

| | |
|---|-------|
| List of figures | xi |
| List of tables..... | xiv |
| List of abbreviations..... | xvii |
| List of publications..... | xx |
| Summary..... | xxi |
| Zusammenfassung..... | xxiii |
| 1. Introduction | 1 |
| 1.1. The mammalian gut microbiota | 1 |
| 1.1.1. Composition of the microbiota in humans and mice..... | 1 |
| 1.1.2. The effects of the microbiota on its host..... | 2 |
| 1.1.2.1. Education of the immune system..... | 2 |
| 1.1.2.2. Influence of the gut microbiota on gut morphology and nutrition | 3 |
| 1.1.3. Environmental and host factors influencing the intestinal microbiota composition..... | 4 |
| 1.1.3.1. Diet | 4 |
| 1.1.3.2. Antibiotic treatment..... | 5 |
| 1.1.3.3. Inflammation and infection | 5 |
| 1.1.3.4. Host genotype | 6 |
| 1.2. Analytical tools to study the gut microbiota composition and function..... | 6 |
| 1.2.1. High-throughput amplicon sequencing and quantitative PCR of bacterial 16S rRNA genes | 7 |
| 1.2.2. Meta-omics analyses | 7 |
| 1.2.3. Fluorescence <i>in situ</i> hybridization | 8 |
| 1.2.4. Bacterial isolation and culture | 8 |

| | | |
|----------|---|----|
| 1.3. | <i>Salmonella enterica</i> serovar Typhimurium - a model human pathogen to study microbiota-pathogen interaction in the gut | 9 |
| 1.3.1. | Mechanisms of <i>Salmonella</i> Typhimurium pathogenesis..... | 9 |
| 1.3.2. | <i>Salmonella</i> Typhimurium outcompetes the gut microbiota and benefits from the gut inflammation | 12 |
| 1.4. | Colonization resistance | 13 |
| 1.4.1. | Direct effects of the gut microbiota on the enteric pathogens | 14 |
| 1.4.2. | Indirect effects on pathogen colonization | 15 |
| 1.4.3. | Mouse models developed to study the colonization resistance and the underlined mechanisms | 15 |
| 1.5. | The intestinal mucus layer..... | 16 |
| 1.5.1. | Composition of the mucus layer | 16 |
| 1.5.2. | Interactions of the mucus layer with the gut microbiota and the enteropathogens | 17 |
| 1.5.3. | Mouse models developed to study the role of the mucus layer..... | 18 |
| 1.5.4. | The protein disulfide isomerase AGR2 and its functions..... | 19 |
| 2. | Objectives..... | 21 |
| 3. | Materials and Methods | 22 |
| 3.1. | Materials | 22 |
| 3.1.1. | Chemicals, Consumables and Instruments..... | 22 |
| 3.1.2. | Oligonucleotides, probes and antibodies | 26 |
| 3.1.3. | Plasmids and strains | 32 |
| 3.1.4. | Media and buffers..... | 34 |
| 3.2. | Methods | 41 |
| 3.2.1. | Bacterial culture methods | 41 |
| 3.2.1.1. | Cryoconservation of bacteria..... | 41 |
| 3.2.1.2. | Bacterial culture conditions..... | 43 |

| | | |
|-----------|---|----|
| 3.2.1.3. | Streptomycin halo assay | 43 |
| 3.2.2. | Bacterial strains | 44 |
| 3.2.2.1. | <i>Salmonella</i> strains | 44 |
| 3.2.2.2. | The Altered Schaedler Flora strains | 44 |
| 3.2.2.3. | Isolation of the Oligo-MM strains | 44 |
| 3.2.2.4. | Preparation of bacterial inocula as frozen stocks | 46 |
| 3.2.3. | Molecular biology methods | 46 |
| 3.2.3.1. | Genomic DNA extraction | 46 |
| 3.2.3.2. | RNA extraction and microarray analysis | 47 |
| 3.2.3.3. | 16S rRNA gene amplification and sequencing | 48 |
| 3.2.3.4. | AGR2 gene amplification | 49 |
| 3.2.3.5. | Generation of plasmids containing full length 16S rRNA gene | 49 |
| 3.2.3.6. | 16S rRNA gene-based taxonomic assignment of the bacterial strains | 50 |
| 3.2.3.7. | Plasmid extraction | 50 |
| 3.2.3.8. | Preparation of electro-competent bacteria | 50 |
| 3.2.3.9. | Electro-transformation of plasmid DNA | 51 |
| 3.2.3.10. | P22-transduction | 51 |
| 3.2.3.11. | Genome sequencing | 52 |
| 3.2.3.12. | Metagenomics analysis | 52 |
| 3.2.3.13. | 16S rRNA gene amplicon sequencing | 53 |
| 3.2.3.14. | Quantitative PCR of bacterial 16S rRNA genes | 55 |
| 3.2.3.15. | Fluorescence <i>in situ</i> hybridization (FISH) | 56 |
| 3.2.3.16. | Immunofluorescence microscopy | 58 |
| 3.2.3.17. | Lipocalin-2 quantification | 59 |
| 3.2.4. | Mouse experiments | 60 |
| 3.2.4.1. | Mice used in this study | 60 |

| | | |
|----------|--|----|
| 3.2.4.2. | Animal inoculation experiments..... | 60 |
| 3.2.4.3. | Animal infection experiments | 60 |
| 3.2.4.4. | Ethics statement | 61 |
| 3.2.4.5. | Histopathological analysis..... | 61 |
| 3.2.4.6. | Statistical analysis | 61 |
| 4. | Results – Establishment of a novel gnotobiotic mouse model to study host-microbiota-pathogen interactions | 63 |
| 4.1. | The Oligo-Mouse Microbiota, a consortium of mouse-derived commensal strains..... | 63 |
| 4.1.1. | Isolation of the Oligo-MM strains | 63 |
| 4.1.2. | Morphology and taxonomic assignment of the Oligo-MM strains | 64 |
| 4.1.3. | Representation of the ASF and Oligo-MM strains in a conventional murine gut microbiota | 66 |
| 4.1.3.1. | Phylum distribution and abundance | 66 |
| 4.1.3.2. | OTU distribution and abundance..... | 68 |
| 4.1.4. | Deposition of the Oligo-MM strains at the German type culture collection (DSMZ)..... | 70 |
| 4.2. | The Oligo-MM ¹⁰ can be reproducibly transplanted to gnotobiotic mice from a frozen mixture.... | 70 |
| 4.3. | The Oligo-MM ¹² stably colonizes the murine gut and is vertically transmitted over at least 4 filial generations..... | 76 |
| 4.4. | The Oligo-MM ¹² consortium partially restores colonization resistance against <i>Salmonella</i> | 78 |
| 4.5. | Functional analysis correlates functional capacity of intestinal microbiota and CR against <i>Salmonella</i> | 82 |
| 4.6. | Colonization resistance of Oligo-MM ¹² mice can be increased by transfer of ASF ⁷ | 86 |
| 4.7. | Establishment of a fluorescence <i>in situ</i> hybridization assay to detect, localize and quantify individual Oligo-MM strains..... | 98 |

| | | |
|--------|---|-----|
| 5. | Results - The role of the mucus layer and the microbiota during <i>Salmonella enterica</i> serovar Typhimurium infection..... | 104 |
| 5.1. | AGR2 ^{ko} mice exhibit a defect in MUC2 secretion in the cecal mucosa..... | 105 |
| 5.2. | AGR2 ^{ko} mice show significantly attenuated inflammation 1 day post <i>S. Tm</i> infection compared to littermate controls in sm-treated mice | 105 |
| 5.3. | Microarray analysis..... | 108 |
| 5.4. | Presence of <i>S. Tm</i> in cecal tissue is reduced in AGR2 ^{ko} mice as compared to littermate controls. | 109 |
| 5.5. | Microbiota of AGR2 ^{ko} mice is less susceptible to streptomycin-treatment than the microbiota of AGR2 ^{het} littermates despite similar sm concentration along the intestinal tract of both AGR2 ^{ko} and AGR2 ^{het} mice..... | 111 |
| 5.6. | Streptomycin-treatment leads to pronounced alteration of gut microbiota composition in both AGR2 ^{het} and AGR2 ^{ko} mice..... | 116 |
| 5.7. | Ampicillin treatment renders AGR2 ^{ko} mice susceptible to <i>S. Tm</i> -induced colitis | 118 |
| 5.8. | Enrichment of <i>Deferribacteres</i> phylum correlates with protection against <i>S. Tm</i> -induced colitis. | 123 |
| 5.9. | Generation of AGR2 germfree mice to study <i>S. Tm</i> -microbiota interactions under highly defined conditions | 125 |
| 5.10. | <i>S. Tm</i> T3SS-1 expression is downregulated in sm-treated AGR2 ^{ko} mice | 127 |
| 6. | Discussion | 130 |
| 6.1. | The Oligo-MM: a defined microbial consortium to study microbiota-host pathogen interaction in gnotobiotic mice..... | 130 |
| 6.1.1. | The Oligo-MM can be used as platform to identify bacteria and mechanisms underlying colonization resistance..... | 130 |
| 6.1.2. | Which mechanisms underlie colonization resistance mediated by the Oligo-MM? | 131 |
| 6.1.3. | Minimal gut microbiota as a tool for gnotobiotic studies..... | 133 |

| | | |
|----------|---|-----|
| 6.1.4. | What are the potential limitations of the Oligo-MM model? | 136 |
| 6.1.4.1. | Do all Oligo-MM strains colonize the mouse gut? | 136 |
| 6.1.4.2. | Are Gram-positive strains systematically underestimated? | 137 |
| 6.1.4.3. | Localization and quantification of individual bacterial strains using FISH | 139 |
| 6.1.4.4. | How long do the Oligo-MM strains need to establish a stable microbial community in mouse gut? | 139 |
| 6.1.4.5. | Culturomics as a tool to improve taxonomic classification | 140 |
| 6.2. | The AGR2 ^{ko} mice: A mouse model to study the role of the mucus layer and the microbiota during <i>S. Tm</i> infection..... | 143 |
| 6.2.1. | Does mutation of AGR2 gene only affect the cecal mucus layer? | 143 |
| 6.2.1.1. | AGR2 ^{ko} mice do not develop spontaneous colitis in contrast to other mucin-deficient mouse models..... | 143 |
| 6.2.1.2. | AGR2 ^{ko} and AGR2 ^{het} mice exhibit differential phenotype and gene expression | 143 |
| 6.2.1.3. | AGR2 ^{ko} and AGR2 ^{het} mice exhibit differential microbiota composition | 145 |
| 6.2.2. | Which other mechanisms could protect sm-treated AGR2 ^{ko} mice against <i>S. Tm</i> infection? | 146 |
| 6.2.2.1. | <i>S. Tm</i> exhibits reduced T3SS-1 expression in sm-treated AGR2 ^{ko} mice | 146 |
| 6.2.2.2. | Effects of antibiotic treatments on the host and on <i>S. Tm</i> | 147 |
| 7. | Appendix | 149 |
| 8. | Literature | 165 |
| 9. | Acknowledgments | 194 |
| 10. | Curriculum Vitae | 198 |

List of figures

| | |
|---|----|
| Figure 1. Phylogenetic comparison of the intestinal microbiota composition of humans and mice..... | 2 |
| Figure 2. Schematic representation of <i>Salmonella</i> Typhimurium pathogenesis..... | 11 |
| Figure 3. Schematic representation of <i>S. Tm</i> growth within the normal and the inflamed gut..... | 13 |
| Figure 4. Structure and organization of the intestinal mucus layer..... | 17 |
| Figure 5. Presentation of the AGR2 mouse model from Park <i>et al.</i> | 20 |
| Figure 6. Morphology of the Oligo-MM strains..... | 64 |
| Figure 7. Representation of Oligo-MM and ASF strains in a conventional mouse microbiota based on 16S rRNA gene sequences..... | 67 |
| Figure 8. Oligo-MM ¹⁰ inoculation in ASF ⁵ mice using frozen stocks harboring 10 Oligo-MM strains is efficient and reproducible. | 71 |
| Figure 9. Data from figure 8 analyzed using open-reference approach based on a custom 16S sequence database. | 73 |
| Figure 10. Comparison of fecal and cecal microbiota composition of ASF ⁵ mice colonized with the Oligo- MM ¹⁰ consortium analyzed using open-reference approach based on a custom 16S sequence database. | 74 |
| Figure 11. Microbiota complexity of ASF ⁵ -colonized mice increases after Oligo-MM ¹⁰ inoculation. | 75 |
| Figure 12. Oligo-MM ¹² consortium stably colonizes germfree mice and is vertically transmitted over at least 4 filial generations. | 77 |
| Figure 13. Fecal microbiota composition and diversity 40 days after transplantation with Oligo-MM ¹² or complex microbiota. | 79 |
| Figure 14. Fecal microbiota composition of ASF ⁵ mice colonized with the Oligo-MM ¹² or mock- inoculated, analyzed using a hydrolysis probe based quantitative PCR assay..... | 80 |
| Figure 15. Oligo-MM ¹² consortium partially restores colonization resistance against <i>S. Tm</i> ^{avir} | 82 |
| Figure 16. Functionome analysis correlates functional diversity with colonization resistance. | 86 |
| Figure 17. Functionome analysis correlates microbiota complexity with functional diversity. | 88 |

| | |
|--|-----|
| Figure 18. Establishment of gnotobiotic mice harboring an increased microbiota complexity..... | 90 |
| Figure 19. Microbiota complexity correlates with increased colonization resistance against <i>S. Tm</i> ^{avir} | 92 |
| Figure 20. Functionome analysis indicates potential metabolic pathways involved in CR against <i>S. Tm</i> .. | 95 |
| Figure 21. KEGG module analysis of single ASF and Oligo-MM strains..... | 98 |
| Figure 22. Establishment of a FISH assay to localize and quantify single strains in the Oligo-MM ¹² mouse gut..... | 100 |
| Figure 23. Detection and relative quantification of, YL58, a Gram-positive strain present in Oligo-MM ¹² mouse cecum. | 102 |
| Figure 24. Detection and relative quantification of YL58 and YL44 by FISH analysis reveals misestimation of this strain using gDNA-based quantitative approaches..... | 103 |
| Figure 25. <i>AGR2</i> ^{ko} mice show defective mucin secretion compared to <i>AGR2</i> ^{het} littermate controls..... | 105 |
| Figure 26. <i>AGR2</i> ^{ko} mice show attenuated inflammation 1 day post- <i>S. Tm</i> ^{wt} oral infection compared to <i>AGR2</i> ^{het} mice..... | 107 |
| Figure 27. Presence of <i>S. Tm</i> in cecal tissue is reduced in <i>AGR2</i> ^{ko} mice as compared to littermate controls. | 110 |
| Figure 28. Microbiota of <i>AGR2</i> ^{ko} mice is less susceptible to streptomycin treatment than the microbiota of <i>AGR2</i> ^{het} littermates..... | 112 |
| Figure 29. Microbiota of <i>AGR2</i> ^{ko} and <i>AGR2</i> ^{het} mice encounter same amount of effective streptomycin over-time along the intestinal tract..... | 113 |
| Figure 30. Comparison of microbiota composition of <i>AGR2</i> ^{ko} and <i>AGR2</i> ^{het} untreated mice analyzed using 16S rRNA gene amplicon sequencing. | 115 |
| Figure 31. Fecal microbiota composition of <i>AGR2</i> ^{ko} and <i>AGR2</i> ^{het} mice shows pronounced alterations after streptomycin treatment. | 117 |
| Figure 32. Microbiota of <i>AGR2</i> ^{ko} and <i>AGR2</i> ^{het} mice are highly susceptible to ampicillin treatment. | 119 |
| Figure 33. Analysis of microbiota composition of <i>AGR2</i> ^{ko} and <i>AGR2</i> ^{het} mice pretreated with ampicillin reveals gut microbiota composition different from sm-treated mice..... | 120 |

| | |
|--|-----|
| Figure 34. Ampicillin reduces colonization resistance against <i>S. Tm</i> ^{wt} in AGR2 ^{ko} mice. | 122 |
| Figure 35. Comparison of microbiota composition of AGR2 ^{ko} mice before and after sm- or amp-treatment. | 124 |
| Figure 36. Comparison of AGR2 ^{ko} and AGR2 ^{het} mice after antibiotic treatment depending on their pathological score at day 1 p.i..... | 125 |
| Figure 37. AGR2 germfree mice are highly susceptible to <i>S. Tm</i> infection..... | 126 |
| Figure 38. T3SS-1 expression is reduced in AGR2 ^{ko} mice after streptomycin treatment as compared to ampicillin treatment. | 128 |

List of tables

| | |
|--|----|
| Table 1. Chemicals, kits and reagents | 22 |
| Table 2. Antibiotics used in this study..... | 24 |
| Table 3. Specific instruments and materials | 25 |
| Table 4. Oligonucleotides and probes | 26 |
| Table 5. MID barcodes for 454 multiplexing | 28 |
| Table 6. 16S rRNA gene specific primers and hydrolysis probes for qPCR assay | 29 |
| Table 7. Primary antibodies..... | 31 |
| Table 8. Secondary antibodies..... | 32 |
| Table 9. Plasmids in <i>S. Tm</i> | 32 |
| Table 10. Plasmids generated to sequence the full 16S rRNA genes of the Oligo-MM and ASF strains ... | 32 |
| Table 11. <i>S. Tm</i> and <i>E. coli</i> strains | 33 |
| Table 12. Luria-Bertani (LB) medium..... | 34 |
| Table 13. LB agar and soft agar | 34 |
| Table 14. LB 0.3 M NaCl..... | 34 |
| Table 15. Brain-heart infusion (BHI) medium* | 35 |
| Table 16. Anaerobic <i>Akkermansia</i> medium (AAM)..... | 35 |
| Table 17. Schaedler blood agar | 36 |
| Table 18. WSB broth/agar..... | 36 |
| Table 19. AII medium | 37 |
| Table 20. Peptone-glycerol broth | 37 |
| Table 21. Phosphate Buffered Saline (PBS) 10X | 38 |
| Table 22. TE Buffer | 38 |
| Table 23. CTAB/NaCl Buffer | 38 |
| Table 24. Paraformaldehyde (PFA) 4 %..... | 38 |
| Table 25. Sucrose 20 % | 39 |

| | |
|--|-----|
| Table 26. Composition of hybridization buffers (HB) for FISH..... | 39 |
| Table 27. Composition of washing buffers (WB) for FISH..... | 39 |
| Table 28. Blocking buffer for ELISA..... | 39 |
| Table 29. Washing buffer for ELISA | 40 |
| Table 30. Substrate buffer for ELISA..... | 40 |
| Table 31. Percoll gradient | 40 |
| Table 32. Accession numbers of the strains deposited at DSMZ..... | 42 |
| Table 33. Isolation and cultivation of the Oligo-MM strains..... | 45 |
| Table 34. Fluorophores and optimal formamide (FA) concentrations established for the FISH probes targeting the Oligo-MM strains. | 56 |
| Table 35. Taxonomic assignment of the Oligo-MM strains | 65 |
| Table 36. Quantitative representation of Oligo-MM and ASF strains in a conventional mouse microbiota | 68 |
| Table 37. Taxonomic assignment of the Oligo-MM strains using EzTaxon database | 142 |
| Table 38. Microbial composition of the Oligo-MM ¹⁰ inoculum determined by qPCR..... | 149 |
| Table 39. Microbial composition in feces determined by amplicon sequencing using the Silva database to assign taxonomy at the family level..... | 149 |
| Table 40. Microbial composition in small intestines determined by amplicon sequencing using the Silva database to assign taxonomy at the family level | 150 |
| Table 41. Microbial composition in feces determined by amplicon sequencing using a custom sequence collection to assign taxonomy at the genus level | 151 |
| Table 42. Microbial composition in small intestines determined by amplicon sequencing using a custom sequence collection to assign taxonomy at the genus level..... | 153 |
| Table 43. Microbial composition in the frozen inoculum determined by amplicon sequencing using a custom sequence collection to assign taxonomy at the genus level..... | 153 |

| | |
|--|-----|
| Table 44. Microbial composition in feces and cecal content determined by amplicon sequencing using a custom sequence collection to assign taxonomy at the genus level..... | 154 |
| Table 45. Oligo-MM ¹² fecal composition over generations analyzed by qPCR | 155 |
| Table 46. Microbial composition in feces determined by amplicon sequencing using the Silva database to assign taxonomy at the family level..... | 157 |
| Table 47. Microbial composition in feces of ASF and Oligo-MM strains before infection determined by qPCR | 158 |
| Table 48. Microbial composition in feces of ASF- and Oligo-MM-colonized mice before infection determined by qPCR..... | 159 |
| Table 49. Gene sets upregulated in cecal epithelium of AGR2 ^{ko} mice as compared to AGR2 ^{het} littermates | 161 |
| Table 50. Gene sets downregulated in cecal epithelium of AGR2 ^{ko} mice as compared to AGR2 ^{het} littermates | 161 |

List of abbreviations

| | |
|--------------------|--|
| AAM | Anaerobic Akkermansia media |
| AGR2 | Anterior gradient homolog 2 |
| Amp | Ampicillin |
| ASF | Altered Schaedler flora |
| BHI | Brain heart infusion |
| BSA | Bovine serum albumin |
| CCF | Commensal colonization factors |
| CFU | Colony forming unit |
| CON | Conventional |
| CR | Colonization resistance |
| DAIME | Digital image analysis in microbial ecology |
| ddH ₂ O | Ampuwa water |
| dH ₂ O | Distilled water |
| DSMZ | Deutsche Sammlung von Mikroorganismen und Zellkulturen |
| DSS | Dextran sodium sulfate |
| DTL | Detection limit |
| EHEC | Enterohemorrhagic <i>E. coli</i> |
| ELISA | Enzyme-linked immunosorbent assay |
| ER | Endoplasmic reticulum |
| FA | Formamide |
| FCS | Fetal calf serum |
| FISH | Fluorescence <i>in situ</i> hybridization |
| gDNA | Genomic DNA |
| GI | Gastrointestinal |
| H&E | Hematoxylin and eosin |

| | |
|----------|---|
| HB | Hybridization buffer |
| KEGG | Kyoto encyclopedia of genes and genomes |
| LB | Luria-Bertani |
| Lcn2 | Lipocalin-2 |
| LEfSe | LDA Effect Size |
| LPS | Lipopolysaccharide |
| mLN | Mesenteric lymph nodes |
| MUC2 | Mucin 2 |
| NanoSIMS | High-resolution secondary ion mass spectrometry |
| O.C.T. | Optimal cutting temperature |
| Oligo-MM | Oligo-Mouse Microbiota |
| OMP | Outer membrane protein |
| o.n. | Overnight |
| OTU | Operational taxonomic units |
| PBS | Phosphate buffered saline |
| PCoA | Principal Coordinate Analysis |
| PFA | Paraformaldehyde |
| PMN | Polymorphonuclear neutrophils |
| PRR | Pattern recognition receptor |
| PTS | Proline, threonine and serine-rich domain |
| QIIME | Quantitative Insights Into Microbial Ecology |
| qPCR | Quantitative polymerase chain reaction |
| RATS | Robust Automated Threshold Selection |
| RNS | Reactive nitrogen species |
| ROS | Reactive oxygen species |
| Rpm | Revolutions per minute |
| RT | Room temperature |

| | |
|--------------|--|
| SCFA | Short-chain fatty acid |
| SCV | <i>Salmonella</i> -containing vacuole |
| SFB | Segmented filamentous bacteria |
| Sm | Streptomycin |
| SPF | Specific pathogen-free |
| SPI | <i>Salmonella</i> pathogenicity island |
| spp. | Species |
| <i>S. Tm</i> | <i>Salmonella enterica</i> serovar Typhimurium |
| T3SS | Type three secretion system |
| T3SS-1 | T3SS encoded by SPI-1 |
| T3SS-2 | T3SS encoded by SPI-2 |
| T6SS | Type six secretion system |
| Th17 | T helper cell |
| WT | Wild-type |

List of publications

Brugiroux S, Beutler M, Pfann C, Garzetti D, Ruscheweyh HJ, Ring D, Diehl M, Herp S, Lötscher Y, Hussain S, Bunk B, Pukall R, Huson DH, Münch PC, McHardy AC, McCoy KD, Macpherson AJ, Loy A, Clavel T, Berry D, Stecher B. (2016) Genome-guided modular design of a novel defined mouse microbiota that confers colonization resistance against *Salmonella enterica* serovar Typhimurium. **Nat Microbiol.** (Accepted for publication)

Loy A, Pfann C, Steinberger M, Hanson B, Herp S, **Brugiroux S**, Gomes Neto JC, Boekschoten MV, Schwab C, Urich T, Ramer-Tait AE, Rattei T, Stecher B, Berry D. The putative gut pathobiont *Mucispirillum schaedleri* - Intestinal lifestyle and genome evolution by extensive horizontal gene transfer. **ISME.** (Submitted)

Studer N, Desharnais L, Beutler M, **Brugiroux S**, Terrazos M, Menin L, McCoy KD, Kuehne S, Minton N, Stecher B, Bernier-Latmani R, Hapfelmeier S. Functional intestinal microbial secondary bile acid production by 7-alpha-dehydroxylating *Clostridium scindens* in a gnotobiotic mouse model. **Front Cell Infect Microbiol.** (Submitted)

Uchimura Y, Wyss M, **Brugiroux S**, Limenitakis J, Stecher B, McCoy KD, and Macpherson AJ. (2016) Complete Genome Sequences of Twelve Species of a Stable Defined Moderately Diverse Mouse Microbiota 2 (sDMDMm2). **Genome Announc.** 4(5): e00951-16.

Lagkouvardos I, Pukall R, Abt B, Fösel BU, Meier-Kolthoff JP, Kumar Neeraj, Bresciani A, Martinez I, Just S, Ziegler Caroline, **Brugiroux S**, Wenning M, Bui TP, Hugenholtz F, Plugge CM, Peterson DA, Hornef MW, Baines JF, Smidt H, Walter J, Kristiansen K, Nielsen HB, Haller D, Overmann J, Stecher B, Clavel T. (2016) The mouse intestinal bacterial collection (miBC): Host-specific insight into cultivable diversity and genomic novelty of the mouse gut microbiome. **Nat Microbiol.** 1:16131.

Li H, Limenitakis JP, Fuhrer T, Geuking MB, Lawson MA, Wyss M, **Brugiroux S**, Keller I, Macpherson JA, Rupp S, Stolp B, Stein JV, Stecher B, Sauer U, McCoy KD, Macpherson AJ. (2015) The outer mucus layer hosts a distinct intestinal microbial niche. **Nat Commun.** 6:8292.

Berry D, Stecher B, Schintlmeister A, Reichert J, **Brugiroux S**, Wild B, Wanek W, Richter A, Rauch I, Decker T, Loy A, Wagner M. (2013) Host-compound foraging by intestinal microbiota revealed by single-cell stable isotope probing. **Proc Natl Acad Sci U S A.** 110(12):4720-5.

Maier L, Vyas R, Cordova CD, Lindsay H, Schmidt TS, **Brugiroux S**, Periaswamy B, Bauer R, Sturm A, Schreiber F, von Mering C, Robinson MD, Stecher B, Hardt WD. (2013) Microbiota-derived hydrogen fuels *Salmonella* Typhimurium invasion of the gut ecosystem. **Cell Host Microbe.** 14(6):641-51.

Summary

The gastrointestinal tract of mice and men harbors a highly diverse microbiota that confers protection to the host against infections with enteric pathogens such as *Salmonella enterica* serovar Typhimurium (*S. Tm*). This phenomenon is termed as colonization resistance (CR). The tremendous complexity of the intestinal ecosystem precludes investigating the contribution of individual strains to host-bacterial interactions as well as studying their individual role in CR. Therefore, we established a gnotobiotic mouse model which harbors a defined consortium of mouse-derived bacteria able to confer CR against *S. Tm*. This bacterial consortium was named as the Oligo-Mouse Microbiota (Oligo-MM) and comprises twelve isolates abundant in the mouse intestine which are assigned to five major eubacterial phyla (*Firmicutes*, *Bacteroidetes*, *Actinobacteria*, *Verrucomicrobia* and *Proteobacteria*). Firstly, this work presents isolation and characterization of the individual members of the consortium and the generation of a gnotobiotic mouse line stably colonized with the Oligo-MM. Secondly, the establishment of Oligo-MM specific molecular tools including a qPCR assay and probes for fluorescence *in situ* hybridization (FISH) is reported. Furthermore, draft genome sequences were generated for all strains and enabled functional metagenomic analysis. All strains were deposited at the German Type Culture collections (DSMZ). Finally, an innovative approach which combines mouse infection experiments and comparative metagenomics was employed to identify bacterial mechanisms potentially involved in CR against *S. Tm*. In conclusion, the Oligo-MM consortium will be a useful tool to understand the role of single species in a complex microbial ecosystem and decipher molecular mechanisms underlying host-microbiota pathogen interaction.

Gut inflammation and disease induced by *S. Tm* is the result of the interplay between *S. Tm* virulence factors, the mucosal immune system, physical barriers and the microbiota. The intestinal mucus layer is known to provide protection against enteric infections and mucus-deficient mice have been shown to be more susceptible to infection with enteric pathogens such as *S. Tm* when compared to control mice. Anterior gradient homolog 2 (AGR2) is a member of the protein disulfide isomerase family involved in correct folding and export of the major component of the colonic mucus layer, MUC2. In the second part of this thesis, AGR2^{ko} mice deficient in mucus secretion were employed to investigate the role of the intestinal mucus layer and the microbiota in *S. Tm* infection using the antibiotic-treated *Salmonella* colitis model. Surprisingly, streptomycin (sm)-treated AGR2^{ko} mice were shown to be protected to early *S. Tm*-induced colitis in contrast to their heterozygous littermate controls (AGR2^{het}). This effect was not seen in mice pretreated with a different antibiotic, ampicillin. Microbiota composition analysis combined with indicator taxa analysis identified bacterial members assigned to the *Deferribacteres* phylum as candidates

of protective microbiota in sm-treated AGR2^{ko} mice. Additionally, expression of the *S. Tm* type III secretion system 1 (T3SS-1) was found to be downregulated in sm-treated AGR2^{ko} mice. This reveals microbiota-mediated regulation of T3SS-1 as novel potential mechanism involved in reduced symptoms of *S. Tm*-induced colitis. Finally, germfree rederivation of AGR2^{ko} and AGR2^{het} mice and generation of isobiotic mice using the Oligo-MM consortium will serve as toolbox to disentangle the mechanisms involved in protection against *S. Tm* in mucin-deficient mice.

Zusammenfassung

Der gastrointestinale Trakt von Menschen und Mäusen wird jeweils von einer höchst diversen mikrobiellen Gemeinschaft, genannt Mikrobiota, besiedelt, welche den Wirt vor Infektionen durch enterische Pathogene wie *Salmonella enterica* serovar Typhimurium (*S. Tm*) schützt. Dieses Phänomen wird als Kolonisationsresistenz (KR) bezeichnet. Die enorme Komplexität des intestinalen Ökosystems erschwert die genaue Untersuchung der individuellen Bakterien in Bezug auf ihre Interaktion mit dem Wirt, sowie ihre individuelle Rolle bei der KR. In dieser Arbeit wurde ein definiertes Konsortium von mausstämmigen Bakterien etabliert, welches KR gegenüber *S. Tm* im gnotobiotischen Mausmodell vermittelt. Dieses bakterielle Konsortium wird als die Oligo-Maus Mikrobiota (Oligo-MM) bezeichnet und enthält zwölf dem Maudarm entstammende Isolate, welche fünf eubakterielle Hauptphyla (*Firmicutes*, *Bacteroidetes*, *Actinobacteria*, *Verrucomicrobia* und *Proteobacteria*) repräsentieren. Diese Studie beschreibt erstens die Isolierung und Charakterisierung der individuellen Stämme des Konsortiums und die Erstellung einer gnotobiotischen Mauslinie, die stabil mit Oligo-MM kolonisiert wird. Zweitens wird die Entwicklung von Oligo-MM-spezifischen molekularen Werkzeugen wie einem spezifischen quantitativen PCR-Assay sowie von Sonden für die Fluoreszenz *in situ* Hybridisierung (FISH) beschrieben. Des Weiteren wurden Genomsequenzen für alle Stämme generiert, welches die funktionelle metagenomische Analyse ermöglichte. Alle Stämme wurden im Deutschen Zentrum für Mikroorganismen und Zellkulturen (DSMZ) hinterlegt. Letztendlich wurde ein innovatives Vorgehen angewandt, welches Mausinfektionsexperimente und vergleichenden Metagenomanalysen kombiniert, um bakterielle Mechanismen zu identifizieren, die möglicherweise eine Rolle bei der KR gegen *S. Tm* spielen. Zusammenfassend wird das Oligo-MM Konsortium zum molekularen Verständnis der Rolle einzelner Bakterien im komplexen mikrobiellen Ökosystem beitragen und die molekularen Mechanismen der Erreger-Wirtsinteraktion entschlüsseln.

Durch *S. Tm* hervorgerufene Darmentzündungen und Infektion sind das Ergebnis des Zusammenspiels von *S. Tm* Virulenzfaktoren, dem mukosalen Immunsystem, physischen Barrieren und der Mikrobiota. Der Darmschleimhaut bietet Schutz gegen Darminfektionen. Im Vergleich zu Kontrollmäusen sind Muzin-defiziente Mäuse anfälliger für Infektionen durch Erreger wie *S. Tm*. Anterior gradient homolog 2 (AGR2) ist ein Mitglied der Proteindisulfidisomerase Familie, welche für die korrekte Faltung und den Export der Hauptkomponente der Darmschleimhautschicht, MUC2 verantwortlich ist. Im zweiten Teil dieser Arbeit wurden AGR2^{ko} Mäuse mit defekter Muzinsekretion verwendet, um die Rolle der intestinalen Muzinschicht und der Mikrobiota bei der *S. Tm* Infektion im antibiotika-behandelten *Salmonella* Kolitismodell zu untersuchen. Überraschenderweise waren Streptomycin (Sm)-behandelte AGR2^{ko}-Mäuse geschützt gegen frühzeitige *S. Tm*-induzierte Kolitis im

Vergleich zu ihren heterozygoten Wurfgeschwistern (AGR2^{het}). Dieser Effekt wurde nicht bei Mäusen beobachtet, welche mit einem anderen Antibiotikum, Ampicillin, vorbehandelt wurden. Die Analyse der Mikrobiota-Zusammensetzung in Kombination mit einer Indikator-taxa-Analyse konnte bakterielle Vertreter des Phylums *Deferribacteres* als Kandidaten der protektiven Mikrobiota in Sm-behandelten AGR^{ko}-Mäusen identifizieren. Zudem war die Expression des *S. Tm* Typ III Sekretionssystems (T3SS-1) in Sm-behandelten AGR2^{ko}-Mäusen deutlich herunterreguliert. Dieses Resultat identifiziert die Mikrobiota-gesteuerte Regulation des T3SS-1 als neuen potentiellen Mechanismus bei der Pathogenese der *S. Tm*-Infektionen. Schlussendlich wird die Rederivierung keimfreier AGR2^{ko}- und AGR2^{het}-Mäuse und die Züchtung von isobiotischen Mäusen unter Verwendung vom Oligo-MM Konsortiums zur Aufklärung der genauen Mechanismen beitragen, die in Mucin-defizienten zum Schutz gegen *S. Tm* beitragen.

1. Introduction

The gut harbors the most dense and complex microbial ecosystem within the human body, termed as microbiota (Ley, Lozupone et al. 2008). This thesis focuses at the role of the gut microbiota in enteric infections. The first part of the introduction takes a glance at the complexity of the gut microbiota, its various functions and the challenge to study the interactions between the gut microbiota, the host and the enteric pathogens such as *Salmonella enterica* serovar Typhimurium (*S. Tm*) in experimental animal models. The second part introduces the techniques to analyze the gut microbiota composition. In the third part, the human enteropathogen *S. Tm* is introduced. The fourth part gives an overview on colonization resistance against enteric pathogens and experimental animal models developed to study it. Finally, the last part introduces the intestinal mucus layer, its protective role towards the host and its various interactions with the gut microbiota.

1.1. The mammalian gut microbiota

1.1.1. Composition of the microbiota in humans and mice

The gastrointestinal tract is inhabited by approximately 1000 bacterial species, making up 10^{12} cells per gram of large intestinal content (Marchesi and Shanahan 2007). In order to study the functions of the gut microbiota and its role in health and disease, most of the *in vivo* studies have so far employed a well-defined model organism: the laboratory mouse (*mus musculus*).

The composition of the gut microbiota of humans and mice is rather similar at the taxonomic phylum level. The microbiota of both is dominated by anaerobic bacteria belonging to the *Firmicutes* and the *Bacteroidetes* making up 90 %. The *Actinobacteria*, the *Proteobacteria*, the TM7 and the *Verrucomicrobia* are present at a lower abundance (**Figure 1A**) (Eckburg, Bik et al. 2005, Ley, Backhed et al. 2005). However, at the taxonomic genus level, the gut microbiota of humans and mice is rather different. Opposite to the mouse microbiota, the gut microbiota of humans harbors more *Prevotella*, *Faecalibacterium* and *Ruminococcus* genera. On the other side, the gut microbiota of mice harbors more *Lactobacillus*, *Alistipes*, *Turicibacter* and *Mucispirillum* genera than the human microbiota (Krych, Hansen et al. 2013, Nguyen, Vieira-Silva et al. 2015) (**Figure 1B**). Such differences were also shown at the taxonomic family level (Seedorf, Griffin et al. 2014) and may hamper direct translation of data obtained from mouse experiments to the human system.

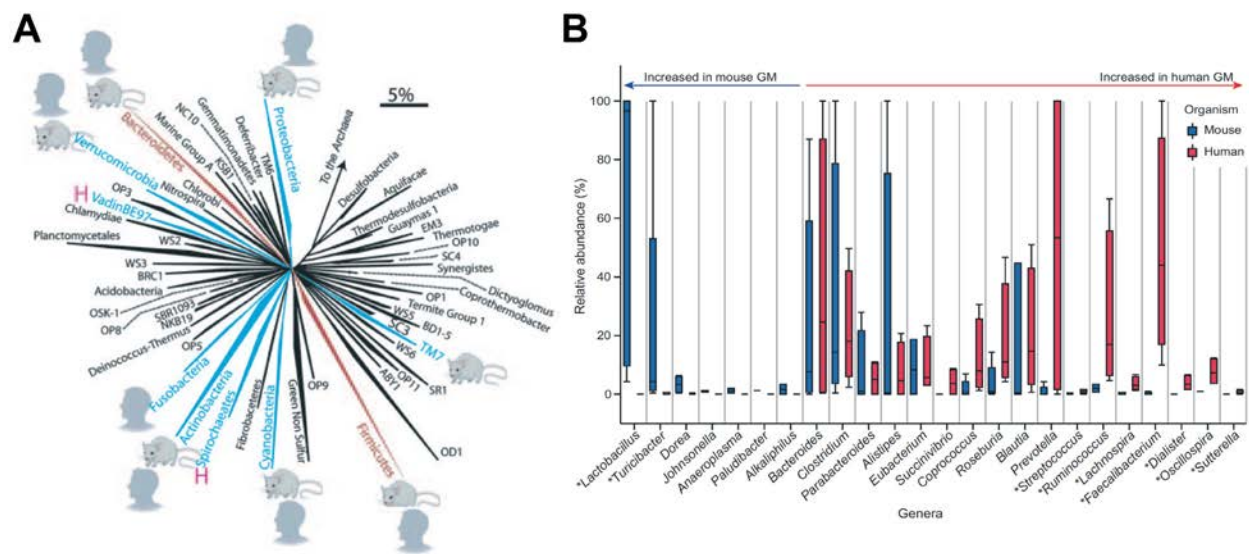


Figure 1. Phylogenetic comparison of the intestinal microbiota composition of humans and mice.

(A) Intestinal microbiota composition of humans and mice is very similar at the taxonomic phylum level. Divisions detected in mouse cecum and in human colonic microbiota are indicated by the mouse symbol (Ley, Backhed et al. 2005) and the human-head symbol (Eckburg, Bik et al. 2005), respectively. “H” denotes additional divisions represented in the human fecal microbiota, as determined from GenBank entries. Divisions dominant in mice and humans are colored red, rarer divisions are blue, and undetected divisions are black. The bar indicates changes per nucleotide. Taken from (Ley, Backhed et al. 2005) with permission. Copyright 2015 National Academy of Sciences, U.S.A. (B) Similarities and discrepancies of both microbial ecosystems at the taxonomic genus level in feces using four human datasets and five mouse datasets. Genera with significant differences ($P < 0.05$) between human and mouse microbiota are annotated with an asterisk. Taken from (Nguyen, Vieira-Silva et al. 2015) under the terms of the Creative Commons Attribution License (<http://creativecommons.org/licenses/by/3.0>).

1.1.2. The effects of the microbiota on its host

The enormous amount of microorganisms which are directly adjacent to the single-layered intestinal epithelial border requires that host and commensal microbiota develop strategies to coexist. In most cases, the interactions appear to be of mutual benefit for both the gut microbiota and its host. It is well known that the gut microbiota inflicts beneficial effects on its natural host. However, in some cases, the gut microbiota can also be deleterious for the host.

1.1.2.1. Education of the immune system

Starting right after birth, the gut microbiota educates the immune system (Lotz, Gutle et al. 2006). This phenomenon has been intensively studied in humans, where newborns encounter the first bacterial invaders while passing through the maternal vagina. Controversially, another study detected bacteria even

in the placenta, suggesting that bacterial colonization could occur before birth (Aagaard, Ma et al. 2014). However, these results are highly discussed in the field (Aagaard 2014). Thus, members of the vaginal microbiota constitute the first microbial community established in the gut and some members of this microbiota stably colonize. Further on, once in the gut, these pioneer colonizers enter in contact with the epithelial border (Dominguez-Bello, Costello et al. 2010). This first contact is essential for educating the immune system of newborns (Lotz, Gutle et al. 2006), participating in milk digestion (Gagnon, Savard et al. 2015) and aiding other commensals to colonize the gastrointestinal tract (Penders, Thijs et al. 2006). It is known that when the first microbial community differs from the community of vaginal microbiota (*e.g.* babies born by caesarian), newborns harbor another gut microbiota in their early age. This correlates with the risk of developing asthma and multiple allergies later in life, in humans (Kero, Gissler et al. 2002). Moreover, germfree mice colonized with bacterial strains isolated from humans have an impaired immune system compared to animals colonized with murine isolates (Chung, Pamp et al. 2012). Therefore, both the microbiota composition and its adaptation to its host are important to educate the immune system.

In adult mice, it is well documented that the members of the gut microbiota can influence the intestinal immune system and the barrier function. They can influence the innate immune system by inducing the production of antimicrobial peptides (*e.g.* REGIII β , REGIII γ) (Vaishnava, Behrendt et al. 2008) and by maturing lymphoid tissues via their recognition by host pattern recognition receptors (PRR) (Bouskra, Brezillon et al. 2008). Moreover, they can influence the adaptive immune system by inducing regulatory immune responses (Atarashi, Tanoue et al. 2013), by promoting the differentiation of T helper cell (Th17) (Atarashi, Nishimura et al. 2008) and by inducing the production of secretory immunoglobulin A (Macpherson and Uhr 2004). Finally, the gut microbiota can influence the barrier function by modulating the structure of mucus layers (Johansson, Jakobsson et al. 2015) and regulating intestinal epithelial permeability (Stefka, Feehley et al. 2014).

1.1.2.2. Influence of the gut microbiota on gut morphology and nutrition

Besides, the gut microbiota is known to influence the intestinal morphology, physiology and motility (Berg 1996). Using germfree animals, it was shown that commensals increase the number of goblet cells (Stefka, Feehley et al. 2014) and the production of mucus (Jakobsson, Rodriguez-Pineiro et al. 2015). They also participate to microvilli formation, increase the rate of the epithelial cell turnover, and contribute to the development of the gut-associated lymphoid tissues, the Peyer's patches and the mesenteric lymph nodes (Falk, Hooper et al. 1998, Round and Mazmanian 2009, Ohland and Jobin 2015).

Furthermore, the gut microbiota fulfills a variety of metabolic functions, which can contribute to nutrition and is therefore beneficial for the host (Nicholson, Holmes et al. 2012). The metabolites shaped and modified by the gut microbiota are termed metabolome. The microbiota can promote glucose absorption as well as catabolize host dietary nutrients (Backhed, Ding et al. 2004) and mucus glycans (Johansson, Jakobsson et al. 2015). Additionally, bacterial metabolites such as amino acids (Zheng, Xie et al. 2011), carbohydrates (Flint, Scott et al. 2012) or vitamins (Koenig, Spor et al. 2011) can have also beneficial effects on the host. Finally, the microbiota ferment dietary fibers and complex-carbohydrates into short-chain fatty acids (SCFA) such as butyrate (Donohoe, Holley et al. 2014), propionate and acetate (Caspari and Macy 1983). The SCFA, in particular butyrate, are known to influence epithelial cell proliferation (Donohoe, Collins et al. 2012), mucosal immune response and mucus secretion (Vanhoutvin, Troost et al. 2009). However, these effects are controversial and highly discussed in the field (Hamer, Jonkers et al. 2010, Bultman and Jobin 2014).

1.1.3. Environmental and host factors influencing the intestinal microbiota composition

Under healthy conditions, the composition of the gut microbiota differs largely within and between individuals depending on different factors such as aging and ethnic group (Yatsunenkov, Rey et al. 2012), intestinal location (Zhang, Geng et al. 2014), lifestyle habit (Ley, Hamady et al. 2008), foregoing infection (Gradel, Nielsen et al. 2009), diet (Carmody, Gerber et al. 2015), pregnancy (Koren, Goodrich et al. 2012), previous antibiotic therapy (Liou and Turnbaugh 2012), atmospheric pressure (Adak, Maity et al. 2014) and housing conditions in case of experimental animals (Ma, Bokulich et al. 2012, Rogers, Kozłowska et al. 2014). Severe changes in the composition of the gut microbiota, termed as dysbiosis, have further been associated with various diseases. In this section, some factors involved in dysbiosis are described in more details.

1.1.3.1. Diet

The diet can promote dysbiosis (Goodman, Kallstrom, 2011). Dietary habits such as herbivore, carnivore or insectivore lifestyles are known to influence the gut microbiota in humans and in other organisms (Ley, Hamady et al. 2008, Ley, Lozupone et al. 2008). Nutrient sources such as high fat and high sugar diets (Carmody, Gerber et al. 2015), carbohydrates (Aguirre, Eck et al. 2015), artificial sweeteners (Suez, Korem et al. 2014) or vitamins (*e.g.* vitamins A and B12) (Cha, Chang et al. 2010,

Degnan, Barry et al. 2014) can also affect the composition of the gut microbiota. For example, the artificial sweeteners increase the Bacteroidales and decrease the Clostridiales. This dysbiosis can lead to an increase of glucose intolerance and metabolic disorders (Suez, Korem et al. 2014). Furthermore, Faith *et al.* developed a modeling approach to predict the reaction of microbiota after a change of diet, based on the diet composition. This model could allow the manipulation of the microbiota to improve global human health and prevent or treat various diseases (Faith, McNulty et al. 2011).

1.1.3.2. Antibiotic treatment

Antibiotic treatment promotes severe dysbiosis, despite the high abundance of antibiotic resistances in the microbiome (Sommer, Dantas et al. 2009, Maurice, Haiser et al. 2013). Dysbiosis can have deleterious effects on the host. Antibiotic-induced dysbiosis is associated with an increased adiposity suggesting that a dysbiotic microbiota is more efficient in extracting energy from the diet than a conventional microbiota (Flint 2012, Liou and Turnbaugh 2012). Moreover, antibiotic-induced dysbiosis can facilitate enteric infections by both genuine and opportunistic pathogens (*e.g. Clostridium difficile*, vancomycin-resistant *Enterococcus* and *Salmonella enterica* serovar Typhimurium) and inhibit immune responses (*e.g.* production of the antibacterial lectin RegIII γ) (Brandl, Plitas et al. 2008, Ng, Ferreyra et al. 2013). Further, long-term disturbances triggered by antibiotic treatment are associated with several pathologies such as colitis, diarrhea and allergies (Hill, Siracusa et al. 2012, Varughese, Vakil et al. 2013, Satokari, Fuentes et al. 2014). Additionally, in a dose-dependent manner, antibiotics are also known to influence the quorum-sensing systems of the gut bacteria (Struss, Pasini et al. 2012).

1.1.3.3. Inflammation and infection

Chronic and acute intestinal inflammation in humans and mice are associated with severe dysbiosis. In particular, in chronic inflammatory disease, relative abundance of *Firmicutes* and *Bacteroidetes* was shown as shifted and relative abundance of *Deferribacteres* and *Proteobacteria* was observed as increased (Morgan, Tickle et al. 2012, Schwab, Berry et al. 2014). However, it is unclear whether this dysbiosis is responsible for inflammation or occurs consequently. During infection, enteropathogens trigger inflammatory responses using different virulence factors such as flagella and type three secretion systems (T3SS). This leads to dysbiosis (Belzer, Gerber et al. 2014) as well as drastic changes in the gut ecosystem such as increased hypoxia (*i.e.* diminished availability of oxygen) (Harris, Carter et al. 2011), increased mucus secretion (Xue, Zhang et al. 2014) and massive induction of immune

response (*e.g.* cytokines, IL-1 β , interferon- γ) (Rhee, Walker et al. 2005, Muller, Hoffmann et al. 2009) (also reviewed in (Kaiser, Diard et al. 2012)).

1.1.3.4. Host genotype

For both humans and mice, it is known that host genotype shapes the gut microbiota. In humans, this was shown by a study on monozygotic and dizygotic twin pairs (Goodrich, Waters et al. 2014). In mice, evidence comes from genetically modified mouse models (Ley, Backhed et al. 2005, Krych, Hansen et al. 2013). However, it remains unclear whether genetic mutations have direct or indirect effects on microbiota composition. For example, the major component of the intestinal mucus layer is mucin 2 (MUC2). MUC2-deficient mice were shown to harbor a different microbiota as compared to wild-type (WT) mice (Sovran, Loonen et al. 2015). However, it is unclear whether this difference is due to their lack of intestinal mucus layer (Van der Sluis, De Koning et al. 2006), their different profile of gene expression compared to their WT littermates (*e.g.* for genes involved in immune response, lipid metabolism pathways and cell-cycle control) (Sovran, Loonen et al. 2015) or other consequences of *muc2* mutation. Therefore, various strategies aim to decrease variations in microbiota composition such as cohousing WT and mutant mice, using littermates as reference group, standardizing diet, minimizing stress factors, and so on (Laukens, Brinkman et al. 2015).

In conclusion, regarding the high complexity of the interactions between the gut microbiota and its host, it is challenging to understand host-microbiota relationships at a molecular level. Therefore, one of the strategies to study these interactions is to simplify the system by using well-characterized animal models in combination with well-defined microbiota and specific-analytical methods.

1.2. Analytical tools to study the gut microbiota composition and function

A variety of different analysis tools has been developed to analyze the composition and the localization of the gut microbiota. While methods based on counting of 16S rRNA gene copies as well as bacterial culture methods can be used to study relative abundance of individual microbial taxa, fluorescence *in situ* hybridization (FISH) allows the localization and the quantification of single cells *in situ*. We used three different analysis methods to compensate the bias of each of the single methods. The strengths and limitations of each method are outlined below.

1.2.1. High-throughput amplicon sequencing and quantitative PCR of bacterial 16S rRNA genes

High-throughput 16S rRNA amplicon sequencing is one of the most powerful approaches to study microbiota composition (Sogin, Morrison et al. 2006). It provides a relatively cheap and high-throughput dataset of sequences, which can be used to describe the gut microbiota composition to a low taxonomic level, and offers the parallel analysis of a large amount of samples in a short time scale. However, results vary depending on the analysis platform, the amplified 16S rRNA gene region (*i.e.* primer bias), the sequencing depth, the 16S rRNA gene used for taxonomic assignment and the bioinformatics analysis pipeline used (Koren, Knights et al. 2013, Schmidt, Matias Rodrigues et al. 2015). Furthermore, chimera generated during PCR amplification constitute another source for errors (Edgar, Haas et al. 2011).

The quantitative polymerase chain reaction (qPCR) assay provides more sensitive and specific detection of bacterial strains than other gDNA-based methods. It is currently also cheaper than the amplicon sequencing technique. However, it does not allow the detection of bacterial contaminants as it only detects targeted bacterial strains.

1.2.2. Meta-omics analyses

While metagenomics is used to predict the functional capacity of the entire gut microbiota community using genomic DNA (gDNA) sequencing, metatranscriptomics is used to get an overview on the transcriptional activity using RNA sequencing (Gill, Pop et al. 2006, Xiong, Frank et al. 2012). Importantly, two subjects with similar metagenomic profiles can have different metatranscriptomic activities (Franzosa, Morgan et al. 2014). This can be because metabolic pathways predicted to be in the same microbiota can be in different bacteria. Moreover, functional analyses are biased regarding how genes are related to the reference proteins.

Recently, metaproteomics and metabolomics analyses have been used to identify the functional activity of a microbial community in more details (Nicholson, Holmes et al. 2005, Verberkmoes, Russell et al. 2009).

In conclusion, gDNA-based methods are powerful tools to study microbiota composition and function. However, they can bias the data due to gDNA extraction efficiency as Gram-negative and Gram-positive bacteria have different cell walls, which exhibit different susceptibility to lysis methods

(Salonen, Nikkila et al. 2010, Maukonen, Simoes et al. 2012). This leads to a bias in favor of Gram-negative bacteria, which are easier to lyse. Bacterial genomes can harbor one to several copies of the same 16S rRNA gene, which can be either identical or different. This also leads to misestimation of the relative abundance of bacterial strains and can complicate the taxonomic assignment (Watanabe, Kojima et al. 2013).

1.2.3. Fluorescence *in situ* hybridization

Fluorescence *in situ* hybridization (FISH) uses probes targeting the 16S rRNA. FISH probes are fluorescently labelled to specifically detect bacterial communities at the single-cell level, study ecological niches in tissue sections and determine the relative abundance of individual microbial community members using image analysis software such as the digital image analysis in microbial ecology software (DAIME) or BacSpace (Daims, Lucker et al. 2006, Earle, Billings et al. 2015). It can also be combined with other techniques such as high-resolution secondary ion mass spectrometry (NanoSIMS) to visualize bacterial metabolic activities *in vivo* (Berry, Stecher et al. 2013). However, despite the efforts made to optimize the FISH protocols, the fluorescent signal intensity, the microscopic resolution and the image analysis, it is challenging to establish a specific FISH protocol for gut tissues. This is mainly due to the high bacterial density in the gut and the auto-fluorescence of the gut tissue and plant fibers.

1.2.4. Bacterial isolation and culture

Bacterial isolation and culture is essential to characterize the physiological properties of bacterial strains *in vitro*, determine its genome sequence and perform proof of experimental concept. The genome sequence allows gaining insights into function and metabolic pathways of the organism and facilitating the development of specific analytical tools. Eventually, strategies for genetic manipulation can also be developed based on the genomic information. However, despite 52 phyla identified in the domain Bacteria, only half of them have cultured representative strains (nicely reviewed in (Rappe and Giovannoni 2003)). Therefore, efforts are made to circumvent technical problems (*e.g.* working under anaerobic atmosphere) and to develop new cultivating methods such as enrichment culture (Clavel, Henderson et al. 2006), high-throughput methods (Connon and Giovannoni 2002), gel microdroplet approach (Zengler, Toledo et al. 2002) or synergistic bacterial growth (Kaeberlein, Lewis et al. 2002).

1.3. *Salmonella enterica* serovar Typhimurium - a model human pathogen to study microbiota-pathogen interaction in the gut

Salmonella enterica serovar Typhimurium (*S. Tm*) is a facultative anaerobic, non-spore-forming, Gram-negative bacterium, which is taxonomically assigned to the Enterobacteriaceae family. In humans, food-borne infections with nontyphoidal *Salmonella* strains (*e.g.* *S. Tm*) lead usually to self-limiting diarrhea and can, in some cases, also cause bacteremia (*e.g.* young children and immunocompromised patients) (Fabrega and Vila 2013). To infect successfully its host, *S. Tm* harbors a tremendous amount of virulence factors encoded within five *Salmonella* pathogenicity islands (SPI) in the chromosome and a virulence plasmid (pSLT). Initiation and amplification of the pro-inflammatory signals by *S. Tm* results in activation of macrophages and dendritic cells (Rydstrom and Wick 2007), granulocyte transmigration in the gut lumen, mucosal edema, epithelial damage, reduced numbers of mucus-loaded goblet cells (Barthel, Hapfelmeier et al. 2003) and mucin secretion (Day, Mandal et al. 1978). Moreover, *S. Tm* has to compete with the gut microbiota and deal with the inflammatory milieu in the gut. Here, the pathogenesis of *S. Tm* is reviewed with its most relevant virulence factors, followed by *S. Tm* interaction with the gut microbiota in the healthy and inflamed gut.

1.3.1. Mechanisms of *Salmonella* Typhimurium pathogenesis

The majority of studies have been performed in a mouse model for *S. Tm*-induced colitis, the streptomycin-treated (sm-treated) mouse colitis model (Barthel, Hapfelmeier et al. 2003). *S. Tm* pathogenesis is schematized below (**Figure 2**).

After infection of sm-treated mice, *S. Tm* reaches the intestine and crosses the mucus layer in order to reach the epithelial border using chemotactic flagella-mediated motility (Stecher, Hapfelmeier et al. 2004). Using different adhesins, *S. Tm* attaches to the enterocytes in the small intestine preferentially, where M cells of the Peyer's patches are infected (Gerlach, Jackel et al. 2007).

So far, three mechanisms for *S. Tm* entry into host cells have been described. (1) After its adhesion to epithelial cells, *S. Tm* employs a type three secretion system (T3SS) termed as T3SS-1 and encoded on *Salmonella* pathogenicity island 1 (SPI-1). Using a needle complex and a translocon machinery, T3SS-1 injects at least fourteen different effector proteins into the host cell (Kaiser, Diard et al. 2012). This leads to actin cytoskeletal rearrangement, internalization of *S. Tm* via a Trigger-like mechanism, and initiation of gut inflammation through the induction of pro-inflammatory cytokines (*e.g.* IFN γ , IL-1 β and MIP2) (Hapfelmeier, Ehrbar et al. 2004, Patel and Galan 2005). (2) After its adhesion to

epithelial cells, *S. Tm* uses an outer membrane protein (OMP) termed the Rck, which is encoded on pSLT, to enter epithelial cells via a Zipper-like mechanism. Rck interacts with its host receptor (still unknown) to manipulate the host signaling and trigger *S. Tm* internalization. *S. Tm* is the first pathogen to be described as able to induce both Zipper and Trigger mechanisms for host cell invasion (Velge, Wiedemann et al. 2012). (3) *S. Tm* is directly sampled from the gut lumen by dendritic cells, which open the tight junctions and send dendrites to the lumen (Rescigno, Rotta et al. 2001).

Once inside the phagocytic or non-phagocytic cells, *S. Tm* is contained in a *Salmonella*-containing vacuole (SCV) (Garcia-del Portillo, Foster et al. 1992). In order to survive and replicate intracellularly, *S. Tm* expresses a second T3SS, termed as T3SS-2 and encoded on SPI-2, as well as corresponding effector proteins (Figueira and Holden 2012). Among other, the SPI-2-encoded effector proteins are reported to block fusion of the SCV with lysosomes (Uchiya, Barbieri et al. 1999), to manipulate the vesicular trafficking pathway (*e.g.* transcytosis of the SCV to the basolateral membrane) (Garvis, Beuzon et al. 2001) and to induce the formation of *Salmonella*-induced filaments (Garcia-del Portillo, Zwick et al. 1993). Eventually, T3SS-2 activity enables intracellular replication, induction of profound inflammation and systemic spread (Hapfelmeier and Hardt 2005).

Effector proteins encoded by T3SS-1 and T3SS-2 can also induce systemic dissemination of *S. Tm* to other organs such as mesenteric lymph nodes, liver, spleen and gallbladder (Lawley, Chan et al. 2006). To favor dissemination, *S. Tm* can induce epithelial and macrophage cell death (Monack, Raupach et al. 1996, Paesold, Guiney et al. 2002). These events trigger acute and chronic inflammatory responses through the activation of cytokines such as IFN γ (Monack, Bouley et al. 2004). Moreover, *S. Tm* has several mechanisms to promote its survival in the host such as turning into non-replicating persisters within macrophages or inducing biofilm formation (Papavasileiou, Papavasileiou et al. 2010, Helaine, Cheverton et al. 2014). During persistent infection, *S. Tm* can be transmitted to a new host using fecal shedding (Lam and Monack 2014).

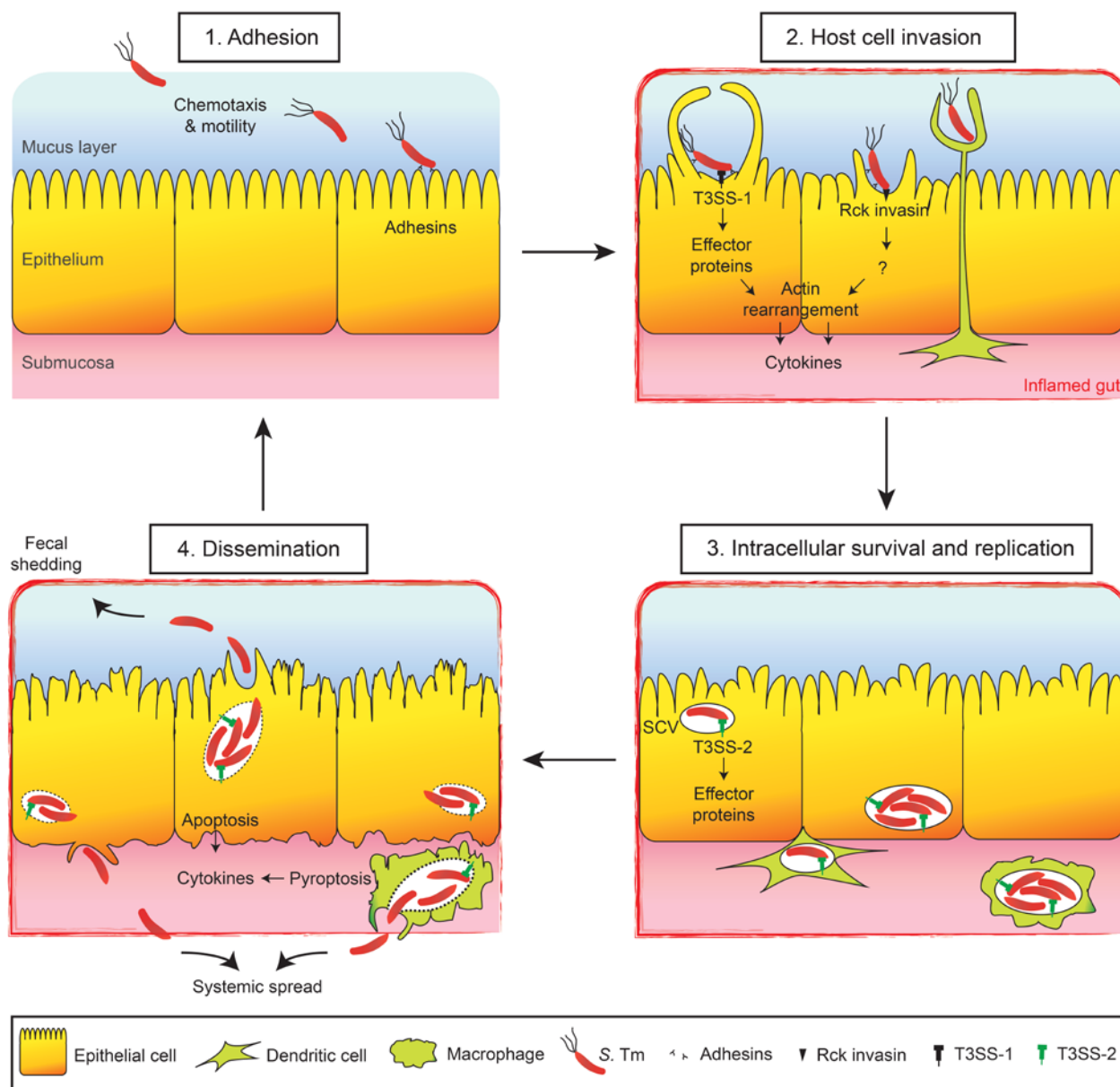


Figure 2. Schematic representation of *Salmonella Typhimurium* pathogenesis.

1. Adhesion: After ingestion, *S. Tm* swims towards the gut epithelium along chemotactic gradients. After penetrating the mucus layer, it adheres to the epithelial surface using diverse adhesins. **2. Host cell invasion:** In order to invade into epithelial cells, *S. Tm* can use two mechanisms. Firstly, *S. Tm* can use its T3SS-1 to inject several effector proteins into the cellular cytoplasm. T3SS-1 effectors are also known to induce the expression of pro-inflammatory cytokines. Secondly, *S. Tm* uses its Rck invasin to interact with the epithelial cell. In both cases, it triggers actin rearrangement and lead to the engulfment of *S. Tm* into the epithelial cell. The host receptor of Rck invasion remains unknown. Finally, *S. Tm* can also be sampled by dendritic cells directly from the gut lumen. **3. Intracellular survival and replication:** Once inside the host cells, *S. Tm* uses its T3SS-2 to inject effector proteins into the cell cytoplasm. Thereby, it manipulates the host cell (e.g. vesicular trafficking pathways) in order to survive and replicate into the *Salmonella*-containing vacuole (SCV). T3SS-2 effectors are also known to cause tissue-wide inflammation. Moreover, macrophages are able to phagocytose *S. Tm*, which can survive intracellularly and replicate. **4. Dissemination:** In order to disseminate, *S. Tm* uses different mechanisms, which remain unclear. For example, *S. Tm* can induce epithelial cell apoptosis and dendritic cell pyroptosis.

1.3.2. *Salmonella Typhimurium* outcompetes the gut microbiota and benefits from the gut inflammation

Upon infection, *S. Tm* encounters a dense and autochthonous microbiota that prevents *S. Tm* infection. In order to successfully colonize and infect its host, *S. Tm* has developed several strategies to outcompete the microbiota (**Figure 3**).

The ability of *S. Tm* to colonize the gut correlates with the presence of close related species (Stecher, Chaffron et al. 2010). *S. Tm* can also exploit hydrogen and sugars (*e.g.* sialic acid), which are microbiota-derived to colonize the gut (Maier, Vyas et al. 2013, Ng, Ferreyra et al. 2013). Using flagella and chemotaxis, *S. Tm* follows the gradient of high-energy nutrients (*e.g.* mucin-derived sugars and electron acceptors) and reaches the epithelial cells to initiate inflammation (Stecher, Hapfelmeier et al. 2004). Moreover, *S. Tm* can exploit inflammation to outcompete the microbiota. Indeed, the mucosal inflammation increases the release of mucins and other glycoconjugate nutrients, which favors *S. Tm* colonization and helps the remaining pathogens in the lumen to sense the epithelial border (Stecher, Barthel et al. 2008). Moreover, during inflammation, polymorphonuclear neutrophils (PMN) that transmigrate into the intestinal lumen release reactive oxygen species (ROS) and reactive nitrogen species (RNS) to kill *S. Tm* (Loetscher, Wieser et al. 2012). The by-products of releasing ROS and RNS are tetrathionate and nitrate, respectively, which are used by *S. Tm* as respiratory electron acceptors (Winter, Thiennimitr et al. 2010, Rivera-Chavez, Winter et al. 2013). This ability to perform anaerobic respiration boosts *S. Tm* growth and enables it to outcompete obligate anaerobic commensals (Rivera-Chavez, Winter et al. 2013). Furthermore, to survive inflammatory responses, *S. Tm* developed resistances against some anti-microbial peptides (*e.g.* RegIII β) (Stelzer, Kappeli et al. 2011). Other antimicrobials are released to enable the acquisition of essential micronutrients. It is the case for the acquisition of iron against which the mucosa excretes the enterochelin-sequestering protein lipocalin-2 (Lcn2) to limit iron availability. *S. Tm* bypasses this host-defense by producing the salmochelin, which is an Lcn2-resistant glycosylated enterochelin derivative (Raffatellu, George et al. 2009). Similarly, calprotectin is released by PMNs to sequester zinc in the inflamed gut. *S. Tm* overcomes this calprotectin-mediated zinc chelation by expressing a zinc transporter (ZnuABC), which is known to enhance *S. Tm* growth and allow *S. Tm* to overgrow the gut microbiota (Liu, Jellbauer et al. 2012).

In conclusion, in order to infect its host successfully, *S. Tm* developed strategies to overgrow the gut microbiota, to benefit from mucosal inflammation and to resist host-defense mechanisms. All together, these mechanisms negatively affect gut microbiota in particular the anaerobic commensals, which are

presumably more sensitive to inflammation and to antimicrobials (Stecher, Robbiani et al. 2007). However, the gut microbiota can also play a protective role during *S. Tm* infection.

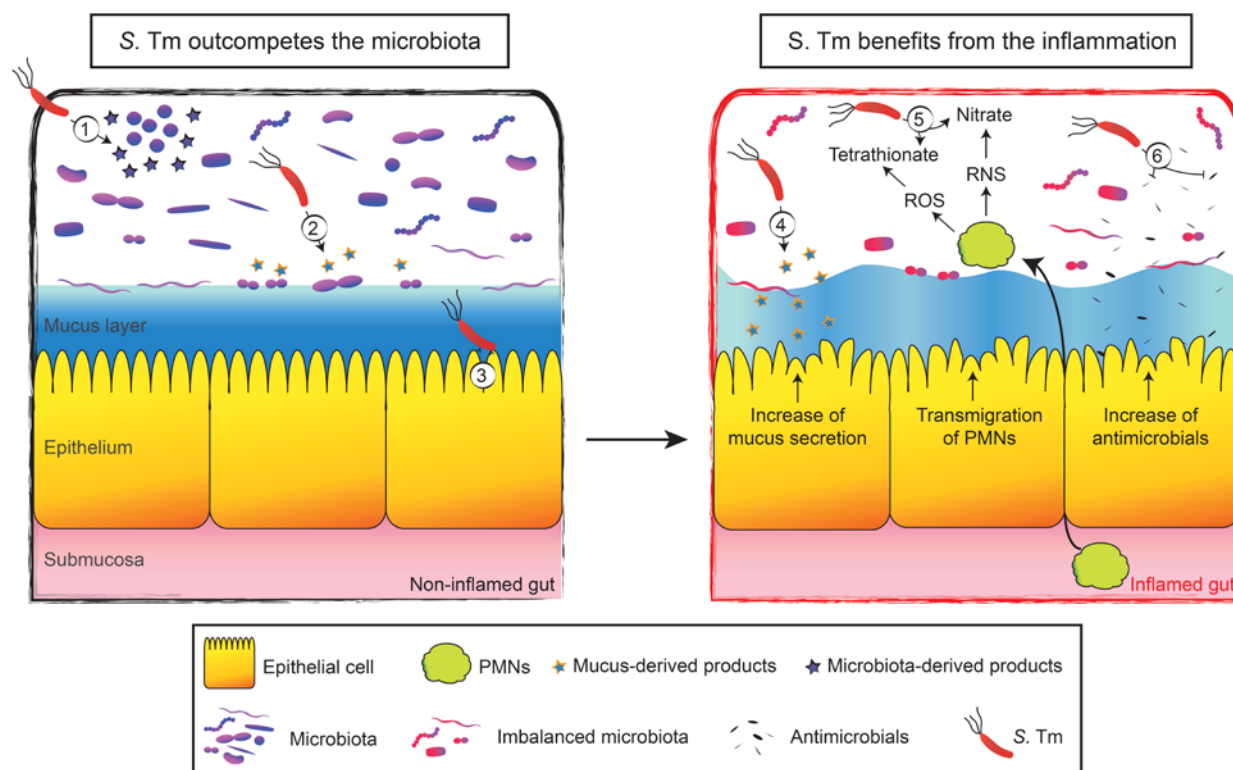


Figure 3. Schematic representation of *S. Tm* growth within the normal and the inflamed gut.

Upon entering the intestinal tract, *S. Tm* encounters the gut microbiota, which is already established and well-adapted to the gut ecosystem. To successfully colonize and invade the gut, *S. Tm* uses different mechanisms. **1.** *S. Tm* utilizes the microbiota-derived products (e.g. H_2). **2.** *S. Tm* uses mucus-derived carbohydrates, which are degraded by mucolytic bacteria (e.g. sialic acid). **3.** *S. Tm* uses chemotaxis and motility to penetrate the mucus layer and reach the epithelial border. Moreover, *S. Tm* benefits from inflammation as it **4.** senses the chemotactic gradient emanating from the mucus layer, which is increased by inflammation. **5.** *S. Tm* uses tetrathionate and nitrate, which result from inflammation, as anaerobic electron acceptor. **6.** *S. Tm* resists antimicrobials such as lipocalin and calprotectin.

1.4. Colonization resistance

Previous studies have shown that antibiotic treatment (e.g. with streptomycin) enhanced infections by enteropathogens such as *Salmonella* spp. (Miller, Bohnhoff et al. 1956), *E. coli*, *Klebsiella pneumoniae* and *Pseudomonas aeruginosa* in mice (van der Waaij, Berghuis-de Vries et al. 1971). Similar observations were also reported for other enteropathogens such as *Shigella sonnei* (Pongpech, Hentges et al. 1989), *Clostridium difficile* (Reeves, Koenigsnecht et al. 2012), *Enterococcus faecium* (Ubeda, Bucci et al.

2013) and *S. Tm* (Stecher, Robbiani et al. 2007). These studies highlight the protective role of the gut microbiota for its host against enteric pathogens. This is termed as colonization resistance (CR). Here, I first review the direct and indirect CR effects mediated by the gut microbiota on enteropathogens, and then the animal models used to study CR *in vivo*.

1.4.1. Direct effects of the gut microbiota on the enteric pathogens

The gut microbiota can interfere with pathogen growth and inhibit enteric infections in many ways. One potential mechanism is the competition for nutrients or micronutrient. This has been postulated as the Freter's nutrient-niche hypothesis. It states that a bacterium cannot invade a resident microbiota if its metabolic niche is already occupied by other strains (Freter, Brickner et al. 1983). Competition mechanisms include nutrients such as amino acid and sugars as well as micronutrients like iron and H₂ (Deriu, Liu et al. 2013, Maier, Vyas et al. 2013, Sassone-Corsi and Raffatellu 2015). Supporting this idea, microbiota complexity positively correlates with CR against enteric pathogens in many cases (*e.g. S. Tm*) (Stecher, Chaffron et al. 2010). Another mechanism of CR is the production of antimicrobial compounds and toxins by the microbiota. Some commensals are known to secrete antimicrobial peptides called microcins or bacteriocins, which kill bacterial competitors including pathogens (*e.g. E. coli* Nissle, *Clostridium difficile*, *Bifidobacterium* spp. and *Lactobacillus* spp.) (Allison, Fremaux et al. 1994, Nedialkova, Denzler et al. 2014, Buffie, Bucci et al. 2015). Moreover, fermentation of carbohydrates leads to production of short chain fatty acids (SCFA) such as acetate, propionate and butyrate. Acetate is known to prevent the release of Shiga toxin during infection with enterohaemorrhagic *E. coli* (EHEC) and to modulate the expression of invasion genes of *S. Tm* in the large intestine (Durant, Carrier et al. 2000, Lawhon, Maurer et al. 2002, Fukuda, Toh et al. 2011). Propionate and butyrate are known to repress virulence (*e.g. S. Tm*) (Lawhon, Maurer et al. 2002). Furthermore, commensals (*e.g. strains belonging to the Bacteroidetes* phylum) can secrete antibacterial toxins using the type VI secretion system (T6SS) in a contact-dependent manner (Russell, Wexler et al. 2014). Finally, another mechanism of CR is the competition between commensals and enteropathogens for adhesion to the host epithelium. However, this was shown in cell cultures only (Alemka, Clyne et al. 2010, Ren, Li et al. 2012) and mechanisms by which adherent commensals inhibit attachment and virulence of enteropathogens remain unclear (Greene and Klaenhammer 1994).

1.4.2. Indirect effects on pathogen colonization

Studies using germfree mice clearly demonstrate the essential role of the microbiota for educating the gut immune system and inducing maturation of the epithelial border (Backhed 2012). One potential mechanism is the effect on the innate immune system. Microbial colonization is associated with the induction of innate immune responses such as expression of antimicrobial peptides (*e.g.* C-type lectins and α -defensins) (Cash, Whitham et al. 2006, Vaishnava, Behrendt et al. 2008), cytokines (*e.g.* IL-1 β and IL-22) (Satoh-Takayama, Vosshenrich et al. 2008, Hasegawa, Kamada et al. 2012) and inducible nitric oxide synthase (Allen, Lafuse et al. 2012). Additionally, the gut microbiota can also trigger adaptive immune responses and interfere with the differentiation of T cell subpopulations such as Th17 cells, which are involved in pro-inflammatory responses and regulatory T cells, which play a role in the anti-inflammatory immune responses and tolerance (Atarashi, Tanoue et al. 2011). The microbiota also promotes differentiation and activation of B cells, as well as secretion of Immunoglobulin A (Hapfelmeier, Lawson et al. 2010). This plays an important role in maintaining the gut homeostasis. Thirdly, by interacting with epithelial cells, commensal bacteria can also protect from enteric infections. Microbiota-released SCFA can provide nutrition for colonocytes, modulate host signaling pathways, suppress inflammation and increase the mucosal barrier function by promoting the formation of tight junctions (reviewed in (Ploger, Stumpff et al. 2012)). Butyrate was also shown to stimulate mucus expression and secretion (Shimotoyodome, Meguro et al. 2000, Gaudier, Rival et al. 2009).

1.4.3. Mouse models developed to study the colonization resistance and the underlined mechanisms

It is well-established that conventional mice are more resistant to enteric infections (*e.g.* *S. Tm* and *Citrobacter rodentium*) as compared to germ-free mice (Kamada, Kim et al. 2012). However, the conventional microbiota harbors approximately 1000 bacterial species, making up 10^{12} cells per gram of large intestinal content (Marchesi and Shanahan 2007). Therefore, mice which harbor a simplified and well-defined gut microbiota (*i.e.* gnotobiotic mice) have been developed to study the contribution of single bacterial strain to CR. Numerous studies have used mice harboring bacteria derived from humans (Fukuda, Toh et al. 2011, Ganesh, Klopffleisch et al. 2013, Lee, Donaldson et al. 2013, Faith, Ahern et al. 2014, Slezak, Krupova et al. 2014). However, human microbiota colonized mice were shown to exhibit an impaired immune system and an increased susceptibility to *Salmonella* infection, as compared to mice colonized with a murine microbiota (Chung, Pamp et al. 2012). Moreover, Sedorf *et al.*, provided evidence that a mouse-adapted microbiota better invades and colonizes the mouse gut than

xenobiota (Seedorf, Griffin et al. 2014). Therefore, mice harboring a limited mouse-adapted microbiota were developed (Itoh and Mitsuoka 1985, Reeves, Koenigsnecht et al. 2012). As an example, the altered Schaedler flora (ASF) harbors eight strains and has been widely used (Dewhirst, Chien et al. 1999). However, mice colonized with the ASF strains were shown to exhibit large cecal size (Wymore Brand, Wannemuehler et al. 2015), abnormal T cell repertoire (Geuking, Cahenzli et al. 2011), lack of colonization resistance (Stecher, Chaffron et al. 2010) and abnormal metabolic capacity (Norin and Midtvedt 2010, Berry, Stecher et al. 2013). These observations highlight the importance of improving current gnotobiotic mouse models based on murine isolates to study CR mechanisms.

1.5. The intestinal mucus layer

1.5.1. Composition of the mucus layer

The mucus layer represents one of the first physical barriers encountered by the gut microbiota and the enteropathogens. In the large intestine, the mucus layer is mainly composed of a secreted gel-forming mucin named MUC2 (Gum, Hicks et al. 1994). MUC2 forms a network composed of a core protein, rich in the amino acids proline, threonine and serine (PTS), which are repeated in tandem and constitute the PTS domain. In the endoplasmic reticulum (ER), the core protein is dimerized at the C-termini and trimerized at the N-termini via disulfide bonds (**Figure 4A**) (Asker, Axelsson et al. 1998, Godl, Johansson et al. 2002). The polymer is then conveyed to the Golgi apparatus where the PTS domain is heavily O-glycosylated, becoming the mucin domain. This resulting mature mucin is finally condensed into granulae before being secreted by specialized cells termed goblet cells (Johansson, Gustafsson et al. 2010). When released on the apical side of the intestinal epithelium, MUC2 expands and divides into 2 layers: the inner mucus layer, which is firmly adherent and close to the epithelial border, and the outer mucus layer, which is loose and closer to the gut lumen (**Figure 4B**). In healthy conditions, the inner layer is devoid of bacteria, while the outer layer can be colonized (**Figure 4C**) (Johansson, Phillipson et al. 2008). Proteomic analysis suggests that the loose property of the second mucus layer results from proteolytic cleavage of the firm mucus layer by host endogenous proteases (Johansson, Thomsson et al. 2009). However, the role of mucin-degrading bacteria cannot be entirely excluded (*e.g. Bifidobacterium* spp., *Ruminococcus* spp., *Akkermansia muciniphila*) (Hoskins, Agustines et al. 1985, Png, Linden et al. 2010, Subramani, Johansson et al. 2010).

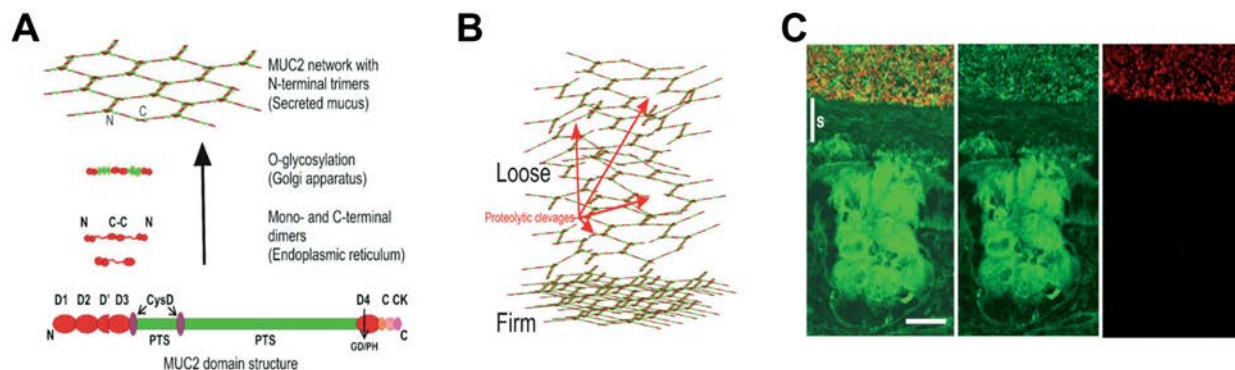


Figure 4. Structure and organization of the intestinal mucus layer.

(A) MUC2 contains cysteine-rich N- and C-terminal parts, four complete von Willebrand D domains (D1-D4) and PTS domains, which are rich in proline, threonine and serine. In the endoplasmic reticulum, MUC2 is dimerized at the C-termini and trimerized at the N-termini. In the Golgi apparatus, PTS domains are heavily O-glycosylated and become the mucin domain. Finally, mucin is condensed and stored into granulae in goblet cells before being secreted. (B) The secreted mucus is organized into two layers: the inner mucus layer, which is firmly adherent and close to the epithelial border (Firm) and the outer mucus layer, which is a nonattached, soluble mucus layer (Loose). (A-B) Taken from (Johansson, Larsson et al. 2011) with permission. (C) MUC2 immunostaining (green) revealed MUC2-positive goblet cells and mucus layers in distal colon. Bacteria (red) were detected by FISH using a general bacterial probe (Eub338). The inner mucus layer (s) is devoid of bacteria, which are only detected in the outer mucus layer. Scale bar: 20 μ m. Taken from (Johansson, Phillipson et al. 2008) with permission. Copyright (2005) National Academy of Sciences, U.S.A.

1.5.2. Interactions of the mucus layer with the gut microbiota and the enteropathogens

The mucus layer represents an essential and dynamic platform of interactions between the host and the gut bacteria.

Firstly, the mucus layer is an ecological niche. Indeed, the outer mucus layer harbors a different microbial composition as compared to the gut lumen (Li, Limenitakis et al. 2015). The bacterial strains hosted by the mucus layer can degrade and feed on the mucus layer. They are termed mucolytic bacteria (*e.g. Bacteroides acidifaciens* and *Akkermansia muciniphila*) (Berry, Stecher et al. 2013, Marcobal, Southwick et al. 2013). Furthermore, bacteria hosted by the mucus layer can benefit from bacterial- or host-derived substrates others than mucin. For example, *E.coli* can use fucose released from mucin by *Bacteroides thetaiotaomicron* and host-derived phospholipids enclosed in the outer mucus layer (Pacheco, Curtis et al. 2012, Li, Limenitakis et al. 2015). Finally, bacteria can also bind to the mucus layer. This can affect pathogen invasion and virulence (*e.g. S. Tm*), as well as allow bacteria to adhere to the mucus layer and avoid regular shedding (Cheng and Bjerknes 1983, Huang, Lee et al. 2011, Hansson 2012, Zarepour, Bhullar et al. 2013).

Besides being a nutrient source for bacteria, the mucus layer represents a physical and a chemical barrier. First, it has a protective role against enteric pathogens (*e.g. Yersinia enterocolitica*, *Citrobacter rodentium* and *S. Tm*) as well as commensal bacteria (Johansson, Phillipson et al. 2008, Zarepour, Bhullar et al. 2013). Second, it represents also a chemical barrier, as it binds numerous antimicrobial compounds targeting pathogens and commensals (Vaishnava, Behrendt et al. 2008). This limits bacterial contact from the mucosal epithelium and thus, contributes to maintain the gut homeostasis.

Finally, mucus layer benefits from commensals. Among others abnormalities, germfree mice exhibit a thinner mucus layer compared to conventional mice (Johansson, Phillipson et al. 2008). This suggests that the microbiota has beneficial effects on maturation of the mucus layer. For examples, *Bacteroides thetaiotaomicron* can use fucose as an energy source to generate a microbial signal that induces host fucosylated glycan synthesis (Hooper, Xu et al. 1999). Then, fucosylated glycans can be cleaved by commensals such as *B. thetaiotaomicron* that release fucose, which was shown to repress virulence gene expression of EHEC (Keeney and Finlay 2013). Moreover, *B. thetaiotaomicron* can release acetate, which also modulates the expression of genes involved in synthesis and glycosylation of mucin. Consequently, this leads to an increase in the number of goblet cells of the colonic epithelium (Wrzosek, Miquel et al. 2013). Finally, acetate can be used by *Faecalibacterium prausnitzii* to produce another SCFA, such as butyrate (Wrzosek, Miquel et al. 2013). SCFA are known to be beneficial for the epithelial border and modulate mucin gene expression (Gaudier, Jarry et al. 2004, Bultman and Jobin 2014).

1.5.3. Mouse models developed to study the role of the mucus layer

Mouse models harboring defective or altered mucus layer exhibit different phenotypes. In MUC2-deficient mice, intestinal bacteria penetrate the inner mucus layer and enter in direct contact with intestinal epithelial cells (Johansson, Ambort et al. 2011). In consequence, MUC2^{ko} mice develop spontaneous and severe colitis as well as tumors, depending on their genetic background (*e.g. MUC2^{ko}, Winnie and Eeyore* mice) and hygiene conditions (Heazlewood, Cook et al. 2008, Bao, Guo et al. 2014). Moreover, these mice are known to be more susceptible to enteric infections and chemically induced colitis (Heazlewood, Cook et al. 2008, Bergstrom, Kissoon-Singh et al. 2010). Their histopathology is characterized by epithelial cell dysfunction, abnormal number and morphology of goblet cells, and endoplasmic reticulum stress (Heazlewood, Cook et al. 2008).

Mice lacking TMF/ARA160, a Golgi-associated protein expressed in colonic enterocytes, and mice exhibiting defective core 1-derived O-glycans in intestinal epithelial cells (TM-IEC *Clgalt^{ko}* mice) harbor an altered mucosal architecture (*e.g. thicker mucus or abnormal glycosylation*) (Bel, Elkis et al.

2014, Sommer, Adam et al. 2014). These mice are more resistant to chemically induced colitis and do not develop spontaneous colitis (Bel, Elkis et al. 2014, Sommer, Adam et al. 2014). Moreover, studies showed that abnormal mucus layer affects the gut microbiota composition (Sommer, Adam et al. 2014) and that the colitis phenotype can be transmissible by fecal transplantation (Bel, Elkis et al. 2014). Furthermore, mice lacking the blood group glycosyltransferase β -1,4-N-acetylgalactosaminyltransferase 2 (*B4galnt2*) exhibit also an altered mucin structure. *B4galnt2*-deficient mice show different microbiota composition and lower susceptibility to *S. Tm*-induced inflammation, as compared to mice expressing *B4galnt2* (Rausch, Steck et al. 2015).

1.5.4. The protein disulfide isomerase AGR2 and its functions

Anterior gradient homolog 2 (AGR2) is a member of the protein disulfide isomerase family (Persson, Rosenquist et al. 2005), which is expressed in several cell types such as mucus-containing goblet, Paneth and enteroendocrine cells (Wang, Hao et al. 2008). AGR2 localizes to the ER lumen and is indirectly associated with ER membrane-bound ribosomes (Higa, Mulot et al. 2011). It was shown to be essential for correct folding and export of MUC2 (Park, Zhen et al. 2009), and to be involved in maintenance of ER homeostasis (Zhao, Edwards et al. 2010). AGR2 was also found to be secreted in intestinal mucus layer (Bergstrom, Berg et al. 2014). However, the extracellular functions of AGR2 remain unknown. Finally, AGR2 can be used as diagnostic marker for cancers (Kovalev, Shishkin et al. 2006), as dysregulation of AGR2 gene expression has been associated with tumor growth and metastasis in several cancers such as brain (Hong, Wang et al. 2013), ovarian (Sung, Choi et al. 2014) and pancreatic cancers (Ramachandran, Arumugam et al. 2008).

In order to study the role of AGR2 *in vivo*, AGR2^{ko} mice were generated using different targeting constructs and promoters for the expression of Cre recombinase (Park, Zhen et al. 2009, Zhao, Edwards et al. 2010, Gupta, Wodziak et al. 2013). Compared to AGR2^{wt} mice, all AGR2^{ko} mice show a decrease secretion of heavily glycosylated proteins (*e.g.* mucins), loss of intestinal goblet cells, none or few MUC2 protein detectable, body weight loss and morphologic abnormalities (*e.g.* enlarged stomach, small and large intestine). AGR2^{ko} mice can also show dysregulation of immune response (*e.g.* increased expression of several pro-inflammatory cytokines), increased neutrophil infiltration and increased ER stress response. Moreover, premature death was observed and associated to intestinal obstruction (Gupta, Wodziak et al. 2013) and severe spontaneous terminal ileitis and colitis (Park, Zhen et al. 2009, Zhao, Edwards et al. 2010). It has been suggested that severity of spontaneous colitis could be due to mouse genetic background and housing conditions (*e.g.* in gnotobiotic facility).

In this study, I used AGR2 mouse model from Park *et al.* In these AGR2^{ko} mice, MUC2 core protein is undetectable in colon and mice show only mild spontaneous colitis in healthy conditions (**Figure 5A,B**). Finally, AGR2^{ko} mice are more susceptible to colitis (*e.g.* dextran sodium sulfate (DSS)-induced colitis) than their AGR2^{wt} littermates (**Figure 5C,D**) (Park, Zhen et al. 2009).

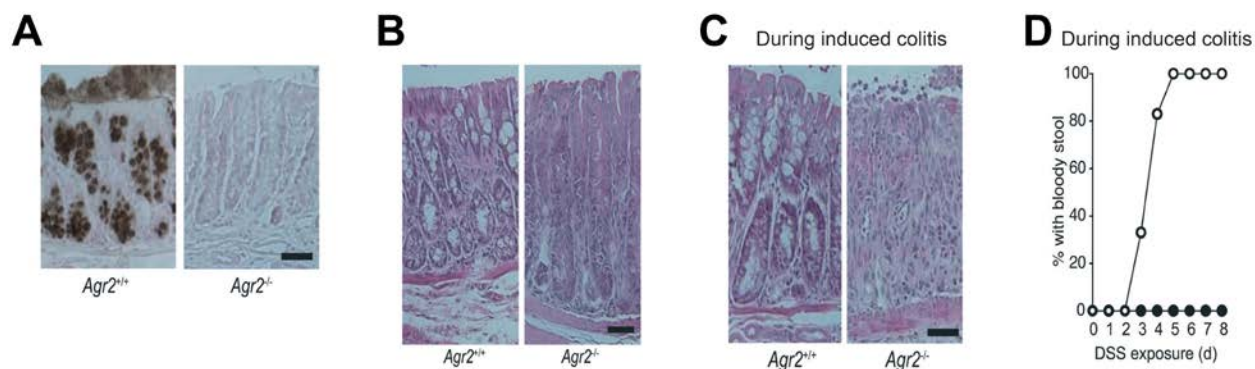


Figure 5. Presentation of the AGR2 mouse model from Park *et al.*

(**A**) Immunohistochemical detection of MUC2 (brown) in colon shows that AGR2^{ko} (AGR2^{-/-}) mice are devoid of intestinal mucus layer. (**B**) Hematoxylin and eosin (H&E) staining of colon from AGR2^{ko} and AGR2^{wt} (AGR2^{+/+}) mice. AGR2^{ko} mice show loss of colonic goblet cells and enlarged colon. (**C-D**) AGR2^{ko} and AGR2^{wt} mice were exposed to DSS (1.5 % in drinking water) for 7-8 days. (**C**) H&E staining of colon from DSS-exposed mice. AGR2^{ko} mice show severe epithelial damage compared to AGR2^{wt} mice. (**D**) Percentage of AGR2^{ko} (empty circle) and AGR2^{wt} (full circle) mice that develop bloody stools during DSS exposure. AGR2^{ko} mice are more susceptible to DSS-induced colitis than AGR2^{wt} mice. Scale bars: 50 μ m. Taken from (Park, Zhen et al. 2009) with permission.

2. Objectives

The conventional gut microbiota confers colonization resistance (CR) to infection with enteropathogens, including *S. Tm*. CR is absent in mice harboring a low complexity microbiota (LCM). However, CR is restored by cohousing of LCM mice with a conventional donor animal (Stecher, Chaffron et al. 2010). This observation underlines the importance of a complex gut microbiota in establishing normal CR. The mammalian gut is inhabited by 500-1,000 bacterial species (Marchesi and Shanahan 2007). So far, the identity of CR mediating bacteria has remained unknown. Furthermore, it is unclear if a reduced and defined number of bacteria might be able to restore CR in gnotobiotic mice. For identifying and characterizing potentially protective members of the microbiota and eventually study CR in a mechanistic manner, I aimed to generate a gnotobiotic mouse model. A number of gnotobiotic mouse models, most of them based on humanized microbiota have been established in the past. To my knowledge, none of these models was shown to restore CR against *S. Tm*.

In the first part of this thesis, I aimed to establish a defined consortium of murine commensal bacteria and test for their ability to restore CR against *S. Tm* in gnotobiotic mice. To this end, I planned to optimize methods for bacterial cultivation and develop analytical tools to characterize and specifically detect each strain *in vivo* and test their ability to provide CR against *S. Tm*.

Salmonella Typhimurium uses chemotaxis and motility to reach the epithelial border and to induce colitis (Stecher, Hapfelmeier et al. 2004). The intestinal mucus layer consisting of highly glycosylated mucins forms a tight physical barrier and prevents access of both commensals and pathogens from the single-layered epithelial border. Several commensals can breakdown mucin glycoproteins and thereby release carbon sources (*e.g.* fucose), which can be used as nutrient source by other non-mucolytic bacteria and pathogens (Pacheco, Curtis et al. 2012, Berry, Stecher et al. 2013, Ng, Ferreyra et al. 2013). Therefore, the mucus layer takes a two-sided role in bacterial infections, which has hitherto been only poorly studied.

In the second part of my thesis, I aimed to investigate the role of the mucus layer during *S. Tm* infection, using mucin-deficient mice. As mice lacking the major intestinal mucin MUC2 develop spontaneous colitis at early age (Van der Sluis, De Koning et al. 2006) and thus cannot be used to study *S. Tm* pathogenesis, we used mice deficient in anterior gradient homolog 2 (AGR2). AGR2-deficient mice show absent MUC2 secretion but do not develop spontaneous colitis at young age (Park, Zhen et al. 2009). Therefore, I used the AGR2-deficient mouse model to investigate the role of the mucus layer during *S. Tm* infection.

3. Materials and Methods

3.1. Materials

3.1.1. Chemicals, Consumables and Instruments

Table 1. Chemicals, kits and reagents

| Item | Supplier |
|---|--|
| ABTS | Biozol (Eching) |
| Acetic acid | Roth (Karlsruhe) |
| Agar Bacto™ | Becton Dickinson (New Jersey, US) |
| Agarose | Sigma-Aldrich Chemie (Munich) |
| Bovine serum albumin | GE Healthcare Life Sciences (Freiburg) |
| Brain Heart Infusion | Oxoid, Thermo Fisher Scientific biosciences (St. Leon-Rot) |
| Chloroform | Roth (Karlsruhe) |
| CloneJET™ PCR Cloning kit | Thermo Fisher Scientific biosciences (St. Leon-Rot) |
| Cysteine (-L) Hydrochloride Monohydrate | Sigma-Aldrich Chemie (Munich) |
| Cystine (-L) | Sigma-Aldrich Chemie (Munich) |
| 4',6-diamidino-2-phenylindole (DAPI) | Roth (Karlsruhe) |
| ddH ₂ O | Ampuwa |
| Defibrinated horse blood | Oxoid, Thermo Fisher Scientific biosciences (St. Leon-Rot) |
| Defibrinated sheep blood | Oxoid, Thermo Fisher Scientific biosciences (St. Leon-Rot) |
| D-glucose | Roth (Karlsruhe) |
| DirectPCR-Tail | Peqlab, VWR (Erlangen) |
| DreamTaq PCR Master Mix (2x) | Thermo Fisher Scientific biosciences (St. Leon-Rot) |
| EDTA | Roth (Karlsruhe) |
| Ethanol | Roth (Karlsruhe) |

| Item | Supplier |
|--|---|
| FastStart Essential DNA Probes Master | Roche (Rotkreuz) |
| GeneRuler 1kb DNA Ladder | Thermo Fisher Scientific biosciences (St. Leon-Rot) |
| Glycerol Rothipuran | Roth (Karlsruhe) |
| Hemin | Sigma-Aldrich Chemie (Munich) |
| Hexadecyltrimethyl ammonium bromide (CTAB) | Roth (Karlsruhe) |
| HRP-streptavidin | Biozol (Eching) |
| Isopropanol | Roth (Karlsruhe) |
| K ₂ HPO ₄ | Roth (Karlsruhe) |
| KCl | Fluka, Sigma-Aldrich Chemie (Munich) |
| KH ₂ PO ₄ | Roth (Karlsruhe) |
| Lipocalin-2/NGAL DuoSet (Mouse) | R&D Systems (Minneapolis, US) |
| Lysozyme from hen egg | Sigma-Aldrich Chemie (Munich) |
| MacConkey agar | Roth (Karlsruhe) |
| Menadione | Sigma-Aldrich Chemie (Munich) |
| Mucin from porcine stomach | Sigma-Aldrich Chemie (Munich) |
| NaCl | Roth (Karlsruhe) |
| Na ₂ HPO ₄ unhydrated | Roth (Karlsruhe) |
| Na ₂ CO ₃ | Merck Chemicals (Schwalbach) |
| Na ₂ S.9H ₂ O | Sigma-Aldrich Chemie (Munich) |
| Normal goat serum | Biozol (Eching) |
| Tissue-Tek Optimal Cutting Temperature (O.C.T.) compound | Sakura Finetek, (Torrance) |
| Tween-20 | Roth (Karlsruhe) |
| Palladium chloride | Sigma-Aldrich Chemie (Munich) |
| Pancreatic digest of casein | Becton Dickinson (New Jersey, US) |
| Paraffin, Paraplast Plus | Roth (Karlsruhe) |
| Paraformaldehyde | Roth (Karlsruhe) |

| Item | Supplier |
|--|---|
| Phalloidin FluoProbes [®] 647 | Interchim (Montluçon) |
| Phenol/chloroform/isoamylalcohol | Roth (Karlsruhe) |
| Primer and probe synthesis | Metabion (Martinsried) |
| Proteinase K | Roth (Karlsruhe) |
| Proteose peptone No 3 | Becton Dickinson (New Jersey, US) |
| Sodium acetate | Roth (Karlsruhe) |
| Sodium dodecyl sulfate (SDS) | Serva (Heidelberg) |
| Sucrose (D-Saccharose) | Roth (Karlsruhe) |
| Sytox green nucleic acid stain | Invitrogen, Thermo Fisher Scientific biosciences (St. Leon-Rot) |
| Tris | MP Biomedicals (Eschwege) |
| Tryptone | Roth (Karlsruhe) |
| Trypticase soy broth | Oxoid, Thermo Fisher Scientific biosciences (St. Leon-Rot) |
| Vectashield mounting medium | Biozol (Eching) |
| Xylol | Roth (Karlsruhe) |
| Yeast extract | MP Biomedicals (Eschwege) |
| Yeast t-RNA | Roche (Rotkreuz) |

Table 2. Antibiotics used in this study

| Antibiotic | Supplier | Final concentration |
|----------------------|------------------|----------------------------|
| Ampicillin | Roth (Karlsruhe) | 100 µg/ml |
| Chloramphenicol | Roth (Karlsruhe) | 30 µg/ml |
| Kanamycin sulfate | Roth (Karlsruhe) | 30 µg/ml |
| Streptomycin sulfate | Roth (Karlsruhe) | 50 µg/ml |

Table 3. Specific instruments and materials

| Item | Supplier |
|---|--|
| Agencourt AMPure XP kit | Beckman Coulter (USA) |
| Aluminum crimp seals (diam. 11 mm) | Sigma-Aldrich (Munich) |
| Aluminum crimp seals (diam. 20 mm) | Sigma-Aldrich (Munich) |
| Blank antimicrobial susceptibility disks | Oxoid, Thermo Fisher Scientific biosciences (St. Leon-Rot) |
| Bottle-Top-Filter (0.2 μm) | A.Hartenstein (Wuerzburg) |
| Butyl-rubber stoppers (diam. 11 mm) | Sigma-Aldrich (Munich) |
| Butyl-rubber stoppers (diam. 20 mm) | Geo-Microbial Technologies |
| Crimper (diam. 11 mm) | Sigma-Aldrich (Munich) |
| Crimper (diam. 20 mm) | VWR (Erlangen) |
| Cryotome CM1950 | (Leica, Wetzlar) |
| Cryotubes | Thermo Fisher Scientific biosciences (St. Leon-Rot) |
| Decrimper (diam. 20 mm) | VWR (Erlangen) |
| Diagnostic slides (10 wells, 76 x 25 x 1 mm) | Thermo Fisher Scientific biosciences (St. Leon-Rot) |
| Electroporation cuvette (1mm) | Eppendorf (Wesseling-Berzdorf) |
| Filter Millex (0.22 μm) | Merck Chemicals (Schwalbach) |
| Flexible vinyl Anaerobic Airlock chamber Type B | Coy laboratory products |
| Flexible film isolator | Harlan (Rossdorf) |
| Glass beads (0.5-0.75 mm) | Schieritz & Hauenstein |
| Glass beads (<106 μm) | Sigma-Aldrich (Munich) |
| Gnotocages | Han, Bioscape (Emmendingen) |
| LightCycler480 Multiwell Plate 96, white | Roche (Rotkreuz) |
| LightCycler96 | Roche (Rotkreuz) |
| Nanodrop | Thermo Fisher Scientific biosciences (St. Leon-Rot) |
| NucleoSipn Gel and PCR Clean-up kit | Macherey-Nagel (Düren) |
| NucleoSipn Plasmid kit | Macherey-Nagel (Düren) |
| Plasmid Plus Midi Kit | Qiagen (Hilden) |

| Item | Supplier |
|---|---------------------------|
| QIAamp DNA Stool Mini Kit | Qiagen (Hilden) |
| Superfrost Plus slides (75 x 25 x 1 mm) | A.Hartenstein (Wuerzburg) |
| Wheaton glass serum bottles (1.5 ml) | Sigma-Aldrich (Munich) |
| Wheaton glass serum bottles (100 ml) | Sigma-Aldrich (Munich) |

3.1.2. Oligonucleotides, probes and antibodies

Table 4. Oligonucleotides and probes

| Designation | Sequence (5' - 3') | Specificity | Reference |
|--|--|---------------|---|
| 16S rRNA gene amplification, cloning and sequencing | | | |
| fD1 | CGATATCTCTAGAAGAGTTTGAT CCTGGCTCAG | All bacteria* | Adapted from (Weisburg, Barns et al. 1991) |
| fD2 | CGATATCTCTAGAAGAGTTTGAT CATGGCTCAG | All bacteria* | Adapted from (Weisburg, Barns et al. 1991) |
| rP1 | GATATCGGATCCACGGTTACCTT GTTACGACTT | All bacteria* | Adapted from (Weisburg, Barns et al. 1991) |
| fD1- <i>EcoRV</i> - <i>XbaI</i> | CCGATATCTCTAGAAGAGTTTGA TCCTGGCTCAG | All bacteria* | Adapted from (Weisburg, Barns et al. 1991) |
| fD2- <i>EcoRV</i> - <i>XbaI</i> | CCGATATCTCTAGAAGAGTTTGA TCATGGCTCAG | All bacteria* | Adapted from (Weisburg, Barns et al. 1991) |
| rP1- <i>EcoRV</i> - <i>BamHI</i> | CCGATATCGGATCCACGGTTACC TTGTTACGACTT | All bacteria* | Adapted from (Weisburg, Barns et al. 1991) |
| 16S-27f | AGAGTTTGATCMTGGCTCAG | All bacteria* | (Lane, Stackebrandt et al. 1991) |
| pJet1-FP | ACTACTCGATGAGTTTTTCGG | pJET 1.2 | Fermentas |
| pJet1-RP | TGAGGTGGTTAGCATAGTTC | pJET 1.2 | Fermentas |
| 338F-M13 | GTAAACGACGGCCAGTGCTCCT ACGGGWGGCAGCAGT | All bacteria* | (Gronbach, Flade et al. 2014) |
| 1044R-rM13 | GGAAACAGCTATGACCATGACT ACGAGCTGACGACARCCATG | All bacteria* | (Gronbach, Flade et al. 2014) |
| A-M13 | CCATCTCATCCCTGCGTGTCTCC GACTCAG/MID sequence/GTAAACGACGGCCAGT G | All bacteria* | (Gronbach, Flade et al. 2014) |
| B-rM13 | CCTATCCCCTGTGTGCCTTGCA GTCTCAGGAAACAGCTATGAC CATGA | All bacteria* | (Gronbach, Flade et al. 2014) |

| Designation | Sequence (5' - 3') | Specificity | Reference |
|--------------------------------------|-------------------------|---|----------------------------------|
| M13_F | GTAAAACGACGGCCAG | pCR [®] 2.1-TOPO [®] | Invitrogen |
| M13_R | CAGGAAACAGCTATGAC | pCR [®] 2.1-TOPO [®] | Invitrogen |
| AGR2 gene specific primers | | | |
| AGR2-KO-fwd | ACCTACATGGCCTTCCTTCC | <i>Agr2</i> ^{ko} -specific | (Park, Zhen et al. 2009) |
| AGR2-wt-fwd | TATCCAGGCTCAGCAGGTTT | <i>Agr2</i> ^{wt} -specific | (Park, Zhen et al. 2009) |
| AGR2-rev | ACCATCAAGGGTCTGTTGCT | <i>Agr2</i> ^{ko} and <i>Agr2</i> ^{wt} | (Park, Zhen et al. 2009) |
| 16S rRNA specific FISH probes | | | |
| YL2_180 | CACCATGCGGTGGGGCGGAGCA | YL2 | Unpublished |
| YL27_180 | AGATGCCTCCCCTCGGCCACA | YL27 | Unpublished |
| YL31_180 | CCATGCGACCCAACTGCATCA | YL31 | Unpublished |
| YL32_180 | CCATGCGGCACTGTGCGCTTA | YL32 | Unpublished |
| Muc1437 | CCTTGCGGTGGCTTCAGAT | YL44 | (Derrien, Collado et al. 2008) |
| BET940 | TTAATCCACATCATCCACCG | YL45 | (Demaneche, Sanguin et al. 2008) |
| YL58_180 | CCATGCAGCCCTGTGCGCTTA | YL58 | Unpublished |
| YL58_180_negctrl | TAAGCGCACAGGGCTGCATGG | None of the Oligo-MM strains | Unpublished |
| I46_180 | AGTATGCGCTCTGTATACCTA | I46 | Unpublished |
| I48_180 | TCATGCGATCTTGATATCCTA | I48 | Unpublished |
| I49_180 | GCCATGTGGCTTTTGTGTTA | I49 | Unpublished |
| KB1_180 | GCCATGCGGCATAAACTGTTA | KB1 | Unpublished |
| KB18_180 | CCATGCGATAAGATAATGTCA | KB18 | Unpublished |
| EUB338 I | GCT GCC TCC CGT AGG AGT | Most bacteria | (Amann, Binder et al. 1990) |
| EUB338 III | GCT GCC ACC CGT AGG TGT | <i>Verrucomicrobiales</i> | (Daims, Bruhl et al. 1999) |

Designations of unpublished FISH probes were followed by the starting position (e.g. xxx_180) of the probe when aligned to the 16S rRNA gene of *E. coli*. * targeting the 16S rRNA of most of the bacteria.

Table 5. MID barcodes for 454 multiplexing

| Designation | MID sequence | Designation | MID sequence |
|--------------------|---------------------|--------------------|---------------------|
| MID1 | ACGAGTGCGT | MID21 | TGCGTGAGCA |
| MID2 | ACGCTCGACA | MID22 | ACAGCTCGCA |
| MID3 | AGACGCACTC | MID23 | CTCACGCAGA |
| MID4 | AGCACTGTAG | MID24 | GATGTCACGA |
| MID5 | ATCAGACACG | MID25 | GCACAGACTA |
| MID6 | ATATCGCGAG | MID26 | GAGCGCTATA |
| MID7 | CGTGTCTCTA | MID27 | ATCTCTGTGC |
| MID8 | CTCGCGTGTC | MID28 | CTGTGCGCTC |
| MID9 | TAGTATCAGC | MID29 | CGACTATGAT |
| MID10 | TCTCTATGCG | MID30 | GCGTATCTCT |
| MID11 | TGATACGTCT | MID31 | TCTGCATAGT |
| MID12 | TACTGAGCTA | MID32 | ATCGAGTCAT |
| MID13 | CATAGTAGTG | MID33 | GTGATGATAC |
| MID14 | CGAGAGATAC | MID34 | CATAGAGAGC |
| MID15 | ATACGACGTA | MID35 | ATGCAGCATA |
| MID16 | TCACGTACTA | MID36 | ATCATGCACT |
| MID17 | TCGATCGAGT | MID37 | TGAGCTAGCT |
| MID18 | CAGTCAGTAG | MID38 | GATGACTGAC |
| MID19 | ACACTGACAC | MID39 | CACAGTCACA |
| MID20 | GTACGATCGT | MID40 | TGCTAGCATG |

Table 6. 16S rRNA gene specific primers and hydrolysis probes for qPCR assay

| Designation | Sequence (5' - 3') | Specificity |
|---------------------|-------------------------------|--------------------|
| Isol46_Exonucl._fwd | ACGGTAGCTAAAACCGGATAGGT | |
| Isol46_Exonucl._rev | GCCTTGATGGGCGCTTTAA | I46 |
| Probe_Isol46 | FAM-TACAGAGCGCATACTCAGT-BHQ1 | |
| Isol49_Exonucl._fwd | GCACTGGCTCAACTGATTGATG | |
| Isol49_Exonucl._rev | CCGCCACTCACTGGTGATC | I49 |
| Probe_Isol49 | HEX-CTTGCACCTGATTGACGA-BHQ1 | |
| YL58_Exonucl._fwd | GAAGAGCAAGTCTGATGTGAAAGG | |
| YL58_Exonucl._rev | CGGCACTCTAGAAAAACAGTTTCC | YL58 |
| Probe_YL58 | FAM-TAACCCCAGGACTGCAT-BHQ1 | |
| YL27_Exonucl.2_fwd | TCAAGTCAGCGGTAAAAATTTCG | |
| YL27_Exonucl.2_rev | CCCACTCAAGAACATCAGTTTCAA | YL27 |
| Probe2_YL27 | HEX-CAACCCCGTCGTGCC-BHQ1 | |
| YL31_Exonucl.2_fwd | AGGCGGGATTGCAAGTCA | |
| YL31_Exonucl.3_rev | CCAGCACTCAAGAACTACAGTTTCA | YL31 |
| Probe2_YL31 | FAM-CAACCTCCAGCCTGC-BHQ1 | |
| YL32_Exonucl.2_fwd | AATACCGCATAAGCGCACAGT | |
| YL32_Exonucl.2_rev | CCATCTCACACCACCAAAGTTTT | YL32 |
| Probe2_YL32 | HEX-CGCATGGCAGTGTGT-BHQ1 | |
| KB1_Exonucl._fwd | CTTCTTTCTCCCGAGTGCTT | |
| KB1_Exonucl._rev | CCCCTCTGATGGGTAGGTTACC | KB1 |
| Probe_KB1 | FAM-CACTCAATTGGAAAGAGGAG-BHQ1 | |
| YL2_Exonucl._fwd | GGGTGAGTAATGCGTGACCAA | |
| YL2_Exonucl._rev | CGGAGCATCCGGTATTACCA | YL2 |
| Probe_YL2 | HEX-CGGAATAGCTCCTGGAAA-BHQ1 | YL2 |

| Designation | Sequence (5' - 3') | Specificity |
|----------------------|------------------------------------|--------------------|
| KB18_Exonucl.2_fwd | TGGCAAGTCAGTAGTGAAATCCA | |
| KB18_Exonucl.2_rev | TCACTCAAGCTCGACAGTTTCAA | KB18 |
| Probe2_KB18 | FAM-CTTAACCCATGAACTGC-BHQ1 | |
| YL44_Exonucl._fwd | CGGGATAGCCCTGGGAAA | |
| YL44_Exonucl._rev | GCGCATTGCTGCTTTAATCTTT | YL44 |
| Probe_YL44 | HEX-TGGGATTAATACCGCATAGTA-BHQ1 | |
| YL45_Exonucl._fwd | AGACGGCCTTCGGGTTGTA | |
| YL45_Exonucl._rev | CGTCATCGTCTATCGGTATTATCAA | YL45 |
| Probe_YL45 | FAM-ACCACTTTTGTAGAGAACGA-BHQ1 | |
| Isol48_Exonucl._fwd | GGCAGCATGGGAGTTTGCT | |
| Isol48_Exonucl._rev | TTATCGGCAGGTTGGATACGT | I48 |
| Probe_Isol48 | HEX-CAAACCTCCGATGGCGAC-BHQ1 | |
| ASF356_Exonucl.2_fwd | CGGCAAGGTAAGCGATATGTG | |
| ASF356_Exonucl.2_rev | CGCTTTCCTCTCCTGTACTCTAGCT | ASF356 |
| Probe2_ASF356 | FAM-TAACTTAAGGATAGCATAACGAACT-BHQ1 | |
| ASF360_Exonucl.4_fwd | TGAGTGCTAAGTGTTGGGAGGTT | |
| ASF360_Exonucl.4_rev | CGGAGTGCTTAATGCGTTAGCT | ASF360 |
| Probe4_ASF360 | FAM-CCGCCTCTCAGTGCT-BHQ1 | |
| ASF361_Exonucl._fwd | TCGGATCGTAAAACCCTGTTG | |
| ASF361_Exonucl._rev | ACCGTCGAAACGTGAACAGTT | ASF361 |
| Probe_ASF361 | HEX-TAGAGAAGAAAGTGCGTGAGAG-BHQ1 | |
| ASF457_Exonucl._fwd | GACTGGAACAACCTACCGAAAGGT | |
| ASF457_Exonucl._rev | CAGGTCTCCCCAACTTTTCCT | ASF457 |
| Probe_ASF457 | FAM-TAATGCCGGATGAGTTATA-BHQ1 | ASF457 |
| ASF500_Exonucl._fwd | AGGCGGGACTGCAAGTCA | |

| Designation | Sequence (5' - 3') | Specificity |
|----------------------|--------------------------------|-----------------------|
| ASF500_Exonucl._rev | CAAATGCAGGCCACAGGTT | ASF500 |
| Probe_ASF500 | HEX-ATGTGAAAACCACGGGC-BHQ1 | |
| ASF502_Exonucl.3_fwd | GACCCCAGTACCGCATGGTA | |
| ASF502_Exonucl.3_rev | TCAGACGCGGGCCTATCTTA | ASF502 |
| Probe3_ASF502(SB2) | HEX-AGAGGTAAAAACTGAGGTGGT-BHQ1 | |
| ASF519_Exonucl._fwd | TGTGGCTCAACCATAAAATTGC | |
| ASF519_Exonucl._rev | GCATTCCGCCTACCTCAAATAT | ASF519 |
| Probe_ASF519 | HEX-TTGAAACTGGTTGACTTGAG-BHQ1 | |
| Salmo_Exonucl._fwd | TGGGAAACTGCCTGATGGA | |
| Salmo_Exonucl._rev | CTTGCGACGTTATGCGGTATT | <i>S. Typhimurium</i> |
| Probe_Salmo | FAM-ATAACTACTGGAAACGGTGGC-BHQ1 | |
| Univ_Exonucl.2_fwd | TGCATGGYYGTCGTCAGC | |
| Univ_Exonucl.2_rev | CRTCRTCCCCRCCTTCCTC | All strains |
| Probe2_Univ. | HEX-AACGAGCGCAACCC-BHQ1 | |

All primers and probes were designed by Markus Beutler and are unpublished. Identity of Oligo-MM strains are indicated in blue, identity of ASF strains are in orange. Salmo: targets *S. Typhimurium*; Univ: targets all strains. Fwd: forward primer; Rev: reverse primer; Probe: hydrolysis probe labelled at the 5' end either with FAM (6-carboxyfluorescein) or HEX (6-carboxyhexafluorescein) and conjugated at the 3' end with BHQ1 (black hole quencher 1).

Table 7. Primary antibodies

| Antibody | Origin | Supplier | Final concentration |
|--|---------------|-----------------------------------|----------------------------|
| α - <i>Salmonella</i> B test serum anti-O | Rabbit | Becton Dickinson (New Jersey, US) | 1:400 |
| α -MUC2 H-300 | Rabbit | Santa cruz (Heidelberg) | 1:200 |

Table 8. Secondary antibodies

| Antibody | Origin | Supplier | Final concentration |
|----------------------------------|--------|---|---------------------|
| α -rabbit IgG dylight 549 | Goat | Jackson ImmunoResearch (Baltimore, US) | 1:400 |

3.1.3. Plasmids and strains

Table 9. Plasmids in *S. Tm*

| Plasmid | Genotype | Reference |
|---------|---|------------------------------------|
| pM973 | T3SS-2 (SPI-2) promotor <i>ssaG</i> coupled with GFP <i>mut2</i> coding sequence | (Hapfelmeier, Stecher et al. 2005) |
| pM974 | T3SS-1 (SPI-1) promotor of the <i>sicAsipBCDA</i> operon coupled with GFP <i>mut2</i> coding sequence | (Ackermann, Stecher et al. 2008) |
| pM979 | Constitutively expressed GFP <i>mut2</i> coding sequence (ribosomal <i>rpsM</i> promoter) | (Stecher, Hapfelmeier et al. 2004) |
| pWKS30 | Ampicillin resistance cassette | (Wang and Kushner 1991) |

Table 10. Plasmids generated to sequence the full 16S rRNA genes of the Oligo-MM and ASF strains

| Plasmid | Backbone | Origin of the insert | Restriction enzymes | Reference |
|----------|--|----------------------|---------------------|-------------|
| pSAB3 | pJET 1.2 | YL27 | <i>NotI</i> | Unpublished |
| pSAB4 | pJET 1.2 | YL58 | <i>HindIII</i> | Unpublished |
| pSAB6 | pJET 1.2 | I46 | <i>NotI</i> | Unpublished |
| pSAB7 | pJET 1.2 | I48 | <i>HindIII</i> | Unpublished |
| pSAB8 | pJET 1.2 | I49 | <i>HindIII</i> | Unpublished |
| pSAB9 | pJET 1.2 | KB1 | <i>NotI</i> | Unpublished |
| pSAB10 | pJET 1.2 | ASF502 | <i>NotI</i> | Unpublished |
| pSAB12 | pJET 1.2 | KB18 | <i>HindIII</i> | Unpublished |
| pSAB13 | pJET 1.2 | ASF500 | <i>NotI</i> | Unpublished |
| pMB1 | pJET 1.2 | <i>S. Tm</i> M557 | <i>HindIII</i> | Unpublished |
| pM1452 | pCR [®] 2.1-TOPO [®] | YL2 | <i>HindIII</i> | Unpublished |
| pM1456-1 | pCR [®] 2.1-TOPO [®] | YL31 | <i>HindIII</i> | Unpublished |
| pM1457-1 | pCR [®] 2.1-TOPO [®] | YL32 | <i>HindIII</i> | Unpublished |

| Plasmid | Backbone | Origin of the insert | Restriction enzymes | Reference |
|----------|--|----------------------|---------------------|-------------|
| pM1459-1 | pCR [®] 2.1-TOPO [®] | YL44 | <i>HindIII</i> | Unpublished |
| pM1460-1 | pCR [®] 2.1-TOPO [®] | YL45 | <i>NcoI</i> | Unpublished |
| pM1411-1 | pSB-Bluescript | ASF356 | <i>NotI</i> | Unpublished |
| pM1412-4 | pSB-Bluescript | ASF360 | <i>NotI</i> | Unpublished |
| pM1413-1 | pSB-Bluescript | ASF361 | <i>NotI</i> | Unpublished |
| pM1414-1 | pSB-Bluescript | ASF457 | <i>NotI</i> | Unpublished |
| pM1417-1 | pSB-Bluescript | ASF519 | <i>NotI</i> | Unpublished |

Table 11. *S. Tm* and *E. coli* strains

| Strains | Lab-internal strain designation | Genotype | Reference |
|---|---------------------------------|---|-----------------------------------|
| <i>S. Tm</i> strains | | | |
| <i>S. Tm</i> ^{wt} | SB300 | <i>S. Tm</i> strain SL1344 | (Hoiseth and Stocker 1981) |
| <i>S. Tm</i> ^{wt,gfp} | SB300_pM973 | <i>S. Tm</i> carrying plasmid pM973 | Unpublished |
| <i>S. Tm</i> ^{wt,amp} | SB300_pWKS30 | <i>S. Tm</i> carrying plasmid pWKS30 (Wang and Kushner 1991) | (Stecher, Denzler et al. 2012) |
| <i>S. Tm</i> ^{avir} | M557 | <i>invG</i> ; <i>sseD::aphT</i> | (Hapfelmeier, Ehrbar et al. 2004) |
| <i>S. Tm</i> ^{cheY} | M957 | <i>cheY::cm</i> | (Stecher, Barthel et al. 2008) |
| <i>S. Tm</i> ^{avir2} | M2702 | <i>invG</i> ; <i>ssaV</i> | (Maier, Vyas et al. 2013) |
| <i>S. Tm</i> ^{avir2} _p ^{sicAgfp} | M2702_pM974 | <i>S. Tm</i> carrying plasmid pM974 | Unpublished |
| <i>S. Tm</i> ^{avir2,cheY} | SAB1-1 | <i>invG</i> ; <i>ssaV</i> ; <i>cheY::cm</i> | Unpublished |
| <i>E. coli</i> strains | | | |
| <i>E. coli</i> DH5 α | | | Invitrogen |

3.1.4. Media and buffers

Liquid media and buffers were prepared as described in the following tables and sterilized by autoclaving at 121 °C, 1 bar, 20 min, unless otherwise stated.

Table 12. Luria-Bertani (LB) medium

| Components | Per liter medium |
|-------------------|-------------------------|
| NaCl | 5 g |
| Yeast Extract | 5 g |
| Tryptone | 10 g |

All components were dissolved in dH₂O.

Table 13. LB agar and soft agar

| Components | Per liter medium |
|-------------------|-------------------------|
| NaCl | 5 g |
| Yeast Extract | 5 g |
| Tryptone | 10 g |
| Agar* | 15 g |

All components were dissolved in dH₂O. * Soft agar: add 7 g/L instead.

Table 14. LB 0.3 M NaCl

| Components | Per liter medium |
|-------------------|-------------------------|
| NaCl | 17.53 g |
| Yeast Extract | 5 g |
| Tryptone | 10 g |

All components were dissolved in dH₂O.

Table 15. Brain-heart infusion (BHI) medium*

| Components | Per liter medium |
|---|------------------|
| Brain Heart Infusion | 37 g |
| Distilled water (dH ₂ O) | 1 L |
| Autoclave and then add under anaerobic and sterile conditions: | |
| Cysteine-HCl.H ₂ O [#] | 0.25 g |
| Na ₂ S.9H ₂ O [#] | 0.25 g |

All components were dissolved in dH₂O. [#] Sterile filtered. * for BHI agar, add 15 g/L agar.

Table 16. Anaerobic *Akkermansia* medium (AAM)

| Components | Per liter medium |
|--|------------------|
| Brain Heart Infusion | 18.5 g |
| Trypticase soy broth | 15 g |
| Yeast extract | 5 g |
| K ₂ HPO ₄ | 2.5 g |
| Hemin | 1 mg |
| Glucose | 0.5 g |
| Distilled water (dH ₂ O) | 1 L |
| Autoclave and then add under sterile conditions: | |
| Na ₂ CO ₃ (5% stock solution) [□] | 0.4 g |
| Cysteine hydrochloride [#] | 0.5 g |
| Menadione [#] | 0.5 g |
| Fetal calf serum (complement-inactivated) [#] | 3 % |
| Mucin from porcine stomach [□] | 0.25 % |

All components were dissolved in dH₂O except for the hemin, which was resuspended in ethanol p.a. supplemented with NaOH until it is entirely dissolved and for the menadione, which was resuspended in ethanol p.a. [□] Autoclaved. [#] Sterile filtered.

Table 17. Schaedler blood agar

| Components | Per liter medium |
|---|-------------------------|
| Pancreatic digest of casein | 10 g |
| Proteose Peptone No 3 | 5 g |
| Glucose | 5 g |
| Yeast extract | 5 g |
| Tris | 3 g |
| Hemin | 10 mg |
| L-Cystine | 0.4 g |
| Agar | 15 g |
| Autoclave and then add under sterile conditions: | |
| Fetal calf serum (complement-inactivated) [#] | 3 % |
| Defibrinated sheep or horse blood | 50 ml |

All components were dissolved in dH₂O except for the hemin, which was resuspended in ethanol p.a. supplemented with NaOH. [#] Sterile filtered. (Schaedler, Dubs et al. 1965).

Table 18. WSB broth/agar

| Components | Per liter medium |
|---|-------------------------|
| Wilkinson-Chalgreen Anaerobe broth (Oxoid) | 33 g |
| Glucose | 4 g |
| Hemin | 10 µg |
| L-Cystine | 0.4 g |
| Agar* (Serva) | 15 g |
| Autoclave, cool to 50 °C and then add sterily: | |
| Defibrinated sheep blood | 50 ml |

All components were dissolved in dH₂O except for the hemin, which was resuspended in ethanol p.a. supplemented with NaOH. * Optional.

Table 19. AII medium

| Components | Per liter medium |
|--|-------------------------|
| Brain Heart Infusion (Oxoid) | 18.5 g |
| Yeast Extract (Oxoid) | 5 g |
| Trypticase soy broth (Oxoid) | 15 g |
| K ₂ HPO ₄ | 2.5 g |
| Hemin | 10 µg |
| Glucose | 0.5 g |
| Palladium chloride* | 0.33 g |
| Agar* (Serva) | 15 g |
| Autoclave and then add under anaerobic conditions: | |
| Na ₂ CO ₃ [‡] | 42 mg |
| Cysteine hydrochloride [#] | 50 mg |
| Menadione [#] | 5 µg |
| Fetal calf serum (complement-inactivated) [#] | 3 % |

All components were dissolved in dH₂O except for the hemin, which was resuspended in ethanol p.a. supplemented with NaOH and for the menadione, which was resuspended in ethanol p.a. * Optional. Adapted from (Aranki and Freter 1972). [‡] Autoclaved. [#] Sterile filtered.

Table 20. Peptone-glycerol broth

| Components | Per liter broth |
|-------------------|------------------------|
| Peptone | 20 g |
| Glycerol | 50 ml |

All components were dissolved in dH₂O.

Table 21. Phosphate Buffered Saline (PBS) 10X

| Components | Per liter buffer |
|---|-------------------------|
| NaCl | 80 g |
| KCl | 2 g |
| Na ₂ HPO ₄ unhydrated | 6,1 g |
| KH ₂ PO ₄ | 2,4 g |

All components were dissolved in dH₂O.

Table 22. TE Buffer

| Components | Final concentration |
|-------------------|----------------------------|
| Tris-HCl | 10 mM |
| EDTA | 1 mM |

All components were dissolved in ddH₂O. pH was adjusted to 8.0 with NaOH.

Table 23. CTAB/NaCl Buffer

| Components | Final concentration |
|-------------------|----------------------------|
| CTAB | 10 % |
| NaCl | 0.7 M |

All components were dissolved in ddH₂O.

Table 24. Paraformaldehyde (PFA) 4 %

| Components | Per liter buffer |
|---|-------------------------|
| ddH ₂ O | 300 ml |
| PFA | 40 g |
| NaOH (1 M) | 100 µl |
| PBS (10X) in ddH ₂ O, pH 7.4 | 100 ml |

Components were heated up to 60 °C and stirred vigorously until PFA is dissolved. DdH₂O was filled up to 1 L and pH was adjusted. Buffer was sterile filtered and stored at -20 °C.

Table 25. Sucrose 20 %

| Components | Per liter buffer |
|--------------------------------|-------------------------|
| Sucrose (D-Saccharose) | 200 g |
| PBS (1X) in ddH ₂ O | 1 L |

Buffer was sterile filtered and stored at 4 °C.

Table 26. Composition of hybridization buffers (HB) for FISH

| Formamide (%): | 0 | 5 | 10 | 15 | 20 | 25 | 30 | 35 | 40 | 45 | 50 | 55 | 70 |
|-----------------------|----------|----------|-----------|-----------|-----------|-----------|-----------|-----------|-----------|-----------|-----------|-----------|-----------|
| 5 M NaCl | 180 | 180 | 180 | 180 | 180 | 180 | 180 | 180 | 180 | 180 | 180 | 180 | 180 |
| 1 M Tris / HCl | 20 | 20 | 20 | 20 | 20 | 20 | 20 | 20 | 20 | 20 | 20 | 20 | 20 |
| ddH ₂ O | 799 | 749 | 699 | 649 | 599 | 549 | 499 | 449 | 399 | 349 | 299 | 249 | 99 |
| Formamide | 0 | 50 | 100 | 150 | 200 | 250 | 300 | 350 | 400 | 450 | 500 | 550 | 700 |
| 10 % SDS | 1 | 1 | 1 | 1 | 1 | 1 | 1 | 1 | 1 | 1 | 1 | 1 | 1 |

Volumes are in μ l.

Table 27. Composition of washing buffers (WB) for FISH

| Formamide (%): | 0 | 5 | 10 | 15 | 20 | 25 | 30 | 35 | 40 | 45 | 50 | 55 | 70 |
|-----------------------|----------|----------|-----------|-----------|-----------|-----------|-----------|-----------|-----------|-----------|-----------|-----------|-----------|
| 5 M NaCl | 9.0 | 6.3 | 4.5 | 3.2 | 2.2 | 1.5 | 1.0 | 0.7 | 0.5 | 0.3 | 0.2 | 0.1 | 0 |
| 1 M Tris / HCl | 1 | 1 | 1 | 1 | 1 | 1 | 1 | 1 | 1 | 1 | 1 | 1 | 1 |
| 0.5 M EDTA | 0 | 0 | 0 | 0 | 0.5 | 0.5 | 0.5 | 0.5 | 0.5 | 0.5 | 0.5 | 0.5 | 0.5 |
| ddH ₂ O | to 50 ml | | | | | | | | | | | | |

Volumes are in ml.

Table 28. Blocking buffer for ELISA

| Components | Per liter buffer |
|--------------------------------|-------------------------|
| Bovine serum albumin (BSA) | 20 g |
| PBS (1X) in ddH ₂ O | 1 L |

Buffer was freshly prepared each time (not autoclaved, not sterile filtered).

Table 29. Washing buffer for ELISA

| Components | Per liter buffer |
|--------------------------------|-------------------------|
| Tween-20 | 0.5 ml |
| PBS (1X) in ddH ₂ O | 1 L |

Buffer was freshly prepared each time (not autoclaved, not sterile filtered).

Table 30. Substrate buffer for ELISA

| Components | Per liter buffer |
|----------------------------------|-------------------------|
| NaH ₂ PO ₄ | 13.8 g |
| dH ₂ O | 1 L |

Buffer was autoclaved, stored at RT and pH was adjusted to 4.0.

Table 31. Percoll gradient

20 % Percoll:

| Components | Per liter DMEM |
|-------------------|-----------------------|
| Percoll | 200 ml |

40 % Percoll:

| Components | Per liter 1X PBS |
|-------------------|-------------------------|
| Percoll | 400 ml |

One volume 40 % Percoll was gently pipetted under 1 volume 20 % Percoll, using a Pasteur pipette. Percoll gradient solution was stored at 4 °C.

3.2. Methods

3.2.1. Bacterial culture methods

3.2.1.1. Cryoconservation of bacteria

***S. Tm* and *E. coli* strains.** Bacteria streaked out from cryostocks were grown overnight (o.n.) on agar plates supplemented with the appropriate antibiotics at 37 °C. A single bacterial colony was inoculated in 3 ml LB medium (with the appropriate antibiotics) and grown o.n. at 37 °C on a wheel rotor. Further, the o.n. culture was spun down at 4 °C for 20 min at 5,000 rpm. The supernatant was removed and the bacterial pellet was resuspended in 1 ml peptone-glycerol broth and stored in cryotubes at -80 °C.

Anaerobic bacterial strains. 0.5 ml of pre-reduced 20 % glycerol supplemented with palladium crystals was aliquoted in 1.5 ml anoxic glass vials and sealed in the anaerobic chamber and autoclaved. Afterwards, 0.5 ml of actively growing anaerobic cultures, grown in respective culture media, was added into the autoclaved vials and immediately frozen at -80 °C.

Strain deposition at the German type culture collection (DSMZ). Except of the strains ASF492, which could not be cultivated, all ASF and Oligo-MM¹² strains were deposited at the German type culture collection (DSMZ; Deutsche Sammlung von Mikroorganismen und Zellkulturen). Individual strains were sent as a frozen stock to the DSMZ. There, the frozen stocks were revived and the resulting cultures were lyophilized and sent back in order to confirm the strain purity and identity using Gram staining, 16S rRNA gene amplification and sequencing, as described below. The corresponding accession numbers are listed in **Table 32**.

Table 32. Accession numbers of the strains deposited at DSMZ

| Strain ID | Accession number |
|------------------|-------------------------|
| ASF356 | DSM26116 |
| ASF360 | DSM28184 |
| ASF361 | DSM 28185 |
| ASF457 | DSM 26150 |
| ASF500 | DSM 29473 |
| ASF502 | DSM 26118 |
| ASF519 | DSM 26086 |
| YL2 | DSM 26074 |
| YL27 | DSM 28989 |
| YL31 | DSM 26117 |
| YL32 | DSM 26114 |
| YL44 | DSM 26127 |
| YL45 | DSM 26109 |
| YL58 | DSM 26115 |
| I46 | DSM 26113 |
| I48 | DSM 26085 |
| I49 | DSM 32035 |
| KB1 | DSM 32036 |
| KB18 | DSM 26090 |

3.2.1.2. Bacterial culture conditions

Aerobic culture conditions. Bacteria from -80 °C cryostocks were grown o.n. on LB agar supplemented with the appropriate antibiotics at 37 °C. For mouse experiments, a single colony was inoculated in 3 ml LB medium containing 0.3 M NaCl (LB^{0.3}), supplemented with the appropriate antibiotics and grown at 37 °C on a wheel rotor for 12 h. Further, the o.n. culture was diluted 1:20 in fresh LB^{0.3} medium and grown at 37 °C on a wheel rotor for 4 h. The subculture was washed in ice-cold 1X PBS and the bacterial pellet was resuspended in cold 1X PBS at a concentration of $\sim 1.10^8$ cfu/ml.

Anaerobic culture conditions. Anaerobic media, solutions and glass bottles were pre-reduced at least 2 days before use under anoxic conditions (Formiergas: 3 % H₂, Rest N₂) in an anaerobic chamber. Cryostocks were defrozen at 37 °C into a water-bath. A single vial was inoculated into a sealed wheaton bottle containing 10 ml of pre-reduced medium. Liquid cultures were gassed (7 % H₂, 10 % CO₂, rest N₂) and incubated until growth was observed. Anaerobic bacterial strains were grown either in anaerobic brain-heart infusion (BHI) broth or in anaerobic *Akkermansia* medium (AAM). To improve growth of YL44, AAM was supplemented with gastric mucin.

Bacterial cultures for genomic DNA extraction and genome sequencing. Bacterial cultures were set up as described above except for that media were filtered using a bottle-top-filter system (0.2 µm) before autoclaving.

3.2.1.3. Streptomycin halo assay

This assay was performed by Diana Ring (AG Stecher, MvP, Munich).

E. coli strain DH5 α (Invitrogen) was streaked out on LB agar plates from -80 °C cryostocks and incubated o.n. at 37 °C. Next, a single colony was grown in 3 ml LB medium for 12 h, on a wheel rotor, at 37 °C. LB agar plates were overlaid with either 6 ml LB soft agar mixed with 100 µl of an o.n. culture of *E. coli* DH5 α or 15 ml LB soft agar mixed with 250 µl bacterial culture, depending on agar plate size. Blank antimicrobial susceptibility disks (Oxoid) were laid on each plate and 5 µl sample was spotted on each disk. A standard curve was performed using serial dilutions of streptomycin from 500 mg/ml to 5×10^{-13} mg/ml with 10-fold diluting steps. Plates were incubated o.n. at 37 °C and inhibition zone (halo) size was measured using a ruler. Size of the blank disk was substrated to all values.

3.2.2. Bacterial strains

3.2.2.1. Salmonella strains

Salmonella spp. strains used in this study are listed in **Table 11**. The M2702 derivative SAB1-1 (*invG*; *ssaV*; *cheY::cm*) was constructed by P22 transduction of *cheY::cat* (Cm^R) allele from the *S. Tm* strain M957 into the recipient strain M2702 (*invG*; *ssaV*).

3.2.2.2. The Altered Schaedler Flora strains

The Altered Schaedler Flora (ASF) strains ASF356, ASF360, ASF361, ASF457, ASF500 and ASF519 were obtained from Charles River Laboratories.

In order to isolate ASF502, an ASF-colonized C57Bl/6 mouse (ETH, Zurich) was killed and imported into an anaerobic chamber. The cecum content was resuspended in pre-reduced 1X PBS and plated on Schaedler blood agar (**Table 17**). Plates were exported into an anaerobic jar and incubated at 37 °C under anaerobic conditions. Single colonies were restreaked on fresh agar until pure growth is observed, and then transferred into 10 ml AAM and incubated at 37 °C. Strain identity was confirmed by 16S rRNA gene sequencing and sequences were blasted against NCBI blast (Altschul, Gish et al. 1990) and the Ribosomal Database Project (RDP) (Wang, Garrity et al. 2007).

Taxonomic classification of the ASF strains is detailed further in **Table 35**.

3.2.2.3. Isolation of the Oligo-MM strains

Isolation of I46, I48 and I49 strains by Ricco Robbiani (ETH, Zurich). Fecal pellets were collected from C57Bl/6J mice (Janvier, ETH, Zurich), directly resuspended in PBS and plated on Wilkins-Chalgren agar supplemented with 5 % defibrinated sheep blood (WSB agar). Plates were incubated in an anaerobic atmosphere (7 % H₂, 10 % CO₂, rest N₂) at 37 °C for 3-5 days. Strains were identified by 16S rRNA gene sequencing and sequences were blasted against RDP.

Isolation of YL2, YL27, YL31, YL32, YL44, YL45 and YL58 strains by Yvonne Loetscher (ETH, Zurich). C57Bl/6J mice (Janvier, ETH, Zurich) harboring a conventional gut microbiota were killed and then imported into an anaerobic chamber. Cecum contents were resuspended into a diluting fluid as described in (Aranki, Syed et al. 1969) and either directly plated on AII agar or plating on WSB agar after a heat treatment at 80 °C for 10 min or a chloroform-treatment as previously described (Itoh and Freter

1989). Plates were transferred into anaerobic jars, gassed (7 % H₂, 10 % CO₂, rest N₂) and incubated at 37 °C for one week. Single colonies were restreaked on fresh agar until pure growth is observed, and then transferred into pre-reduced AII liquid medium and incubated at 37 °C, in anaerobic conditions. Strains were identified by 16S rRNA gene sequencing and sequences were blasted against RDP.

Isolation of KB1 and KB18 strains. Feces from a TCR^{MOG92-106}/I-A^s transgenic (RR) SJL/J mouse (Berer, Mues et al. 2011) was heat-inactivated at 70°C for 15 min and frozen at -20°C (Kerstin Berer, MPI, Munich). Fecal pellets were imported in the anaerobic chamber and resuspended into pre-reduced 1X PBS. Serial dilutions were either plated on BHI agar or transferred into BHI medium. Freshly inoculated bottles were heated for 1h at 70 °C and cooled down on ice. Agar plates and liquid bottles were incubated at 37 °C under anaerobic conditions (7% H₂, 10% CO₂, rest N₂) until growth was observed. KB1 was isolated as a single colony from a BHI agar plate after an o.n. incubation. KB18 was isolated using a serial dilution approach and 8 days incubation. Strains were identified by 16S rRNA gene sequencing and sequences were blasted against NCBI and RDP.

Table 33. Isolation and cultivation of the Oligo-MM strains

| Strain ID | Mouse line of origin | Isolation media | Culture media | Reference |
|-----------|--|-----------------|----------------------|-------------|
| YL2 | C57Bl/6J | AII agar | AAM or BHI | Unpublished |
| YL27 | C57Bl/6J | AII agar | AAM or BHI | Unpublished |
| YL31 | C57Bl/6J | WSB agar | AAM or BHI | Unpublished |
| YL32 | C57Bl/6J | WSB agar | AAM or BHI | Unpublished |
| YL44 | C57Bl/6J | WSB agar | AAM ^{Mucin} | Unpublished |
| YL45 | C57Bl/6J | WSB agar | AAM or BHI | Unpublished |
| YL58 | C57Bl/6J | WSB agar | AAM or BHI | Unpublished |
| I46 | C57Bl/6J | WSB agar | AAM or BHI | Unpublished |
| I48 | C57Bl/6J | WSB agar | AAM or BHI | Unpublished |
| I49 | C57Bl/6J | WSB agar | AAM or BHI | Unpublished |
| KB1 | TCR ^{MOG92-106} /I-A ^s transgenic (RR) SJL/J | BHI agar | AAM or BHI | Unpublished |
| KB18 | TCR ^{MOG92-106} /I-A ^s transgenic (RR) SJL/J | BHI medium | BHI | Unpublished |

Taxonomic classification is detailed further in **Table 35**.

3.2.2.4. Preparation of bacterial inocula as frozen stocks

Oligo-MM¹⁰. The ten Oligo-MM strains (YL2, YL31, YL32, YL44, YL45, YL58, I46, I48, I49 and KB1) were anaerobically and individually grown. Then, OD₆₀₀ of the cultures was determined. Purity of bacterial culture was confirmed by Gram staining. Further on, actively growing cultures were imported into the anaerobic chamber and mixed in a 1:1 ratio according to their OD₆₀₀ measurements (except for the YL45 bacterial culture, which is translucent). In order to cryopreserve the frozen stock at -80 °C, 1 vol. bacterial mixture was mixed to 1 vol. 20 % glycerol solution supplemented with palladium black crystals, as previously described. Mixtures were aliquoted in 1.5 ml glass vials, sealed with butyl-rubber stoppers and frozen at -80 °C.

ASF⁶. Similarly to the procedure described above, six ASF strains (ASF356, ASF360, ASF361, ASF457, ASF502 and ASF519) were anaerobically grown and actively growing cultures were imported into the anaerobic chamber. For each ASF strain, 3 ml culture was centrifuged 5 min, 8,000 rpm at 4 °C and cell pellets were directly frozen at -20 °C for further analyses. Cultures were mixed all together in a 1:1 ratio according to their OD₆₀₀ measurements and aliquoted such as 1 vol. bacterial suspension was mixed with 1 vol. glycerol solution supplemented with palladium black crystals. Mixtures were aliquoted in 1.5 ml glass vials, sealed with butyl-rubber stoppers and frozen at -80 °C. To inoculate ASF⁷ mixture, ASF⁶ inoculum was supplemented by ASF500 which was inoculated to mice as actively growing culture.

For each bacterial inoculum, 3-6 ml of the mixture was centrifuged 5 min, 8,000 rpm at 4 °C and pellets were directly frozen at -20 °C for DNA extraction to confirm strain identity and presence using amplicon sequencing or/and qPCR.

3.2.3. Molecular biology methods

3.2.3.1. Genomic DNA extraction

Genomic DNA extraction from bacterial cultures. Genomic DNA extraction was performed using a standard phenol/chloroform/isoamylalcohol protocol. Concentrations indicated in the next paragraph are given as final concentration. Briefly, bacterial pellets of Gram-positive strains were resuspended in TE buffer (**Table 22**) supplemented with 0.5 % SDS and 20 mg/ml lysozyme. Then, bacterial suspensions were incubated at 37 °C for 1 h 30 min. Further on, suspensions were supplemented with 0.1 µg/ml proteinase K and incubated at 55 °C for 1 h. The bacterial pellets of Gram-negative strains were directly resuspended in TE buffer supplemented with 0.5 % SDS and 0.1 µg/ml proteinase K, then incubated at 55 °C for 1 h. Next, 0.64 M NaCl and 0.1 volume (vol.) CTAB/NaCl buffer (**Table 23**) were added and

incubated at 65 °C for 10 min. Then, 1 vol. of phenol/chloroform/isoamylalcohol and the suspensions were mixed, and then centrifuged. Supernatants were transferred into a new tube and gDNA was precipitated with 0.7 vol. isopropanol and 0.1 vol. 3 M sodium acetate. Tubes were mixed and centrifuged at full speed at 4 °C for 30 min. Genomic DNA was washed with 1 vol. ice-cold 70 % ethanol p.a. and centrifuged at 4 °C for 15 min. Finally, gDNA was dissolved using 20-50 µl TE buffer and stored at 4 °C for further whole genome sequencing or at -20 °C for other applications. Genomic DNA concentration was determined using Nanodrop (Peqlab Biotechnology) and DNA integrity was confirmed by agarose gel electrophoresis.

Genomic DNA extraction from mouse intestinal contents and Oligo-MM¹⁰ inoculum. Small intestinal, cecal and fecal gDNA were extracted using the QIAamp DNA Stool Mini Kit (Qiagen) following the manufacturer's instructions with two modifications: protocol was initialized by a bead-beating step (3 min, 50 Hz) in buffer ASL using 2 glass bead sizes (0.5-0.75 mm and <106 µm) and lysozyme was added to the lysis buffer at a 20 mg/ml final concentration.

Genomic DNA extraction from mouse biopsies. In order to genotype genetically modified mouse lines (*i.e.* AGR2 and MUC2 mice), murine gDNA was extracted using biopsies from tails or ears. Briefly, tail biopsies were suspended in 200 µl DirectPCR-Tail reagent (Peqlab Biotechnology) supplemented with 0.4 mg/ml final concentration of proteinase K. After an o.n. incubation at 55 °C, 500 rpm, proteinase K was heat-inactivated at 85 °C for 45 min. Further on, suspensions were centrifuged 2 min at 11,000 rpm and directly used as a template for PCR or frozen at -20 °C. In order to extract gDNA from ear biopsies, the same protocol with adapted volumes of DirectPCR-Tail reagent (100 µl instead of 200 µl).

3.2.3.2. RNA extraction and microarray analysis

Intestinal epithelial cell (IEC) isolation. Cecal IEC isolation was performed together with Eva Rath (TUM-ZIEL, Freising-Weihestephan, Germany) using a standard Percoll gradient protocol. Concentrations indicated in the next paragraph are given as final concentration. Briefly, after mouse sacrifice, cecum was sampled and cecal epithelial cells were exposed by inversion. In tube 1, tissues were resuspended in 1 volume (vol.) DMEM, supplemented with 1 mM DTT and vortexed for 1 min. Then, tissue suspensions were incubated at 37 °C for 15 min, at 200 rpm and vortexed for 1 min. Cecal tissues were transferred into a new tube (tube 2) with 1 vol. 1X PBS supplemented with 1.5 mM EDTA, then vortexed for 1 min. Cecal tissue suspensions were incubated at 37 °C for 10 min, at 200 rpm and vortexed for 1 min. Meanwhile, IEC suspensions in tube 1 were centrifuged at 4 °C for 7 min, at 300xg and IEC pellets were resuspended in 5 ml DMEM, and then stored on ice. In tube 2, Cecal tissues were discarded

and IEC suspensions were centrifuged at 4 °C for 7 min, at 300xg. Then, IEC pellets were resuspended with the 5 ml DMEM from tube 1. IEC suspensions were carefully pipetted onto the Percoll gradient (**Table 31**) and centrifuged at 4 °C for 30 min, at 600xg. IEC were isolated from the Percoll gradient using a Pasteur pipette into a new tube, supplemented with 0.025 vol. DMEM, and centrifuged at 4 °C for 5 min, at 300xg. IEC were washed once in 1X PBS, and then resuspended in adequate buffer.

IEC RNA extraction. The RNA was extracted by Eva Rath (TUM-ZIEL, Freising-Weihenstephan, Germany). Total RNA was isolated from cecal IEC using the column-based RNeasy Mini kit (Qiagen, Hilden, Germany) according to the manufacturer's instructions. RNA quality and concentration was determined by spectrophotometric analysis (ND-1000 spectrophotometer, NanoDrop and Agilent bioanalyzer) and the RNA integrity number was >6 for all samples. Total RNA was sent to Mark Boekschoten (WU Agrotechnology & Food Sciences, Wageningen, Netherlands).

Microarray analysis. The analysis was performed by Mark Boekschoten (WU Agrotechnology & Food Sciences, Wageningen, Netherlands). Genome-wide mRNA expression profiles were analyzed using the Gene set enrichment analysis (GSEA) approach, as described in (Subramanian, Tamayo et al. 2005). Gene sets were considered as significantly down- or upregulated when False Discovery Rate value (FDR q-val) was below 0.25.

3.2.3.3. 16S rRNA gene amplification and sequencing

Polymerase chain reaction (PCR) on bacterial genomic DNA targeting the 16S rRNA gene was carried out in order to clone and sequence the amplicon. PCR was performed as previously described (Weisburg, Barns et al. 1991). Briefly, one PCR reaction contained 0.125 µM each forward primers (fD1 and fD2, **Table 4**), 0.25 µM reverse primer (rP1, **Table 4**), 2 X DreamTaq PCR Master Mix and 200-300 ng bacterial genomic DNA. PCR was performed using a peqSTAR 2X Gradient Thermocycler (Peqlab Biotechnology). PCR conditions were: 95 °C for 5 min, followed by 35 cycles of 95 °C for 30 s, 50 °C for 30 s and 72 °C for 1 min. After 72 °C for 10 min, as final elongation step, PCR tubes were held at 8 °C for short term storage. A portion of all PCR products was subjected to agarose gel electrophoresis on a 1 % agarose gel. When a single PCR product band was detected at 1.5 kb, PCR products were purified directly from the PCR mix using NucleoSpin Gel and PCR Clean-up kit. When multiple amplicons were present, the 1.5 kb band was extracted from the gel using the same kit. Concentration of PCR products was determined using Nanodrop (Peqlab Biotechnology). Next, PCR products were directly cloned in plasmid vectors, as described below.

3.2.3.4. AGR2 gene amplification

In order to genotype AGR2 mice, PCR was performed using gDNA extracted from mouse biopsies. PCR protocol was adapted from (Park, Zhen et al. 2009). Briefly, one PCR reaction contained 0.25 μ M each primers (AGR2-KO-fwd, AGR2-wt-fwd and AGR2-rev) (**Table 4**), 2 X DreamTaq PCR Master Mix and 2 μ l template genomic DNA taken from supernatant. PCR was performed using a peqSTAR 2X Gradient Thermocycler (Peqlab Biotechnology). PCR conditions were: 94 °C for 5 min, followed by 30 cycles of 95 °C for 45 s, 59 °C for 45 s and 72 °C for 2 min. After 72 °C for 7 min, as final elongation step, PCR tubes were held at 8 °C for short term storage. PCR products were subjected to agarose gel electrophoresis on a 2 % agarose gel. A single PCR product band was detected at 267 bp for AGR2^{wt} genotype and at 374 bp for AGR2^{ko} genotype.

3.2.3.5. Generation of plasmids containing full length 16S rRNA gene

PSAB-labelled plasmids. Plasmids labelled with pSAB (**Table 10**) were generated using the CloneJETTM PCR Cloning kit (Thermo Fisher Scientific biosciences) and following manufacturer's instructions. Briefly, 75 ng purified PCR products amplified using primers fD1, fD2 and rP1 were blunted for 5 min at 70 °C. Next, blunted products were inserted into 50 ng pJET1.2 cloning vector and incubated at RT for 30 min. Ligation mixture was transformed into electro-competent *E. coli* DH5 α , as detailed in **section 3.2.3.9**. Inserts were sequenced by GATC Biotechnology (Sanger sequencing approach) using universal primers pJet1-FP and pJet1-RP (**Table 4**).

PM-labelled plasmids. To generate plasmids pM1456-1, pM1457-1, pM1459-1 and pM1460-1 (**Table 10**), the 16S rRNA gene was amplified using the primers fD1-*EcoRV-XbaI*, fD2-*EcoRV-XbaI* and rP1-*EcoRV-BamHI* (**Table 4**). Next, purified PCR products were inserted in the linear pCR[®]2.1-TOPO[®] vector in a 5 min cloning step, using the TOPO[®] Cloning kit and following manufacturer's instructions (Invitrogen). Inserts were sequenced from both sides (Microsynth, Balgach, Switzerland) using the primers M13_F (GTAAAACGACGGCCAG, Invitrogen) and M13_R (CAGGAAACAGCTATGAC, Invitrogen). This work was performed by Yvonne Loetscher (ETH, Zurich). To generate plasmids pM1411-1, pM1412-4, pM1413-1, pM1414-1 and pM1417-1 (**Table 10**), 16S rRNA gene was amplified using fD1-*EcoRV-XbaI*, fD2-*EcoRV-XbaI* and rP1-*EcoRV-BamHI* primers. Next, purified PCR products were inserted in linearized pSB-Bluescript SK II vector (Stratagene). To generate pM1411-1, pM1412-4 and pM1413-1, pSB-Bluescript SK II vector was linearized using *EcoRV*; for pM1414-1 using *NotI/HindIII* and for pM1417-1 using *NotI/BamHI*. To generate pM1414-1, 16S rRNA gene sequence was

previously cloned in pCR[®]2.1-TOPO[®] vector and from there cloned in pSB-Bluescript SK II vector. These plasmids were generated by Prof. Bärbel Stecher.

Next, plasmid vectors were transformed in electro-competent *E. coli* DH5 α , as detailed in **section 3.2.3.9**. Plasmids are listed in **Table 10**.

3.2.3.6. 16S rRNA gene-based taxonomic assignment of the bacterial strains

Identification of bacterial strains was achieved by sequencing the 16S rRNA gene previously cloned in plasmid vectors from both sides by GATC Biotechnology (Sanger sequencing approach) using appropriate primer pairs. Resulting sequences were trimmed and assembled using the software CLC DNA Workbench (version 6.0.2) and 16S rRNA gene sequences were blasted against the Ribosomal Database Project (RDP) (Wang, Garrity et al. 2007), NCBI blast (Altschul, Gish et al. 1990), Greengenes (DeSantis, Dubosarskiy et al. 2003) and Silva (Quast, Pruesse et al. 2013) databases in order to taxonomically assign the bacterial strains newly isolated. After comparison of all databases, SINA ([Silva Incremental Aligner](#)), the Silva Web Aligner, was preferred for taxonomic assignments.

3.2.3.7. Plasmid extraction

Plasmids previously transformed in electro-competent bacterial strains *E. coli* DH5 α or *S. Tm*^{wt} as described in **section 3.2.3.9**. were extracted using NucleoSpin Plasmid kit according to the manufacturer's instructions. Briefly, transformed *E. coli* or *S. Tm* strains were streaked out from cryostocks on LB or MacConkey agar, respectively, supplemented with appropriate antibiotics and incubated o.n. at 37 °C. Next, single colony was picked to inoculate 3-5 ml LB culture supplemented with appropriate antibiotics and incubate o.n. at 37 °C under agitation. Overnight cultures were spun down at 4 °C for 15 min at 5,000 rpm and plasmids were extracted from bacterial pellets according to the manufacturer's instructions. Extracted plasmids were transformed in appropriate *S. Tm* strains, used to sequence 16S rRNA gene or linearized to generate standard curves for qPCR.

3.2.3.8. Preparation of electro-competent bacteria

A single bacterial colony was inoculated in 3-10 ml LB medium and grown o.n. at 37 °C on a wheel rotor. Further, o.n. culture was used to inoculate (1:20) 10-100 ml LB medium, incubated at 37 °C and 180 rpm.

At an OD₆₀₀ of 0.5-0.8, the culture was chilled on ice for 30 min and subsequently spun down at 4 °C, 15 min and 4,500 rpm. The supernatant was removed and pelleted cells were washed three times in 1 vol. sterile ice-cold dH₂O, one time in 0.5 vol. sterile dH₂O and one time in 0.1 vol. sterile ice-cold 10 % glycerol, respectively. After each step bacteria were spun down at 4 °C, 15 min and 4,500 rpm. Finally, bacteria were suspended in 0.02 vol. ice-cold 10 % glycerol, distributed into 80 µl aliquots, which were shock-frozen in liquid nitrogen and stored at -80 °C.

3.2.3.9. Electro-transformation of plasmid DNA

A frozen stock of electro-competent cells was thawed on ice and 1-10 µl of the plasmid DNA was added. Bacteria were incubated for 10 min on ice, subsequently transferred into an ice-cold 1 mm electroporation cuvette and pulsed at 1,800 V/cm, 5 ms using Gene Pulser Xcell (Bio-Rad). Following this, 900 µl LB medium was added and bacteria were incubated for 1 h in a thermomixer at 37 °C and 850 rpm. Afterwards, bacteria were spun down at room temperature (RT) for 2 min, 10,000 rpm and 900 µl from the supernatant were removed. Pelleted cells were suspended in the remaining liquid and plated on LB agar plates supplemented with the appropriate antibiotic(s).

3.2.3.10. P22-transduction

Preparation of P22-lysates. A single colony of the *S. Tm* donor strain was inoculated in 3 ml LB medium supplemented with 5 mM CaCl₂ and grown o.n. at 37 °C on a wheel rotor. Further, 500 µl of the o.n. culture were added to 10 µl P22-lysate (kindly provided by Prof. Dr. M. Hensel) and incubated for 15 min at 37 °C. Next, the mixture was used to inoculate 5 ml LB culture, which was incubated o.n. at 37 °C on a wheel rotor. On the next day 50 µl chloroform were added to the o.n. culture followed by an incubation for 30 min at 37 °C. Next, the culture was spun down at 4 °C, for 10 min at 4,500 rpm and the supernatant was filtered through (0.45 µm) and 20 µl chloroform were added to the 1.5 ml filtrate. Filtered lysate was stored at 4 °C for further use. Sterility of the lysate was verified by plating 50 µl on LB agar followed by an o.n. incubation at 37 °C.

P22-transduction. A single colony of the *S. Tm* recipient strain was inoculated in 3 ml LB medium supplemented with 5 mM CaCl₂ and grown o.n. at 37 °C on a wheel rotor. Next, 100 µl of the o.n. culture were added to 10 µl P22-lysate and incubated for 15 min at 37 °C. Subsequently, the bacteria-phage mixture was added to 900 µl LB medium supplemented with 10 mM EGTA and incubated in a thermomixer at 37 °C and 850 rpm. After 1 h incubation, the bacterial culture was spun down at RT for 2

min at 10,000 rpm and 900 μ l of the supernatant were removed. Pelleted bacteria were resuspended in the remaining liquid and plated on 10 mM EGTA LB agar plates supplemented with the appropriate antibiotic(s).

3.2.3.11. Genome sequencing

Complete genome sequence of strain KB18 was obtained by PacBio sequencing (DSMZ, Braunschweig, Germany). For the remaining eleven Oligo-MM strains, whole-genome shotgun sequencing was performed using the Illumina technology (Eurofins Genomics GmbH, Ebersberg, Germany). Libraries of 500 bp insert size were prepared from the isolated genomic DNA and sequenced as 300 bp paired-end runs on an Illumina MiSeq v3 instrument. Raw Illumina reads were *de novo* assembled using the careful mode of SPAdes version 3.5.0 (Bankevich, Nurk et al. 2012) with a minimum read coverage cutoff of 20 and minimum contig length of 500 bp. The quality of the Illumina draft genome assemblies was assessed with QUAST (Gurevich, Saveliev et al. 2013). Automatic annotation of the twelve Oligo-MM genomes was performed with RAST (Aziz, Bartels et al. 2008) to obtain a general overview of the genetic and functional content. Filtered raw reads from Illumina MiSeq sequencing of the eleven Oligo-MM genomes have been deposited in the Sequence Read Archive (SRA) under SRA Study Accession Number SRP060697 and following SRA Experiment Accession Numbers: I46-SRX1092348, I48-SRX1092357, I49-SRX1092347, KB1-SRX1092355, KB18-SRX1092360, YL2-SRX1092353, YL27-SRX1092362, YL31-SRX1092358, YL32-SRX1092359, YL44-SRX1092354, YL45-SRX1092361 and YL58-SRX1092352.

3.2.3.12. Metagenomics analysis

Metagenomics analysis was performed by Carina Pfann and Ass.-Prof. David Berry (DOME, University of Vienna, Austria). The functional and metabolic capacity of the Oligo-MM community was predicted from annotated shotgun genomes and compared to those of the ASF community and of a conventional mouse gut microbiota by mapping against the KEGG (Kyoto Encyclopedia of Genes and Genomes) database. Input files for assembled Oligo-MM (see above) and ASF genomes (Wannemuehler, Overstreet et al. 2014) were either single genomes or artificial metagenomes, created by merging contigs of each community into a multi-fasta file. Metagenomic reads, derived from eight different samples to cover the heterogeneity of a conventional mouse gut microbiota (Sequence Read Archive accession numbers SRX313003 (JCVI 2013), DRX013306 (Milk 2014) and ERX166941 (Nanjing University 2013), and

MG-RAST accession numbers M4W0E1C1225, M4W0E2C1220, M4W1E1C1240, M4W1E2C1241 and M4W12E2C1226 (Wang, Linnenbrink et al. 2014)), were merged and assembled with Ray-Meta version 2.3.1 with default parameters (Boisvert, Raymond et al. 2012). KEGG mapping was performed using a custom pipeline. Gene prediction was done with Prodigal version 2.60 (Hyatt, Chen et al. 2010, Hyatt, LoCasio et al. 2012) and the predicted protein files of the three groups (Oligo-MM, ASF and conventional) were aligned separately against a reduced KEGG database (<http://huttenhower.sph.harvard.edu/kegg/>) using RAPSearch version 2.23 (Ye, Choi et al. 2011, Zhao, Tang et al. 2012). Custom Python scripts were used for assignment against the KEGG database and to obtain information about the presence and completeness of each KEGG module, expressed as value between 0 (module complete, dark green) and 4 (module absent, white).

3.2.3.13. 16S rRNA gene amplicon sequencing

Generation and barcoding of 16S rRNA gene sequences. The variable regions V3-V6 of the 16S rRNA gene were amplified by PCR using gDNA extracted from intestinal contents or the Oligo-MM¹⁰ inoculum as detailed in **section 3.2.3.1**. PCR comprised two consecutive steps. In the first step, primers targeting the 16S rRNA gene (*italic*) and specific primers carrying the 5'M13/rM13 adapters (**bold**) 338F-M13 (**GTAAACGACGGCCAGTGCTCCTACGGWGGCAGCAGT**) and 1044R-rM13 (**GGAAACAGCTATGACCATGACTACGCGCTGACGACARCCATG**) are used to amplify the V3-V6 region of the bacterial 16S rRNA gene. One PCR reaction contained 500 nM of each primer (338F-M13 and 1044R-rM13, see **Table 4**), 2 X DreamTaq PCR Master Mix and 50 ng template gDNA. PCR reaction was performed in duplicates using a peqSTAR 2X Gradient Thermocycler (Peqlab Biotechnology). PCR conditions were: 95 °C for 10 min, followed by 20 cycles of 95 °C for 30 s, 55 °C for 30 s and 72 °C for 45 s and a final elongation step at 72 °C for 10 min. Duplicate reactions were pooled and loaded on a 1 % agarose gel in order to confirm successful PCR amplification. After purification of PCR products using the NucleoSpin Gel and PCR Clean-up kit and manufacturer's instructions, concentration and quality of the purified PCR products were assessed using Nanodrop (Peqlab Biotechnology). In order to barcode each PCR product with a specific MID sequence and to add the 454-specific Lib-L tag, a second PCR was performed using M13/rM13-specific primers containing the 454-specific Lib-L primers (underline) A-M13 (CCATCTCATCCCTGCGTGTCTCCGACTCAG/MID sequence/**GTAAACGACGGCCAGTG**) and B-rM13 (CCTATCCCCTGTGTGCCTTGGCAGTCTCAG**GGAAACAGCTATGACCATGA**). The 40 different MID 10 bp error-correcting barcodes for multiplexing are listed in **Table 5**. PCR was performed using 400 nM of each primer (A-M13 and B-rM13). These primers extended the first PCR products and this extension was visualized on a 2 % agarose gel.

Purification of barcoded 16S rRNA gene sequences. In order to purify barcoded 16S rRNA gene sequences, amplicons of the second PCR were pooled and purified by ethanol precipitation. Briefly, the total volume was adjusted to 400 μ l using ddH₂O. Then, 0.1 vol. 3M sodium acetate and 2.5 vol. ethanol p.a. were added, mixed and centrifuged for 30 min, at 13,000 rpm, 4 °C. DNA pellets were suspended in 1.25 vol. 70 % ethanol and centrifuged for 15 min, at 13,000 rpm, 4 °C. Finally, DNA was air-dried and suspended in 50 μ l ddH₂O. In a second time, purified PCR products were run on a 0.8 % agarose gel, bands corresponding to the barcoded 16S rRNA gene sequences were excised and amplicons were extracted using the NucleoSpin Gel and PCR Clean-up kit. Amplicons were eluted in ddH₂O, further purified using Agencourt AMPure XP kit and finally resuspended in ddH₂O. Concentration and quality of the purified barcoded amplicon sequences were assessed using a Nanodrop (Peqlab Biotechnology). Samples were stored at -20 °C.

Amplicon sequencing platform. Amplicon sequencing was performed at Eurofins, on a 454 GS FLX Titanium platform from one side (Lib-L-A) according to the recommended procedures (454 Roche).

Bioinformatic analysis. Sequence analysis was performed by Dr. Debora Garzetti (AG Stecher, MvP, Munich). The QIIME (Quantitative Insights Into Microbial Ecology) (Caporaso, Kuczynski et al. 2010) software package version 1.8 was used for read denoising and pre-processing, OTU clustering, taxonomic assignment, alpha diversity analysis and Principal Coordinate Analysis (PCoA) (Krzanowski 2000). Briefly, OTU clustering was performed at the 97 % similarity level using an open-reference method, based on a custom sequence collection of the full length 16S rRNA gene sequences of the 12 Oligo-MM and 5 ASF strains (ASF360, ASF361, ASF457, ASF502 and ASF519). Taxonomy was assigned by the RDP classifier against either the Silva database (Quast, Pruesse et al. 2013) or the custom sequence collection. Alpha diversity was determined using the metric of observed species as measure of within-sample diversity. In order to compare all samples at equal sequencing depth for diversity analyses, the minimum number of reads present in all the analyzed samples was chosen as rarefaction level. Statistically differentially abundant operational taxonomic units (OTUs) were identified using LEfSe with $\alpha=0.01$ and LDA score=2.0 (Segata, Izard et al. 2011). Microbiota composition shown in **section 5**. was analyzed the same way than detailed above except of the denoising step that was not performed.

3.2.3.14. Quantitative PCR of bacterial 16S rRNA genes

Quantitative polymerase chain reaction (qPCR) was established by Markus Beutler (AG Stecher, MvP, Munich).

Generation of template plasmid DNA for standard curves. Plasmids containing full length 16S rRNA gene sequences from the 12 Oligo-MM strains, 7 ASF strains (ASF356, ASF360, ASF361, ASF457, ASF500, ASF502 and ASF519) and *Salmonella* Typhimurium M557 (**Table 11**) were transformed in *E. coli* DH5 α . From 100 ml o.n. cultures, plasmids were purified using the Plasmid Plus Midi Kit following manufacturer's instructions. Next, plasmid DNA was linearized using appropriate restriction enzymes, which have no restriction site within the 16S rRNA gene sequence. After digestion, linearized plasmids were cleaned up using NucleoSpin Gel and PCR Clean-up kit and following manufacturer's instructions.

Design of 16S rRNA specific primers and hydrolysis probes. In order to design 16S rRNA specific primers and hydrolysis probes, Primer Express 3 (Applied Biosystems, Life Technologies) software was applied to an alignment of full length 16S rRNA gene sequences. To enable duplex qPCR assays, hydrolysis probes were 5'-labelled with either 6-carboxyfluorescein (FAM) or 6-carboxyhexafluorescein (HEX). Additionally, each probe was conjugated with the black hole quencher 1 (BHQ1) at the 3' end. Primers and probes were synthesized by Metabion (**Table 6**).

Standard curves and qPCR conditions. Standard curves were determined using linearized plasmid as DNA template. Stocks of 10 ng/ μ l each linearized plasmid were prepared and 16S rRNA gene copy numbers were calculated in order to prepare 10-fold dilutions (from 10^8 to 10^2 gene copies per μ l). Plasmid DNA was diluted in 100 ng/ μ l yeast t-RNA solution (Roche). Standard curves were run in triplicates only once to evaluate single qPCR assays. In further experiments, software LightCycler96 version 1.1 reproduced standard curves based on single DNA template with known DNA quantity as well as the efficiency derived from the standard curve of each qPCR assay which was initially run. Efficiency of each qPCR was calculated based on the slope of standard curves (qPCR efficiency: $(10^{(-1/\text{slope of standard curve})} - 1) \times 100$) using 1:10 dilution of linearized plasmid, as DNA template. Efficiencies of qPCR reactions were within the range of 90-110 %. QPCR reactions were performed in 96 well plates using the thermo cycler LightCycler96 (Roche). One PCR reaction (total volume: 20 μ l) contained 300 nM of each primer, 250 nM of the corresponding hydrolysis probe (see **Table 6**), FastStart Essential DNA Probes Master and 5 ng template gDNA. PCR reactions with DNA templates extracted from feces or cecal content were run in duplicates. PCR conditions were: 95 °C for 10 min, followed by 45 cycles of 95 °C for 15 s and 60 °C for 1 min. Fluorescence for each cycle was recorded after the step at 60 °C. Quantification cycle (Cq) as well as the baseline were automatically determined by the software LightCycler96 version 1.1 (Roche).

3.2.3.15. Fluorescence *in situ* hybridization (FISH)

Design of specific probes. In order to design strain-specific oligonucleotides, full length 16S rRNA gene sequences were aligned using CLC DNA Workbench 6.0.2 software (**Table 4**). To increase the fluorescent signal intensity, the oligonucleotides were double-labelled with either fluorescein isothiocyanate (FITC), cyanine 3 (Cy3) or Cy5 at the 3' and 5' ends (**Table 34**). All FISH probes were synthesized by Metabion (Munich).

Optimization of probe specificity. To optimize the hybridization conditions of each probe, formamide (FA) concentration series were performed using a standard FISH protocol as previously described (Daims, Stoecker et al. 2005). The concentration of FA was increased in the hybridization buffer, while the concentration of NaCl was decreased in the washing buffer, concomitantly (**Tables 26 and 27**). Further on, all individual probes were tested with the optimal concentrations of FA on target and non-target strains in order to confirm their specificity (**Table 34**).

Table 34. Fluorophores and optimal formamide (FA) concentrations established for the FISH probes targeting the Oligo-MM strains.

| Designation | Fluorophores | Fluorescence signal* | Work <i>in vivo</i> | Optimal formamide concentration |
|------------------|-----------------|----------------------|---------------------|---------------------------------|
| YL2_180 | 2xCy3 | Yes | No | 20 % |
| YL27_180 | 2xCy3 or 2xFITC | Yes | Yes | 30 % |
| YL31_180 | 2xCy3 | Yes | Yes | 35 % |
| YL32_180 | 2xCy3 or 2xFITC | Yes | Yes ^s | n.d. |
| Muc1437 | 2xCy3 or 2xFITC | Yes | Yes | 30 % |
| BET940 | 2xCy3 | Yes | Yes | 30 % |
| YL58_180 | 2xFITC | Yes | Yes | 30 % |
| YL58_180_negctrl | 2xFITC | No | Yes | n.d. |
| I46_180 | 2xCy3 | Yes | Yes ^s | n.d. |
| I48_180 | 2xCy3 or 2xFITC | Yes | No | n.d. |
| I49_180 | 2xCy3 or 2xFITC | Yes | No | n.d. |
| KB1_180 | 2xCy3 | Yes | Yes ^s | n.d. |
| KB18_180 | 2xCy3 | No | No | n.d. |

* The intensity of the fluorescence signal was evaluated at 35 % FA concentration on the corresponding pure bacterial culture, which was PFA-fixed. n.d.: not determined. § Work but need to be optimized.

Fixation of bacterial samples. One volume (vol.) of actively growing culture was directly fixed in 3 vol. of ice-cold 4 % paraformaldehyde (PFA) and incubated for 3 to 12 h at 4 °C. Later on, the suspension was washed 3 times in ice-cold 1X PBS in order to remove residual PFA. Finally, the pellet was suspended in 1 vol. ice-cold 1X PBS and 1 vol. ice-cold 96 % ethanol p.a. Then, PFA-fixed samples were kept at -20 °C. For FISH analysis, 3 to 5 µl were spotted on a 10-well epoxy-coated slide, dried for 5 min at 46 °C and directly used for FISH.

Fixation of mouse samples. Cecum were fixed in 4 % paraformaldehyde (PFA) for 12 h at 4 °C, washed in 20 % sucrose o.n. at 4 °C, cryo-embedded in O.C.T., flash frozen in liquid nitrogen and then stored at -80 °C. Cecal cryosections (5-7 µm thick) were mounted on superfrost plus glass slides using a cryotome CM1950 (Leica, Wetzlar) and air-dried at RT, at least o.n.

FISH. Fluorescence *in situ* hybridization (FISH) was performed using double-labelled 16S rRNA-targeted oligonucleotide probes according to a standard protocol (Daims, Stoecker et al. 2005). Briefly, fixed-bacterial or -mouse samples were dehydrated using increasing concentrations of ethanol 50 %, 80 % and 96 % for 3 min each and were air-dried. Hybridization buffers (HB) were prepared as described in **Table 26** and vigorously mixed by vortexing. The FISH probes were added to HB at 5 ng/µl final concentration and pipetted on the air-dried samples. Hybridization was performed for 4 h in a humid chamber saturated with HB at 46 °C in an oven, where the samples were protected from light. Later on, the slides were washed for 10 min at 48 °C in a water-bath using washing buffer (WB) (**Table 27**), rinsed 5 sec into ice-cold ddH₂O and air-dried. DAPI staining was performed using a solution of 1 µg/ml final concentration in ddH₂O for 30 min at 4 °C in the dark. Sections were mounted with Vectashield and sealed with nail polish. Slides were observed under a Leica TCS SP5 confocal microscope (Leica, Wetzlar) within 24 h. TIFF images (1024 x 1024) were obtained using the software LAS AF (Leica, Wetzlar) and analyzed using the software DAIME (Digital Image Analysis in Microbial Ecology, version 2.0) (Daims, Lucker et al. 2006). In order to remove fluorescent background, FITC and Cy3 channels were subtracted to Cy3 and FITC channels, respectively (twice for YL44 analysis and thrice for YL58 analysis). Biovolume quantification was performed on object layers extracted from TIFF images using automatic 2D segmentation RATS (Robust Automated Threshold Selection) algorithm (Kittler, Illingworth et al. 1985) and ignoring objects up to 5 pixels.

3.2.3.16. Immunofluorescence microscopy

Fixation and preparation of cecal cryosections. Cecum were fixed in 4 % paraformaldehyde (PFA) for 12 h at 4 °C, washed in 20 % sucrose o.n. at 4 °C, cryo-embedded in O.C.T., flash frozen in liquid nitrogen and then stored at -80 °C. Cecal cryosections (5-7 µm thick) were mounted on superfrost plus glass slides using a cryotome CM1950 (Leica, Wetzlar) and air-dried at RT, at least o.n.

Fixation and preparation of paraffin-embedded cecal sections. In order to preserve the mucus layer on epithelial surfaces, cecum were fixed in water-free Carnoy's solution (60 % absolute ethanol, 30 % chloroform, 10 % glacial acetic acid) and stored one to two weeks at 4 °C. Fixed-cecum were dehydrated twice in absolute ethanol for 30 min each and then, twice in absolute xylol for 1 h each. Further on, cecum were incubated in a 1:1 xylol/paraffin solution for 1 h at 60 °C. In order to remove xylol, xylol/paraffin solution was replaced by paraffin and incubated at 60 °C for 45 min. This step was repeated until xylol was evaporated. Then, cecal tissues were embedded in paraffin into histo-cassettes and cooled down at RT. Using a microtome type Reichert-Jung Hn-40, paraffin sections (5 µm thick) were stretched at 45 °C in 80 % ethanol bath in order to preserve the mucus layer, dried o.n. under the hood and incubated 2-3 h at 37 °C. Before dewaxing, sections were fixed on the slide for 10 min at 60 °C. This protocol was adapted from (Johansson and Hansson 2012).

Immunofluorescent staining of cecal cryosections. Prior immunofluorescent staining, cecal cryosections were fixed in 4 % PFA for 5 min at 4 °C. Paraffin-embedded cecal sections were dewaxed using xylol for 10 min at 60 °C then xylol for 10 min at RT and rehydrated using decreasing concentrations of ethanol 100 %, 95 % and 80 % for 5 min each at RT. This step was adapted from (Johansson and Hansson 2012). Immunofluorescent staining was performed as described in (Stecher, Robbiani et al. 2007). Cecal sections were washed in 1X PBS and blocked with 10 % (w/v) normal goat serum in PBS for 1 h. *S. Tm* was stained using a polyclonal rabbit anti-Salmonella O antigen group B serum (α -*Salmonella* B, 1:400, 10 % normal goat serum) and a dylight 549-conjugated goat anti-rabbit antibody (α -rabbit-dylight 549, 1:400, 10 % normal goat serum). The specificity of α -*Salmonella* B antiserum was checked extensively by analyzing cecum cryosections from uninfected mice, as negative controls. MUC2 was stained using a α -MUC2 H-300 (1:200, 10 % normal goat serum) and a dylight 549-conjugated goat anti-rabbit antibody (α -rabbit-dylight 549, 1:400, 10 % normal goat serum). DNA was stained with sytox green (0.1 µg/ml final concentration) and/or DAPI (1 µg/ml final concentration). F-actin was stained with phalloidin FluoProbes[®] 647 (1:300, 10 % normal goat serum). Sections were mounted with Vectashield and sealed with nail polish. Slides were observed under a Leica TCS SP5 confocal microscope (Leica, Wetzlar) within 24 h. TIFF images were obtained using the software LAS AF (Leica, Wetzlar).

Intracellular immunofluorescent staining in epithelial tissue cryosections. This staining and the corresponding analysis shown in **Figure 27** were performed by Dr. Mikael Sellin (ETH, Zurich), as described in (Sellin, Muller et al. 2014). Briefly, cecal tissue was fixed in 4 % PFA/4 % sucrose, saturated in PBS/20 % sucrose, embedded in O.C.T., flash frozen in liquid nitrogen and stored at -80 °C. Cryosections (20 µm thick) were air-dried, rehydrated with PBS, permeabilized using 0.5 % Triton X-100 and blocked with 10 % normal goat serum. For quantification of *S. Tm* in whole tissue, epithelium and lamina propria, cryosections were stained for ICAM-1/CD54 (clone 3E2, Becton Dickinson), AlexaFluor-647 conjugated phalloidin (Molecular Probes) and DAPI (Sigma-Aldrich). Samples were mounted with Mowiol (Calbiochem). A Zeiss Axiovert 200 m microscope with 10x-100x objectives, a spinning disc confocal laser unit (Visitron) and two Evolve 512 EMCCD cameras (Photometrics) were used for imaging. For quantification of *S. Tm*, imaging was performed at 400x and 1,000x. Postcapture processing and analysis used the Visiview (Visitron) and Image J x64. Intracellular *S. Tm* was manually enumerated blindly in six to nine nonconsecutive sections per mouse. All data represent averages/section.

3.2.3.17. Lipocalin-2 quantification

Lipocalin-2 (Lcn2) levels were determined by enzyme-linked immunosorbent assay (ELISA) in cecal content. This assay was performed by Diana Ring (AG Stecher, MvP, Munich) using kit and protocol from R&D Systems (Minneapolis, US). Briefly, 96-well plates were coated with Lcn2 capture antibody (1:200, 1X PBS) and incubated o.n. at 4 °C. On the next day, plates were washed 3 times using washing buffer (washing step) and incubated with blocking buffer for 1 h, at RT. After another washing step, plates were loaded with standard and mouse samples (Standard: starting concentration at 60 ng/ml, then 1:3 dilutions until 0.027 ng/ml in blocking buffer. Mouse samples: undiluted, 1:20 and 1:200 in 1X PBS) then incubated 1 h, at RT. After two washing steps, plates were loaded with Lcn2 detection antibody (1:200, blocking buffer) and incubated 1 h, at RT. After two washing steps, plates were loaded with HRP-streptavidin (1:1000, 1X PBS) and incubated 1 h, at RT. Plates were finally washed six times in washing buffer and developed with liquid substrate using 0.1 mg/ml ABTS diluted in substrate buffer and supplemented with 0.05 % H₂O₂ just before use. After 30 to 45 min at RT, absorbance was measured at λ₄₀₅ using a plate reader. Lipocalin-2 was detected in the concentration range of 0.25-60 ng/ml. Detection limit (DTL) was calculated for each experiment using the lowest concentration of Lcn2 detected in the assay (Lcn2, ng/ml) respective to the highest amount of cecal content (A_C, g) such as:

$$DTL = \frac{\text{lowest Lcn2}}{20} \times \frac{100}{\text{highest Ac}}$$

DTL was comprised between 0.18 and 0.57 ng/mg cecal content, as shown in figures (red dotted line).

3.2.4. Mouse experiments

3.2.4.1. Mice used in this study

Germfree C57Bl/6 mice were purchased from the Clean Mouse Facility (CMF, University of Bern, Switzerland) and housed under germfree conditions. They were directly inoculated with a mixture of either five ASF strains (ASF360, ASF361, ASF457, ASF502, ASF519) or four ASF strains (ASF356, ASF361, ASF502, ASF519). These mice were termed ASF⁵ and ASF⁴, respectively. C57Bl/6 mice colonized with the defined Oligo-MM¹² consortium and termed as Oligo-MM¹², were generated and provided by Prof. McCoy and Prof. Macpherson (University of Bern, Switzerland). Specific pathogen-free (SPF) C57Bl/6J mice harboring a conventional microbiota were purchased from Janvier (Le Genest-Saint-Isle). AGR2^{tm1.2Erle} mice, termed in this study as AGR2, were obtained from David Erle (Park, Zhen et al. 2009), bred and kept under SPF conditions at the MvP mouse facility in individually ventilated cages (IVCs). AGR2 germfree mice, termed in this study as AGR2^{GF}, were rederived from AGR2 heterozygous (AGR2^{het}) and homozygous (AGR2^{ko}) conventional mice by Prof. Bleich and Dr. Basic (Hannover medical school, Hannover). Gnotobiotic mice ASF⁵, ASF⁴, Oligo-MM¹² and AGR2^{GF} were bred under germfree conditions in flexible film isolators (Harlan Laboratories).

3.2.4.2. Animal inoculation experiments

All gnotobiotic experiments were performed in gnotocages (Han, Bioscape, Emmendingen), at the Max-von-Pettenkofer Institute (LMU, Munich). Gnotobiotic mice, 6 to 8 week old, were orally and rectally inoculated with about 100 µl bacterial mixture of frozen stocks (SPF cecum content, Oligo-MM¹⁰ consortium, ASF⁶ consortium, other single strains) or actively growing culture (*e.g.* ASF500).

3.2.4.3. Animal infection experiments

Germfree and gnotobiotic animal infection. Animals were infected by oral gavage with *S. Tm*^{avir} or *S. Tm*^{wt} in 50 µl 1X PBS at 12 to 24 week old depending on previous treatments. Strain identity and corresponding infective doses are indicated elsewhere, in result and legend parts.

SPF animal infection. SPF C57Bl/6 and AGR2 mice were housed in IVCs, pretreated by oral gavage either with streptomycin (25 mg/mouse) or ampicillin (25 mg/mouse) one day prior infection and infected by oral gavage with *S. Tm*. Strain identity and corresponding infective doses are indicated elsewhere, in result and legend parts.

All mice were sacrificed in S2 conditions by cervical dislocation. Live bacterial loads in feces, cecal content, liver, spleen and mLN were determined by plating on MacConkey agar with respective antibiotics (streptomycin 50 µg/ml and ampicillin 100 µg/ml).

3.2.4.4. Ethics statement

All animal experiments were reviewed and approved by the local ethics committee (55.2-1-54-2532-49-11, 55.2-1-54-2532-13-15 and 55.2-1-54-2532-145-14) and performed according to the legal requirements.

3.2.4.5. Histopathological analysis

Histology of the cecum was done at necropsy. Cecal tissue was embedded in Tissue-Tek Optimal Cutting Temperature (O.C.T.) compound, flash frozen in liquid nitrogen and stored at -80 °C. Cryosections (5 µm thick) of the cecal tissue were stained using hematoxylin and eosin (H&E), and then scored as described in (Stecher, Robbiani et al. 2007). Briefly, evaluation scored submucosal edema (score 0-3), polymorphonuclear neutrophils infiltration into the lamina propria (score 0-4), loss of goblet cells (score 0-3) and epithelial damage (score 0-3). The total histopathological score for each tissue section was determined as the sum of all of these individual scores. Combined score 0-3: no to minimal signs of inflammation that are not sign of a disease. Combined score 4-7: moderate inflammation. Combined score above 8: severe inflammation.

3.2.4.6. Statistical analysis

Determination of significance of differences among mouse groups was assessed using the exact Mann-Whitney U test (MW) for comparison of two groups and the one-way ANOVA nonparametric Kruskal-Wallis test for comparison of more than two groups. Statistical tests were performed using the software GraphPad Prism version 5.01 for Windows (GraphPad Software, La Jolla California USA,

www.graphpad.com). P values of less than 0.05 (two-tailed for MW) were considered as statistically significant. * P<0.05, ** P<0.01, *** P<0.001.

4. Results – Establishment of a novel gnotobiotic mouse model to study host-microbiota-pathogen interactions

Gnotobiotic mice harboring a defined gut microbiota are widely used to study the complex mechanisms involving host-microbiota-pathogen interactions. Moreover, it is well established that the gut microbiota coevolves with its host (Seedorf, Griffin et al. 2014). Most of the gnotobiotic mouse models currently used is based on bacterial strains isolated from humans (Faith, Ahern et al. 2014, Slezak, Krupova et al. 2014). Up-to-date, the bacterial community of the Altered Schaedler Flora (ASF) model is the only one involving only mouse-derived bacteria (Dewhirst, Chien et al. 1999). However, ASF strains are not available in public strain collections, yet.

In this first chapter, I will present the establishment of a novel gnotobiotic mouse model based on a collection of mouse-derived strains. In order to generate a mouse-derived consortium, we isolated and characterized twelve intestinal commensal strains from specific pathogen-free (SPF) mice, the Oligo-Mouse Microbiota (Oligo-MM). To colonize germfree mice in a reproducible manner, we established a method to inoculate the Oligo-MM as a single dose. To specifically detect the Oligo-MM strains and analyze microbial community composition, we developed three Oligo-MM specific analysis tools: a 16S rRNA gene-based amplicon sequencing approach, a quantitative fluorescence *in situ* hybridization (FISH) approach and a quantitative PCR assay. Moreover, we show that the Oligo-MM mediates colonization resistance (CR) against the human enteric pathogen *Salmonella enterica* serovar Typhimurium (*S. Tm*). Therefore, the Oligo-MM is a highly useful reductionist model system to study host-microbiota-pathogen interactions.

4.1. The Oligo-Mouse Microbiota, a consortium of mouse-derived commensal strains

4.1.1. Isolation of the Oligo-MM strains

To isolate mouse-derived commensal strains, we used cecal and fecal specimen from conventional mice raised in SPF conditions (**Table 33**). In order to sample cecal contents, mice were sacrificed, imported into an anaerobic chamber and dissected under anoxic conditions. To increase the proportion of spore-forming bacteria, a part of the fecal samples was sampled, heat-treated and directly frozen at -20 °C. Cecal and fecal contents were resuspended in anaerobic media and either plated on rich media or directly

used to inoculate liquid cultures. Furthermore, plates and cultures were incubated under anaerobic conditions. Once obtained in pure culture, the strains were grown using different anaerobic media, as detailed in **Materials & Methods (3.2.1.2)**. We also established a method to cryopreserve anaerobic strains in glass vials at -80 °C using reducing agents, such as palladium black.

4.1.2. Morphology and taxonomic assignment of the Oligo-MM strains

In order to confirm the purity of each culture, we performed Gram staining and assessed bacterial morphology by light microscopy. We observed rather heterogeneous morphologies between individual pure cultures (**Figure 6**).

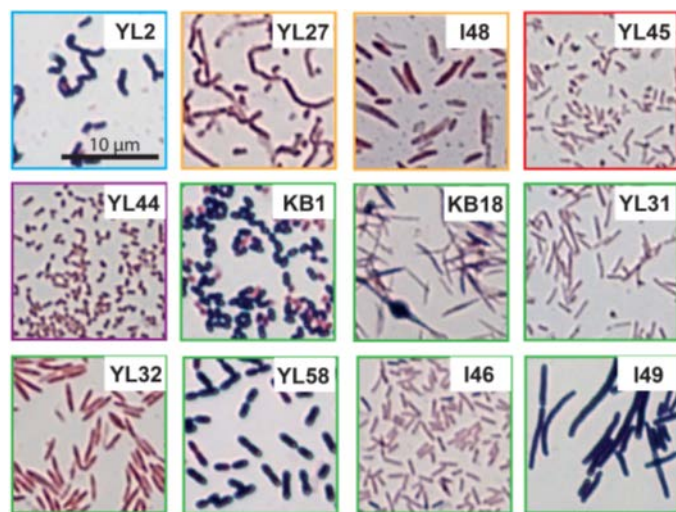


Figure 6. Morphology of the Oligo-MM strains.

Pure cultures (late logarithmic or stationary growth phase) were Gram-stained and bacteria were imaged using a light microscope (100-fold magnification). Color code refers to the phylum: bright blue: Actinobacteria; light orange: Bacteroidetes; red: Proteobacteria; purple: Verrucomicrobia and green: Firmicutes. Scale bar: 10 μm. For taxonomic assignment, refer to **Table 35**.

To taxonomically assign each strain, we used 16S rRNA gene sequencing. The full length 16S rRNA genes were amplified, cloned into a plasmid vector and sequenced. The 16S rRNA genes were aligned against different 16S rRNA databases (RDP, SILVA, NCBI blast, Greengenes) for taxonomic assignment (**Table 35**).

Finally, we isolated more than sixty strains from the mice. Out of this initial collection, we selected strains to meet the following criteria. The strains are cultivable in a reproducible fashion, cryopreservable and represent a diverse range of bacterial phyla abundant in the murine gut. In this way, twelve strains (the Oligo-MM¹², **Table 35**) were selected: six strains were assigned to the phylum *Firmicutes* (YL31, YL32, YL58, I46, I49 and KB1), one strain to the *Bacteroidetes* (I48), one strain to the *Actinobacteria* (YL2), one strain to the *Proteobacteria* (YL45) and one strain to the *Verrucomicrobia*

(YL44). Two strains were included at a later time point: one strain assigned to the phylum *Firmicutes* (KB18) and one to the *Bacteroidetes* (YL27). The initial characterization was performed using only the first ten strains (the Oligo-MM¹⁰). Finally, among the Oligo-MM¹² strains, four were taxonomically assigned as species *Incertae Sedis*, suggesting that they represent a novel species or even genus.

Table 35. Taxonomic assignment of the Oligo-MM strains

| Taxonomic classification | Strain ID | Taxonomic Identity (Genus) | SINA alignment score |
|--------------------------------------|-------------|--|----------------------|
| phylum <i>Actinobacteria</i> | | | |
| class Actinobacteria | | | |
| order Bifidobacteriales | | | |
| family Bifidobacteriaceae | YL2 | <i>Bifidobacterium</i> | 0.998 |
| phylum <i>Bacteroidetes</i> | | | |
| class Bacteroidia | | | |
| order Bacteroidales | YL27 | Bacteroidales; <i>Incertae Sedis</i> | 0.989 |
| family Bacteroidaceae | I48 | <i>Bacteroides</i> | 0.999 |
| phylum <i>Proteobacteria</i> | | | |
| class Betaproteobacteria | | | |
| order Burkholderiales | | | |
| family Sutterellaceae | YL45 | <i>Parasutterella</i> | 0.978 |
| phylum <i>Verrucomicrobia</i> | | | |
| class Verrucomicrobiae | | | |
| order Verrucomicrobiales | | | |
| family Verrucomicrobiaceae | YL44 | <i>Akkermansia</i> | 0.998 |
| phylum <i>Firmicutes</i> | | | |
| class Bacilli | | | |
| order Lactobacillales | | | |
| family Enterococcaceae | KB1 | <i>Enterococcus</i> | 0.998 |
| family Lactobacillaceae | I49 | <i>Lactobacillus</i> | 0.999 |
| class Clostridia | | | |
| order Clostridiales | | | |
| family Lachnospiraceae | YL32 | Lachnospiraceae; <i>Incertae Sedis</i> | 0.997 |
| | YL58 | <i>Blautia</i> | 0.997 |
| family Ruminococcaceae | YL31 | <i>Flavonifractor</i> | 0.989 |
| | KB18 | Ruminococcaceae; <i>Incertae Sedis</i> | 0.986 |
| class Erysipelotrichia | | | |
| order Erysipelotrichales | | | |
| family Erysipelotrichaceae | I46 | Erysipelotrichaceae; <i>Incertae Sedis</i> | 0.996 |

Full length 16S rRNA gene sequences were aligned against the SILVA database using SINA alignment.

4.1.3. Representation of the ASF and Oligo-MM strains in a conventional murine gut microbiota

In order to determine if the isolated strains are abundant members of a conventional mouse microbiota, we generated a phylogenetic tree including full-length 16S rRNA gene sequences of a normal microbiota, the Oligo-MM¹² and 8 ASF (ASF356, ASF360, ASF361, ASF457, ASF492, ASF500, ASF502 and ASF519; ASF⁸) strains. We used full-length 16S rRNA gene sequences from the cecum of unmanipulated SPF mice harboring a conventional microbiota (Stecher, Robbiani et al. 2007). In this study, cecal contents from conventional mice were recovered and cecal DNA was extracted. The full length bacterial 16S rRNA genes were amplified by PCR, cloned into plasmid vectors and the inserts were sequenced. To this data set were included the full-length 16S rRNA gene sequences from the ASF⁸ and Oligo-MM¹² strains.

4.1.3.1. Phylum distribution and abundance

The ASF and Oligo-MM¹² consortia harbor members taxonomically assigned to three and five of the most abundant bacterial phyla, respectively, from the seventeen phyla identified in the murine gut so far (Linnenbrink, Wang et al. 2013). In our dataset, we identified 7 different bacterial phyla. Two phyla, the *Cyanobacteria* and the *Tenericutes*, were only found in the samples from conventional mice (**Figure 7**). These two phyla were of low abundance, as only four and two reads were assigned to the *Tenericutes* and the *Cyanobacteria*, respectively (**Table 36**). One phylum was unique to the Oligo-MM¹²: the *Actinobacteria* (YL2). The phylum *Deferribacteres*, representing 4.2 % of the total reads in the conventional mouse gut (**Table 36**) is represented in the ASF (ASF457) but not in the Oligo-MM¹². Compared to other studies, we found that another phylum, the *TM7*, was neither detected in the conventional mouse gut nor represented by ASF⁸ or Oligo-MM¹² (Krych, Hansen et al. 2013). To conclude, ASF⁸ and Oligo-MM¹² consortia represent three and four phyla, respectively found in the conventional mouse gut and one phylum, the *Actinobacteria*, was unique to the Oligo-MM¹².

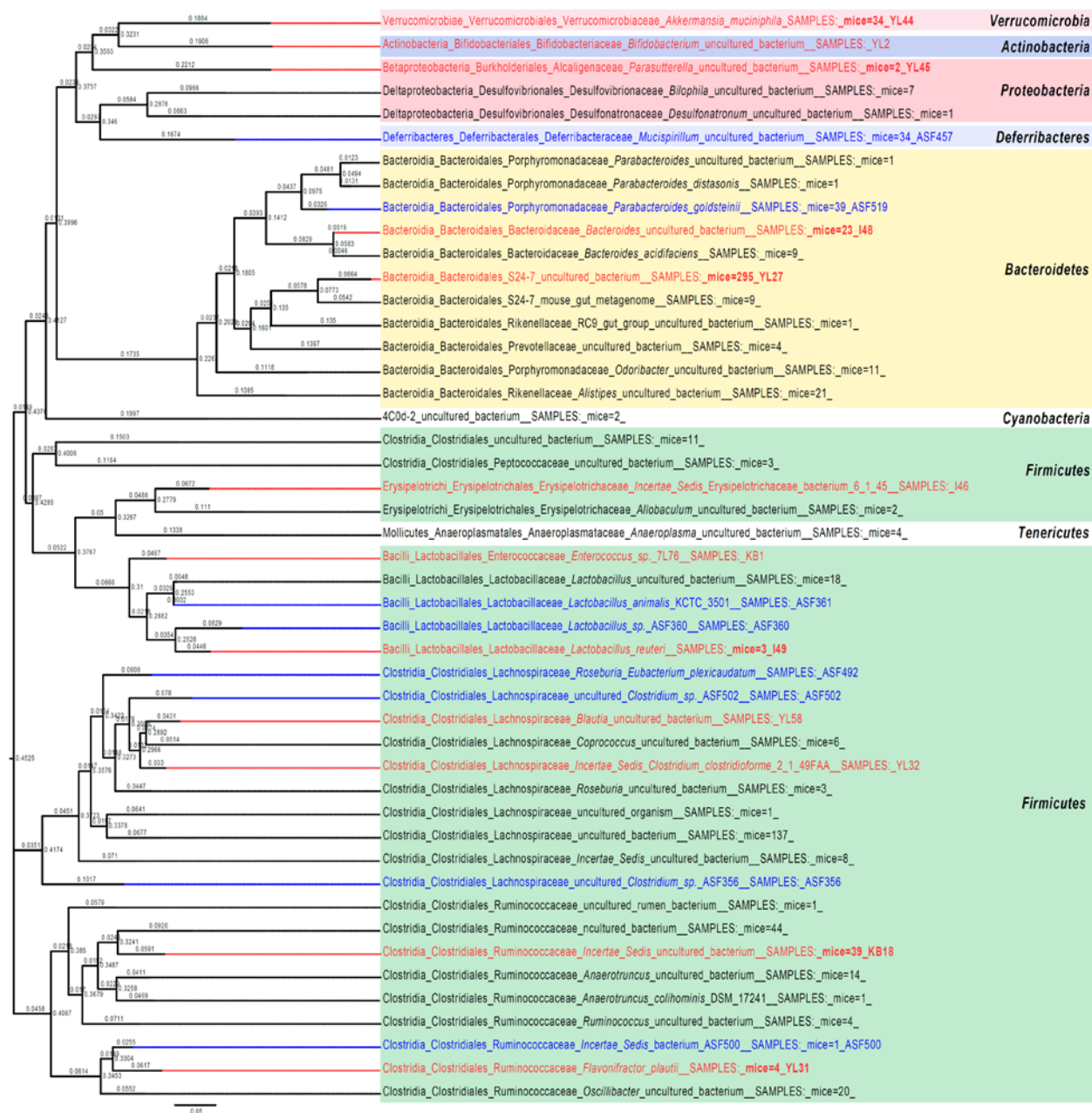


Figure 7. Representation of Oligo-MM and ASF strains in a conventional mouse microbiota based on 16S rRNA gene sequences.

Full length 16S rRNA gene sequences of the 12 Oligo-MM strains (red) as well as the 8 ASF strains (blue) (Dewhirst, Chien et al. 1999) were compared against a set of 865 full-length high quality 16S rRNA gene sequences from 2 types of conventional unmanipulated SPF mice (Stecher, Robbani et al. 2007). All sequences were aligned against the SILVA database version 111 NR (Quast, Pruesse et al. 2013) using MEGABLAST version 2.2.28+ on a 97 % identity level, yielding 47 different taxonomic identities. The best hit of each of the 47 taxonomies from the database was used for the generation of a multiple sequence alignment using Infernal, respectively. A phylogenetic tree was generated using fasttree (Price, Dehal et al. 2009). The number of sequences per taxonomic identity in the conventional mice is indicated (e.g. mice=20). The Oligo-MM strains, which have at least one representative in the mouse dataset, are highlighted in bold. Color code refers to the phylum: bright blue: *Actinobacteria*; light orange: *Bacteroidetes*; red:

Proteobacteria; purple: *Verrucomicrobia*; green: *Firmicutes*; light blue: *Deferribacteres* and white: others. Data analysis was performed by Hans-Joachim Ruscheweyh, University of Tübingen.

4.1.3.2. OTU distribution and abundance

For seven Oligo-MM¹² strains, representatives at the OTU (Operational Taxonomic Unit) level were detected in the conventional mouse microbiota. Five were apparently not present in this community. However, we used other mice for isolation of the Oligo-MM strains (**Table 36**). Interestingly, YL27 was assigned to the most abundant taxon (*i.e.* S24-7) of the mouse microbiota. In contrast, three ASF strains were represented at the OTU level while five were not detected. We conclude that the Oligo-MM¹² consortium is quantitatively and qualitatively more complex than the ASF consortium and represents a diverse spectrum of the mouse microbiota. However, this data shows that a significant number of taxa represented in a conventional microbiota are not included in either consortium of strains.

Table 36. Quantitative representation of Oligo-MM and ASF strains in a conventional mouse microbiota

| Phylum | Class | Family | Genus | Species | Reads* | Strain ID |
|------------------------|---------------------|---------------------|------------------------|---------------------|------------|-------------|
| <i>Bacteroidetes</i> | Bacteroidia | S24-7 | | | 295 | YL27 |
| <i>Firmicutes</i> | Clostridia | Lachnospiraceae | | | 137 | |
| <i>Firmicutes</i> | Clostridia | Ruminococcaceae | | | 44 | |
| <i>Firmicutes</i> | Clostridia | Ruminococcaceae | <i>Incertae Sedis</i> | | 39 | KB18 |
| <i>Bacteroidetes</i> | Bacteroidia | Porphyromonadaceae | <i>Parabacteroides</i> | <i>goldsteinii</i> | 39 | ASF519 |
| <i>Verrucomicrobia</i> | Verrucomicrobiae | Verrucomicrobiaceae | <i>Akkermansia</i> | <i>muciniphila</i> | 34 | YL44 |
| <i>Deferribacteres</i> | Deferribacteres | Deferribacteraceae | <i>Mucispirillum</i> | | 34 | ASF457 |
| <i>Bacteroidetes</i> | Bacteroidia | Bacteroidaceae | <i>Bacteroides</i> | | 23 | I48 |
| <i>Bacteroidetes</i> | Bacteroidia | Rikenellaceae | <i>Alistipes</i> | | 21 | |
| <i>Firmicutes</i> | Clostridia | Ruminococcaceae | <i>Oscillibacter</i> | | 20 | |
| <i>Firmicutes</i> | Bacilli | Lactobacillaceae | <i>Lactobacillus</i> | | 18 | |
| <i>Firmicutes</i> | Clostridia | Ruminococcaceae | <i>Anaerotruncus</i> | | 14 | |
| <i>Bacteroidetes</i> | Bacteroidia | Porphyromonadaceae | <i>Odoribacter</i> | | 11 | |
| <i>Firmicutes</i> | Clostridia | | | | 11 | |
| <i>Bacteroidetes</i> | Bacteroidia | S24-7 | | | 9 | |
| <i>Bacteroidetes</i> | Bacteroidia | Bacteroidaceae | <i>Bacteroides</i> | <i>acidifaciens</i> | 9 | |
| <i>Firmicutes</i> | Clostridia | Lachnospiraceae | <i>Incertae Sedis</i> | | 8 | |
| <i>Proteobacteria</i> | Deltaproteobacteria | Desulfovibrionaceae | <i>Bilophila</i> | | 7 | |
| <i>Firmicutes</i> | Clostridia | Lachnospiraceae | <i>Coproccoccus</i> | | 6 | |

| Phylum | Class | Family | Genus | Species | Reads* | Strain ID |
|-----------------------|---------------------|---------------------|------------------------|------------------------|----------|-------------|
| <i>Firmicutes</i> | Clostridia | Ruminococcaceae | <i>Flavonifractor</i> | <i>plautii</i> | 4 | YL31 |
| <i>Firmicutes</i> | Clostridia | Ruminococcaceae | <i>Ruminococcus</i> | | 4 | |
| <i>Tenericutes</i> | Mollicutes | Anaeroplasmataceae | <i>Anaeroplasma</i> | | 4 | |
| <i>Bacteroidetes</i> | Bacteroidia | Prevotellaceae | uncultured | | 4 | |
| <i>Firmicutes</i> | Bacilli | Lactobacillaceae | <i>Lactobacillus</i> | <i>reuteri</i> | 3 | I49 |
| <i>Firmicutes</i> | Clostridia | Lachnospiraceae | <i>Roseburia</i> | | 3 | |
| <i>Firmicutes</i> | Clostridia | Peptococcaceae | | | 3 | |
| <i>Proteobacteria</i> | Betaproteobacteria | Alcaligenaceae | <i>Parasutterella</i> | | 2 | YL45 |
| <i>Firmicutes</i> | Erysipelotrichi | Erysipelotrichaceae | <i>Allobaculum</i> | | 2 | |
| <i>Cyanobacteria</i> | 4C0d-2 | | | | 2 | |
| <i>Bacteroidetes</i> | Bacteroidia | Rikenellaceae | | | 1 | |
| <i>Bacteroidetes</i> | Bacteroidia | Porphyromonadaceae | <i>Parabacteroides</i> | <i>distasonis</i> | 1 | |
| <i>Bacteroidetes</i> | Bacteroidia | Porphyromonadaceae | <i>Parabacteroides</i> | | 1 | |
| <i>Firmicutes</i> | Clostridia | Ruminococcaceae | <i>Incertae Sedis</i> | | 1 | ASF500 |
| <i>Firmicutes</i> | Clostridia | Ruminococcaceae | <i>Anaerotruncus</i> | <i>colihominis</i> | 1 | |
| <i>Firmicutes</i> | Clostridia | Ruminococcaceae | | | 1 | |
| <i>Firmicutes</i> | Clostridia | Lachnospiraceae | | | 1 | |
| <i>Proteobacteria</i> | Deltaproteobacteria | Desulfonatronaceae | <i>Desulfonatronum</i> | | 1 | |
| <i>Firmicutes</i> | Bacilli | Enterococcaceae | <i>Enterococcus</i> | | - | KB1 |
| <i>Firmicutes</i> | Erysipelotrichi | Erysipelotrichaceae | <i>Incertae Sedis</i> | | - | I46 |
| <i>Firmicutes</i> | Clostridia | Lachnospiraceae | <i>Clostridium</i> | <i>clostridioforme</i> | - | YL32 |
| <i>Firmicutes</i> | Clostridia | Lachnospiraceae | <i>Blautia</i> | | - | YL58 |
| <i>Actinobacteria</i> | Actinobacteria | Bifidobacteriaceae | <i>Bifidobacterium</i> | | - | YL2 |
| <i>Firmicutes</i> | Clostridia | Lachnospiraceae | <i>Eubacterium</i> | <i>plexicaudatum</i> | - | ASF492 |
| <i>Firmicutes</i> | Clostridia | Lachnospiraceae | <i>Clostridium</i> | | - | ASF356 |
| <i>Firmicutes</i> | Clostridia | Lachnospiraceae | <i>Clostridium</i> | | - | ASF502 |
| <i>Firmicutes</i> | Bacilli | Lactobacillaceae | <i>Lactobacillus</i> | | - | ASF360 |
| <i>Firmicutes</i> | Bacilli | Lactobacillaceae | <i>Lactobacillus</i> | <i>animalis</i> | - | ASF361 |

The number of sequences per taxonomic identity in the conventional mice (reads) is listed in descending order. Oligo-MM strains as well as their respective abundance in conventional microbiota are highlighted in bold (right column). Color code refers to the phylum: bright blue: *Actinobacteria*; light orange: *Bacteroidetes*; red: *Proteobacteria*; purple: *Verrucomicrobia*; green: *Firmicutes*; light blue: *Deferribacteres* and white: others. * Number of 16S rRNA gene sequences per taxonomic identity in conventional mice is taken from Stecher *et al.*, 2007 (Stecher, Robbiani *et al.* 2007). Total number of reads analysed: 818 reads.

4.1.4. Deposition of the Oligo-MM strains at the German type culture collection (DSMZ)

Despite their broad application in preclinical research, ASF strains are not publicly available, which hampers *in vitro* and *in vivo* studies and limits utility of gnotobiotic ASF mouse model to analyze host-microbiota-pathogen interactions. Therefore, in order to ensure long-term preservation and public accessibility, each strain was deposited in the German type culture collection (DSMZ; Deutsche Sammlung von Mikroorganismen und Zellkulturen). Briefly, each strain was sent to the DSMZ as a frozen vial, where lyophilized bacterial glass ampoules were generated. The ampoules were recovered from the DSMZ and strain purity and identity was confirmed by 16S rRNA gene sequencing. The accession numbers of the strains are listed in **Table 32**.

4.2. The Oligo-MM¹⁰ can be reproducibly transplanted to gnotobiotic mice from a frozen mixture

To test whether the Oligo-MM strains can stably colonize the murine intestine, we aimed to inoculate ten of the strains (Oligo-MM¹⁰) into gnotobiotic ASF-colonized mice and follow bacterial colonization over time. To achieve this, we first established a protocol which allows reproducible colonization of gnotobiotic mice using a standard inoculum.

In order to standardize inoculation of the Oligo-MM¹⁰ into gnotobiotic mice and to avoid repeated anaerobic culturing which might lead to significant experimental variation, we tested a method to inoculate the Oligo-MM¹⁰ mixture from frozen stocks. We reasoned that a frozen mixture containing all strains could be used as direct inoculum and thereby limit variations as *e.g.* introduced by bacterial growth state. In order to prepare the frozen stock, each Oligo-MM¹⁰ strain was grown individually. Actively growing cultures were mixed under anaerobic conditions and frozen at -80 °C as glycerol stocks. Frozen vials were thawed and used directly to orally and rectally inoculate mice under germfree conditions.

Next, we tested if gnotobiotic mice could be reproducibly colonized with the Oligo-MM¹⁰. The mice used in these explorative experiments were colonized with a low-complexity microbiota harboring five ASF strains (the ASF⁵ mice) and bred in a germfree isolator. For the experiments, ASF⁵ mice were exported from the isolator and transferred into gnotocages. In order to monitor the Oligo-MM¹⁰ composition over the course of 43 days, we performed two independent experiments where ASF⁵ mice were inoculated with the frozen Oligo-MM¹⁰ or left untreated as controls. In the first experiment, mice

were sacrificed either at day 0 before Oligo-MM¹⁰ inoculation (d0, ASF⁵) or at days 10 and 20 (d10, d20, ASF⁵ + Oligo-MM¹⁰). In the second experiment, mice were sacrificed at days 22 and 43 (d22, d43, ASF⁵ + Oligo-MM¹⁰) or left untreated for 43 days (d43, ASF⁵). All mice were housed in gnotocages throughout the experiments to avoid any possible contaminations (**Figure 8A**).

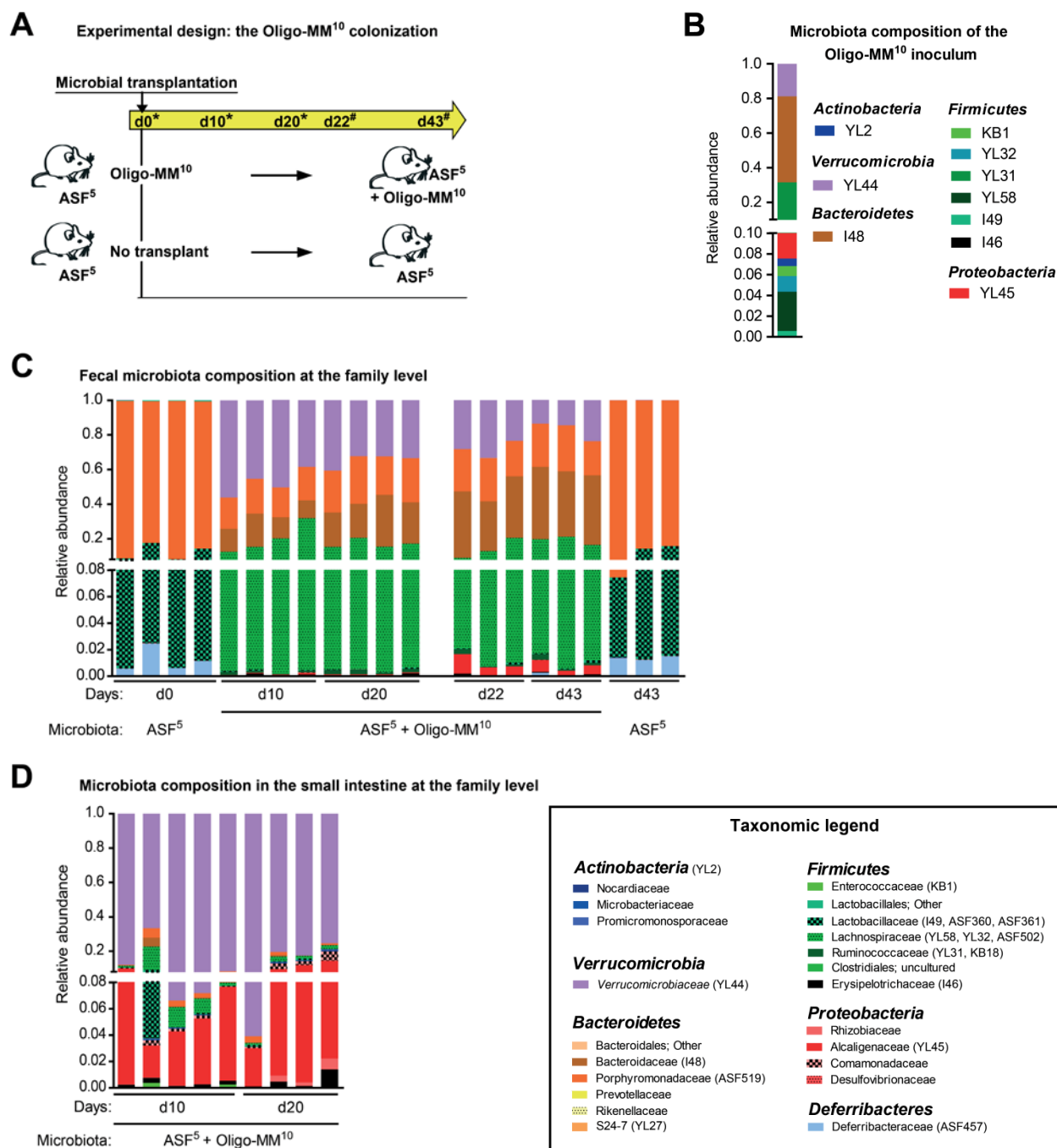


Figure 8. Oligo-MM¹⁰ inoculation in ASF⁵ mice using frozen stocks harboring 10 Oligo-MM strains is efficient and reproducible.

Gnotobiotic mice stably colonized with 5 ASF strains (ASF360, ASF361, ASF457, ASF502 and ASF519; ASF⁵) were inoculated under germfree conditions with a frozen vial containing either 10 Oligo-MM strains (I46, I48, I49, KB1, YL2, YL31, YL32, YL44, YL45, YL58; Oligo-MM¹⁰) or the sterile media, as a negative control (no transplant). Briefly, Oligo-MM¹⁰ strains were separately grown to exponential phase and mixed before freezing. Frozen vials were defrozen at room temperature and directly used for oral and rectal inoculation. Microbial transplantation was performed at two independent occasions as indicated with star (*) and hash (#) symbols. In the first experiment, feces were sampled at days 0 (d0) and mice were sacrificed at d10 and d20 post-inoculation. In the second experiment, mice were sacrificed at d22 and d43 post-inoculation. Three mice were left untreated, as a negative control (ASF⁵, d43). **(A)** Experimental design. **(B)** Microbial composition of the Oligo-MM¹⁰ inoculum was determined using a hydrolysis probe based quantitative PCR assay with strain-specific primers and hydrolysis probe combinations. Data are expressed as relative abundance. **(C-D)** Microbiota composition of **(C)** feces at days 0, 10, 20, 22 and 43 and **(D)** small intestine at days 10 and 20 was determined using amplicon sequencing. Sequencing data were processed using the QIIME pipeline and taxonomy was assigned using the Silva database. Data are presented as relative abundance at the taxonomic family level (1 mouse per column). Color code is indicated in taxonomic legend box. Taxonomic affiliation of the Oligo-MM and ASF strains is indicated (brackets).

To confirm the presence of the individual Oligo-MM strains in the frozen Oligo-MM¹⁰ stock, bacterial gDNA was extracted and microbiota composition was analyzed by 16S rRNA amplicon sequencing and quantitative PCR (qPCR). In order to analyze the Oligo-MM¹⁰ composition over time, gDNA was extracted from fecal samples. In addition, DNA was extracted from small intestinal contents. Microbiota composition was analyzed by 16S rRNA amplicon sequencing and qPCR at different time points. Data were analyzed using the QIIME pipeline (Quantitative Insights Into Microbial Ecology) (Caporaso, Kuczynski et al. 2010) using either an open-reference database or a custom database containing all the twelve Oligo-MM and five ASF strains. To get an overview on microbial complexity, the alpha diversity was calculated using the amplicon sequencing data. We also determined the relative cecal weight which is known to be indicative for microbiota complexity (Bleich and Hansen 2012).

All ten Oligo-MM strains were detected in the frozen Oligo-MM¹⁰ inoculum (**Figures 8B and 9C**). Interestingly, I46 was not detected with the qPCR assay, while it was detected by the amplicon sequencing analysis. Processed data of qPCR and amplicon sequencing are shown in annexed **Tables 37, 38 and 39**. Furthermore, about 70 % and 80 % of the fecal microbiota population were assigned to Gram-negative strains using qPCR and amplicon sequencing, respectively (**Figures 8C, 9A and 12**). Analysis of the fecal microbiota revealed that the majority of the Oligo-MM¹⁰ strains are detectable in the mouse gut at day 10, 20, 22 and 43 post-inoculation. Their colonization appeared to be stable over 43 days (**Figures 8C and 9A**). Interestingly, about 80 % of the fecal microbiota was assigned to Gram-negative bacteria (*i.e.* to *Verrucomicrobia* and *Bacteroidetes*) despite the inoculation of a relatively high number of Gram-positive strains (7 out of 10 strains, belonging to the phyla *Firmicutes* and *Actinobacteria*). Most of the Gram-positive strains are present only at very low abundance and four strains, YL2, KB1, I46 and I49, were not detected in fecal samples by amplicon sequencing (**Figures 8C and 9A**).

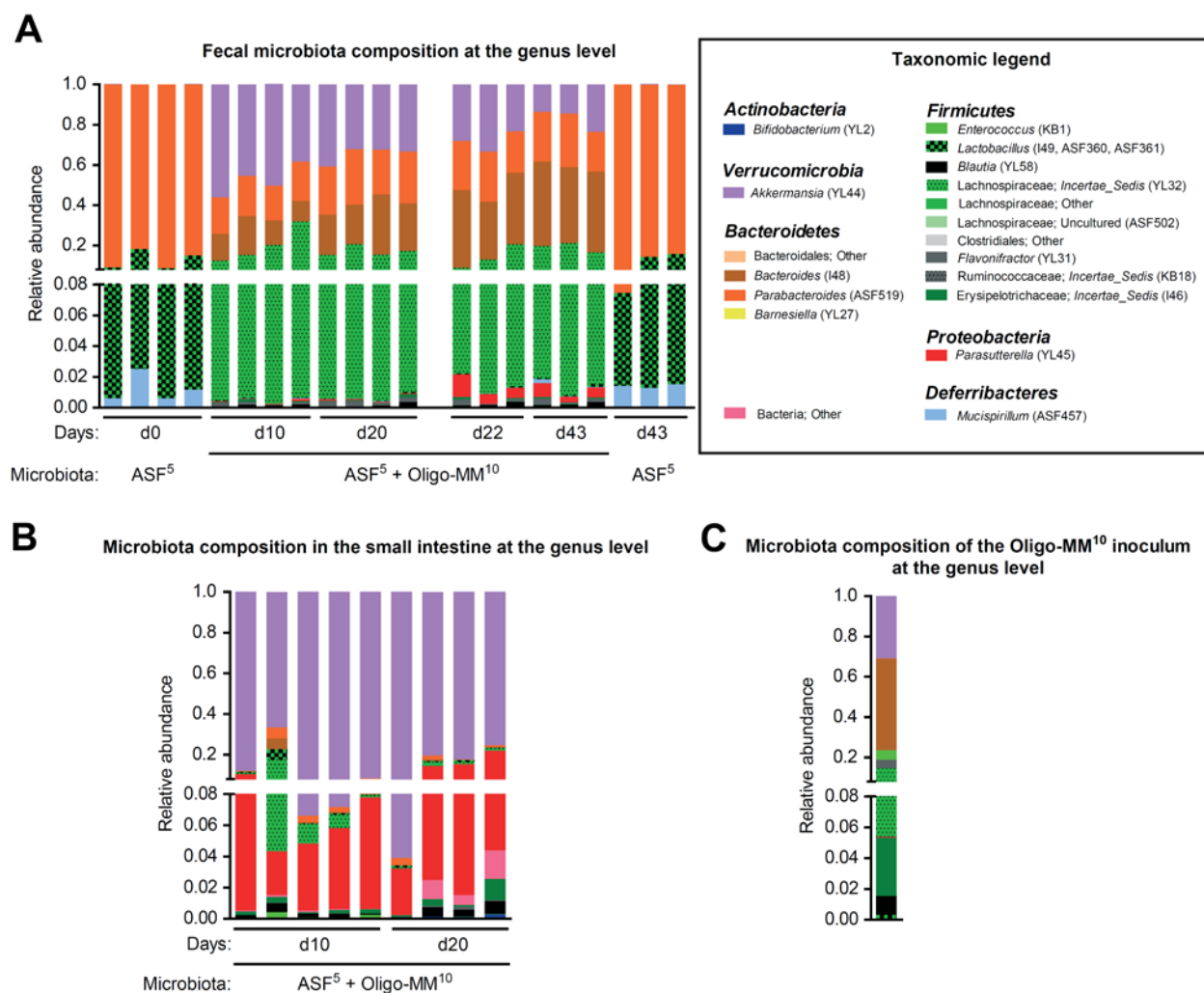


Figure 9. Data from Figure 8 analyzed using open-reference approach based on a custom 16S sequence database.

Microbiota composition was analyzed using the QIIME pipeline and taxonomy was assigned against a custom sequence database of the full length 16S rRNA gene sequences of the Oligo-MM¹² and the ASF⁵ strains. **(A)** Fecal microbiota composition at days 0, 10, 20, 22 and 43. **(B)** Microbiota composition of the small intestine at days 10 and 20. **(C)** Microbial composition of the frozen inoculum. Data are presented as relative abundance at the taxonomic genus level (1 mouse per column). Color code is indicated in taxonomic legend box. Taxonomic affiliation of the Oligo-MM and ASF strains is indicated (brackets).

Significant differences in microbiota composition analyzed by amplicon sequencing were observed between the feces and the small intestine (**Figures 9A,B**). Three strains, YL2, KB1 and I46, were undetected in the feces but detectable in the small intestine. As I49 was assigned to the same genus as ASF360 and ASF361 (*i.e.* Lactobacillaceae, genus *Lactobacillus*), even though the *Lactobacillus* genus was detected, its absence remained unclear. We noticed similarities when comparing amplicon sequencing data processed with an open-reference database and a custom sequence collection (**Figures 8D and 9B**).

Furthermore, we found that cecal and fecal microbiota had comparable microbiota composition (**Figure 10**).

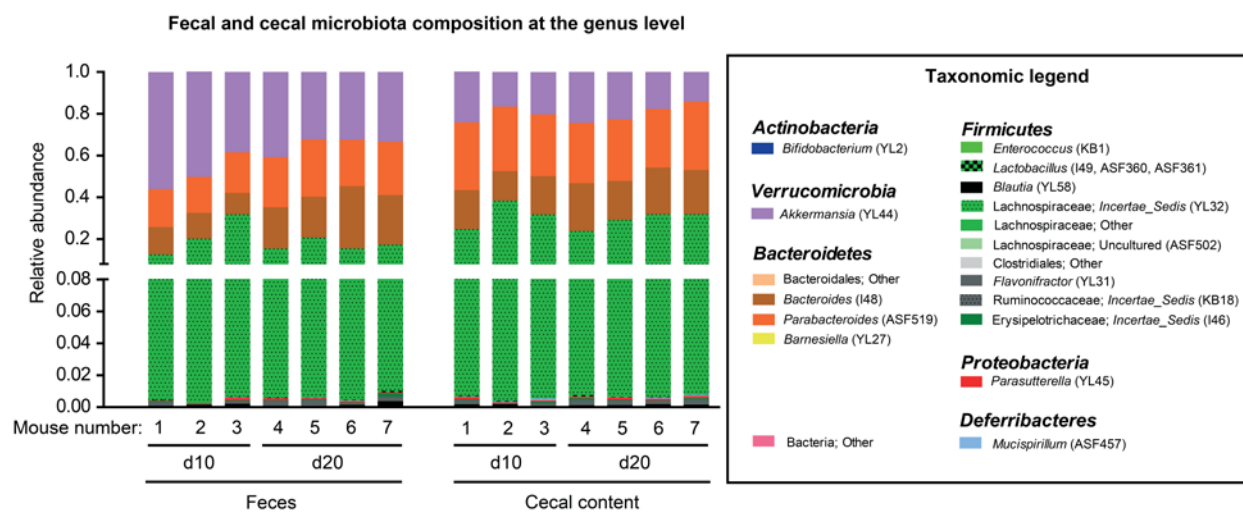


Figure 10. Comparison of fecal and cecal microbiota composition of ASF⁵ mice colonized with the Oligo-MM¹⁰ consortium analyzed using open-reference approach based on a custom 16S sequence database.

Data from **Figure 9**. Briefly, fecal and cecal microbiota compositions at days 10 and 20 (d10 and d20, respectively) were determined using amplicon sequencing. Sequencing data were processed using the QIIME pipeline and taxonomy was assigned against a custom sequence collection of the full length 16S rRNA gene sequences of the 12 Oligo-MM (YL2, YL27, YL31, YL32, YL44, YL45, YL58, KB1, KB18, I46, I48, I49) and 5 ASF strains (ASF360, ASF361, ASF457, ASF502, ASF519). Data are presented as relative abundance at the taxonomic genus level and is representative of 1 experiment (1 mouse per column). Color code is indicated in taxonomic legend box. Taxonomic affiliation of the Oligo-MM and ASF strains is indicated (brackets).

In conclusion, we established a method to reproducibly inoculate the Oligo-MM¹⁰ consortium as a frozen stock to gnotobiotic mice. These data point out that the majority of the Oligo-MM¹⁰ strains stably colonize the mouse gut over a time-course of 43 days. Besides the taxonomic profile, we also analyzed microbiota complexity using alpha diversity based on amplicon sequencing data and relative cecal weight.

To calculate alpha diversity of the fecal microbiota, we used amplicon sequencing data (**Figure 11A**). To determine relative cecal weight, we recorded mouse and cecal weights from the two previous independent experiments as well as six extra control mice colonized with ASF⁵ (**Figure 11B**).

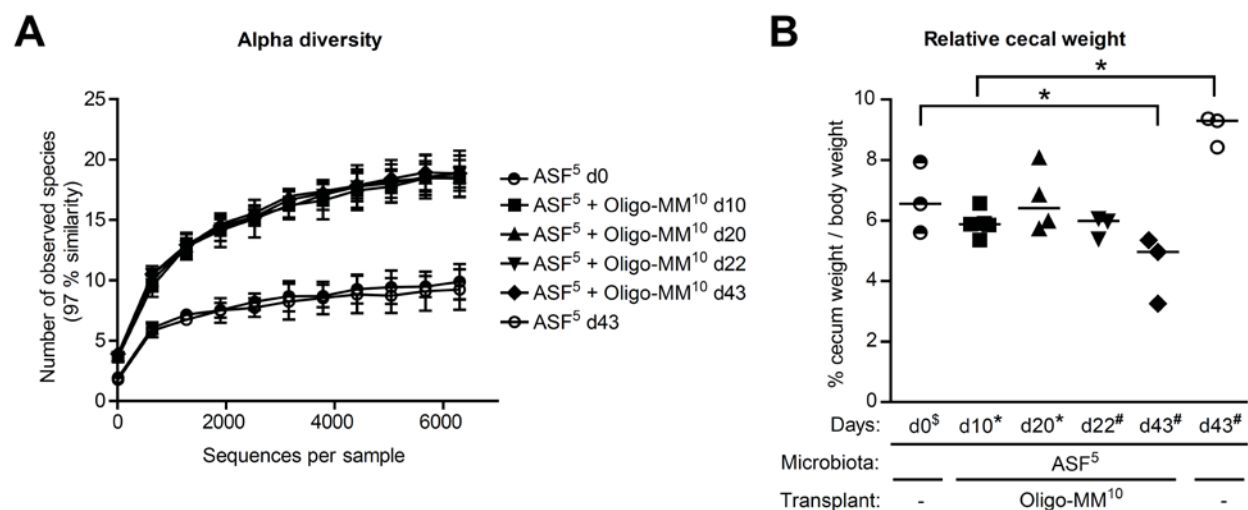


Figure 11. Microbiota complexity of ASF⁵-colonized mice increases after Oligo-MM¹⁰ inoculation.

(A) Alpha diversity was determined as the observed species metric using amplicon sequencing data from **Figure 8**. Data are presented as mean and standard deviation. (B) Mouse cecum and body weight were recorded at different days post-inoculation and at three independent occasions as indicated with dollar ([§]), star (*) and hash (#) symbols. Data were plotted as relative cecal weight (%). Bars represent the median. ASF⁵ mice at d0 and d43 are depicted as half-empty circle and empty circle, respectively. ASF⁵ mice inoculated with the Oligo-MM¹⁰ consortium for 10, 20, 22 and 43 days are depicted as square, triangle, inverted triangle and diamond, respectively. Mann-Whitney U test: * P<0.05. One-way ANOVA Kruskal-Wallis test: (B) P=0.0178.

It has been shown that germfree mice exhibit a relative cecal weight of about 10 % (Stecher, Chaffron et al. 2010). At day 0, the relative cecal weight of ASF⁵ mice ranged between 6 to 8 %. We observed a slight decrease of the relative cecal weight after ten days of Oligo-MM¹⁰ inoculation. Interestingly, we noticed a second significant decrease at day 43 post-inoculation (**Figure 11B**). Surprisingly, the relative cecal weight of ASF⁵ mice was increased (from 6-8 % at d0 to 8-9 % at d43 post-inoculation). The reason for this remains unclear. Moreover, ASF⁵ + Oligo-MM¹⁰ mice showed increased microbiota complexity from day 10 to day 43 post-inoculation, as compared to ASF⁵ mice (**Figure 11A**). This correlates decreased relative cecal weight with increased microbiota complexity, as it was also previously observed (Itoh and Mitsuoka 1985).

Taken together, we established a method to efficiently and reproducibly colonize gnotobiotic mice with a well-defined anaerobic microbial consortium, the Oligo-MM¹⁰. Colonization of all Oligo-MM¹⁰ strains was confirmed along the murine intestinal tract (except of YL2, which could not be detected). Importantly, we established the most complex-defined mouse-derived microbiota described until now. In

the next step, we set out to generate a mouse colony stably colonized with the Oligo-MM strains over several generations, the Oligo-MM mice.

4.3. The Oligo-MM¹² stably colonizes the murine gut and is vertically transmitted over at least 4 filial generations

Next, we aimed to inoculate Oligo-MM strains into germfree mice in order to generate a mouse colony stably colonized with the Oligo-MM over consecutive filial generations.

To create the Oligo-MM¹² consortium, we included two additional strains, YL27 and KB18. YL27 was assigned to the Bacteroidales and KB18 to the Ruminococcaceae (**for further details, refer to Figure 7**). These strains were included as these two phylotypes belong to the most abundant in conventional mice (**Table 35**). Colonization of germfree mice was performed by Prof. Kathy McCoy at the University of Bern (Switzerland) using our established protocol. Two germfree breeding pairs (termed F0) were inoculated with the Oligo-MM¹² and bred under germfree conditions in an isolator. Two breeding pairs from the F2 generation were shipped to our germfree facility and further bred in a germfree isolator. For each generation (from F0 to F4), feces from individual adult mice was sampled. Fecal DNA was extracted and microbiota composition was determined by qPCR (Markus Beutler, AG Stecher). Briefly, specific 16S-targeted primers and hydrolysis probes were designed to detect each 16S rRNA gene by absolute quantification. Relative abundance of each strain is shown by the fraction of individual divided by the sum of all. Besides lower costs compared to amplicon sequencing, one of the advantage of the qPCR assay is that it allows a more accurate quantification of the Oligo-MM¹². However, bacterial contaminants cannot be detected.

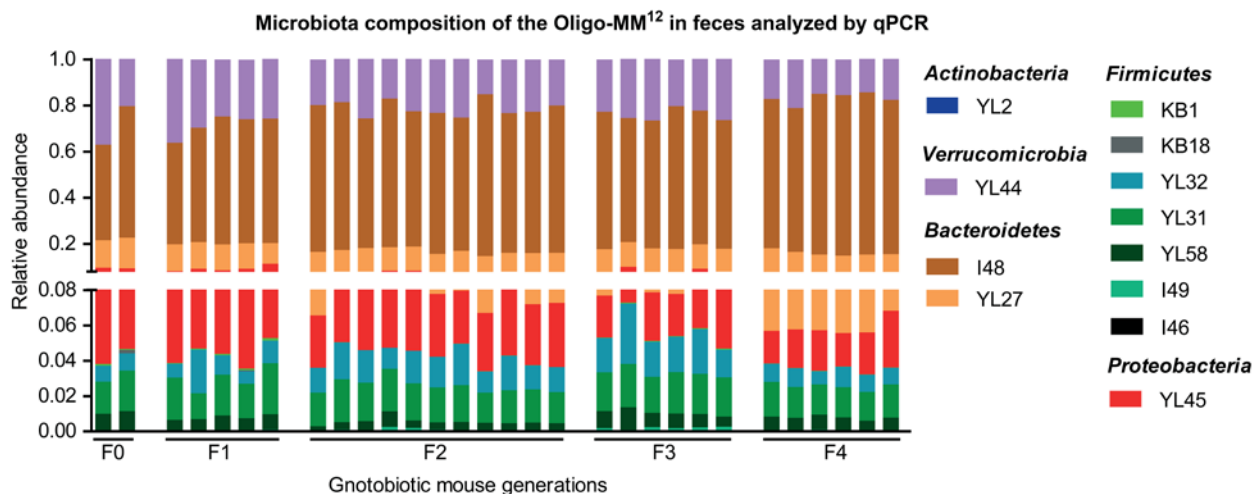


Figure 12. Oligo-MM¹² consortium stably colonizes germfree mice and is vertically transmitted over at least 4 filial generations.

Germfree C57Bl/6 mice were inoculated with a frozen mixture containing 12 Oligo-MM strains (I46, I48, I49, KB1, KB18, YL2, YL27, YL31, YL32, YL44, YL45, YL58; Oligo-MM¹²) and bred for 4 generations in germfree isolators at the Clean Mouse Facility, University of Bern (F0-F1) and Max-von-Pettenkofer Institute (F2-F4). Fecal samples were collected at each generation (F0 to F4). After gDNA extraction, fecal microbiota composition was determined using a hydrolysis probe based quantitative PCR assay. Data are given as relative abundance. One column represents one fecal sample.

We found that composition of the Oligo-MM¹² remained stable over 4 filial generations (**Figure 12 and annexed Table 44**). More than 90 % of the microbial population was composed of three strains (YL44; *Verrucomicrobia* and I48, YL27; *Bacteroidetes*). About 4 % of the fecal microbiota was assigned to YL45 (*Proteobacteria*). The *Firmicutes* strains made up only 5 % of the microbiota detected in the feces of Oligo-MM¹²-colonized mice. In decreasing order of abundance, we detected YL31, YL32 and YL58. I49, KB1 and KB18 were just above detection limit while the isolates I46 and YL2 were never detected with this approach. However, I46 was re-isolated by plating cecal content of a F3 generation mouse. Thereby, we confirmed that I46 colonized the Oligo-MM¹² mice, even though it was not detected by qPCR (data not shown).

Surprisingly, we noted that the majority (95 %) of the fecal microbiota in Oligo-MM¹² mice were Gram-negative strains, mainly assigned to the *Verrucomicrobia* (YL44) and the *Bacteroidetes* (YL27, I48). The minority left (5 %) was Gram-positive strains assigned to the *Firmicutes*. We reasoned that this might be due to a general low DNA extraction efficiency from the Gram-positive strains.

To conclude, we confirmed that eleven of the twelve Oligo-MM¹² strains can colonize murine intestinal tract over 4 filial generations. Regarding YL2, we assume that this strain does either not

colonize the intestine of adult mice or is below the detection limit in the feces or present at higher abundance in other regions of the intestinal tract or is not viable after freezing. In conclusion, the Oligo-MM¹² stably colonizes the murine gut and is vertically transmitted over at least four generations. Up-to-date, this Oligo-MM¹² mouse colony represents the second gnotobiotic mouse model, after the ASF mice, harboring a defined consortium of mouse-derived bacterial strains.

4.4. The Oligo-MM¹² consortium partially restores colonization resistance against *Salmonella*

It has been shown in a previous study that ASF-colonized mice lack colonization resistance (CR) against the enteric pathogen *Salmonella enterica* serovar Typhimurium (*S. Tm*) (Stecher, 2010). Regarding the importance of studying the mechanisms of CR in the gut, we tested whether the Oligo-MM¹² microbiota was able to restore CR against *S. Tm*.

In order to determine whether the Oligo-MM¹² consortium conferred CR against *S. Tm*, we used ASF-colonized mice harboring five ASF strains (ASF⁵), which lack colonization resistance. One group of ASF⁵ mice was inoculated with the Oligo-MM¹² strains (ASF⁵ + Oligo-MM¹²), one group with cecum content from a conventional donor mouse (ASF⁵ + CON) and one mock-inoculated with sterile media as control. After microbiota transplantation, the microbiota was allowed to stabilize for 40 days (**Figure 13A**). It has been shown that a complex conventional microbiota can restore CR in germfree mice against enteropathogens such as *S. Tm* (Stecher, Chaffron et al. 2010). For infection, we used an avirulent *S. Tm* strain (*S. Tm*^{avir}) (Hapfelmeier, Ehrbar et al. 2004) as intestinal inflammation induced by *S. Tm*^{wt} can alter microbiota composition and thereby alleviate colonization resistance (Stecher, Robbiani et al. 2007, Winter, Thiennimitr et al. 2010). Therefore, we can separate colonization resistance from *S. Tm*-mediated virulence mechanisms.

First, we determined gut microbiota composition and complexity at day 40 post-transplantation. We analyzed the fecal microbiota composition using 16S amplicon sequencing as well as qPCR and determined microbiota complexity of each experimental group by calculating the alpha diversity. To test whether the Oligo-MM¹² restores CR against *S. Tm*^{avir}, we orally infected mice with 10⁶ colony forming unit (CFU) *S. Tm*^{avir} and determined the bacterial load at day 1 post-infection (d1 p.i.) in feces and at d2 p.i. in cecum content and mesenteric lymph nodes (mLN). In addition, we also determined the relative cecal weight at d2 p.i.

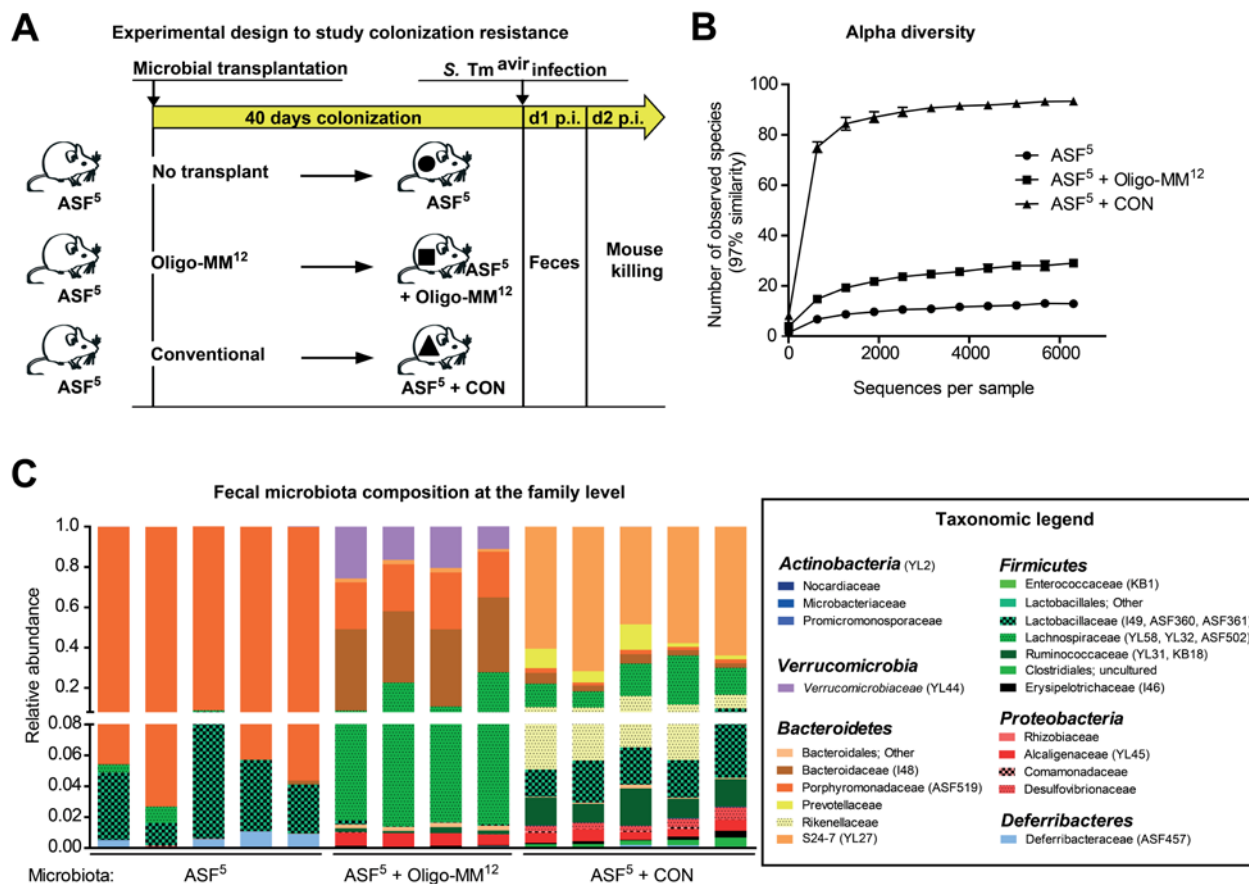


Figure 13. Fecal microbiota composition and diversity 40 days after transplanted with Oligo-MM¹² or complex microbiota.

(A) Experimental design. C57Bl/6 mice colonized with 5 ASF strains (ASF⁵ mice) were inoculated with either the Oligo-MM¹² (ASF⁵ + Oligo-MM¹²; square, 4 mice) or frozen cecum content harvested from a conventional mouse (ASF⁵ + CON; triangle, 5 mice) or mock-inoculated with sterile media as a control (ASF⁵; circle, 5 mice). After 40 days (d40), mice were orally infected with 10⁶ CFU of an avirulent strain of *S. Tm* (*S. Tm*^{avir}). Feces were sampled at day 1 post-infection (p.i.). At day 2 p.i., mice were sacrificed, organs sampled and the relative cecal weight was determined. (B) Alpha diversity was determined at d40 as the observed species metric. Data are presented as mean and standard deviation. ASF⁵; circle, ASF⁵ + Oligo-MM¹²; square, ASF⁵ + CON; triangle. (C) Fecal microbiota composition at d40 was determined using 16S rRNA gene amplicon sequencing. Sequencing data were processed using the QIIME pipeline and taxonomy was assigned against the Silva database. Data are presented as relative abundance at the taxonomic family level. One column represents one mouse. Color code is indicated in taxonomic legend box. Taxonomic affiliation of the Oligo-MM and ASF strains is indicated (brackets).

Using alpha diversity measurement, we confirmed that the three mouse groups harbored different microbiota complexities. In decreasing order, microbiota of ASF⁵ + CON mice was strikingly more complex than the microbiota of ASF⁵ + Oligo-MM¹² mice, which was more complex than the microbiota of ASF⁵ mice (Figure 13B). Using 16S amplicon sequencing, we analyzed fecal microbiota composition. In ASF⁵ mice, four taxonomic family levels were detected suggesting that the five ASF strains would be present in the ASF⁵ mouse group (Figure 13C). However, both ASF360 and ASF361 strains are affiliated

to Lactobacillaceae. Therefore, we used a qPCR assay to detect more specifically bacterial strains. Contrary to ASF361 which was present in all ASF⁵ mice, ASF360 was never detected (**Figure 14**). Its presence remains unclear. In ASF⁵ + Oligo-MM¹² mice, ten taxonomic family levels out of twelve were detected using 16S amplicon sequencing (**Figure 13C**). However, Erysipelotrichaceae and Deferribacteraceae were only detected in very low abundance. As for ASF⁵ mice, several strains were affiliated to the same taxonomic family. Using qPCR, we detected YL31 among the Ruminococcaceae as well as YL32 and YL58 among the Lachnospiraceae (**Figure 14**). Interestingly, ASF457 was better detected using qPCR. Finally, in ASF⁵ + Oligo-MM¹² mice, the bacterial strains YL2, KB1, I49, KB18, ASF502, ASF360 and ASF361 were either not colonizing or under detection limit. In ASF⁵ + CON mice, microbiota composition analysis revealed fifteen different OTUs at the taxonomic family level (**Figure 13C**).

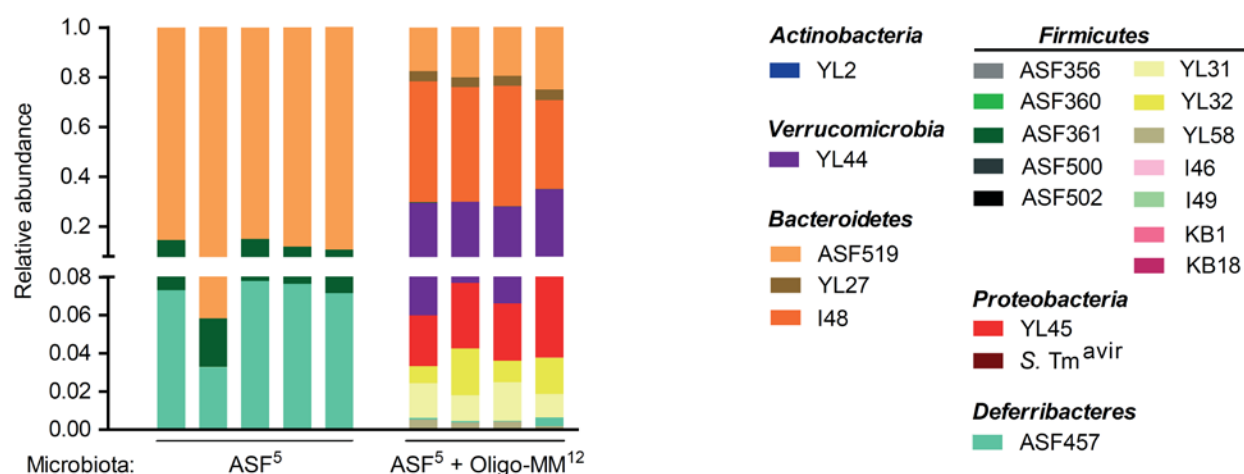


Figure 14. Fecal microbiota composition of ASF⁵ mice colonized with the Oligo-MM¹² or mock-inoculated, analyzed using a hydrolysis probe based quantitative PCR assay.

Fecal DNA from the experiment described in **Figure 13** was analyzed to determine fecal microbiota composition using a hydrolysis probe based quantitative PCR assay. Data are given as relative abundance of the summed total reads of the individual strains. One column represents one fecal sample.

In summary, we confirmed the presence of four bacterial strains in ASF⁵ mice and ten strains in ASF⁵ + Oligo-MM¹² mice. We showed that the majority of the Oligo-MM¹² strains were present in ASF⁵ + Oligo-MM¹² mice. Furthermore, we also set up three experimental groups with an increased microbiota complexity such as four different OTU at the taxonomic family level are present in ASF⁵ mice, ten in ASF⁵ + Oligo-MM¹² mice and fifteen in ASF⁵ + CON mice.

Next, we aimed to study CR in these three mouse groups. Therefore, we infected mice with 10^6 CFU *S. Tm^{avir}* and determined the bacterial load at d1 p.i. in feces and at d2 p.i. in cecum content and mLN. We also determined the relative cecal weight at d2 p.i.

At day 1 p.i., total pathogen loads were significantly reduced in feces from ASF⁵ + Oligo-MM¹² mice compared to the ASF⁵ mice (**Figure 15A**, p-value 0.0079) showing that Oligo-MM¹² consortium increases CR of ASF⁵-colonized mice. Interestingly, there was no significant difference between the ASF⁵ + Oligo-MM¹² and the ASF⁵ + CON mice. At day 2 post-infection, *S. Tm^{avir}* loads were still significantly lower in ASF⁵ + Oligo-MM¹² mice compared to ASF⁵ mice (**Figure 15B**). Similarly, in mLN, *S. Tm^{avir}* loads were intermediate in ASF⁵ + Oligo-MM¹² mice (**Figure 15C**). Relative cecal weight was significantly reduced in ASF⁵ + Oligo-MM¹² mice. Mice transplanted with CON microbiota exhibited a low relative cecal weight which is in the normal range of conventional mice (**Figure 15D**) (Stecher, Chaffron et al. 2010).

These data indicate that the Oligo-MM¹² consortium partially restored CR against *S. Tm^{avir}*. Furthermore, the data suggest that a number of strains from a conventional microbiota are still missing in order to provide full colonization resistance. However, our data indicated that microbiota complexity positively correlates with CR. This could be due to the higher metabolic and functional diversity of a more complex microbiota.

In order to test this idea, we analyzed and compared the functionome of each microbial consortium using metagenomics analysis.

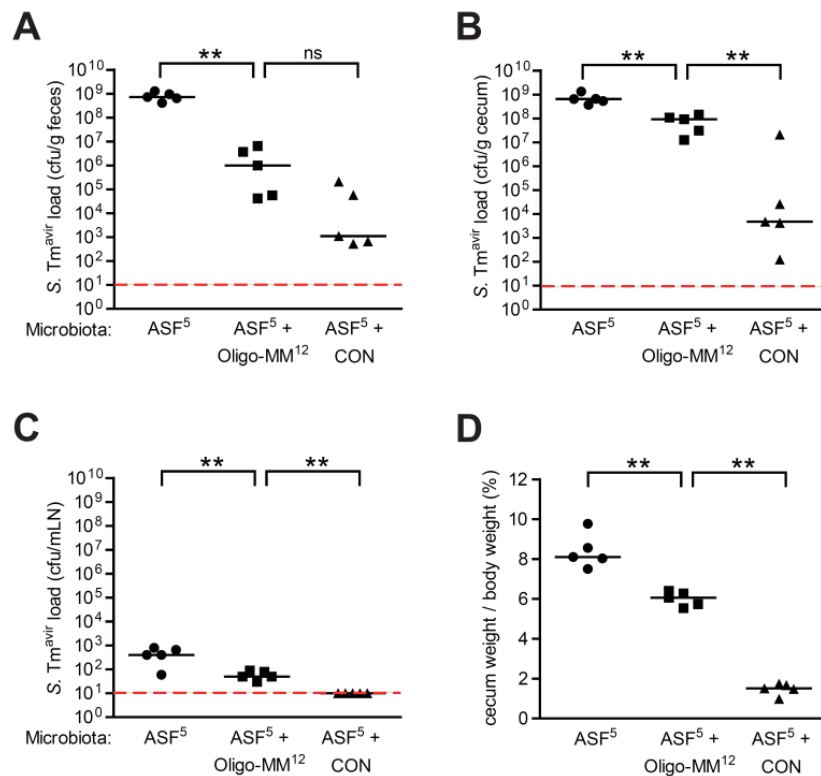


Figure 15. Oligo-MM¹² consortium partially restores colonization resistance against *S. Tm^{avir}*.

S. Tm^{avir} load at day 1 p.i. in (A) feces and at day 2 p.i. in (B) cecum and (C) mesenteric lymph nodes (mLN). (D) Relative cecal weight at day 2 p.i. Dotted lines: detection limit. Bars indicate medians. Mann-Whitney U test: ns=not significant ($P \geq 0.05$), ** $P < 0.01$. One-way ANOVA Kruskal-Wallis test: (A) $P=0.0045$, (B) $P=0.0025$, (C) $P=0.0024$, (D) $P=0.0019$.

4.5. Functional analysis correlates functional capacity of intestinal microbiota and CR against *Salmonella*

To analyze and compare the functionome of each microbial consortium, we first performed whole-genome shotgun sequencing of each Oligo-MM strains. Using either single shotgun genomes of Oligo-MM and ASF strains (Wannemuehler, Overstreet et al. 2014) or metagenomes of conventional mice (JCVI 2013, Nanjing University 2013, Milk 2014, Wang, Linnenbrink et al. 2014), we generated artificial metagenomes which correspond to the three experimental communities: ASF⁵, ASF⁵ + Oligo-MM¹² and ASF⁵ + CON. To determine the presence and completeness of functional modules in each community, predicted protein sequences were aligned against the Kyoto Encyclopedia of Genes and Genomes (KEGG) database (Ogata, Goto et al. 1999) and gene families were organized into different functional units (Kanehisa, Goto et al. 2014).

We found that, ASF⁵ + CON community encodes proteins belonging to more functional modules than ASF⁵ + Oligo-MM¹² and ASF⁵, in decreasing order (**Figure 16**). This observation positively correlates with gut microbiota complexity and CR against *S. Tm^{avir}* (**Figures 13B and 15**). Based on this, we hypothesized that the more functional modules are present within a gut community, the higher is the functional capacity of the community and, therefore, the more CR against *S. Tm^{avir}* is observed. However, deciphering CR mechanisms appears challenging using functionome predictions based on complex gut communities.

Next, we aimed to study CR mechanisms by using decreased microbiota complexity based on ASF and Oligo-MM strains only.

A

1 2 3

1 2 3

| | |
|--|----------------------|
| Microbiota: 1. ASF ⁵ + CON | ■ module complete |
| 2. ASF ⁵ + Oligo-MM ¹² | ■ 1 block missing |
| 3. ASF ⁵ | ■ 2 blocks missing |
| | □ module not present |

Figure 16. Functionome analysis correlates functional diversity with colonization resistance.

Heat maps illustrating KEGG module presence predicted for each artificial metagenome. Briefly, single shotgun genome sequences of 5 ASF and 12 Oligo-MM strains were used to create artificial metagenomes (ASF⁵ and Oligo-MM¹², respectively). KEGG analysis was performed to analyze functional diversity of microbiota ASF⁵, ASF⁵ + Oligo-MM¹² and ASF⁵ + CON. A metagenome from 8 conventional mice was used (JCVI 2013, Nanjing University 2013, Milk 2014, Wang, Linnenbrink et al. 2014). **(A)** KEGG modules absent from ASF⁵ microbial consortium and fully or partially present in ASF⁵ + CON and ASF⁵ + Oligo-MM¹², respectively. **(B)** KEGG modules predicted as present in all three microbial communities, except of putative peptide transport system (M00583) which is only present in ASF⁵ + Oligo-MM¹² community. Each line represents one KEGG module. Color code refers to completeness indicator of KEGG module: dark green: module complete; light green: 1 block missing; apple-green: 2 blocks missing and white: module not present. 1: ASF⁵ + CON; 2: ASF⁵ + Oligo-MM¹² and 3: ASF⁵.

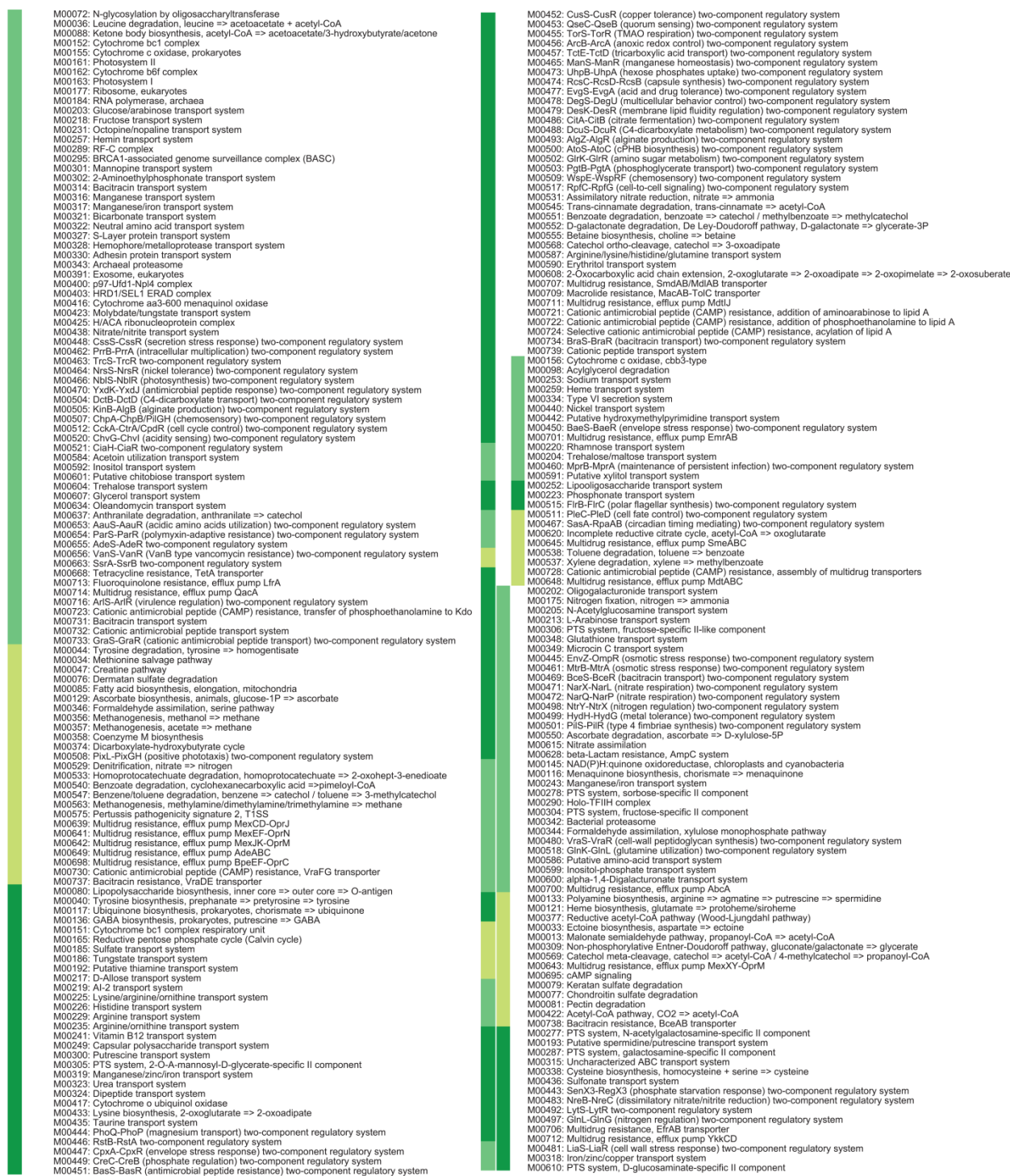
4.6. Colonization resistance of Oligo-MM¹² mice can be increased by transfer of ASF⁷

Our previous results showed that transplantation of the Oligo-MM¹² can increase CR of ASF⁵ mice against *S. Tm*^{avir} and that functional capacity of the microbiota community correlated positively with CR. In order to better study the correlation between CR and functionome, we used two well-defined microbiota: the Oligo-MM¹² and a consortium of eight ASF strains (ASF356, ASF360, ASF361, ASF457, ASF492, ASF500, ASF502, ASF519; ASF⁸). We first predicted and compared the functionome of CON community, the Oligo-MM¹² and the ASF⁸, using metagenomics and KEGG module analysis, as described in **Figure 16**.

We found that CON community encodes proteins belonging to more functional modules than Oligo-MM¹² and ASF⁸, in decreasing order (**Figure 17**). Interestingly, we also found that some functional modules are present in ASF⁸ community but absent from Oligo-MM¹² (**Figure 17A**).

Previously, we hypothesized that the more functional modules are present within a gut community and the more CR against *S. Tm*^{avir} is observed. Therefore, we aimed to generate a microbiota with increased number of functional modules by transplanting Oligo-MM¹² mice with ASF⁸ microbiota.

A



Microbiota: 1. CON
2. Oligo-MM¹²
3. ASF⁸

■ module complete
■ 1 block missing
■ 2 blocks missing
■ module not present

B



Figure 17. Functionome analysis correlates microbiota complexity with functional diversity.

KEGG analysis was performed to analyze functional diversity of microbiota ASF⁸, Oligo-MM¹² and CON. **(A)** Heat maps illustrating KEGG module presence predicted for each artificial metagenome. **(B)** KEGG modules predicted as present in all three microbial communities, except of putative peptide transport system (M00583) which is only present in Oligo-MM¹² community. Each line represents one KEGG module. Color code refers to completeness indicator of KEGG module: dark green: module complete; light green: 1 block missing; apple-green: 2 blocks missing and white: module not present. 1: CON; 2: Oligo-MM¹² and 3: ASF⁸.

To test whether transplantation of Oligo-MM¹² mice with additional ASF strains would influence functionome predictions and CR, we used mice stably colonized with four ASF strains (ASF356, ASF361, ASF502, ASF519; ASF⁴) and mice stably colonized with the twelve Oligo-MM strains (Oligo-MM¹²). ASF⁴ and Oligo-MM¹² mice were bred in different isolators and mice were transferred into gnotocages prior to the start of the experiment. In order to test whether transplantation of additional bacterial strains may influence CR, we inoculated a consortium of seven ASF strains (ASF356, ASF360, ASF361, ASF457, ASF500, ASF502, ASF519; ASF⁷) in either ASF⁴ or Oligo-MM¹² mice. In addition, we transplanted ASF⁴ and Oligo-MM¹² mice with sterile media, as controls (**Figure 18A**). Frozen inoculum of ASF⁷ was prepared as described in **Materials & Methods (3.2.2.4.)**. After inoculation, the microbiota was allowed to stabilize for 40 days in gnotocages under germfree conditions. To analyze microbiota composition, feces were sampled at day 40 post-inoculation, fecal DNA was extracted and microbiota composition was analyzed by qPCR. At day 40 post-inoculation, all mice were orally infected with 5×10^6 CFU *S. Tm*^{avir}. Total pathogen loads were determined at day 1 post-infection (d1 p.i.) in feces and at d2 p.i. in cecal content and in the mLN. We also calculated the relative cecal weight as a marker of microbiota complexity.

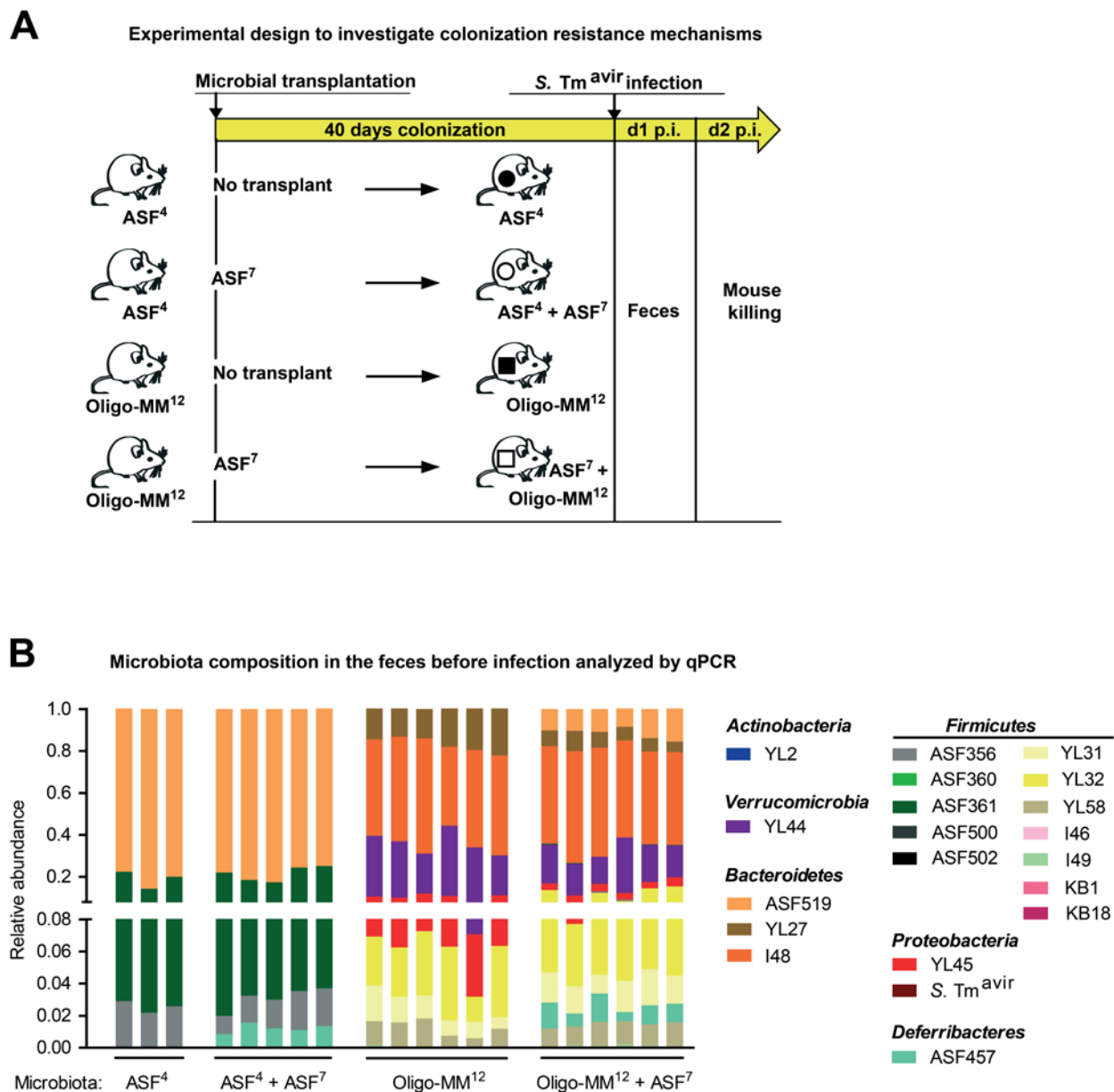


Figure 18. Establishment of gnotobiotic mice harboring an increased microbiota complexity.

(A) Experimental design. C57Bl/6 mice harboring either 4 ASF strains (ASF356, ASF361, ASF502 and ASF519; ASF⁴) or 12 Oligo-MM strains (YL2, YL27, YL31, YL32, YL44, YL45, YL58, KB1, KB18, I46, I48, I49; Oligo-MM¹²) were either inoculated with 7 ASF strains (ASF⁴ + ASF⁷, 5 mice; empty circle and Oligo-MM¹² + ASF⁷, 6 mice; empty square, respectively) or sterile media as control (ASF⁴, 3 mice; circle and Oligo-MM¹², 6 mice; square, respectively). Seven ASF strains were orally and rectally inoculated with 6 ASF strains prepared as a frozen stock (ASF356, ASF360, ASF361, ASF457, ASF502, ASF519) and 1 ASF (ASF500) as actively growing culture. After 40 days, mice were orally infected with 6×10^6 CFU *S. Tm*^{avir}. Feces was sampled at day 1 post-infection (p.i.). At day 2 p.i., mice were sacrificed and organs sampled. Relative cecal weight was determined at day 2 p.i. (B) Fecal microbiota composition was determined using a hydrolysis probe based quantitative PCR assay. Data are shown as relative abundance. One column represents one mouse.

At day 40 post-inoculation, three bacterial strains were detected by qPCR in fecal samples of ASF⁴-colonized mice, four in ASF⁴ + ASF⁷, seven in Oligo-MM¹² and twelve in Oligo-MM¹² + ASF⁷ (**Figure 18B**). Six bacterial strains (ASF360, ASF500, ASF502, YL2, I46, KB18) were never detected and two (I49 and KB1) were only found in feces at low levels.

At day 1 p.i., total pathogen loads were significantly reduced in feces from Oligo-MM¹²-colonized mice compared to ASF⁴ mice showing that stable colonization with the Oligo-MM¹² consortium confers CR against *S. Tm^{avir}* (**Figure 19A**, p-value 0.0275). Surprisingly, ASF⁴ mice harbouring three additional ASF strains (ASF⁴ + ASF⁷ mice) had higher pathogen loads compared to the Oligo-MM¹² mice (p-value 0.0043). This suggests that, in this case, the three additional ASF strains ASF360, ASF457 and ASF500 (with only ASF457 being detected by qPCR) decreased CR against *S. Tm^{avir}*. At day 2 p.i., *S. Tm^{avir}* loads were still significantly lower in Oligo-MM¹² mice as compared to ASF⁴ mice (**Figure 19B**, p-value 0.0238). Similarly, *S. Tm^{avir}* loads were significantly lower in Oligo-MM¹² + ASF⁷-colonized mice as compared to ASF⁴ + ASF⁷-colonized mice (p-value 0.0043). Strikingly, pathogen loads were significantly lower in mice harbouring the Oligo-MM¹² + ASF⁷ consortium as compared to their Oligo-MM¹²-colonized littermate controls (p-value 0.0043) suggesting that the increase of microbiota complexity correlates with the increase in CR, in this case. Thus, the addition of ASF strains can only increase CR in the context of the Oligo-MM¹². This suggests that ASF strains might occupy different niches in ASF⁴-colonized mice as compared to Oligo-MM¹² mice. Interestingly, very low or no pathogen colonization was observed in mLN of Oligo-MM¹²- and Oligo-MM¹² + ASF⁷-colonized mice, respectively, whereas mLN of ASF⁴- and ASF⁴ + ASF⁷-colonized mice were significantly higher colonized by *S. Tm^{avir}*, as compared to Oligo-MM¹²-colonized mice (**Figure 19C**, p-values 0.0357 and 0.0079, respectively). Relative cecal weight was significantly reduced in Oligo-MM¹²- and Oligo-MM¹² + ASF⁷-colonized mice as compared to ASF⁴- and ASF⁴ + ASF⁷-colonized mice (**Figure 19D**).

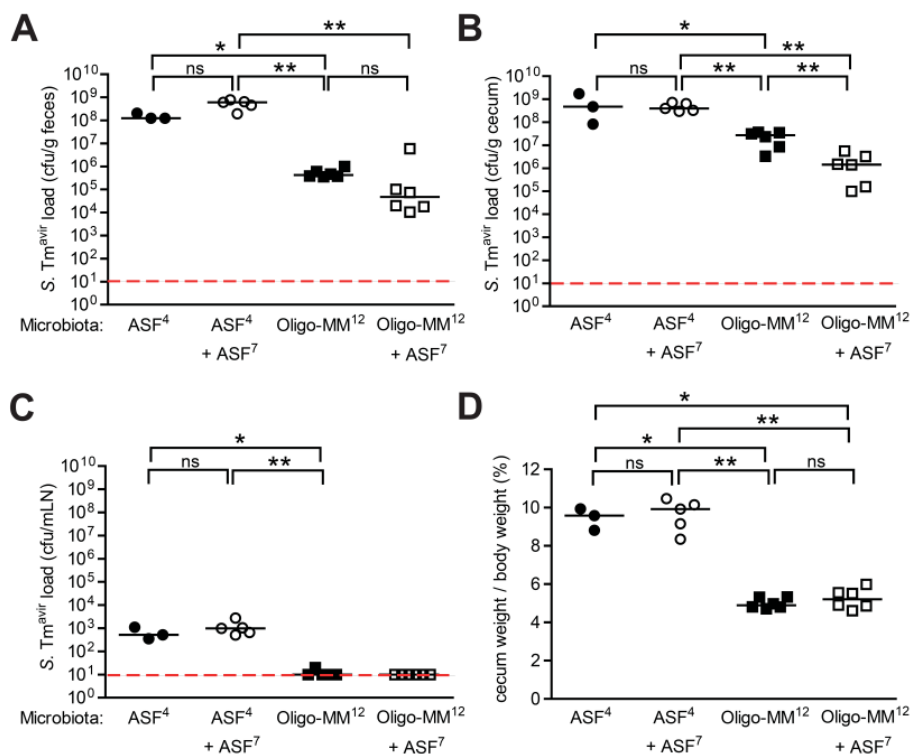


Figure 19. Microbiota complexity correlates with increased colonization resistance against *S. Tm^{avir}*.

S. Tm^{avir} load at day 1 p.i. in (A) feces and at day 2 p.i. in (B) cecum and (C) mesenteric lymph nodes (mLN). (D) Relative cecal weight at day 2 p.i.. Dotted lines: detection limit. Bars represent medians. Mann-Whitney U test: ** $P < 0.01$. One-way ANOVA Kruskal-Wallis test: (A) $P = 0.0013$, (B) $P = 0.0009$, (C) $P = 0.0013$, (D) $P = 0.0028$.

In conclusion, these results clearly show that Oligo-MM¹²-colonized groups are more resistant against *S. Tm^{avir}* colonization than ASF⁴-colonized groups.

In order to investigate potential CR mechanisms, we analyzed and compared the functionome of each microbiota using metagenomics and KEGG module analysis as described in **Figure 16**. We hypothesized that analyzing these well-defined consortia combined with their respective CR phenotypes observed during *S. Tm^{avir}* infection would help us deciphering potential functional modules responsible for CR against *S. Tm^{avir}*.

We found that Oligo-MM¹² + ASF⁷ community encodes proteins belonging to more functional modules than Oligo-MM¹², ASF⁴ + ASF⁷ and ASF⁴, in decreasing order (**Figure 20A**). As previously noticed in **Figure 16**, this observation correlates with gut microbiota complexity and CR property against *S. Tm^{avir}* (**Figures 18B and 19B**). When comparing Oligo-MM¹²- with ASF⁴-colonized mouse groups, the analysis revealed that functional modules pointed out in block “B” was present in Oligo-MM¹²- but not in ASF⁴-colonized mouse groups (**Figure 20B**). Combined with *S. Tm^{avir}* infection experiment (**Figure 19**),

it suggests that either a part or all of these functional modules (*e.g.* nitrate respiration and osmotic stress response) may be implicated in CR mechanisms against *S. Tm^{avir}*. When comparing Oligo-MM¹² + ASF⁷ and Oligo-MM¹² communities, we found that encoded proteins belonging to functional modules showed in block “D” are present in Oligo-MM¹² + ASF⁷-colonized mice but not in Oligo-MM¹² community (**Figure 20D**). Together combined with *S. Tm^{avir}* infection experiment (**Figure 19**), it suggests that functional modules found in this “D” block (*e.g.* type VI secretion system and envelope stress response) may be important for CR. We have previously shown that *S. Tm^{avir}* loads in feces, cecal content and mLN of ASF⁴- and ASF⁴ + ASF⁷-colonized mice were similar (**Figure 19A-C**). According to this functionome analysis, ASF⁴ + ASF⁷ community showed encoded proteins belonging to functional modules presented in block “C” and in a subpart of block “D” which are absent of ASF⁴ community (**Figure 20C,D**) which suggests that these functional modules may not play a direct role in CR against *S. Tm^{avir}*. As an example, type VI secretion system might not be a good candidate involved in CR mechanisms against *S. Tm^{avir}* or may be differentially activated in the context of Oligo-MM¹² + ASF⁷ mice as compared to ASF⁴ + ASF⁷-colonized mice.

We conclude that by using this approach, we are able to generate hypotheses about potential pathways and functions involved in CR.

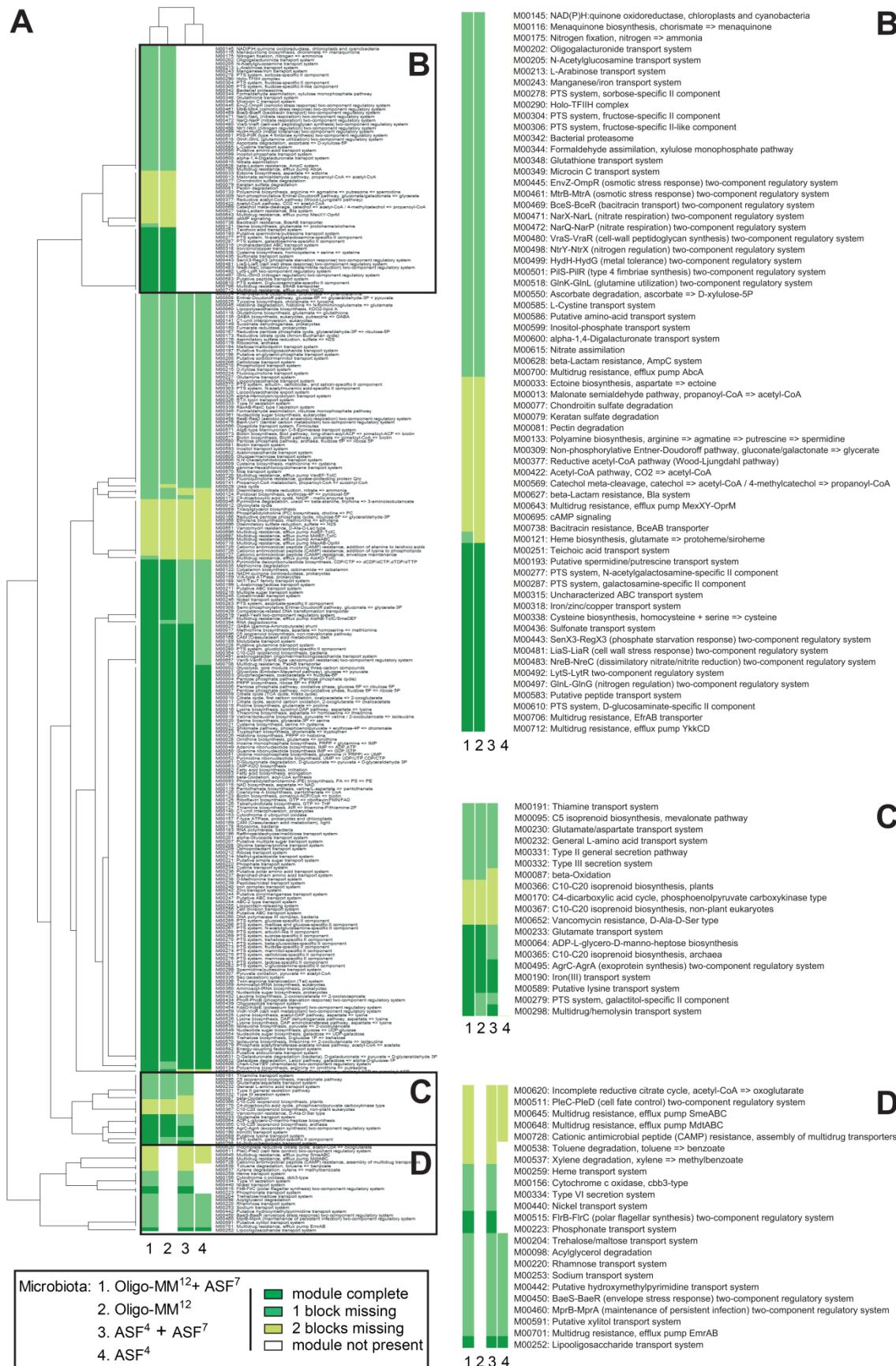


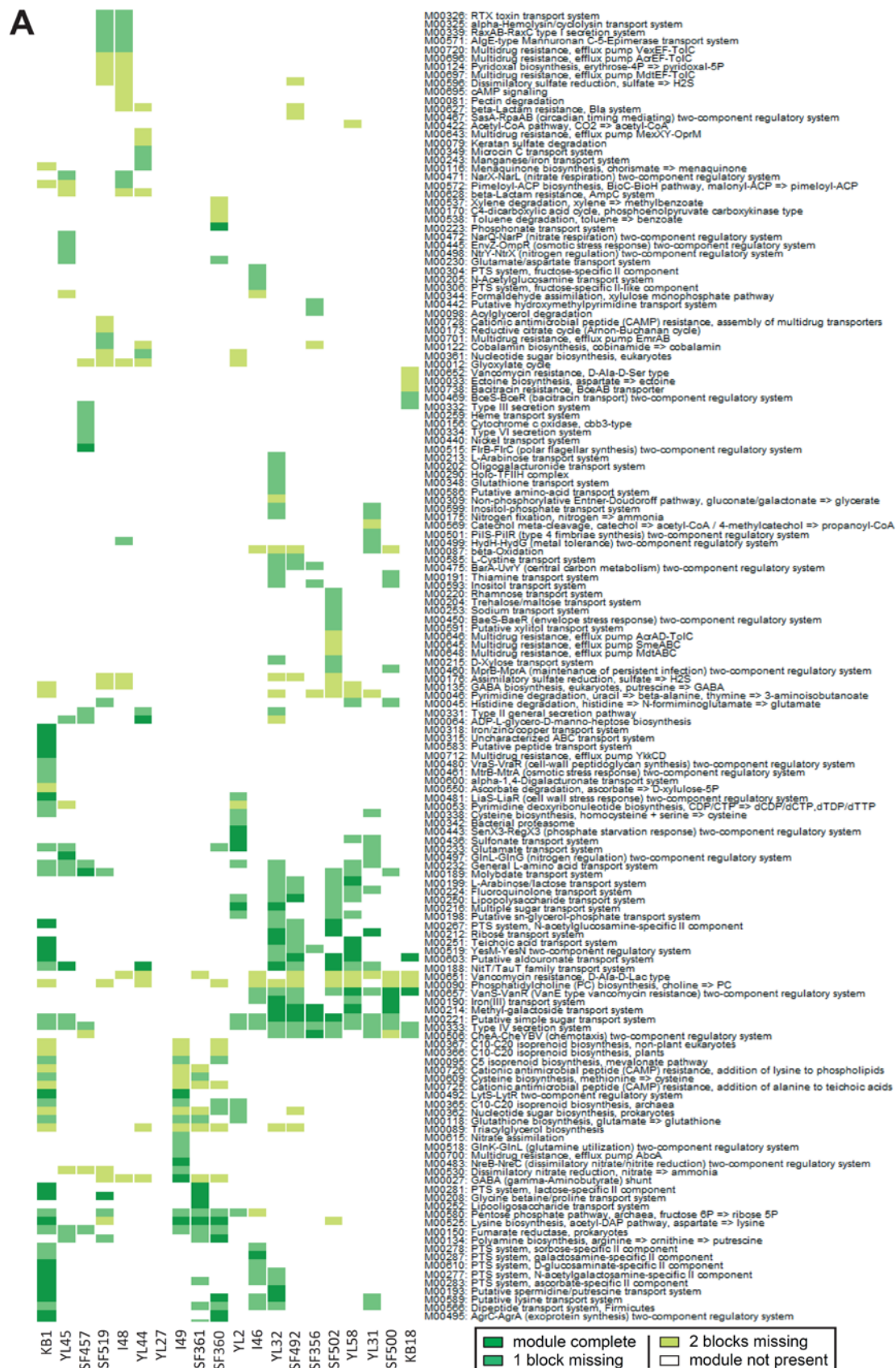
Figure 20. Functionome analysis indicates potential metabolic pathways involved in CR against *S. Tm*

KEGG module analysis was performed to analyze functional capacity of ASF⁴, ASF⁴ + ASF⁷, Oligo-MM¹² and Oligo-MM¹² + ASF⁷ microbiota. *In silico* assemblies (artificial metagenomes) of individual genome sequences were generated. **(A)** Overview. Heat map illustrating presence and absence of KEGG modules in each artificial metagenome. **(B-D)** Zoom in of rectangles. **(B)** Modules only present in Oligo-MM¹²-colonized groups. **(C)** Modules absent from ASF⁴ mice and present in other groups. **(D)** Modules entirely or partially present in ASF-colonized groups. Each line represents one KEGG module. Color code refers to completeness indicator of KEGG module: dark green: module complete; light green: 1 block missing; apple-green: 2 blocks missing and white: module not present. 1: Oligo-MM¹² + ASF⁷; 2: Oligo-MM¹²; 3: ASF⁴ + ASF⁷ and 4: ASF⁴.

Next, we aimed to decipher single bacterial strains involved in CR against *S. Tm*. To this end, we combined previous results from functional analysis of artificial metagenomes with functional analysis of single ASF and Oligo-MM strains.

Firstly, we found that some KEGG modules potentially involved in CR against *S. Tm*^{avir} were specific to few strains only (**Figure 21A**). For example, KEGG module predicted to be involved in envelope stress response (M00450) is only found in ASF502; KEGG modules predicted to be involved in osmotic stress response (M00445 and M00461) are only present in YL45 and KB1, respectively. More generally, KEGG modules predicted to encode proteins involved in respiration, dissimilation, reduction or assimilation of nitrate are present in the bacterial strains YL45, I48, I49, ASF457 and ASF519 (**Figure 21A**). Secondly, we found that some KEGG modules were more likely specific of either Gram-positive or Gram-negative strains (blocks “C” and “D”, respectively) (**Figure 21B**). Finally, other KEGG modules (block “E”) were mostly predicted as conserved functions in all bacterial strains (**Figure 21B**). Importantly, the incompleteness of KEGG modules (*i.e.* one or two block missing) could be due to sequencing errors or incomplete databases. Most likely, the genomes of these organisms contain a high fraction of genes with unknown functions, which remains to be described. All together, these observations suggest that CR might be explained by the presence or the absence of certain KEGG modules.

In conclusion, further experiments are required to determine the contribution of individual strains and their functions in CR against *S. Tm*.



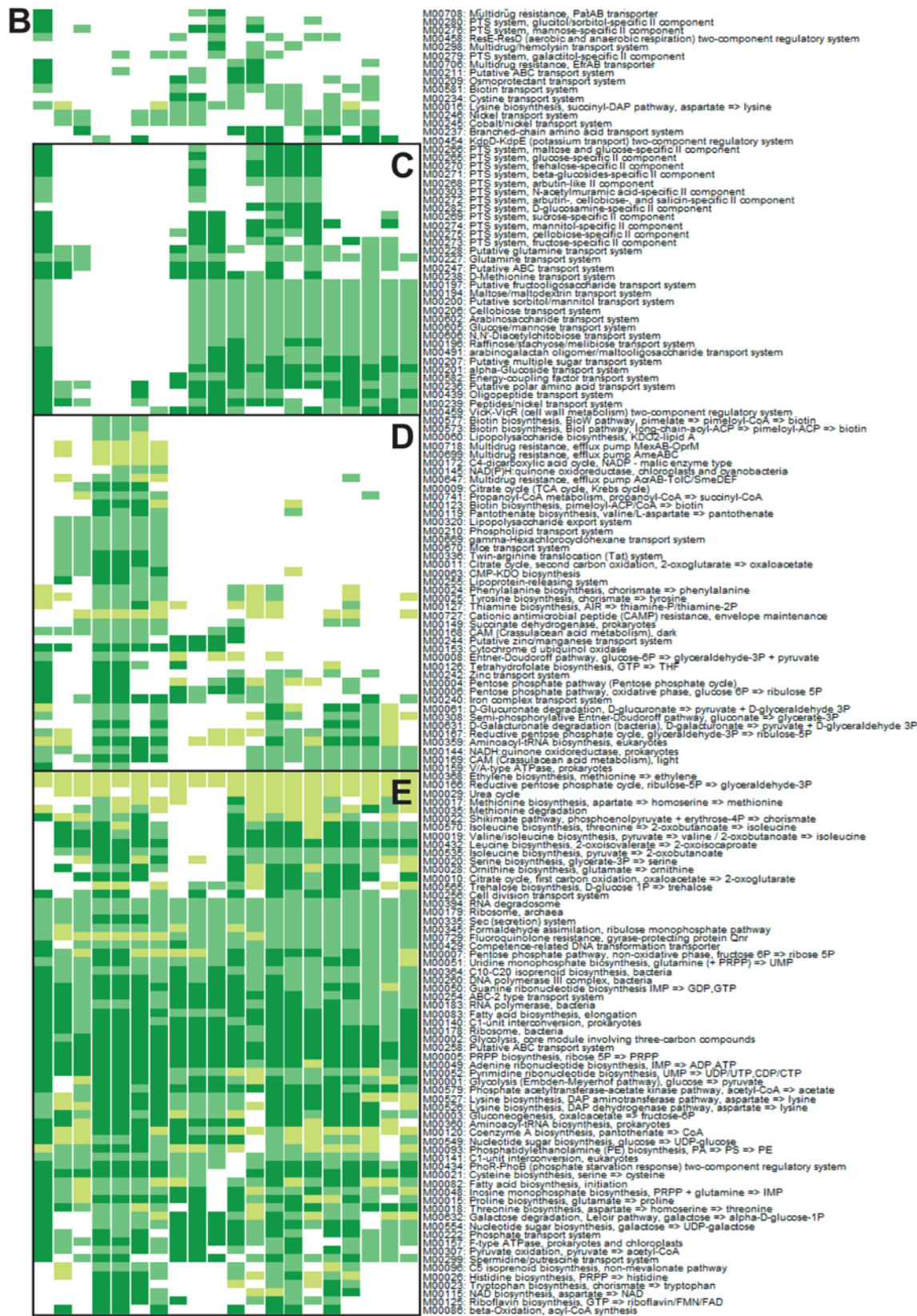


Figure 21. KEGG module analysis of single ASF and Oligo-MM strains.

Heat map illustrating the functionome analysis of 8 ASF strains (ASF356, ASF360, ASF361, ASF457, ASF492, ASF500, ASF502 and ASF519) and 12 Oligo-MM strains (YL2, YL27, YL31, YL32, YL44, YL45, YL58, KB1, KB18, I46, I48, I49) using KEGG analysis. **(A)** Modules mostly specific of few strains. **(B)** Modules present or absent in all strains and mainly present in Gram-positive strains (block **C**), Gram-negative strains (block **D**) or conserved (block **E**). Each line represents one KEGG module. Color code refers to completeness indicator of KEGG module: dark green: module complete; light green: 1 block missing; apple-green: 2 blocks missing and white: module not present. Each column represents one strain.

To conclude, using this well-defined experimental design combined with metagenomics and functionome analyses, we generated new hypotheses and isolated functional modules which could be involved in CR against *S. Tm*^{avir}. As an example, we showed that nitrate respiration and stress responses may be potentially involved in CR mechanisms (**Figures 19 and 20**). We also pointed at other pathways specific to conventional microbiota, which remain to be described (**Figures 15 and 16**). Finally, we demonstrated that the Oligo-MM model is a powerful tool to study CR mechanisms using metagenomics, functionome analysis, qPCR, 16S rRNA gene-based amplicon sequencing and single strain cultivation.

4.7. Establishment of a fluorescence *in situ* hybridization assay to detect, localize and quantify individual Oligo-MM strains

The majority of research groups studies gut microbiota composition by gDNA extraction-based approaches such as qPCR and 16S rRNA gene amplicon sequencing. However, it becomes more and more apparent that such techniques misestimate the true ratio between Gram-positive and Gram-negative bacteria, as Gram-positive bacteria are partially refractory to cell lysis in DNA extraction protocols. This leads to underestimate the abundance of Gram-positive strains. Moreover, such techniques do not provide any information on bacterial localization in the gut, which impedes ecological and interactional studies.

In order to detect and localize single bacterial strains in tissue sections, we established a fluorescence *in situ* hybridization (FISH) assay. To quantify the abundance of specific bacterial populations and confirmed gDNA extraction-based data, we also developed a computational approach using the software digital image analysis in microbial ecology (DAIME) (Daims, Lucker et al. 2006).

FISH was performed as described in **Materials & Methods (3.2.3.15.)**. Briefly, full-length 16S rRNA genes of ASF and Oligo-MM strains were computationally aligned and specific probes were designed using CLC DNA Workbench 6.0.2 software. To increase the fluorescence signal, each oligonucleotide probe was double-labelled with either fluorescein isothiocyanate (FITC) or cyanine 3

(Cy3). To target the entire eubacterial population, a 1:1 mixture of Eub338 I (Amann, Binder et al. 1990) and Eub338 III (Daims, Bruhl et al. 1999) (Eub338 I/III) was double-labelled with cyanine 5 (Cy5). After optimization of fluorescence signal using formamide concentration series (**Table 34**), probe specificity was tested on all other strains. FISH was performed on PFA-fixed cecal cryosections and images were taken using confocal microscopy. Images were analyzed using the DAIME software (Daims, Lucker et al. 2006). It is known that intestinal cells and plant fibers emit auto-fluorescence which hampers computational image analysis. In order to deplete this unspecific auto-fluorescent background, FITC and Cy3 channels were subtracted from Cy3 and FITC channels, respectively, using the DAIME software.

Gut environment harbors different bacterial niches. For example, microbiota composition of mucus layer differs from the gut lumen (Li, Limenitakis et al. 2015). First, we wanted to test whether we could detect mucosal enrichment of a bacterial population using this approach. It is known that *Akkermansia muciniphila* is able to degrade mucin (Derrien, Vaughan et al. 2004). Therefore, we used the Oligo-MM strain YL44. We hypothesized that YL44 might be enriched at the cecal mucus layer.

To confirm that Muc1437 probe allowed detection of YL44 *in vivo*, we used gnotobiotic mice colonized with a low complexity microbiota (LCM) as negative control and LCM mice colonized with YL44 (LCM + YL44) for 21 days, as positive control. We performed FISH and DAIME analysis on these mice as well as on Oligo-MM¹²-colonized mice (Oligo-MM¹²) to analyze the distribution of bacterial population across cecal cross-sections. Sections were hybridized with Muc1437-Cy3 and Eub338 I/III-Cy5, and then DNA was stained with DAPI. Confocal images were taken and merged images were virtually sliced from the epithelial border to the gut lumen (40 μm thick) and slicer templates were applied to grey level images (**Figure 22D-F**). Biovolume of targeted bacterial population (Muc1437-Cy3⁺) was calculated relative to biovolume of all Eub338 I/III-Cy5⁺ population.

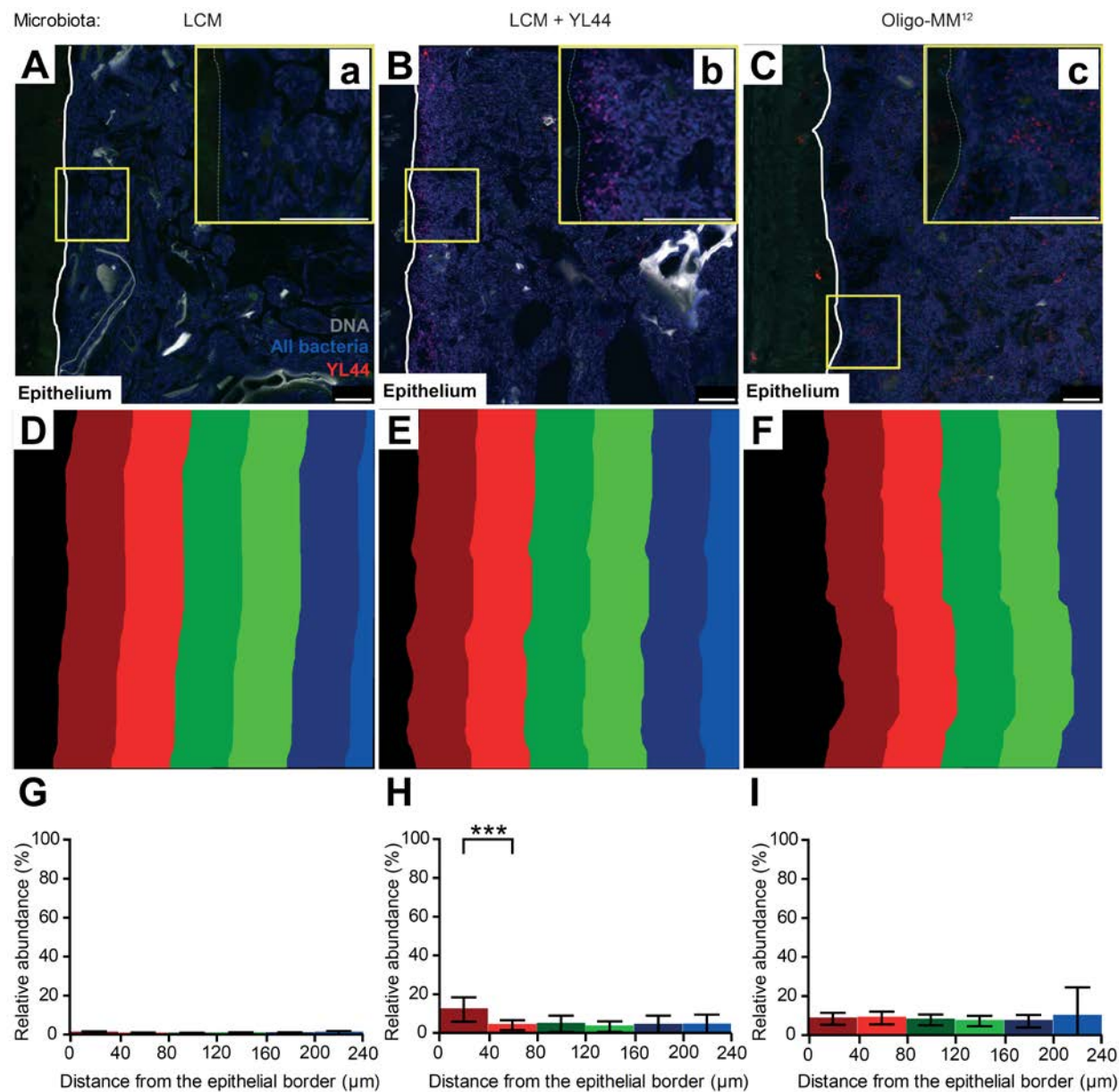


Figure 22. Establishment of a FISH assay to localize and quantify single strains in the Oligo-MM¹² mouse gut.

Gnotobiotic mice stably colonized with a low complexity microbiota (LCM) (**A**, **D**, **G**) were inoculated with YL44 for 21 days (LCM + YL44) (**B**, **E**, **H**). Mice were stably colonized with 12 Oligo-MM strains (I46, I48, I49, KB1, YL2, YL27, YL31, YL32, YL44, YL45, YL58, KB18; Oligo-MM¹²) (**C**, **F**, **I**). Upper right squares in **A-C** are the respective zoom in. (**A-C**) FISH on PFA-fixed cecal cryosections targeting all bacteria (Eub338-I/III, blue), YL44 (Muc1437, red) or gDNA (DAPI, grey). Scale bars: 25 μm. White line: epithelial border. (**D-F**) Slicer template generated by DAIME. Same magnification as for (**A-C**). Colors represent the different virtual layers from the epithelial border (dark red) to the gut lumen (light blue). Thickness: 40 μm. (**G-I**) YL44 biovolume quantification relative to Eub338 probe signal using DAIME in (**G**) LCM-colonized mouse (3 mice, 12 pictures), in (**H**) LCM + YL44-colonized mouse (3 mice, 34 pictures) or in (**I**) Oligo-MM¹²-colonized mice (5 mice, 33 pictures). Detection limit is given by signal detected in (**G**): 0.65 %. Data are given as mean and standard deviation. Mann-Whitney U test: *** $P < 0.001$. One-way ANOVA Kruskal-Wallis test: (**G**) $P = 0.6514$, (**H**) $P < 0.0001$, (**I**) $P = 0.0643$.

On cecal cross-sections of LCM-colonized mice, we observed low Muc1437 signal (**Figure 22A,G**). As this signal was not co-localized with Eub338 I/III signal, we concluded that the signal derived from unspecific binding of the probe to the cecal content, which might be due to the fluorophore itself (Cy3, in this case). We confirmed this hypothesis using another fluorophore (FITC) which appeared to exhibit less unspecific binding (data not shown). On cecal sections of LCM + YL44-colonized mice, we observed that Muc1437 probe hybridized to small coccoid bacterial cells similar to YL44 which seemed to be enriched at the epithelial border (**Figure 22B**). When calculating YL44 relative biovolume, we confirmed that YL44 was significantly enriched between 0 and 40 μm from the epithelial border compared to deeper layers within the lumen (**Figure 22H**). However, on cecal sections of Oligo-MM¹²-colonized mice, YL44 was homogeneously distributed in cecal cross-section (**Figure 22C**). This was confirmed by the relative biovolume showing no enrichment between 0 and 240 μm from the epithelial border (**Figure 22I**).

To sum up, we established a new approach combining FISH and DAIME analysis in order to specifically detect and quantify a bacterial population through cecal cross-sections. We showed that YL44 was enriched at the epithelial border in LCM + YL44-colonized mice but not in Oligo-MM¹²-colonized mice. This suggests that the distribution of YL44 bacterial population in mouse cecum is dependent on microbial context.

Due to different composition of their cell wall, Gram-negative and Gram-positive bacteria exhibit distinct cell wall permeability. This can also affect bacterial lysis during gDNA extraction, which is used for qPCR or 16S rRNA gene-based microbiome analysis (Salonen, Nikkila et al. 2010, Maukonen, Simoes et al. 2012). Therefore, we wanted to validate this approach for a Gram-positive strain assigned to the Lachnospiraceae family (YL58). By FISH, we aimed at comparing relative biovolumes of YL58 and YL44 which are Gram-positive and -negative strains, respectively, with relative 16S rRNA gene copy abundance determined using qPCR and 16S rRNA gene-based amplicon sequencing in stably colonized Oligo-MM¹² mice. To specifically target YL58, we designed probe YL58_180 (**Table 4**). In order to test binding specificity, we used another negative control approach and designed the YL58_180_negctrl probe. YL58_180_negctrl probe is the reverse-complement sequence of YL58_180 and is not targeting any of the Oligo-MM strains. Finally, we compared the relative abundance of 16S rRNA gene copy numbers with the relative biovolume for both strains. All three analyses were performed on Oligo-MM¹² mice (**Figure 23**).

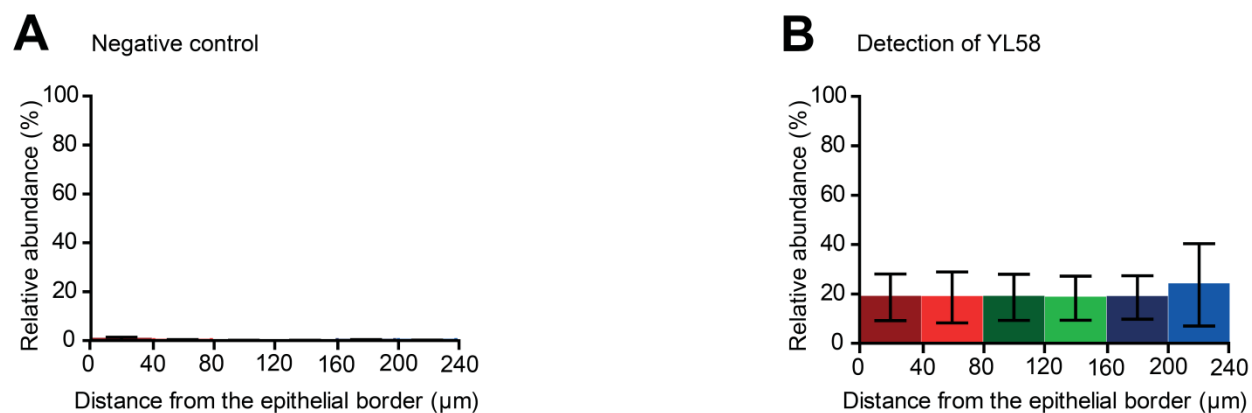


Figure 23. Detection and relative quantification of, YL58, a Gram-positive strain present in Oligo-MM¹² mouse cecum.

FISH on PFA-fixed cecal cryosections of Oligo-MM¹² mice targeting all bacteria (Eub338-I/III), gDNA (DAPI) and either none as negative control (YL58_180_negctrl, reverse complement probe of YL58_180) (A) or YL58 (YL58_180) (B). (A) Background and unspecific signal relative to Eub338-I/III signal quantified using DAIME (3 mice, 9 images). (B) YL58 biovolume quantification relative to Eub338-I/III signal using DAIME (5 mice, 39 images). Colors represent the different virtual layers from the epithelial border (dark red) to the gut lumen (light blue). Thickness: 40 μm. Detection limit is given by signal detected in (A): 0.17 %. Data are presented as mean and standard deviation. One-way ANOVA Kruskal-Wallis test: (A) $P=0.2248$, (B) $P=0.7612$.

We found that YL58 was homogeneously distributed in Oligo-MM¹²-colonized mice between 0 and 240 μm from the epithelial border (Figure 23). As the FISH and DAIME analysis were not performed on all Oligo-MM strains, biovolume data were determined as relative to Eub338 I/III signals. Therefore, we could not directly compare gDNA-extraction and rRNA-based approaches. Interestingly, we could show that $26.1\pm 6.1\%$ and $24\pm 7.7\%$ 16S rRNA gene copy abundance of YL44 were detected using qPCR and 16S rRNA gene-based amplicon sequencing, respectively, whereas about $8.3\pm 5\%$ was detected using FISH (Figure 24). We also found that $0.34\pm 0.09\%$ and $0.24\pm 0.07\%$ 16S rRNA gene copy abundance of YL58 were detected using qPCR and 16S rRNA gene-based amplicon sequencing, respectively, whereas more than 20 % was detected using FISH.

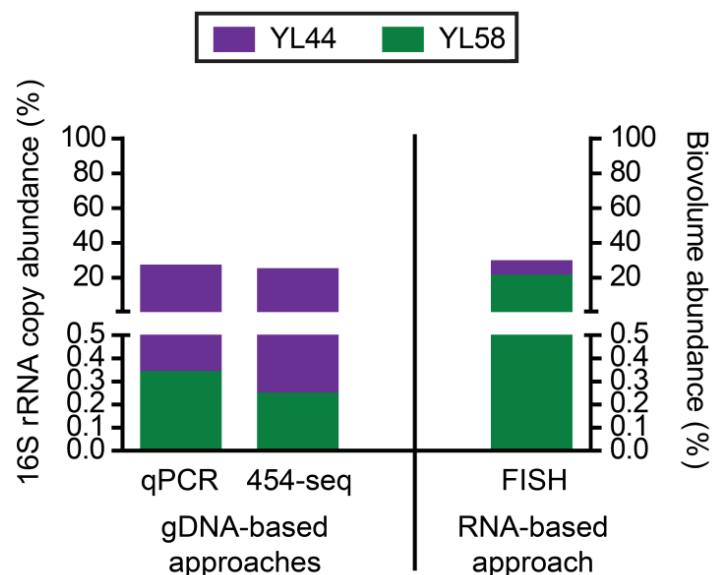


Figure 24. Detection and relative quantification of YL58 and YL44 by FISH analysis reveals misestimation of this strain using gDNA-based quantitative approaches.

Quantitative real-time PCR (qPCR), amplicon sequencing (454-seq) and FISH were performed on the same Oligo-MM-colonized mice ($n = 4$, F2 generation, 8-9 weeks old females) in order to compare different analysis methods. Fecal gDNA were extracted using a modified QIAmp DNA Stool kit protocol including a bead-beating step and relative bacterial abundance was determined by qPCR and amplicon sequencing, as described in **Figures 9 and 12**. Relative abundance of 16S rRNA gene copies is given in percentage. FISH was performed as previously described (see **Figures 22 and 23**) on cecal cryosections. Relative biovolume abundance is given in percentage. Color code refers to the strain: purple: YL44 and green: YL58.

In conclusion, we validated FISH and DAIME analysis for a Gram-positive strain, YL58. We showed that in cecum of Oligo-MM¹²-colonized mice YL58 was equally distributed between 0 and 240 μm from the epithelial border. Moreover, our results point out at under- and over-estimation of the abundance of Gram-positive and -negative strains, respectively, using qPCR and 16S rRNA gene-based amplicon sequencing, as compared to FISH approach.

5. Results - The role of the mucus layer and the microbiota during *Salmonella enterica* serovar Typhimurium infection

The intestinal mucus layer is widely known to provide protection against enteric infections. Mucus-deficient mice were shown to be more susceptible to infection with enteric pathogens such as *Citrobacter rodentium* and *Salmonella enterica* serovar Typhimurium (*S. Tm*) as compared to heterozygous mice (Bergstrom, Kissoon-Singh et al. 2010, Zarepour, Bhullar et al. 2013). However, mucus-deficient mice also develop spontaneous colitis already at young age, which hampers analyzing the course of enteric pathogen infections and induction of inflammation (Van der Sluis, De Koning et al. 2006, Wenzel, Magnusson et al. 2014). Anterior gradient homolog 2 (AGR2) is a member of the protein disulfide isomerase family (Persson, Rosenquist et al. 2005). Expressed in mucus-producing cells, AGR2 is essential for correct folding and export of MUC2, the major component of the cecal and colonic mucus layer (Park, Zhen et al. 2009). Contrary to previous studies (Zhao, Edwards et al. 2010), we never observed spontaneous colitis of AGR2-deficient (AGR2^{ko}) mice in our animal facility.

The second chapter of this thesis deals with the role of the intestinal mucus layer and the microbiota in enteric *S. Tm* infection of AGR2^{ko} mice. We observed that streptomycin-treated AGR2-deficient (AGR2^{ko}) mice but not ampicillin-treated mice were protected against early *S. Tm*-induced colitis (day 1 p.i.) as compared to heterozygous littermate controls (AGR2^{het}). Analyses of the composition of the intestinal microbiota revealed that this protective effect might be due to a differential microbiota composition in AGR2^{ko} vs AGR2^{het} mice rather than the genetic background of the mice. Microbiome analyses of streptomycin- versus ampicillin-treated animals enabled us to narrow down potential protective candidates against *S. Tm*-induced colitis. In addition, by using GFP-reporters of *S. Tm* virulence gene expression, we could show that expression of the type III secretion system 1 (T3SS-1) was downregulated in the protected group and significantly less *S. Tm* were found to invade the mucosa of streptomycin-treated (sm-treated) AGR2^{ko} mice.

5.1. AGR2^{ko} mice exhibit a defect in MUC2 secretion in the cecal mucosa

In 2009, Park *et al.*, showed that AGR2 wild-type (AGR2^{wt}) mice secrete the intestinal mucin MUC2 but not AGR2^{ko} mice (Park, Zhen *et al.* 2009). In order to investigate whether AGR2^{het} mice also secrete MUC2 in cecum, we performed immunofluorescent staining of MUC2, a major component of the cecal mucus layer. As Bergström *et al.*, we found that cecal goblet cells of AGR2^{het} mice secreted MUC2 which was absent in AGR2^{ko} littermates (**Figure 25**) (Bergstrom, Berg *et al.* 2014). Thus, we decided to use AGR2^{het} mice as controls to study the role of the mucus layer in the AGR2^{ko} mouse model. In order to obtain a higher proportion of KO genotype in littermate experimental groups, we bred AGR2^{het} X AGR2^{ko} mice.

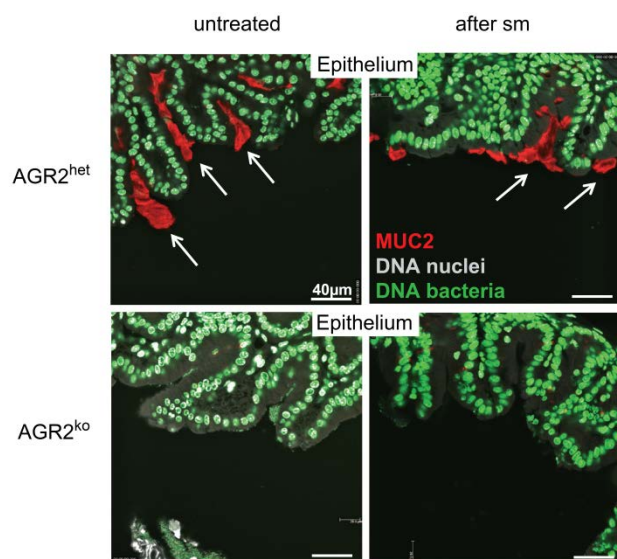


Figure 25. AGR2^{ko} mice show defective mucin secretion compared to AGR2^{het} littermate controls.

Immunofluorescent staining of MUC2 on paraffin embedded cecal sections of AGR2^{ko} and AGR2^{het} mice. Mice were sacrificed before (untreated) or 24 h after streptomycin treatment (sm-treated), cecal tissue was sampled, fixed in Carnoy's solution and embedded in paraffin. Immunofluorescent staining was performed on sections (5 µm thick) using DAPI (light grey) and sytox green (green) to visualize nuclei and bacterial DNA, respectively, as well as anti-MUC2 H-300 antibody (red) to visualize MUC2 production in goblet cells as well as intestinal secretions (arrows). Pictures were taken using confocal microscopy and are representatives of 2 independent experiments (5-6 mice per group, 3 pictures per mouse). Scale bar: 40 µm.

5.2. AGR2^{ko} mice show significantly attenuated inflammation 1 day post *S. Tm* infection compared to littermate controls in sm-treated mice

Because the intestinal microbiota is known to provide colonization resistance (CR) against *S. Tm* in specific pathogen-free (SPF) mice, we used streptomycin (sm) treatment to decrease microbiota density and allow *S. Tm* to colonize mouse intestine and induce colitis (Barthel, Hapfelmeier *et al.* 2003). To test whether mucins were still secreted in AGR2^{het} mice after sm-treatment, we also used immunofluorescent

staining targeted MUC2. We observed that sm-treated AGR2^{het} cecal epithelial cells were still covered by mucus layer while AGR2^{ko} were not showing MUC2 secretion (**Figure 25**).

It is already known that mice deficient in mucus secretion are more susceptible to infection with different enteric pathogens. However, it remains unclear whether this increased susceptibility to infections is correlated with spontaneous colitis. The lack of MUC2 allows the microbial community to come in direct contact with the epithelial border, penetrate deeply in the normally sterile crypt space or even invade into epithelial cells. This leads to spontaneous colitis in the majority of mucus-deficient mouse models such as Muc2^{ko}, AGR2^{ko} and Winnie mouse models (Van der Sluis, De Koning et al. 2006, Zhao, Edwards et al. 2010, Eri, Adams et al. 2011).

In order to determine whether AGR2^{ko} mice, which exhibit reduction of MUC2 secretion in the large intestine, are more susceptible to *S. Tm* infection as compared to AGR2^{het} littermates, we infected sm-pretreated mice with 10⁵ to 10⁶ CFU *S. Tm* wild-type (*S. Tm*^{wt}) harbouring a plasmid that encodes GFP under control of the SPI-2 promoter *pssaG* (*S. Tm*^{wt,gfp}). *S. Tm*^{wt,gfp} infection was performed one day after sm-treatment (25 mg/mouse). Mice were sacrificed and total pathogen loads were determined at days 1, 2 and 3 p.i. in cecal content and mesenteric lymph nodes (mLN). As markers of inflammation and pathology, we determined the inflammation marker lipocalin-2 (Lcn2) concentrations in cecal content and assessed cecal inflammation using a histopathological score, respectively. We also recorded the mouse weight over-time.

At days 0, 1 and 2 p.i., weight loss of sex and age matched AGR2^{ko} mice was significantly more pronounced in AGR2^{ko} mice, in particular 24 h after sm-treatment (**Figure 26A**, p-value <0.0001). The reason for this currently remains unclear. At d1 p.i., total pathogen loads were significantly increased in cecal content of AGR2^{ko} mice as compared to AGR2^{het} mice (**Figure 26B**, p-value 0.0195). This difference disappeared from d2 p.i. on. AGR2^{ko} and AGR2^{het} mice show similar increase of pathogen loads in mLN over-time showing an increased tissue invasion and/or *S. Tm*^{wt,gfp} cell replication (**Figure 26C**, p-value 0.0099). Surprisingly, despite increased *S. Tm*^{wt,gfp} loads in cecal content of AGR2^{ko} mice, AGR2^{ko} mice showed less inflammation in the cecum at d1 p.i. as compared to AGR2^{het} mice (**Figure 26D,F**, p-value 0.0004). This has been confirmed by significantly reduced Lcn2 levels on the cecal content at d1 p.i. (**Figure 26E**).

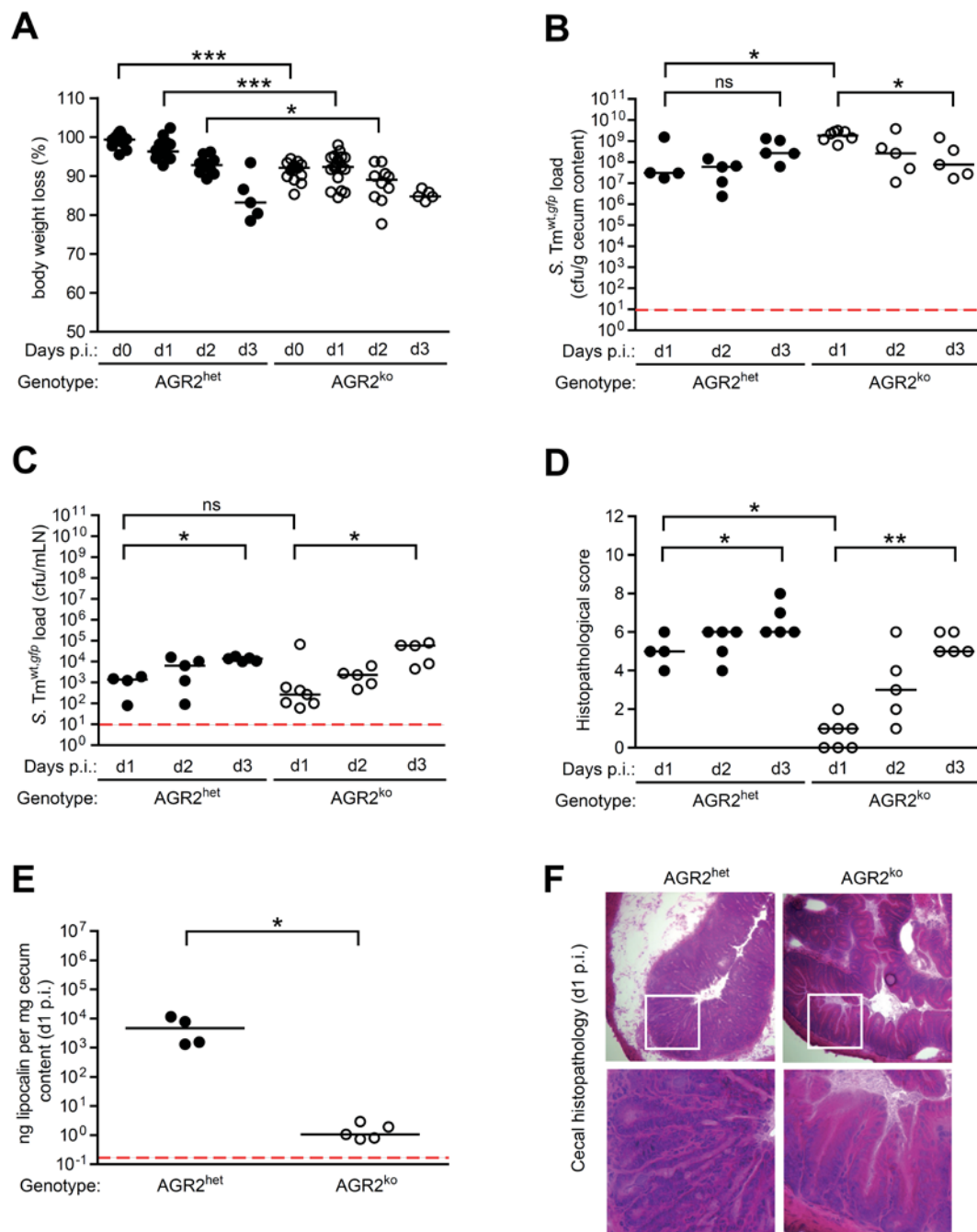


Figure 26. AGR2^{ko} mice show attenuated inflammation 1 day post-*S. Tm*^{wt} oral infection compared to AGR2^{het} mice.

AGR2^{het} and AGR2^{ko} mice were orally gavaged with a single dose of streptomycin (sm; 25 mg/mouse). One day after sm-treatment (d0), mice were orally gavaged with 10⁵ to 10⁶ CFU *S. Tm*^{wt} harbouring pM973 plasmid, which constitutively expresses GFP (*S. Tm*^{wt.gfp}). Infected and uninfected mice were sacrificed either before infection (d0) or post-infection (p.i.) at days 1, 2 or 3 (d1, d2 or d3). (A) Mouse weight was recorded over-time and is relative to the initial weight recorded before sm-treatment. Data are given as percentage. (B-C) *S. Tm*^{wt.gfp} load was determined at days 1, 2 and 3 p.i. in (B) cecum and (C) mesenteric lymph nodes (mLN) by plating. (D) Histopathological analysis of cecal tissue of the infected mice shown in (A-E). Cecal tissue sections were stained using hematoxylin and eosin. The degree of submucosal edema, neutrophil infiltration and epithelial damage was scored in a double-blinded manner. Data are given without the goblet cells score. 0-3: no pathological changes; 4-7: moderate

inflammation; above 8: severe inflammation. **(E)** Lipocalin-2 amount in cecal content at day 1 p.i. was determined using ELISA on 4-5 mice per group, randomly chosen. Data are given as ng lipocalin per mg cecal content. **(F)** Representative hematoxylin and eosin stained sections of infected mice at day 1 p.i. shown in **(D)**. Magnification: 100-fold. Enlarged sections (squares) are shown in the lower panels. Dotted red lines: detection limit. Bars represent the median. Mann-Whitney U test: ns=not significant ($P \geq 0.05$), * $P < 0.05$, ** $P < 0.01$, *** $P < 0.001$. One-way ANOVA Kruskal-Wallis test: **(A)** $P < 0.0001$, **(B)** $P = 0.0195$, **(C)** $P = 0.0099$, **(D)** $P = 0.0004$.

Intriguingly, these data indicate that AGR2^{ko} mice, which lack the intestinal mucus layer, are better protected against *S. Tm*^{wt,gfp}-induced inflammation in cecum, as compared to AGR2^{het} mice. This observation could be explained by (1) altered immune defense or mucosal metabolism and nutrient transport mechanisms in the cecal mucosa of mice (2) differential *S. Tm*^{wt,gfp} loads in cecal tissues due to altered tissue invasion efficiency (3) or different pharmacokinetics of streptomycin and/or as a consequence (4) different microbiota composition in AGR2^{ko} vs AGR2^{het} mice.

5.3. Microarray analysis

Next, we wanted to analyze whether AGR2^{ko} and AGR2^{het} mice exhibit different gene expression profiles in the cecal epithelium. We hypothesized that this difference (*e.g.* increased immune defenses) may lead to the decreased susceptibility to *S. Tm*-induced inflammation observed at d1 p.i.

In order to analyze genome-wide mRNA expression in the cecal epithelium of AGR2^{ko} and AGR2^{het} mice, we isolated cecal epithelial cells and extracted total RNA. Then, we performed microarray analysis and interpreted genome-wide mRNA expression profiles using the Gene set enrichment analysis (GSEA) approach (Subramanian, Tamayo et al. 2005). Gene sets are groups of genes that share common biological function, chromosomal location or regulation. They are defined based on prior biological knowledge and experimental results. Gene sets were considered as significantly down- or upregulated when the False Discovery Rate value (FDR q-val) was below 0.25, which means that less than 25 % of the gene set of interest is estimated as false positive. This setting is considered as reasonable in the setting of an exploratory discovery (Subramanian, Tamayo et al. 2005). The analysis was performed by Mark Boekschoten (WU Agrotechnology & Food Sciences, Wageningen, Netherlands).

Three gene sets were found as significantly enriched in AGR2^{ko} mice as compared to AGR2^{het} littermates *e.g.* gene sets involved in cholesterol biosynthesis (**Annexed Table 49**). This could be due to dysregulation of endoplasmic reticulum (ER) responses, as cholesterol is mainly synthesized by ER (van Meer, Voelker et al. 2008). Most of gene sets found to be downregulated in AGR2^{ko} mice as compared to

AGR2^{het} littermates were predicted to be involved in cell cycle, metabolism, damage response and cancer pathways. These results are in line with previous work showing that AGR2^{ko} mice exhibit elevated endoplasmic reticulum stress response and differential gene expression involved *e.g.* in breast cancer genesis (Zhao, Edwards et al. 2010, Li, Wu et al. 2015). Only few gene sets involved in immune responses (*e.g.* interleukin-2 signaling and immunoregulatory interactions between a lymphoid and a non-lymphoid cells) were found to be downregulated in AGR2^{ko} mice (**Annexed Table 50**).

It is tempting to speculate that the few gene sets involved in immune response mechanisms could play a role in lowering the inflammatory response to *S. Tm* infection in AGR2^{ko} mice. However, even if this type of analysis provides large amounts of predictions, verification of all results is required to confirm these predictions and can be tested using appropriated KO mouse models. In parallel, we followed another approach to decipher protective mechanisms against *S. Tm* present in AGR2^{ko} mice.

5.4. Presence of *S. Tm* in cecal tissue is reduced in AGR2^{ko} mice as compared to littermate controls

It has been well characterized that in order to infect mucosal tissues and cause disease, *S. Tm* employs several virulence factors. The most important are two type III secretion systems (T3SS) T3SS-1 and T3SS-2, located on *Salmonella* pathogenicity island 1 (SPI-1) and SPI-2, respectively (Kaiser, Diard et al. 2012). Whereas T3SS-1 mediates epithelial cell invasion, T3SS-2 allows *S. Tm* to survive and replicate intracellularly in epithelial cells as well as in different cell types in the lamina propria (Patel and McCormick 2014). Together, T3SS-1 and T3SS-2 cooperate to promote bacterial tissue invasion and lead to the induction of a strong mucosal inflammatory response, causing severe enterocolitis in mice. As previously shown, AGR2^{ko} mice are better protected against *S. Tm*^{wt,gfp}-induced cecal inflammation than their AGR2^{het} littermates. Therefore, we hypothesized that this might be reflected by lower *S. Tm* tissue loads in AGR2^{ko} mice compared to AGR2^{het} mice.

In order to test this hypothesis, we used part of cecum sampled at day 1 p.i. from the animal experiment presented in **Figure 26**. The lamina propria was stained using an ICAM-1/CD54 antiserum. The epithelium was visualized by actin-staining with conjugated phalloidin. *S. Tm*^{wt,gfp} expresses GFP only when it resides in a *S. Tm*-containing vacuole, intracellularly. Immunostaining and image analysis were performed by Mikael Sellin (ETH, Zurich), as described in (Sellin, Muller et al. 2014).

At day 1 p.i., loads of the T3SS-2 reporter strain *S. Tm*^{wt,gfp} in epithelial cells and in lamina propria were significantly reduced in AGR2^{ko} mice as compared to their AGR2^{het} littermates (**Figure 27A**,

p-value 0.0159 and 0.0159, respectively). This suggests that *S. Tm*^{wt,gfp} is less invasive and/or that there is less replication of intracellular bacteria in the mucosa of *AGR2*^{ko} as compared to *AGR2*^{het} mice. Overall, *S. Tm*^{wt,gfp} loads were higher in epithelial cells as compared to lamina propria, as also shown previously (**Figure 27A**, p-value 0.0317 and 0.0286, respectively) (Hapfelmeier, Stecher et al. 2005). The cecal mucosa of *AGR2*^{ko} mice was thinner as compared to *AGR2*^{het} mice due to the absence of inflammation (**Figure 27B**).

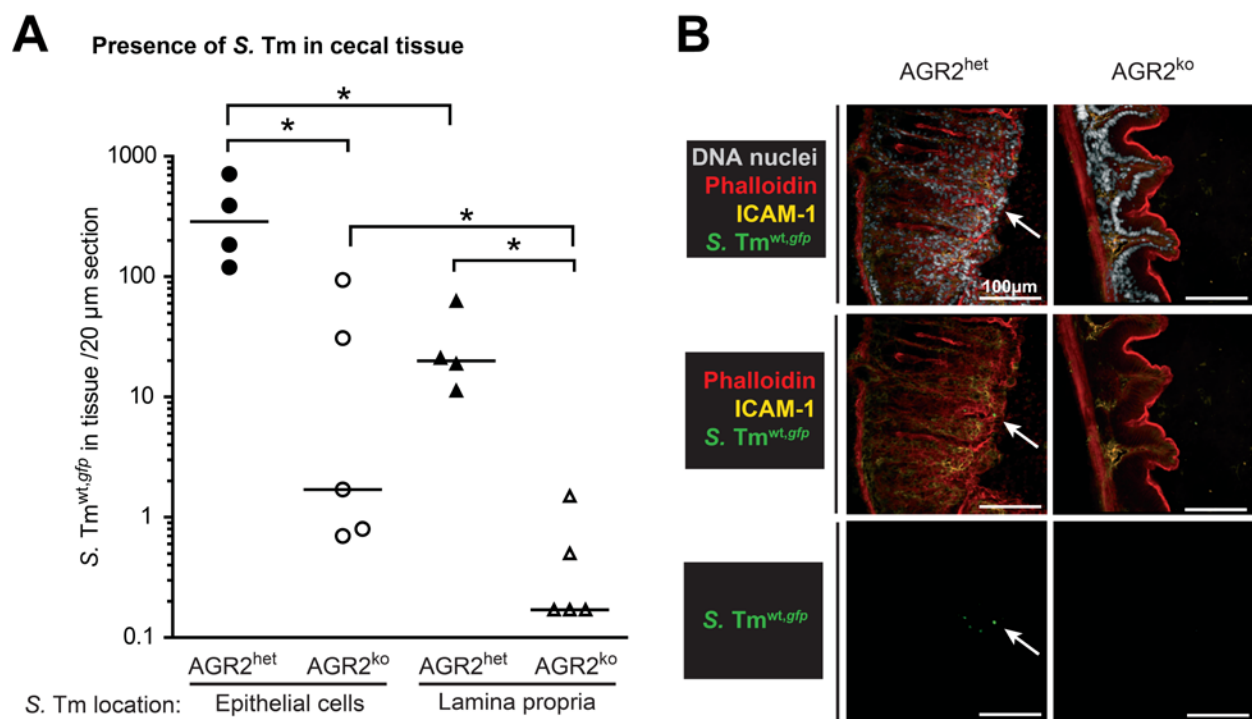


Figure 27. Presence of *S. Tm* in cecal tissue is reduced in *AGR2*^{ko} mice as compared to littermate controls.

AGR2^{het} and *AGR2*^{ko} littermate mice were orally gavaged with a single dose of streptomycin (sm; 25 mg/mouse). After 24 h, mice were orally infected with 5×10^6 CFU *S. Tm*^{wt,gfp}, which constitutively expresses GFP. At day 1 p.i., mice were sacrificed, cecal tissue was fixed in 4 % PFA and frozen in O.C.T. at -80 °C. Intracellular immunostaining of cryosections (20 μm thick) and image analysis were performed by Mikael Sellin, as described in (Sellin, Muller et al. 2014). For quantification of *S. Tm*^{wt,gfp}, imaging was performed at 400x and 1,000x and intracellular *S. Tm*^{wt,gfp} was manually enumerated blindly in six to nine nonconsecutive sections per mouse. 4-5 mice per group. (A) *S. Tm*^{wt,gfp} load in tissue per 20 μm section in epithelial cells (circles) and in lamina propria (triangles). All data represent mean/section of *S. Tm*^{wt,gfp} numbers. Filled symbols; *AGR2*^{het} mice, empty symbols; *AGR2*^{ko} mice. (B) Representative confocal images of cecal sections from *AGR2*^{het} and *AGR2*^{ko} mice. Scale bar: 100 μm. Mann-Whitney U test: * P<0.05. One-way ANOVA Kruskal-Wallis test: (A) P=0.0033.

All together, these observations indicate that the protective effect found at day 1 p.i. in AGR2^{ko} mice may be due to different invasion properties of *S. Tm*^{wt,gfp} and that the mucus layer might be directly or indirectly involved. However, the mechanisms modulating *S. Tm*^{wt,gfp} invasion still remain unknown.

The intestinal microbiota is known to provide CR against *S. Tm* (Stecher, Chaffron et al. 2010, Deriu, Liu et al. 2013). Moreover, both the mucus layer and antibiotic-treatment have been shown to affect and modulate the intestinal microbiota. Thus, we next aimed at studying the effect of sm-treatment and the mucus layer on microbiota density and composition.

5.5. Microbiota of AGR2^{ko} mice is less susceptible to streptomycin-treatment than the microbiota of AGR2^{het} littermates despite similar sm concentration along the intestinal tract of both AGR2^{ko} and AGR2^{het} mice

In order to investigate how oral sm-treatment influences microbiota density in the cecum, we stained commensal bacteria on cecal cryosections of untreated and sm-treated AGR2^{ko} and AGR2^{het} mice, sacrificed 24 hours after treatment with 25 mg of streptomycin. We used sytox green to visualize commensal bacteria and quantified bacteria per area unit within the cecal lumen.

Twenty-four hours after sm-treatment, cecal microbiota density of AGR2^{het} mice decreased by about 98 % (median) as compared to AGR2^{het} untreated mice. No difference was noted in cecal microbiota density of untreated littermates. Microbiota density of sm-treated AGR2^{ko} mice was significantly higher compared to their sm-treated AGR2^{het} littermates (**Figure 28A,B**, p-value <0.0001) showing that sm-treatment is less efficient on the microbiota of AGR2^{ko} than AGR2^{het} mice. This could be due to (1) different pharmacokinetics of streptomycin or (2) different microbiota composition in AGR2^{ko} vs AGR2^{het} mice.

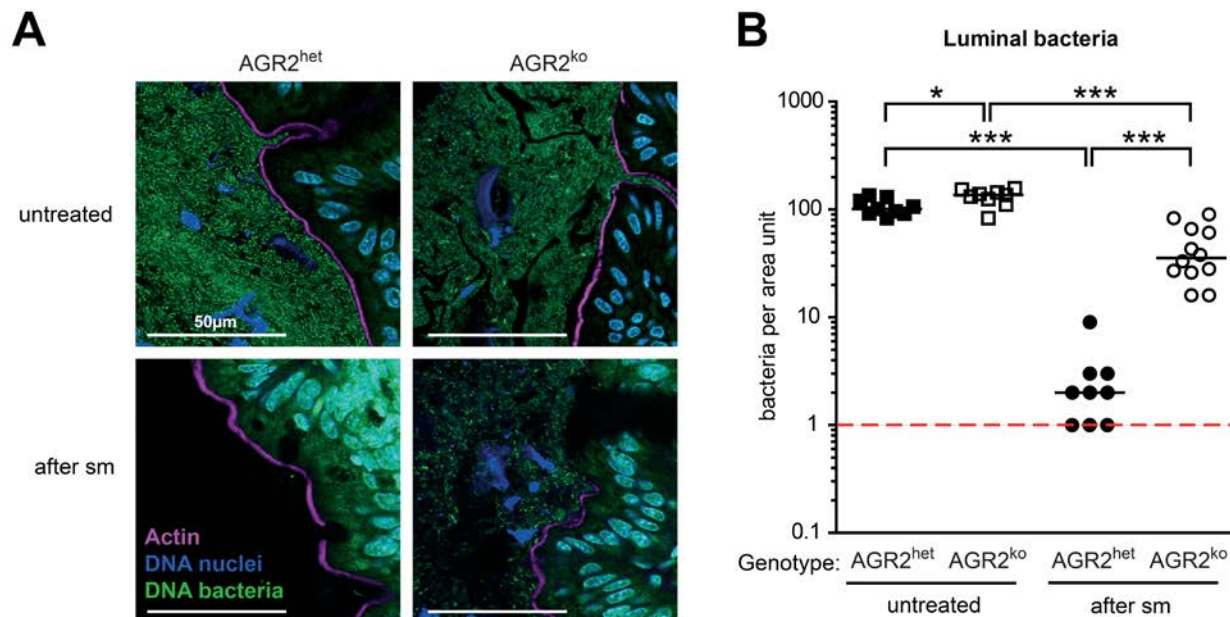


Figure 28. Microbiota of AGR2^{ko} mice is less susceptible to streptomycin treatment than the microbiota of AGR2^{het} littermates.

AGR2^{het} and AGR2^{ko} littermate mice were either orally gavaged with a single dose of streptomycin (sm; 25 mg/mouse) or left untreated. After 24 h, mice were sacrificed, cecum were fixed in 4 % PFA and frozen in O.C.T. at -80 °C. Cryosections (7 µm thick) were stained using phalloidin (purple, actin), sytox green (green, bacterial DNA) and DAPI (blue, nuclei DNA). Confocal images were taken at the epithelial border and luminal bacteria were manually counted in a blind manner such as 4 areas (20 µm² each) per picture were randomly counted, 3 pictures per mouse and 3-4 mice per condition. **(A)** Representative confocal images of cecal sections from AGR2^{het} and AGR2^{ko} mice untreated or pre-treated with streptomycin (after sm-treatment). Scale bars: 50 µm. **(B)** Luminal bacterial counts. Bars represent the median. Dotted red line represents the detection limit. Mann-Whitney U test: * P<0.05, *** P<0.001. One-way ANOVA Kruskal-Wallis test: **(B)** P<0.0001.

The mucus layer has been shown to play a role in antibiotic absorption (Goddard 1998, Hagesaether, Christiansen et al. 2013). To test whether sm was differently absorbed in AGR2^{ko} vs AGR2^{het} mice, we measured sm concentration in different parts of the intestinal tract at different time points after sm-treatment using a bioassay. We determined the sm concentration in the small intestine, the cecal content and the feces, as well as in the serum. To study the dynamics of sm distribution, we sacrificed mice at different time points after oral sm-treatment at 1, 3, 8 and 24 h after sm-treatment (25 mg/mouse).

Interestingly, no difference was observed between AGR2^{ko} and AGR2^{het} mice along the intestinal tract and in the serum (**Figure 29**). This indicates that the increased microbiota density observed in **Figure 28** might be due to differential microbiota composition in AGR2^{ko} mice as compared to AGR2^{het} mice rather than different rates of sm absorption due to differences in the intestinal mucus layer.

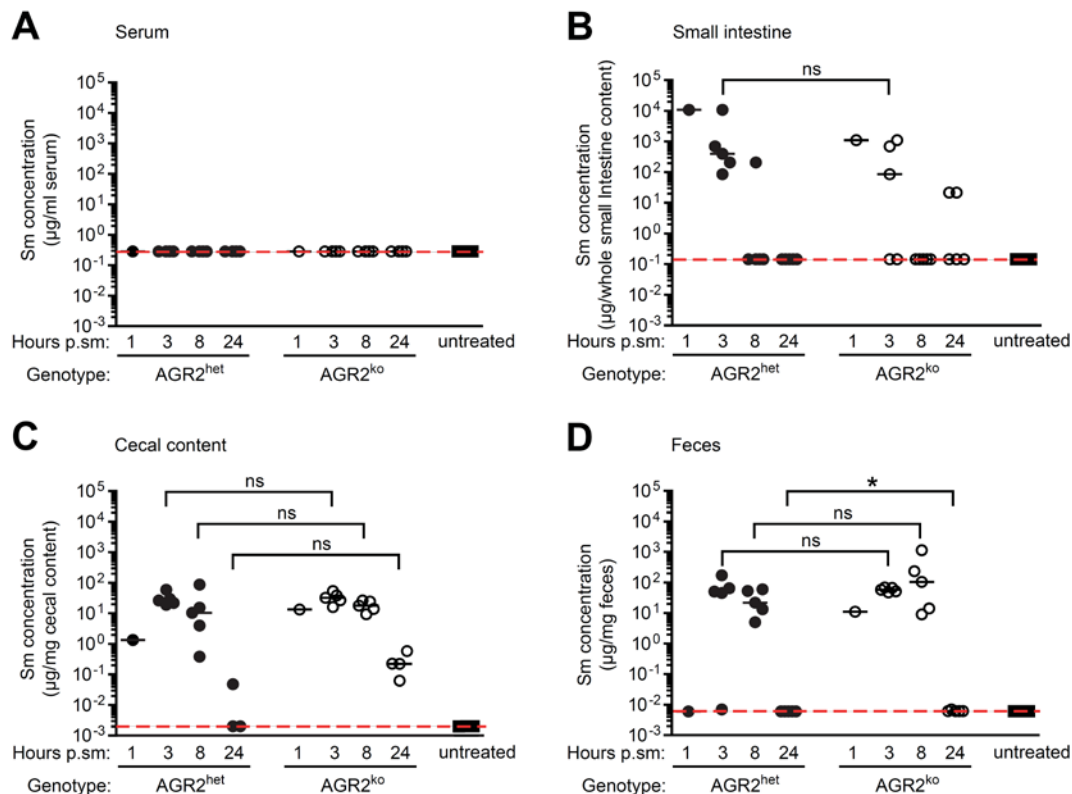


Figure 29. Microbiota of $AGR2^{ko}$ and $AGR2^{het}$ mice encounter same amount of effective streptomycin over-time along the intestinal tract.

$AGR2^{het}$ and $AGR2^{ko}$ mice were orally gavaged with a single dose of streptomycin (sm; 25 mg/mouse). After 1 h, 3 h, 8 h or 24 h post-sm treatment (hours p.sm), mice were sacrificed. Serum and intestinal contents were sampled and concentration of sm was determined using a halo assay. Briefly, blank antimicrobial susceptibility disks were laid on top of sm-sensitive *E. coli* DH5a strain and 5 μ l mouse sample was spotted on each disk. Plates were incubated o.n. at 37 °C and inhibition zone (halo) size was measured using a ruler. Size of the blank disk was substrated to all values. Later on, halo size values were correlated with a standard curve and sample weight or volume in order to determine the exact sm concentration. Untreated littermate mice were taken as negative controls (untreated) to exclude other inhibitory effects in the intestinal content. (A) Sm concentration in serum is given as μ g/ml. (B) Sm concentration in the whole small intestine content is expressed in μ g. (C) Sm concentration in cecal content is given as μ g/mg content. (D) Sm concentration in feces is given as μ g/mg feces. Filled symbols; $AGR2^{het}$ mice, empty symbols; $AGR2^{ko}$ mice. Dotted red lines: detection limit. Bars represent the median. Mann-Whitney U test: * $P < 0.05$, ns=not significant. One-way ANOVA Kruskal-Wallis test: (B) $P=0.0039$, (C) $P=0.0009$, (D) $P=0.0014$.

In order to analyze microbiota composition of $AGR2^{ko}$ and $AGR2^{het}$ mice, bacterial gDNA was extracted from feces and microbiota composition was analyzed by 16S rRNA amplicon sequencing. Data were analyzed using the QIIME pipeline (Quantitative Insights Into Microbial Ecology) (Caporaso, Kuczynski et al. 2010) using an open-reference database. To identify different taxon distribution in $AGR2^{ko}$ vs $AGR2^{het}$ mice, we performed a LDA Effect Size (LEfSe) analysis (Segata, Izard et al. 2011). LEfSe algorithm allows the identification of features (e.g. enriched bacterial taxa) that characterize the differences between two or more biological conditions (e.g. genotype and antibiotic treatment).

Overall, we observed similar microbiota composition at the taxonomic family and genus levels in AGR2^{ko} and AGR2^{het} mice (**Figure 30A,B**). However, Principal Coordinate Analysis (PCoA) showed distinct clustering between AGR2^{ko} and AGR2^{het} microbiota (**Figure 30C**). Strikingly, LefSe analysis revealed that 10 taxa assigned to Prevotellaceae, Bacteroidales, Anaeroplasmatales and Clostridiales were enriched in AGR2^{ko} mice as compared to AGR2^{het} mice. On the other hand, 4 taxa assigned to Erysipelotrichaceae and *Marvinbryantia* were enriched in AGR2^{het} mice as compared to AGR2^{ko} mice (**Figure 30D**). Thus, higher microbiota density observed in AGR2^{ko} mice after sm-treatment could be due to different microbiota composition.

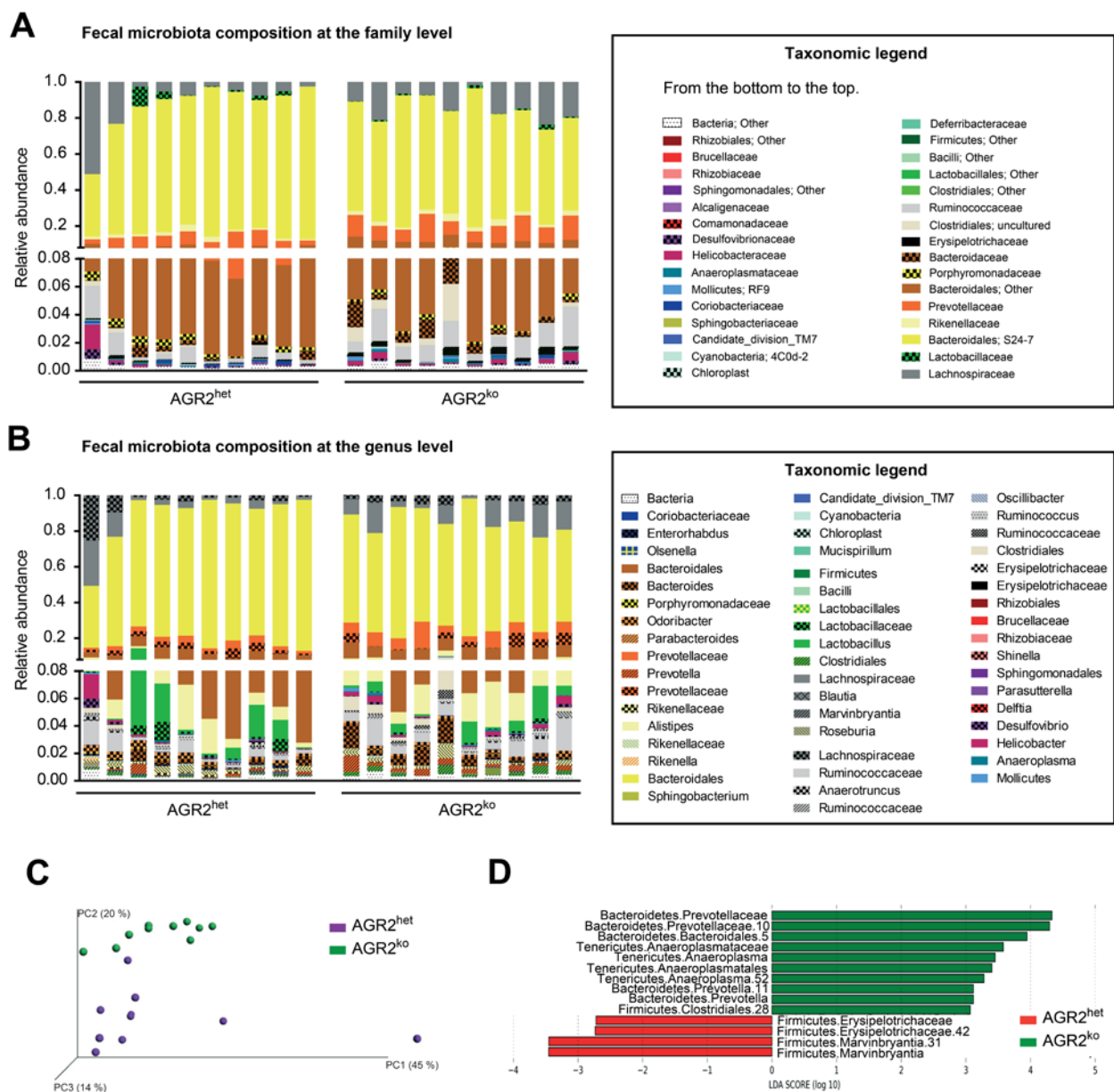


Figure 30. Comparison of microbiota composition of $AGR2^{ko}$ and $AGR2^{het}$ untreated mice analyzed using 16S rRNA gene amplicon sequencing.

Fecal microbiota composition of $AGR2^{ko}$ and $AGR2^{het}$ untreated mice was determined using 16S rRNA gene amplicon sequencing. Sequencing data were processed using the QIIME pipeline and taxonomy was assigned against the Silva database. Data are given as relative abundance at the taxonomic (A) family and (B) genus levels. One mouse per column. Color code is indicated in taxonomic legend boxes. (C) Corresponding Principal Coordinate Analysis (PCoA) plots of Weighted UniFrac distances of 16S rRNA genes. Color code refers to $AGR2$ genotype: green: $AGR2^{ko}$ and purple: $AGR2^{het}$. One mouse per dot. (D) Bacterial taxa enriched in fecal microbiota of $AGR2^{ko}$ and $AGR2^{het}$ untreated mice analyzed using LEfSe analysis. Color code refers to $AGR2$ genotype: green: $AGR2^{ko}$ and red: $AGR2^{het}$.

5.6. Streptomycin-treatment leads to pronounced alteration of gut microbiota composition in both AGR2^{het} and AGR2^{ko} mice

We have shown that sm-treated AGR2^{ko} mice are better protected against *S. Tm*-induced inflammation at d1 p.i. and harbored higher microbiota density in cecum where *S. Tm* invasion was also significantly reduced as compared to their AGR2^{het} littermate controls. These data point at a protective effect of the AGR2^{ko} microbiota during *S. Tm* infection and after sm-treatment.

In order to analyze microbiota composition of AGR2^{ko} and AGR2^{het} mice after sm-treatment, bacterial gDNA was extracted from feces then microbiota composition was analyzed by 16S rRNA amplicon sequencing.

Microbiota composition analysis of AGR2^{het} and AGR2^{ko} mice revealed deep changes after sm-treatment, at taxonomic family and genus levels (**Figure 31**). There was a high variability in microbiota composition in the sm-treated mice. Based on these data, identification of candidates that could be protective in sm-treated AGR2^{ko} mice appeared very challenging.

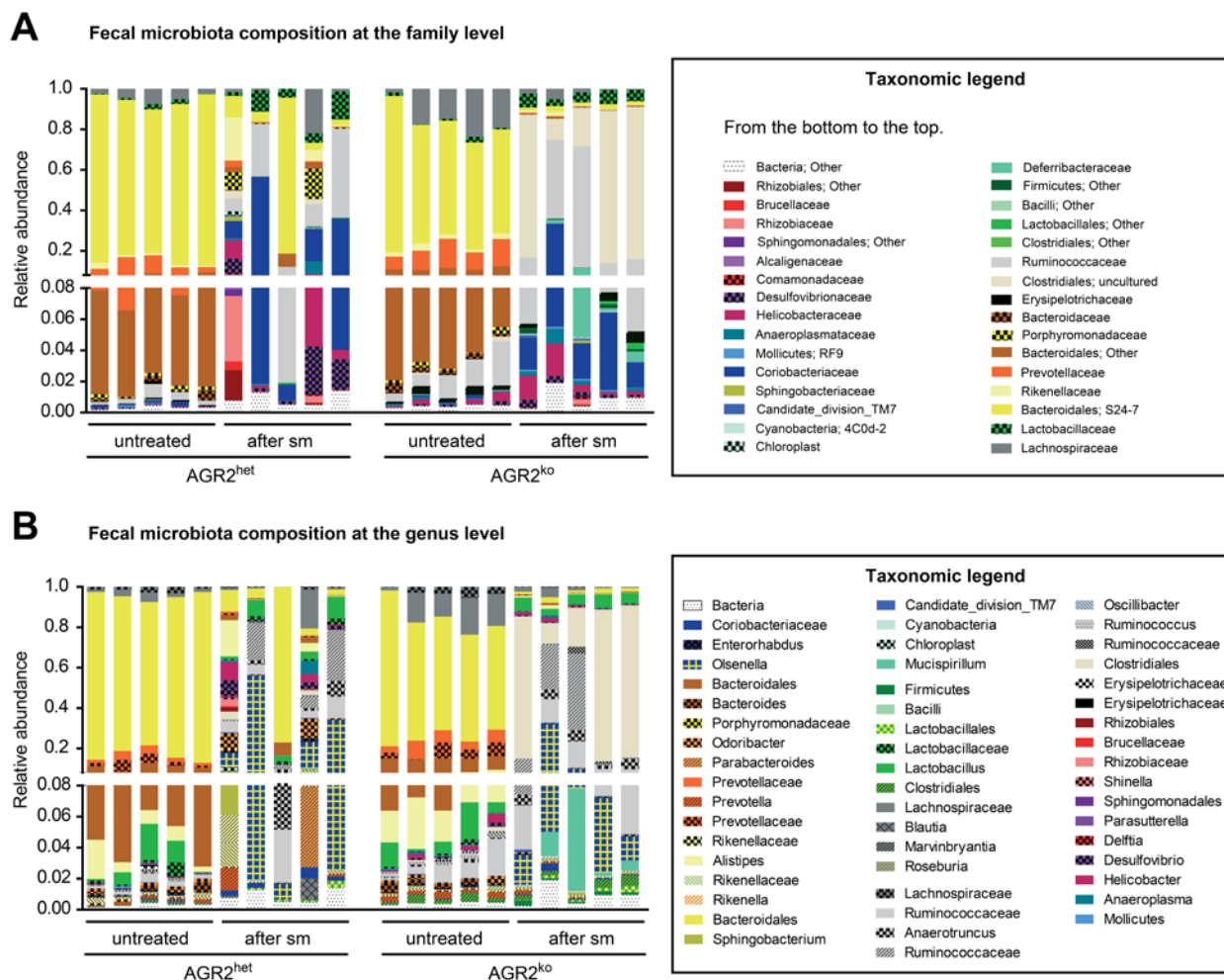


Figure 31. Fecal microbiota composition of $AGR2^{ko}$ and $AGR2^{het}$ mice shows pronounced alterations after streptomycin treatment.

Fecal microbiota composition of $AGR2^{ko}$ and $AGR2^{het}$ mice before (untreated) and 1 day after sm-treatment (after sm) was determined using 16S rRNA gene amplicon sequencing. Sequencing data were processed using the QIIME pipeline and taxonomy was assigned against the Silva database. Data are given as relative abundance at the taxonomic (A) family and (B) genus levels. One mouse per column. Color code is indicated in taxonomic legend boxes.

5.7. Ampicillin treatment renders AGR2^{ko} mice susceptible to *S. Tm*-induced colitis

Streptomycin is an aminoglycoside widely used against Gram-negative bacteria and well known to enable *S. Tm* expansion in gastrointestinal tract (Ng, Ferreyra et al. 2013). Other antibiotics such as ampicillin or metronidazole have been shown to increase colonization of enteric pathogens, such as *S. Tm* and *Citrobacter rodentium* (Endt, Stecher et al. 2010, Wlodarska, Willing et al. 2011). We hypothesized that some members of the intestinal microbiota, which would be sm-resistant might play a role in protecting sm-treated AGR2^{ko} mice from *S. Tm*^{wt}-induced inflammation. We reasoned that treatment with another class of antibiotics would target a different spectrum of the microbiota and thereby overcome differences in microbiota composition caused by sm. We used the broad spectrum antibiotic ampicillin (amp) which targets both Gram-positive and Gram-negative bacteria. To analyze the effect of amp on microbiota density of AGR2^{ko} and AGR2^{het} mice, we first stained commensal bacteria on cecal cryosections of amp-treated mice using sytox green and quantified single bacteria per area unit, as previously described in **Figure 28**.

After amp-treatment, microbiota density of AGR2^{het} mice was reduced to the detection limit (1 bacteria per area unit). Moreover, cecal microbiota density of AGR2^{ko} mice was significantly reduced after amp-treatment as compared to sm-treated AGR2^{ko} mice showing that microbiota of AGR2^{ko} mice is more susceptible to ampicillin than to streptomycin (**Figure 32**). This observation already suggested that microbiota composition of AGR2^{ko} mice differs after sm- and amp-treatment.

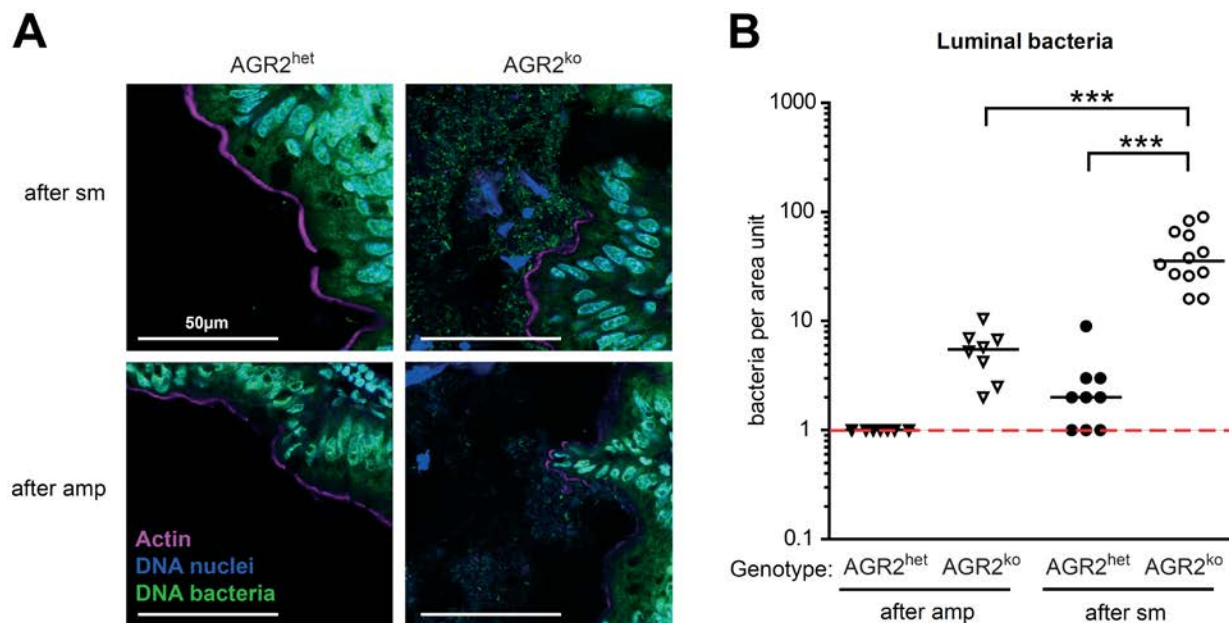


Figure 32. Microbiota of AGR2^{ko} and AGR2^{het} mice are highly susceptible to ampicillin treatment.

AGR2^{het} and AGR2^{ko} littermate mice were orally gavaged with a single dose of either ampicillin (amp; 25 mg/mouse) or streptomycin (sm; 25 mg/mouse). After 24 h, mice were sacrificed, cecal tissue was fixed in 4 % PFA and frozen in O.C.T. at -80 °C. Cryosections (7 μ m thick) were stained using phalloidin (purple, actin), sytox green (green, bacterial DNA) and DAPI (blue, nuclei DNA). Confocal images were taken at the epithelial border and luminal bacteria were manually counted in a blind manner such as 4 areas (20 μ m² each) per picture were randomly counted, 3 pictures per mouse and 3-4 mice per condition. **(A)** Representative confocal images of cecal sections from AGR2^{het} and AGR2^{ko} mice after ampicillin or streptomycin treatment (after amp and after sm, respectively). Scale bars: 50 μ m. **(B)** Luminal bacterial counts. Bars represent the median. Dotted red line represents the detection limit. Mann-Whitney U test: *** P<0.001. One-way ANOVA Kruskal-Wallis test: **(B)** P<0.0001.

In order to analyze microbiota composition of AGR2^{ko} and AGR2^{het} mice after amp-treatment, bacterial gDNA was extracted from feces then microbiota composition was analyzed by 16S rRNA amplicon sequencing. To get an overview on microbial complexity before and after sm- and amp-treatments, we calculated the alpha diversity using the amplicon sequencing data.

As after sm-treatment, microbiota composition analysis of AGR2^{het} and AGR2^{ko} mice revealed pronounced changes after amp-treatment, at all taxonomic levels (**Figure 33A,B**). We observed higher microbiota variability in amp-treated AGR2^{het} mice as compared to amp-treated AGR2^{ko} mice (**Figure 33C**). Using this analysis, we also showed that after antibiotic treatments, AGR2^{ko} microbiota tended to be less complex than AGR2^{het} microbiota, independently of the antibiotic used, although not statistically significant. Untreated AGR2^{ko} and AGR2^{het} mice harbored the most complex intestinal microbiota. Interestingly, sm-treated AGR2^{ko} mice, which were better protected against *S. Tm*^{wt,gfp} at d1 p.i. than their heterozygous littermates, harbor similarly complex microbiota as compared to amp-treated AGR2^{het} mice.

This suggests that microbiota composition and not diversity may account for the protective function of the sm-treated AGR2^{ko} microbiota.

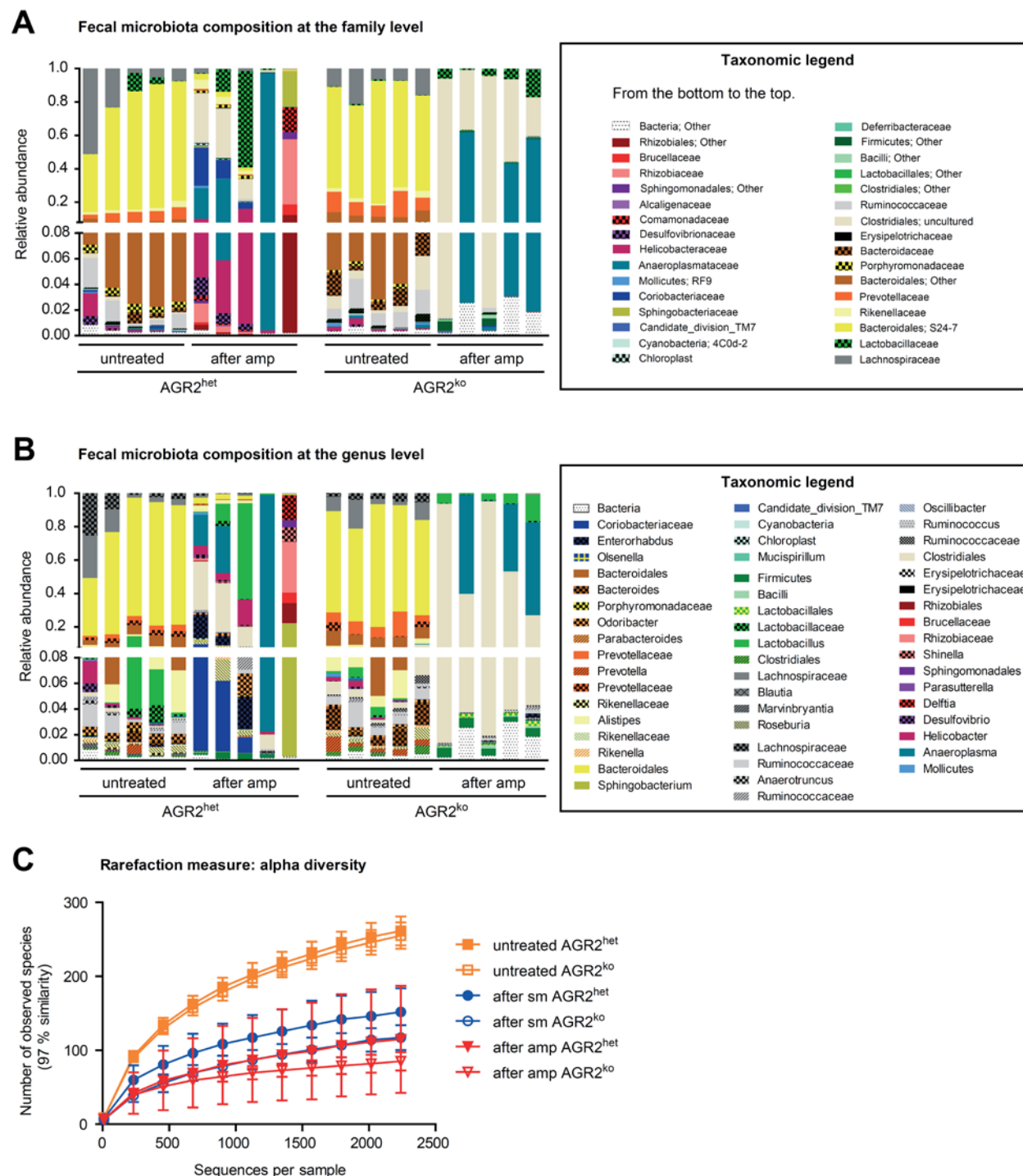


Figure 33. Analysis of microbiota composition of AGR2^{ko} and AGR2^{het} mice pretreated with ampicillin reveals gut microbiota composition different from sm-treated mice.

Fecal microbiota composition of AGR2^{ko} and AGR2^{het} mice before (untreated) and 1 day after amp-treatment (after amp) was determined using 16S rRNA gene amplicon sequencing. Sequencing data were processed using the QIIME pipeline and taxonomy was assigned against the Silva database. Data are given as relative abundance at the taxonomic (A) family and (B) genus levels. One mouse per column. Color code is indicated in taxonomic legend boxes. (C) Alpha diversity was determined as the observed species metric using the QIIME software package version 1.8 from the amplicon sequencing data shown in **Figures 31 and 33**. Data are given as mean and standard deviation. Untreated mice are represented in orange, sm-treated mice in blue and amp-treated mice in red. AGR2^{het} as full symbols and AGR2^{ko} as empty symbols.

Next, we sought to determine whether amp-treated AGR2^{ko} and AGR2^{het} mice were susceptible to *S. Tm*^{wt}-induced colitis. To test this, we treated AGR2^{ko} and AGR2^{het} mice with a single dose of ampicillin (25 mg/mouse) and orally infected them with 10⁶ CFU *S. Tm*^{wt} harbouring a plasmid which contains an ampicillin resistance cassette (*S. Tm*^{wt,amp}). At 24 hours after amp-treatment, mice were sacrificed and total pathogen loads were determined in cecal content. As markers of inflammation and pathology, we determined the *Lcn2* concentration in cecal content and quantified the histopathological changes in cecal tissues, respectively.

Similarly to sm-treated mice, at 24 hours after amp-treatment (d0), AGR2^{ko} mice showed significant weight loss in contrast to AGR2^{het} mice (**Figure 34A**, p-value <0.0001). The reason for this remains unclear. We reasoned that this weight loss might be attributable to antibiotic treatment and/or *S. Tm* infection. At d1 p.i., total pathogen loads were significantly increased in cecal content of AGR2^{ko} mice as compared to AGR2^{het} mice (**Figure 34B**). Interestingly, both AGR2^{ko} and AGR2^{het} mice showed similar signs of cecal inflammation, characteristic for this early time point after oral *S. Tm* infection (**Figure 34C,E**) (Stecher, Robbiani et al. 2007). Similar degree of inflammation was also confirmed by *Lcn2* measurement in cecal content of AGR2^{ko} and AGR2^{het} mice (**Figure 34D**). This suggests that the differences in microbiota composition and not the host genotype account for the protection of sm-treated AGR2^{ko} mice at early time point.

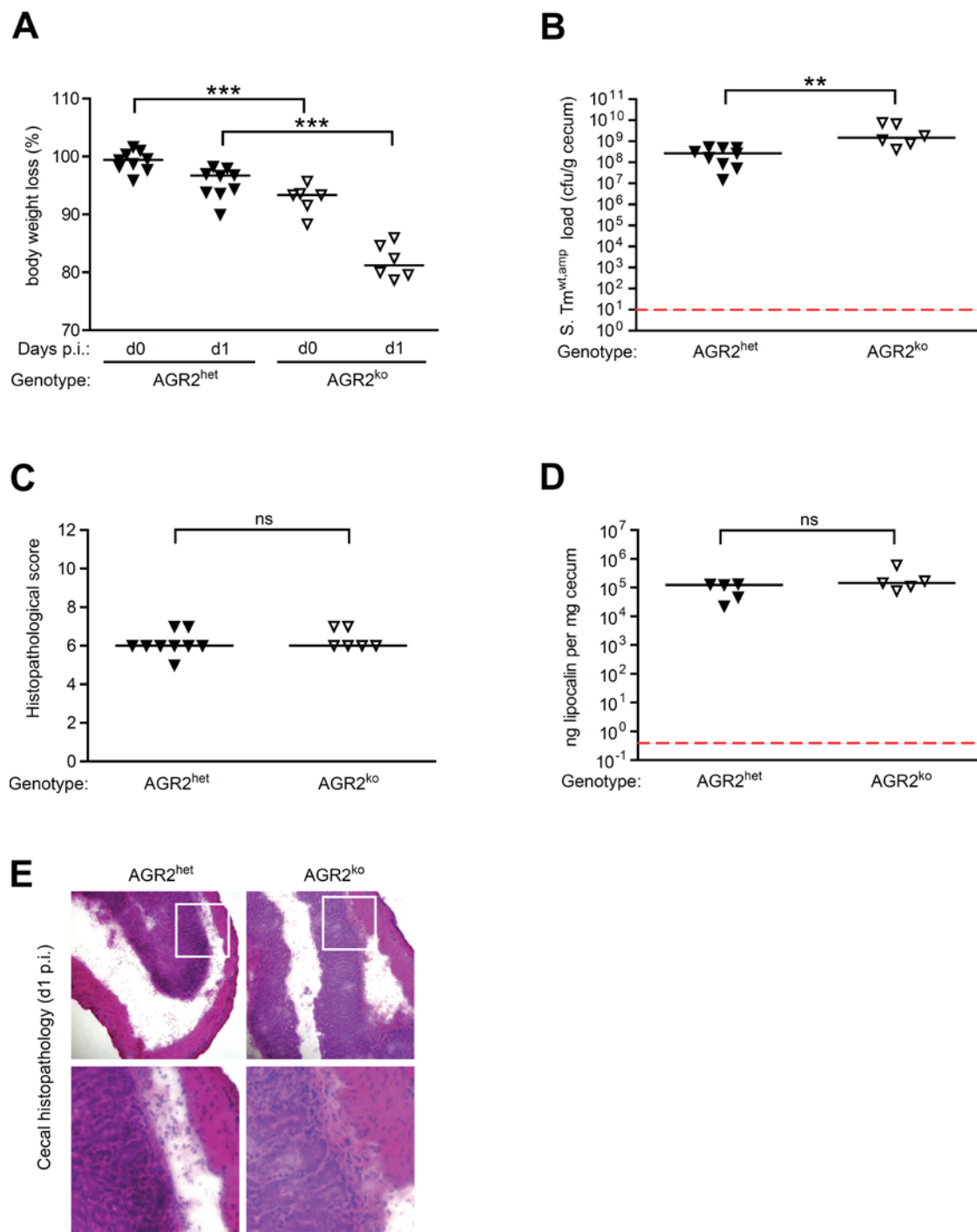


Figure 34. Ampicillin reduces colonization resistance against *S. Tm^{wt}* in AGR2^{ko} mice.

AGR2^{het} and AGR2^{ko} mice were orally gavaged with a single dose of ampicillin (amp; 25 mg/mouse). After 24 h, mice were orally infected with 10⁶ CFU *S. Tm^{wt,amp}* (Stecher, Denzler et al. 2012) harbouring pWKS30 (Wang and Kushner 1991), which contains an ampicillin resistance cassette. Mice were sacrificed at day 1 p.i. (A) Mouse weight was recorded over-time and is relative to the initial weight recorded before amp-treatment. Data are given as percentage. (B) *S. Tm^{wt,amp}* load was determined at day 1 p.i. in cecal content by plating. (C) Histopathological analysis of cecal tissue of infected mice. Cecal tissue sections were stained using hematoxylin and eosin. The degree of submucosal edema, neutrophil infiltration, epithelial damage was scored in a double-blinded manner. Data are

given without the goblet cells score. 0-3: no pathological changes; 4-7: moderate inflammation; above 8: severe inflammation. **(D)** Lipocalin amount in cecal content at day 1 p.i. was determined using ELISA on 5 mice per group, randomly chosen. Data are given as ng lipocalin per mg cecal content. **(E)** Representative hematoxylin and eosin stained sections of infected mice at day 1 p.i. Magnification: 100-fold. Enlarged sections (squares) are shown in the lower panels. Dotted red lines: detection limit. Bars represent the median. Mann-Whitney U test: ns=not significant ($P \geq 0.05$), ** $P < 0.01$, *** $P < 0.001$. One-way ANOVA Kruskal-Wallis test: **(A)** $P < 0.0001$.

These data indicate that both AGR2^{ko} and AGR2^{het} mice are equally susceptible to *S. Tm*^{wt,amp}-induced colitis at d1 p.i., after amp-treatment. Using microbiota composition analyses, we showed that pronounced changes of microbiota composition are not sufficient to allow *S. Tm*^{wt} to induce inflammation in sm-treated AGR2^{ko} mice. Sm-treated AGR2^{ko} mice are protected against *S. Tm*-induced colitis but the reasons remain unclear. We speculated that some taxa or bacteria of the microbiota of sm-treated AGR2^{ko} mice mediate protection.

5.8. Enrichment of *Deferribacteres* phylum correlates with protection against *S. Tm*-induced colitis

So far, our data show that sm-treated AGR2^{ko} mice are protected against *S. Tm*-induced colitis. In contrast, all other groups (AGR2^{ko} and AGR2^{het} amp-treated and sm-treated AGR2^{het} mice) were susceptible. We reasoned that sm-treated AGR2^{ko} microbiota harboured members which could mediate the protective effect. In order to identify these members, we thoroughly compared the microbiota composition of all 4 groups using principal coordinate analysis (PCoA) and the microbiota composition of sm- and amp-treated AGR2^{ko} mice using an algorithm for high-dimensional biomarker discovery: LefSe (Segata, Izard et al. 2011). Using LefSe algorithm, we aimed at identifying taxa which are uniquely enriched in the protective group (sm-treated AGR2^{ko} mice).

Weighted UniFrac PCoA analysis revealed that antibiotic treated mice harbored different microbiota composition as compared to untreated mice (**Figure 35A**). Microbiota composition analyzed using LefSe approach showed forty-eight OTUs enriched in sm-treated AGR2^{ko} mice as compared to amp-treated AGR2^{ko} mice. Enriched OTUs were assigned to six phyla: *Firmicutes*, *Bacteroidetes*, *Actinobacteria*, *Proteobacteria*, *Deferribacteres* and TM7. Three OTUs enriched in amp-treated mice were assigned to the phylum *Firmicutes* (**Figure 35B**). The taxa found to be enriched in AGR2^{ko} protected mice may account for protection against *S. Tm*-induced colitis.

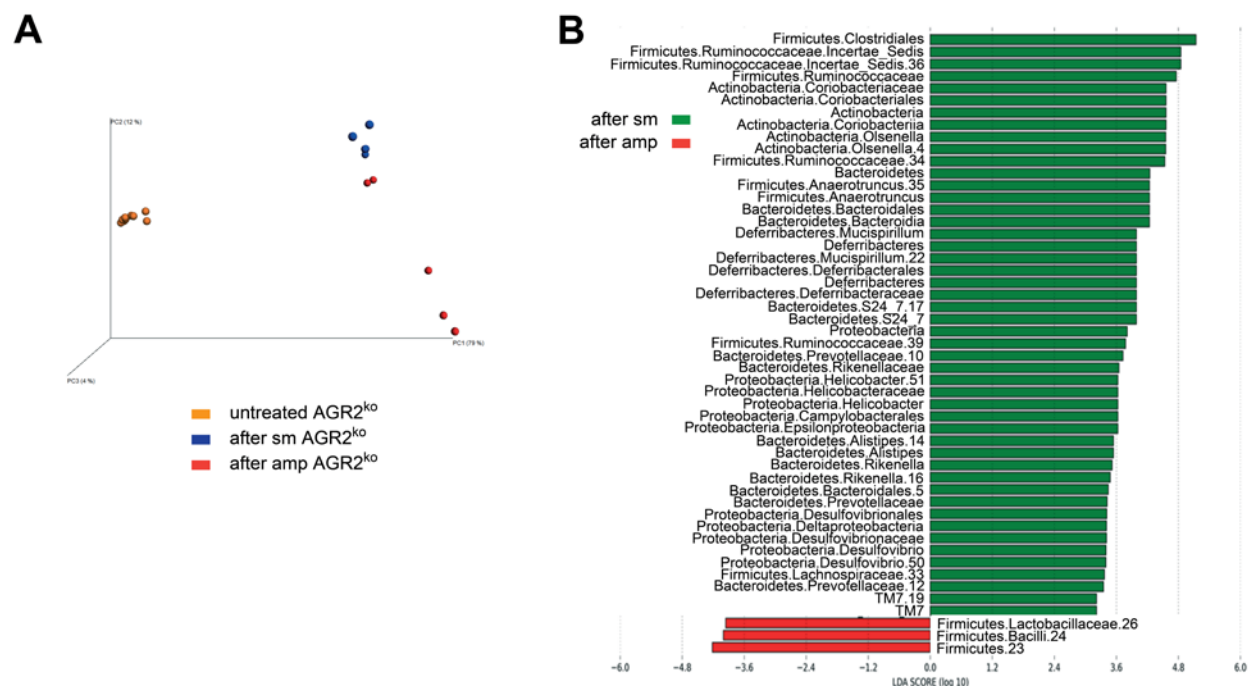


Figure 35. Comparison of microbiota composition of AGR2^{ko} mice before and after sm- or amp-treatment.

(A) Corresponding Principal Coordinate Analysis (PCoA) plots of Weighted UniFrac distances of 16S rRNA genes. Color code refers to pretreatment: orange: untreated; blue: after sm and red: after amp. One mouse per dot. (B) Bacterial taxa enriched in fecal microbiota of AGR2^{ko} either after sm or after amp analyzed using LEfSe analysis. Color code refers to antibiotic treatment: green: after sm and red: after amp.

In order to further narrow down the potential candidates for protective bacteria, we compared the three susceptible mouse groups showing inflammation at d1 p.i. (amp-treated AGR2^{ko} and AGR2^{het} mice and sm-treated AGR2^{het} mice) against the protected group (sm-treated AGR2^{ko} mice).

We found that eight OTUs were enriched in sm-treated AGR2^{ko} mice. Six enriched OTUs were assigned to the phylum *Deferribacteres* and two were assigned to the phylum *Firmicutes* (Figure 36). Regarding the high number of enriched OTUs assigned to the phylum *Deferribacteres*, we hypothesized that members assigned to this phylum (e.g. *Mucispirillum* spp.) might be involved in protection against *S.* Tm-induced colitis in sm-treated AGR2^{ko} mice.

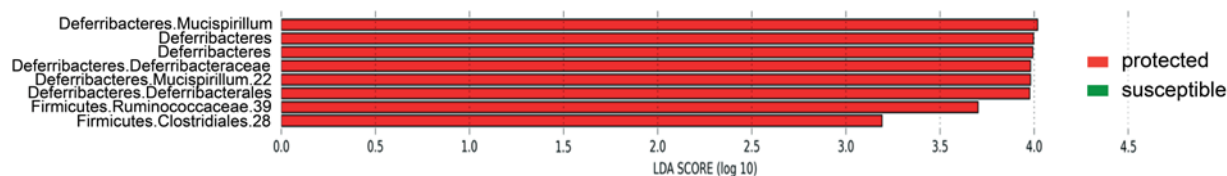


Figure 36. Comparison of AGR2^{ko} and AGR2^{het} mice after antibiotic treatment depending on their pathological score at day 1 p.i.

LEfSe analysis was performed using streptomycin- and ampicillin-treated mice presented in **Figures 26 and 34**, respectively. Mice were ranged according to their pathological score at d1 p.i. 0-3: no pathological changes; 4-7: moderate inflammation; above 8: severe inflammation. AGR2^{ko} sm-treated mice were considered as protected against inflammation (protected). AGR2^{ko} & AGR2^{het} amp-treated mice and AGR2^{het} sm-treated mice were considered as susceptible to inflammation (susceptible). Color code refers to susceptibility to inflammation: green: susceptible and red: protected.

5.9. Generation of AGR2 germfree mice to study *S. Tm*-microbiota interactions under highly defined conditions

Our data so far point at highly complex interactions between the microbiota and the mucus layer. The interplay of these partners leads to protection against *S. Tm*-induced colitis. Using antibiotic treated mice, we could identify bacteria which might interact with *S. Tm* and the mucus layer and influence the outcome of the infection. However, future mechanistic analysis is not possible in mice harbouring a complex and undefined microbiota. Therefore, we sought to investigate the interplay of the microbiota, *S. Tm* and the mucus layer in a gnotobiotic mouse model. AGR2 mice were rederived germfree (AGR2^{GF}) and bred in an isolator under germfree conditions, at the Hannover Medical School.

To test whether AGR2^{GF} mice were susceptible to *S. Tm* infection, we orally infected them with 10⁷-10⁸ CFU *S. Tm*. Already at 20h p.i., we observed high mortality of AGR2^{ko,GF} mice and therefore did not follow up longer time points for ethical reasons. At 20h p.i., mice were sacrificed. Total pathogen loads were determined in cecal content, mLN, spleen and liver. As a marker of inflammation and pathology, we determined the Lcn2 concentration in cecal content and quantified cecal histopathology, respectively.

At 20h p.i., we found similar pathogen loads in cecal content of AGR2^{GF} mice (**Figure 37A**). Equivalent pathogen loads were also found in mLN, whereas spleen and liver showed higher *S. Tm* loads in AGR2^{ko,GF} mice than in AGR2^{het,GF} mice (**Figure 37B**). For both genotypes, we observed high histopathological score as well as high Lcn2 levels pointing at severe inflammation (**Figures 37C,D**).

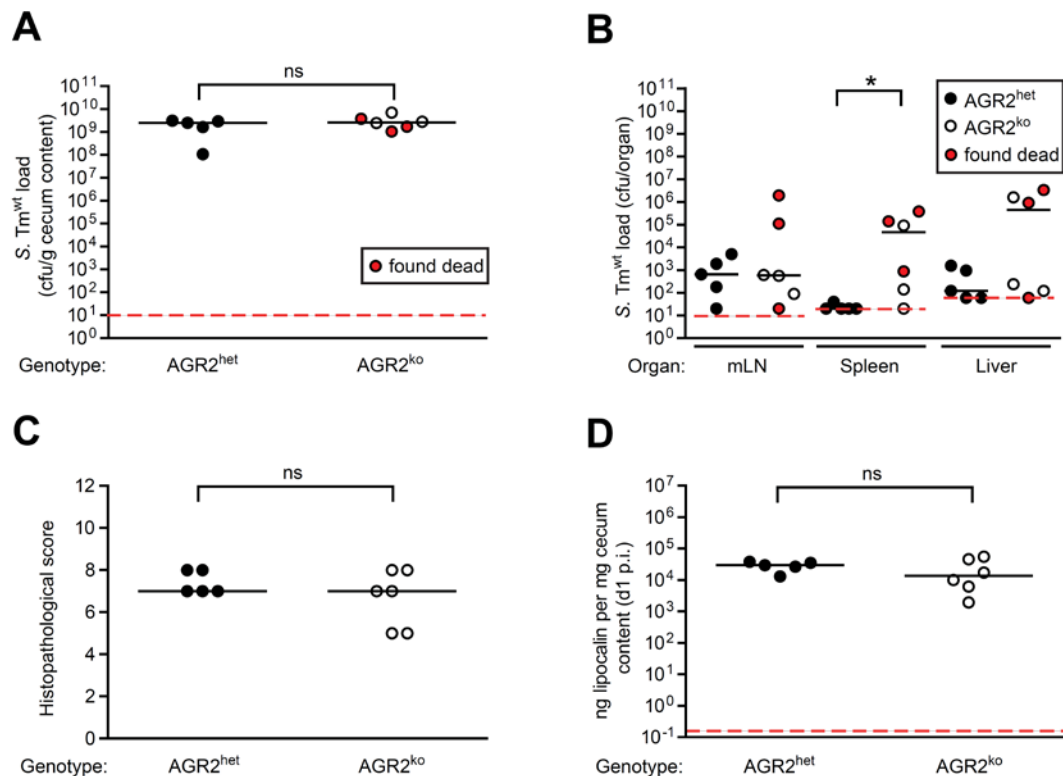


Figure 37. AGR2 germfree mice are highly susceptible to *S. Tm* infection.

AGR2^{het} and AGR2^{ko} littermates were orally gavaged with 10⁷-10⁸ CFU *S. Tm*^{wt}. After 20 h, mice were sacrificed and *S. Tm*^{wt} load was determined in (A) cecal content and in (B) mesenteric lymph nodes (mLN), spleen and liver by plating. (C) Histopathological score of cecal tissue of infected mice. Cecal tissue sections were stained using hematoxylin and eosin. The degree of submucosal edema, neutrophil infiltration and epithelial damage was scored in a double-blinded manner. Data are given without the goblet cells score. 0-3: no pathological changes; 4-7: moderate inflammation; above 8: severe inflammation. (D) Lipocalin-2 concentration in cecal content at 20 h p.i. was determined by ELISA on 2-3 mice per group, randomly chosen. Data are given as ng Lcn2 per mg cecal content.

In conclusion, we demonstrated that the mucus layer was also involved in protection against *S. Tm*-induced colitis in AGR2^{GF} mice but in the opposite way as compared to sm-treated AGR2 mice. Combined with previous data (*cf* Figure 26), we concluded that despite similar pathogen loads in cecal content of both conventional AGR2 and AGR2^{GF} mice, conventional mice are better protected against *S. Tm*-induced inflammation than germfree mice. These data highlight the crucial role of intestinal microbiota to protect its host, even in absence of mucus layer. As the most striking protective effect was observed for sm-treated AGR2^{ko} mice, it appeared plausible that microbiota members enriched in sm-treated AGR2^{ko} mice could be responsible for this protective effect, in a direct or indirect manner. Further gnotobiotic experiments need to be done to confirm this hypothesis.

5.10. *S. Tm* T3SS-1 expression is downregulated in sm-treated AGR2^{ko} mice

In order to invade intestinal epithelial cells and to trigger inflammation, *S. Tm* employs virulence factors including flagella-mediated motility and type III secretion systems (T3SS) (Kaiser, Diard et al. 2012, Thiennimitr, Winter et al. 2012). Whereas motility allows *S. Tm* to penetrate the mucus layer and to access the epithelial border, the SPI-1 type III secretion system (T3SS-1) is required for epithelial cell invasion and induction of inflammation. Moreover, in murine gut tissue, most of *S. Tm* expresses T3SS-1 (T3SS-1⁺) but in gut lumen and *in vitro* only 15 % of *S. Tm* population are T3SS-1⁺ (Ackermann, Stecher et al. 2008). So far, our data show that sm-treated AGR2^{ko} mice exhibit delayed inflammation at day 1 p.i. as compared to sm-treated AGR2^{het} littermates and amp-treated AGR2^{ko} and AGR2^{het} mice. Moreover, our microbiome analysis suggests that microbiota composition of sm-treated AGR2^{ko} mice might be responsible for the protective effect. We hypothesized that deficiency of the mucus layer and/or the microbiota composition in sm-treated AGR2^{ko} mice may affect T3SS-1 expression.

In order to test whether the T3SS-1 expression is altered in sm-treated AGR2^{ko} mice, we infected sm- or amp-treated AGR2^{het} and AGR2^{ko} mice with 10⁴-10⁶ CFU *S. Tm* p^{sicAgfp}. *S. Tm* p^{sicAgfp} is a reporter strain for T3SS-1 expression which harbors *gfp* fused to the promoter of *sicA*, a component of the T3SS-1. Because *S. Tm*-induced inflammation leads to microbiota dysbiosis (Stecher, Robbiani et al. 2007), we used an avirulent *S. Tm* strain, *S. Tm*^{avir2} p^{sicAgfp}. At day 1 p.i., mice were sacrificed and cecum was sampled, fixed and cryopreserved. Cecal cryosections were stained using polyclonal antibodies against *S. Tm* lipopolysaccharide (LPS, α -*Salmonella* B test serum anti-O) and DAPI (DNA). Confocal images were taken randomly at the epithelial border and in cecal lumen. LPS⁺ and GFP⁺ *S. Tm*^{avir2} p^{sicAgfp} cells were counted in order to calculate the relative rate of T3SS-1 expression.

At day 1 p.i., all experimental groups showed similar *S. Tm*^{avir2} p^{sicAgfp} loads (**Figure 38E**). *S. Tm*^{avir2} p^{sicAgfp} in sm-treated AGR2^{ko} mice exhibited significantly less T3SS-1 expression at the epithelial border and in the cecal lumen than in sm-treated AGR2^{het} littermates (**Figure 38A,B**, p-value 0.0021 and 0.0011, respectively and **Figure 38C,D**), suggesting that the mucus layer or the microbiota has an effect on T3SS-1 expression. Conversely to what was observed after sm-treatment, we found that after amp-treatment, AGR2^{ko} mice showed significantly increased T3SS-1 expression as compared to AGR2^{het} littermates at epithelial border (**Figure 38A**, p-value 0.0170). This result indicates that the mucus layer might not be the only factor influencing T3SS-1 expression. Moreover, relative T3SS-1 expression was significantly reduced in sm-treated AGR2^{ko} mice as compared to amp-treated AGR2^{ko} mice, both at

epithelial border and in lumen (**Figure 38A,B**, p-value <0.0001), pointing at a role of intestinal microbiota in T3SS-1 activation.

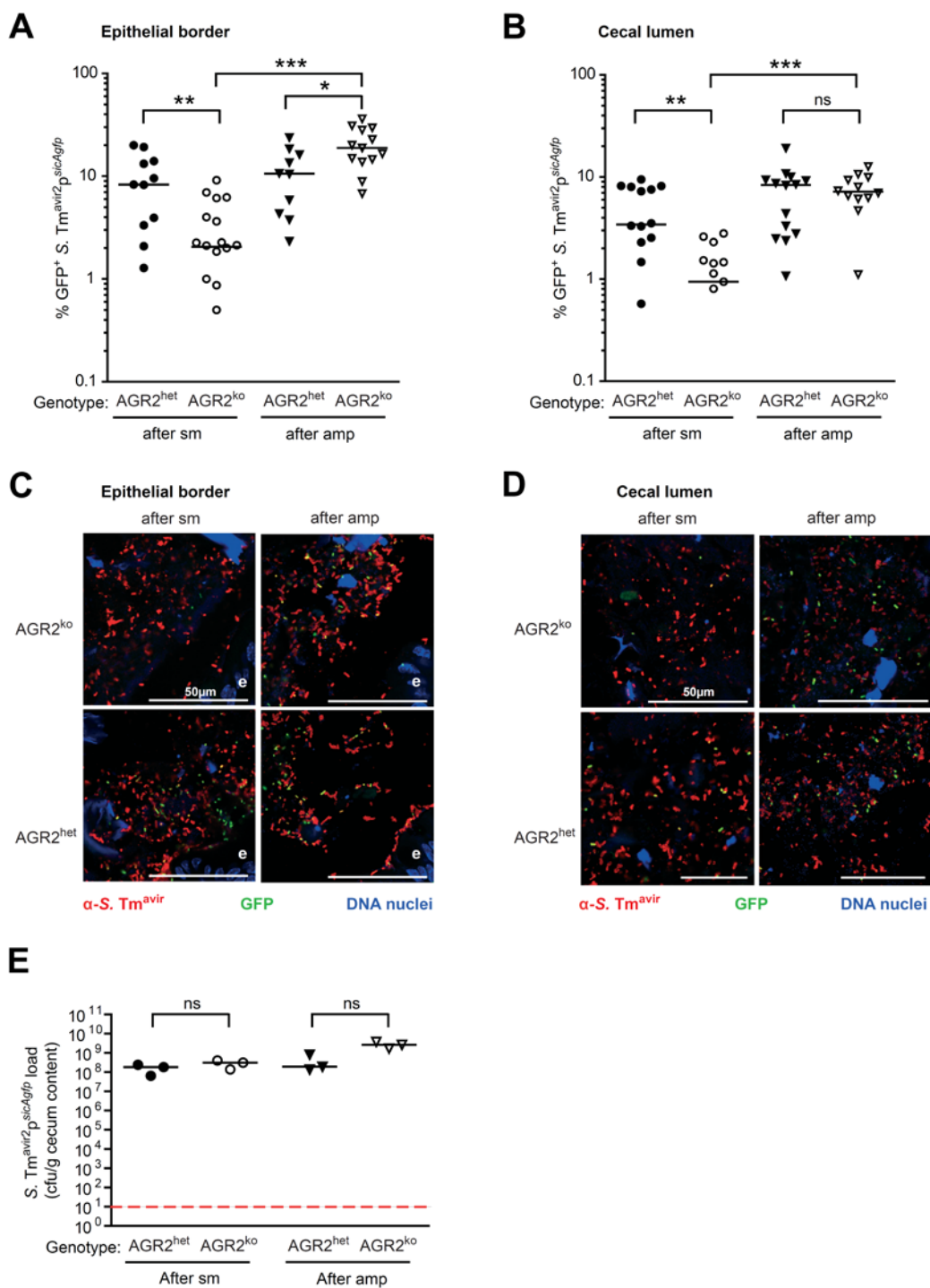


Figure 38. T3SS-1 expression is reduced in $AGR2^{ko}$ mice after streptomycin treatment as compared to ampicillin treatment.

AGR2^{het} and AGR2^{ko} littermate mice were orally gavaged with a single dose of either streptomycin (sm; 25 mg/mouse) or ampicillin (amp; 25 mg/mouse). After 24 h, mice were orally infected with 10⁴ CFU after sm or 10⁶ CFU after amp with *S. Tm*^{avir2}_{p^{sicAgfp}}, an avirulent T3SS-1 reporter strain. At day 1 p.i., mice were sacrificed, cecal tissue was fixed in 4 % PFA and frozen in O.C.T. at -80 °C. Cryosections (7 µm thick) were stained using anti-*Salmonella* B test serum anti-O (red, LPS⁺ *S. Tm*^{avir2}_{p^{sicAgfp}}) and DAPI (blue, nuclei DNA). T3SS-1 expression was represented by GFP signal (green, GFP⁺). Confocal images were taken at the epithelial border and in the lumen. Bacteria were manually counted in a blind manner such as all LPS⁺ *S. Tm*^{avir2}_{p^{sicAgfp}} bacteria were counted first, and then the GFP⁺ cells which colocalized with LPS⁺ *S. Tm*^{avir2}_{p^{sicAgfp}}. 4-8 images at the epithelial border per mouse, 5-7 images in the lumen per mouse and 3 mice per condition. **(A-B)** Bacterial counts **(A)** at epithelial border and **(B)** in cecal lumen. **(C-D)** Representative confocal images of cecal sections from AGR2^{het} and AGR2^{ko} mice after either sm or amp **(C)** at epithelial border or **(D)** in cecal lumen. Scale bars: 50 µm. e; epithelial border. **(E)** *S. Tm*^{avir2}_{p^{sicAgfp}} load was determined at day 1 p.i. in cecum by plating with appropriate antibiotics. Bars represent the median. Dotted red line represents the detection limit. Circle; sm-treated mice, inverted triangle; amp-treated mice, full symbols; AGR2^{het}, empty symbols; AGR2^{ko}. Mann-Whitney U test: ns=not significant (P≥0.05), * P<0.05, ** P<0.01, *** P<0.001. One-way ANOVA Kruskal-Wallis test: **(A)** P<0.0001, **(B)** P<0.0001, **(E)** P=0.0752.

All together, these results indicate that the mucus layer might play an indirect role in T3SS-1 activation by modulating the intestinal microbiota. Indeed, as previously shown, the intestinal microbiota differs in sm-treated AGR2^{ko} mice, which are better protected against *S. Tm*-induced inflammation as compared to sm-treated AGR2^{het} littermates as well as amp-treated AGR2^{ko} and AGR2^{het} mice. Therefore, it is tempting to speculate that the potentially protective microbiota of sm-treated AGR2^{ko} might inhibit T3SS-1 activation and, consequently, delay intestinal inflammation.

6. Discussion

6.1. The Oligo-MM: a defined microbial consortium to study microbiota-host pathogen interaction in gnotobiotic mice

6.1.1. The Oligo-MM can be used as platform to identify bacteria and mechanisms underlying colonization resistance

Numerous approaches have been used to investigate CR mechanisms *in vivo*. Early studies already showed that antibiotic treatment alleviates the protective role of conventional microbiota against enteropathogen infection (Miller, Bohnhoff et al. 1956, van der Waaij, Berghuis-de Vries et al. 1971, Pongpech, Hentges et al. 1989). Attempts were made to identify CR mechanisms by characterizing physiology of the antibiotic-treated mice. For example, antibiotic treatment has been reported to inhibit innate and adaptive immune responses (*e.g.* intestinal expression of RegIII γ and colonic T_{regs}) (Brandl, Plitas et al. 2008, Smith, Howitt et al. 2013), favor the expansion of oxygen-tolerant bacteria such as Enterobacteriaceae (Thijm and van der Waaij 1979) and decrease SCFA levels which are involved in CR (Lawhon, Maurer et al. 2002, Fukuda, Toh et al. 2011, Wichmann, Allahyar et al. 2013). Moreover, antibiotic treatment has been used in combination with transplantation of conventional or low complexity microbiota to identify bacteria that restore CR against enteropathogens (Koopman, Kennis et al. 1984, Stecher, Chaffron et al. 2010, Lawley, Clare et al. 2012). Nowadays, fecal transplantation from healthy human donors is successfully used in humans to treat intestinal infections (*e.g.* against *C. difficile* and *Staphylococcus aureus*) (Konturek, Haziri et al. 2015, Wei, Gong et al. 2015). However, the biggest limitation to study mechanisms underlying CR and identify protective bacteria remains the enormous microbiota complexity. Therefore, comparative microbiome analyses of protective *vs* susceptible cohorts were developed to identify candidate bacterial taxa that correlate with protection against infection (Schubert, Sinani et al. 2015). Elegantly, some studies went one step further and used gnotobiotic mouse models to prove that some candidate strains were indeed responsible for CR (Hsiao, Ahmed et al. 2014, Buffie, Bucci et al. 2015). Gnotobiotic mouse models which are colonized with individual bacteria or mixtures have been proven as a powerful tool to investigate mechanisms underlying CR (Reeves, Koenigsnecht et al. 2012, Ganesh, Klopffleisch et al. 2013).

In this study, we assembled a broad spectrum of phylogenetically different gut bacteria in order to establish a minimal bacterial consortium. In this way, we generated the first defined bacterial consortium of mouse-derived strains which was able to provide significant CR against *S. Tm^{avir}* in mice (**Figure 15**).

Next, we developed a completely new approach to identify possible CR mechanisms by comparing artificial metagenomes of the Oligo-MM¹² strains to the “real” metagenome of conventional mice. In this way, we identified functions which might still be missing in Oligo-MM¹² consortium. We hypothesized that these functions could play a role in CR. And indeed, we validated this hypothesis by using ASF strains, which harbor some of the metabolic pathways present in conventional microbiota but absent from Oligo-MM¹². To my knowledge, this is the first time that a combinatory approach of cultivation and metagenomics is described in order to identify bacteria which confer functionality of a normal gut microbiota.

6.1.2. Which mechanisms underlie colonization resistance mediated by the Oligo-MM?

An approach to analyze the functional capacity (functionome) of a microbial community is based on metagenomics and uses the Kyoto Encyclopedia of Genes and Genomes (KEGG) database (Ogata, Goto et al. 1999) to classify genes into different functional units (Kanehisa, Goto et al. 2014). This approach has already been used successfully on single bacteria, for example, to predict metabolic pathways of *S. Tm* which might play a role during infection (Raghunathan, Reed et al. 2009). It has also been developed to predict the functional capacity of the gut microbiota under different conditions. For example, it was shown that zinc deficiency which leads to impairment of health status alters the metabolic capacity of gut microbiome by depleting pathways involved in lipid metabolism, carbohydrate digestion and mineral absorption. Combined with microbiota composition and host phenotype analyses, the authors correlated several bacterial OTUs (*e.g.* decrease of the taxonomic family Peptostreptococcaceae which belongs to the *Firmicutes*) with zinc depletion (Reed, Neuman et al. 2015). However, to confirm that these OTUs are indeed responsible for pathological states under zinc deficiency conditions, availability of bacterial strains as pure culture would be a valuable tool to perform proof of concept studies in gnotobiotic mice.

In our study, we performed functional analysis based on metagenomics to determine the presence and completeness of functional KEGG modules in individual strains and in different defined bacterial communities. We also identified KEGG modules that are present in conventional microbiota but absent of Oligo-MM¹² (**Figure 17**). Based on this finding, we hypothesized that increasing the metabolic capacity of Oligo-MM¹² could also increase CR against *S. Tm*^{avir}. Therefore, Oligo-MM¹² could be supplemented with bacterial taxa (*e.g.* ASF strains) which are predicted to possess these missing KEGG modules. We tested this hypothesis by transplanting the ASF⁷ consortium in Oligo-MM¹² mice. We found that Oligo-MM¹² +

ASF⁷-colonized mice showed increased CR against *S. Tm*^{avir} as compared to Oligo-MM¹²-colonized mice (**Figure 19**). We concluded that ASF⁷-specific KEGG modules might play a role in CR (**Figure 20, block “D”**). These include T6SS, transport systems for nickel, sodium, heme, phosphanate, trehalose/maltose and rhamnose, as well as degradation systems for xylene, toluene and acylglycerol. It is known that T6SS of *Vibrio cholerae* displays antimicrobial activity against *S. Tm* (MacIntyre, Miyata et al. 2010). Using our metagenomics approach, we found that ASF457 possesses a T6SS. It would be interesting to test whether ASF457 plays a role in CR against *S. Tm* or whether some effector proteins are missing.

Yet, transplantation of conventional microbiota into ASF⁵ mice increased even further CR (**Figure 15**). This suggests that Oligo-MM¹² + ASF⁷ consortium is not as functional as a conventional microbiota to restore CR and that some bacterial taxa are still missing in Oligo-MM¹² to reproduce a conventional-like CR phenotype. Using comparative metagenomics analysis, we identified other KEGG modules that are specific for the conventional microbiota and might also play a role in CR. These include transport systems for carbohydrates and amino acids such as trehalose, glycerol, erythritol, histidine, taurine and lysine/arginine/ornithine. We also identified transport systems for hemin, tungstate, manganese/zinc/iron, sulfate, nitrate/nitrite as well as urea and vitamin B12. Of note, some of these components are already known to influence enteric infections. For example, consumption of vitamin B12 by *Bacteroides thetaiotaomicron* decreases the level of Shiga toxin 2 which is the main virulence factor of EHEC (Cordonnier, Le Bihan et al. 2016). Additionally, we identified an enrichment of various cytochrome modules in the conventional microbiota. As our different defined consortia are mainly composed of strict anaerobic bacteria, it is reasonable to hypothesize that facultative anaerobic bacteria would also play a role in CR, as they would be competing for oxygen with *S. Tm*. It was already known that *E. coli* induces CR against *S. Tm* in GF mice (Hudault, Guignot et al. 2001). Remarkably, the hypothesis that facultative anaerobic (*e.g. E. coli*) could also induce CR when added to the Oligo-MM¹² has been successfully verified in our laboratory (unpublished data). These observations as well as the correlation between microbiota complexity and CR (**Figure 19**) are consistent with the Freter’s nutrient-niche hypothesis (Freter, Brickner et al. 1983). It postulated that a bacterium cannot invade a resident microbiota if its metabolic niche is already occupied by other strains. This suggests that in order to invade a host, a bacterium (*e.g. enteropathogen*) would have to use a specific limiting nutrient more efficiently than the rest of the microbiota.

As previously mentioned, there are other mechanisms involved in CR. For example, the microbiota can also mediate gut epithelial cell maturation (*e.g. via production of SCFA*) (Ploger, Stumpff et al. 2012) and influence gut immune responses (*e.g. via educating the host immune system*) (Backhed 2012, Smith, Howitt et al. 2013). An approach to elucidate the indirect effects of gut microbiota on its host

would be to colonize mice with different defined bacterial consortia and perform metatranscriptomics analysis on host cells to identify differential regulation of genes involved in immune defenses. This would generate hypotheses that could be tested using appropriate mouse KO strains, for example. Ultimate evidence could also be obtained using genetically modifying anaerobic commensals, which is hardly possible for now.

In conclusion, the approach we have taken is a powerful tool to study functional capacity of microbial communities as well as to identify bacterial taxa and metabolic pathways of interest. Moreover, the recent development of mouse-derived strain collections (*e.g.* the Mouse Intestinal Bacterial Collection (Lagkouvardos *et al.*, submitted)) offers new perspectives to functionally mimic a conventional gut microbiota with a fully defined bacterial consortium.

However, comparative metagenomics analysis also presents some limitations. First, it can predict the presence of open reading frames (ORFs) but not their expression. It is also based on databases that only refer to known functions and pathways. Therefore, the completeness of databases as well as the sequence annotation and discovery are additional limitations. It is also plausible that some of our strains (*e.g.* representatives of novel species, genera or families) harbor pathways that remain to be discovered and described. Finally, in metagenomics datasets, a metabolic pathway is considered as complete whether or not its individual components (*e.g.* enzymes) are present in the same bacterium or in several different organisms. Nevertheless, this approach remains as a powerful tool to generate numerous hypotheses. Testing all these hypotheses is challenging particularly due to the fact that the methodology for genetic manipulation of anaerobic bacteria is still very limited. Thus, attempts have to be made in order to develop genetic systems for a wide number of commensal bacteria.

6.1.3. Minimal gut microbiota as a tool for gnotobiotic studies

An experimental strategy to decipher interactions between host and microbiota is first to study the host environment devoid of bacteria (*i.e.* under germfree conditions), and compare it to the situation after adding individual strains or defined bacterial consortia. Germfree (GF) mice are well known to harbor impaired intestinal environment, morphology, motility and physiology (Berg 1996). For example, GF mice show decreased numbers of goblet cells (Stefka, Feehley *et al.* 2014), lower rate of epithelial cell turnover (Falk, Hooper *et al.* 1998) and decreased mucus production (Jakobsson, Rodriguez-Pineiro *et al.* 2015) as well as impaired immune system (Round and Mazmanian 2009). Due to these abnormalities, GF animals are more susceptible to infections with enteropathogens such as *S. Tm* and *Listeria monocytogenes* (Inagaki, Suzuki *et al.* 1996, Hudault, Guignot *et al.* 2001). In an attempt to study host-

microbiota-pathogen interactions using a simplified gut ecosystem as well as to decipher the mechanisms that lead to gut normalization (*i.e.* restoration of a fully functional microbiota by fecal transplantation of a complex microbiota into GF mice), minimal gut microbiota were generated and inoculated to GF mice.

One of the first defined bacterial consortia was named as Schaedler flora and consists of six strains isolated from mice (Schaedler, Dubs et al. 1965). Later, this consortium was modified and became one of the most popular models of minimal mouse-derived microbiota: the “altered Schaedler flora” (ASF) (Orcutt, Giannim et al. 1987). The ASF encompasses eight different strains: *Parabacteroides* spp., *Mucispirillum* spp., *Eubacterium* spp., three *Clostridium* spp. and two *Lactobacillus* spp. (Dewhirst, Chien et al. 1999). Each strain has been fully sequenced and genome information is now publicly available, in contrast to the strains which are still protected by a patent (Wannemuehler, Overstreet et al. 2014, Wymore Brand, Wannemuehler et al. 2015). GF mice colonized with the ASF are partially normalized as compared to conventional mice (Wymore Brand, Wannemuehler et al. 2015). For example, ASF-colonized mice show partial normalization of the cecum morphology (Schaedler, Dubs et al. 1965), the mucosal immune system and the innate defense (Stecher, Chaffron et al. 2010). However, their high susceptibility to *S. Tm* infection compared to GF and conventional mice suggest that ASF mice are not entirely normalized (Stecher, Macpherson et al. 2005, Stecher, Chaffron et al. 2010). This was also confirmed by other studies (Berry, Stecher et al. 2013, Maier, Vyas et al. 2013). Since then, other defined minimal gut microbiota, which are all based on human-derived strains have been developed. The laboratory of J. Gordon uses routinely GF mice colonized with human-derived microbiota to study host-microbiota interactions (*e.g.* in response to diet changes). Thus, Faith *et al* colonized mice with ten sequenced bacterial species to study the response of this defined community to different diets (Faith, McNulty et al. 2011). Using a linear approach, they established a method to predict the variation in abundance of each strain according to the concentration of dietary ingredients fed to the mice. They also found that in response to diet changes, each bacterial strain rather changes its absolute abundance than its gene expression. However, this elegant and prediction model requires to know the exact bacterial species composition of the microbiota and therefore, cannot be applied to conventional microbiota. In another study, different human-derived bacterial consortia were used to identify microbial genes involved in the establishment of *Bacteroides thetaiotaomicron* in the gut (Goodman, McNulty et al. 2009). Using a transposon mutant library, it was shown that genes involved in competition for nutrients (*e.g.* synthesis and utilization of vitamin B12-dependent cofactors) as well as microbiota composition were critical for *B. thetaiotaomicron* fitness in the gut of gnotobiotic mice. Furthermore, a simplified human intestinal microbiota (SIHUMI) consisting of eight bacterial species was established in gnotobiotic rats (Becker, Kunath et al. 2011). Germfree rats colonized with SIHUMI showed metabolic functions such as production of SCFA and degradation of mucins, which were to some extent comparable to conventional

rats. Further on, SIHUMI was also inoculated in GF mice where it was shown to stably colonize the mouse gut overtime and to be vertically transmitted to the offspring (Ganesh, Klopfleisch et al. 2013, Woting, Pfeiffer et al. 2014). By modulating the bacterial composition of SIHUMI, Woting *et al.* investigated the role of two members of SIHUMI (*i.e. Clostridium ramosum* and *Bifidobacterium longum*) towards obesity and metabolic disorders in mice. They demonstrated that, in their animal model, *C. ramosum* was promoting diet-induced obesity independently of *B. longum*, which has been inversely correlated to obesity phenotypes in human (Woting, Pfeiffer et al. 2014, Woting, Pfeiffer et al. 2015). By supplementing SIHUMI consortium with two other strains, *Akkermansia muciniphila* and *S. Tm*, they showed that the mucin degrader *A. muciniphila* was able to exacerbate *S. Tm*-induced inflammation by interfering with the gut mucus homeostasis (Ganesh, Klopfleisch et al. 2013).

To date, GF mice colonized with human-derived strains termed as humanized gnotobiotic mice have been widely used and have provided valuable insights into host-microbiota interactions. The increased accessibility to human microbiota strain collections and genome sequences reflects a great potential to perform mechanistic studies and investigate molecular interactions between host, microbiota and pathogen. However, interactions between microbiota and its host cannot be completely mirrored by humanized gnotobiotic mice. In an elegant study, Seedorf *et al.* investigated the host-specificity of selection and colonization of mouse-adapted vs human-adapted microbiota (Seedorf, Griffin et al. 2014). Knowing that mice can efficiently exchange their gut microbiota due to coprophagic habits, GF mice were co-housed together with mice harboring either mouse- or human-adapted microbiota. After 14 days, gut microbiota of the previous GF mice exhibited 99.8 % of mouse-adapted taxa, showing that mouse-adapted microbiota invade and colonize mouse gut better than human-adapted microbiota. Similarly, some bacterial strains have been reported to be unable to colonize the mouse gut. For example, the human strain *Lactobacillus reuteri* F275 is unable to colonize *Lactobacillus*-free mice, contrary to rodent-adapted strains (Frese, Benson et al. 2011). This could be due to the presence of specific genes such as urease or xylose clusters, which are absent from human-adapted strains. Additionally, a mouse-derived microbiota was shown to better restore CR against enteropathogens (*e.g. S. Tm*) compared to human-derived microbiota (Chung, Pamp et al. 2012). Interestingly, the degree of CR was also reported to differ between gut microbiota of different mouse strains. Using microbiota transplantation experiments between mouse strains, Willing *et al.* showed that microbiota of NIH Swiss mice enhanced CR against *Citrobacter rodentium* compared to C3H/HeJ-associated mouse microbiota (Willing, Vacharaksa et al. 2011). They also found that this enhanced CR occurred in an IL-22 dependent manner, suggesting the importance of the cross-talk between mouse strain-specific microbiota and genetic determinants of its host. This was also confirmed by Chung *et al.* who reported that mice colonized with a human microbiota exhibit an impaired immune system as compared to mice colonized with a murine microbiota (Chung, Pamp et al. 2012). In

conclusion, these observations highlight the tremendous importance of using microbiota, which are specifically adapted to their host at a species level, or even genetic background.

For all these reasons, we used mouse-adapted bacteria to study the interactions between the mouse gut and its microbiota. Except for KB1 and KB18, all bacterial strains were isolated from C57Bl/6J mice and inoculated into C57Bl/6J gnotobiotic mice. To my knowledge, the Oligo-MM consortium is the first defined mouse-adapted microbiota described where all strains as well as their respective genome sequences are publicly available. I am convinced that this model will be a valuable tool to address questions related to host adaptation and specificity of the microbiota. For example, comparative genomic analysis of human- and mouse-adapted strains would highlight to which extends the knowledge acquired on host-microbiota interactions can be transposed from mouse to human gut. To my knowledge, this question has never been addressed using defined microbiota despite some reports questioning the relevance of mouse models for human health (Bibiloni 2012, Nguyen, Vieira-Silva et al. 2015).

6.1.4. What are the potential limitations of the Oligo-MM model?

6.1.4.1. Do all Oligo-MM strains colonize the mouse gut?

In this study, I established a gnotobiotic mouse model which harbors a defined consortium of mouse-adapted gut bacteria. While most of Gram-negative strains were detected at high abundance level using gDNA-based methods (*i.e.* 16S rRNA gene amplicon sequencing and qPCR), Gram-positive strains were barely detected, if at all. This difference of detection between Gram-negative and -positive strains was also reported elsewhere and can have many reasons (Goodman, McNulty et al. 2009, Faith, McNulty et al. 2011, Li, Limenitakis et al. 2015). For example, these strains may colonize below the detection limit or at different intestinal sites than in cecum and feces. Alternatively, their cell wall remains resistant to the DNA extraction method. Lastly, they may not colonize at all. In our study, KB18 and YL2, which are taxonomically assigned to the Ruminococcaceae; *Incertae Sedis* and *Bifidobacterium* spp., respectively, were detected at very low abundance in few mice using gDNA-based methods (**Figures 12 and 18B; annexed Tables 45 and 48**). YL2 was detected at low abundance in the small intestinal content using amplicon sequencing (**Figure 9B; annexed Table 42**). This suggests that YL2 either colonizes preferentially the small intestine or its abundance is too low compared to the other strains to be detected in cecal and fecal contents. KB18 might have a cell wall resistant to gDNA extraction, as its gDNA is already very hard to extract from pure culture (not shown) and its cell wall was shown to be impermeable to FISH probes (not shown) (**Table 34**). Therefore, presence of YL2 and KB18 in cecal and fecal contents

remains unclear. Similarly, I49 (*Lactobacillus* spp.) and KB1 (*Enterococcus* spp) were detected at very low abundance in cecal and fecal contents using qPCR and amplicon sequencing (**Figures 12, 14 and 18B; annexed Tables 45,47 and 48**). They were both detected in small intestinal content (**Figure 9B; annexed Table 42**) and re-isolated on agar from the cecum of a F3 generation offspring stably colonized with the Oligo-MM¹² consortium (not shown). This suggests that KB1 and I49 colonize and are vertically transmissible, despite their detection at low abundance. The fact that some Gram-positive strains are detected at higher loads in small intestine than in cecum can be due either to their preferences for small intestine niches or to an increased relative abundance, for example caused by a decreased relative abundance of bacterial OTUs such as the *Bacteroidetes*, which are highly represented in cecum but not in small intestine (Sarma-Rupavtarm, Ge et al. 2004). Finally, I46 (Erysipelotrichaceae; *Incertae Sedis*) was detectable using amplicon sequencing (**Figure 8C and D; annexed Tables 39 and 40**) and FISH (not shown) but not using qPCR. Moreover, we confirmed its colonization by re-isolating it on agar from the cecum of a F3 generation offspring (not shown). Therefore, we concluded that I46 colonized and was vertically transmitted. By comparing the 16S rRNA gene sequence of the assembled genome and of the 16S rRNA gene-containing plasmid used to establish the qPCR, we found a mismatch in the primers/probe used to perform the qPCR. As we generated new I46-specific primers and probe, we detected I46 by qPCR in cecum, feces and inoculum at similar abundance level than I49 (data unpublished).

6.1.4.2. Are Gram-positive strains systematically underestimated?

Interestingly, in our model, the majority of strains abundantly detected with gDNA-based methods were Gram-negative strains (**Figures 8 and 12**). This can be due to several reasons. It is known that microbiota composition analysis using amplicon sequencing reveals higher abundance of Gram-negative than Gram-positive strains (Goodman, McNulty et al. 2009, Xiong, Frank et al. 2012, Li, Limenitakis et al. 2015, Rojo, Gosalbes et al. 2015). This observation could be due to the gDNA extraction method used. It was shown that members of the *Bacteroidetes* phylum (Gram-negative strains) are easier to lyse than *Actinobacteria* (Gram-positive strains) and that lysis efficiency depends also on the extraction method used (Salonen, Nikkila et al. 2010, Ferrand, Patron et al. 2014). When using 16S rRNA-based amplicon sequencing, number of sequencing reads which determines the detection limit can play a role as some bacterial strains such as *Enterobacter hormachei* and *Proteus vulgaris* have been shown as undetectable below 2,000-3,000 sequencing reads per sample (Belzer, Gerber et al. 2014). Importantly, primer sets used to amplify variable regions of 16S rRNA gene generally lead to underestimation of some key members of the gut microbiota such as *Bifidobacterium longum*, and consequently to overestimation of other members

like *Bacteroides thetaiotaomicron* (Milani, Hevia et al. 2013). In an attempt to investigate the degree of bias of microbiota composition analysis, some studies performed comparative analyses between culture, gDNA-based methods and FISH. Harmsen *et al.* analyzed human fecal microbiota using cultivation and FISH techniques (Harmsen, Gibson et al. 2000). They found that total count of anaerobic bacteria was generally higher using quantification by FISH as compared to plating (except for Clostridia strains). This observation was also confirmed elsewhere (Vieira-Pinto, Bernardo et al. 2007). However, they used only one type of agar medium per targeted phylum, despite the tremendous heterogeneity of gut microbiota. Another study analyzed human microbiota composition using FISH, 16S rRNA gene-based microarray hybridization and amplicon sequencing (Shankar, Hamilton et al. 2014). This study showed that amplicon sequencing data reveals higher variability of microbiota composition compared to microarray analysis. This could either be due to the fact that microarray allows detection of only 775 bacterial phylotypes or that amplicon sequencing targets the V6 hypervariable region of 16S rRNA gene while microarray hybridized the whole amplified gene. It could also be due to chimera formation that occurs during the amplicon sequencing process and which artificially blows up diversity or to PCR amplification biases (Chakravorty, Helb et al. 2007, Paliy, Kenche et al. 2009, Schwab, Berry et al. 2014). Interestingly, they reported that quantification of bacterial abundance was similar using FISH and microarray hybridization for the major microbial bacterial classes (*i.e.* Clostridia, Bacteroidia and combined *Proteobacteria*). However, they did not investigate underestimated microbial OTUs such as *Actinobacteria* and used conventional microbiota to compare gDNA- and rRNA-based techniques, as most of comparative studies.

In this thesis, we used gnotobiotic mice colonized with Oligo-MM¹² strains to compare gDNA- and rRNA-based techniques. We showed that YL44, a Gram-negative strain, was detected at higher relative abundance using gDNA-based methods (*i.e.* 16S rRNA gene-based amplicon sequencing and qPCR) as compared to rRNA-based approach (*i.e.* FISH). Conversely, YL58 was less detected using gDNA-based methods than rRNA-based approach (**Figure 24**). We also highlighted the overestimation of the relative abundance of a Gram-negative strain and the underestimation of a Gram-positive strain, in our model. Therefore, we draw attention on the risk of global misestimation of bacterial strains depending on their cell wall composition which can lead to impaired analysis of microbiota composition. To my knowledge, this thesis reports the first study using gDNA- and rRNA-based techniques applied to a defined “mid-complex” microbiota in order to demonstrate systemic under- and overestimation of Gram-positive and -negative strains, respectively. Our results also underline the importance of using complementary approaches to analyze microbiota composition.

6.1.4.3. Localization and quantification of individual bacterial strains using FISH

FISH exhibits several limitations that hamper its use to study bacterial niches and gut ecology in conventional microbiota. First, it is challenging to test probe specificity in complex and undefined microbial communities. Moreover, mono- or poly-labelled FISH probes can show different sensitivity to detect low abundant bacteria or bacteria with cell walls that exhibit low-permeability properties to probes (*e.g.* some Gram-positive strains) (Pernthaler, Preston et al. 2002). Finally, there is a real limitation to enumerate fluorescently labelled bacteria principally because gut ecosystem harbors many autofluorescent particles (*e.g.* plant fibers). Some studies report manual counting whether others developed automated enumeration approaches (Thiel and Blaut 2005, Earle, Billings et al. 2015). Up-to-date, one study established a software platform to allow quantification of bacteria as well as their localization in the gut (Earle, Billings et al. 2015). To this end, they used GF mice colonized either with a low-complexity microbiota or with a human conventional microbiota. In this thesis, we used a defined “mid-complex” microbiota and developed another approach using the DAIME software to quantify and localize bacterial strains. One of the advantages of DAIME is that it also allows spatial arrangement analysis of bacterial populations to study microbial population interactions, for example (Schillinger, Petrich et al. 2012). We showed that in Oligo-MM¹²-colonized mice, YL44 was enriched at the epithelial border in contrast to YL58 (**Figures 22 and 23**). Moreover, we also showed that the distribution of YL44 in mouse cecum was dependent on the microbiota context (**Figure 22**). Further investigations will be needed to understand the reasons of these different spatial distributions. These results highlight the importance of studying not only the gut microbiota composition, but also the bacterial population niches in the gut environment. Therefore, I am convinced that DAIME will be a powerful tool to study the behavior of single bacteria within the gut ecosystem.

6.1.4.4. How long do the Oligo-MM strains need to establish a stable microbial community in mouse gut?

It is known that colonization of the host with microbial community occurs in a dynamic way and depends on several parameters such as age and sex (Ge, Feng et al. 2006). However, very few studies analyzed the physiological changes induced by the microbiota after inoculation of GF animals. How long does a microbiota require to fulfil its functions in the mouse gut, to optimally interact with the host immune system or to strengthen the mucus layer? Recently, Johansson *et al.* reported that it takes seven to eight weeks for the colonic mucus to normalize and become impenetrable to microbial bacteria after conventionalization of GF mice. They also showed that colonizing microbiota undergoes dynamic changes

for three weeks post-colonization (Johansson, Jakobsson et al. 2015). In our study, we allowed the Oligo-MM¹² strains to stabilize for approximately 40 days before infection. Significant decrease of relative cecal weight at day 43 post-inoculation as compared to day 0 indicate that physiological changes occur even though microbiota composition remains quite stable from day 10 to 43 post-inoculation (**Figures 9A and 11B**). However, we have not analyzed relative cecal weight correlated with microbiota dynamics further and it could be that 40 days may still not be enough for the microbiota to establish and completely normalize its host. Therefore, it would be interesting to study the metabolic dynamics post-inoculation into GF mice in order to analyze the time needed by the microbiota to fully protect the host against enteropathogens and to decipher the chronological events of mechanisms responsible for CR.

6.1.4.5. Culturomics as a tool to improve taxonomic classification

Culturing of intestinal bacterial strains is one of the biggest limitations to study microbiota-host-pathogen interactions, in particular regarding the human microbiome (Brown, de Vos et al. 2013). Since the development of sophisticated microbiome analysis techniques, molecular tools have supplanted culture techniques, as they are considered as time-consuming and challenging. In the early 21st century, some studies compared data obtained using 16S rRNA gene-based techniques with culturing approaches. In this way, it was shown that microbiota composition was slightly less complex as determined by culturing than by culture independent method such as by a 16S rRNA gene library (Wilson and Blichington 1996). Moreover, Wilson *et al.* underlined the complementary use of both techniques, as half of species were only detected by 16S rRNA gene cloning while one third of species were only identified using culturing. Similarly, it was shown that Gram-negative bacteria are mostly underestimated using pyrosequencing, as compared to Gram staining and transmission electron microscopy (Hugon, Lagier et al. 2013). All together, these results highlight the need of using complementary techniques to analyze microbiota composition, as already noted above. It was estimated that only 60-80 % of fecal bacteria counted using microscopic techniques were uncultured (Langendijk, Schut et al. 1995, Hayashi, Sakamoto et al. 2002). More recently, Fodor *et al.* established a list of “most wanted” bacteria, which have less than 90 % identity to two major human-derived databases (*i.e.* GOLD-Human and Human Microbiome Project (HMP) databases), are present in at least 20 % of the samples from different human body sites and are still uncultured (Fodor, DeSantis et al. 2012). In order to isolate and cultivate these bacteria, efforts were made for examples to optimize growth media (Clavel, Henderson et al. 2006), generate novel culture methods such as synergistic growth and the use of gel microdroplets (Kaeberlein, Lewis et al. 2002, Zengler, Toledo et al. 2002, Rappe and Giovannoni 2003). One of the major advances made by the HMP and other sequencing projects was that about 5, 000 human-derived bacterial strains were isolated, cultured and their

genomes sequenced (Fodor, DeSantis et al. 2012). Several studies showed that cultivating a large repertoire of microbial OTUs was possible from few human donors (Goodman, Kallstrom et al. 2011). Increasing the number of culture conditions was termed as culturomics (Pfleiderer, Lagier et al. 2013, Lagier, Hugon et al. 2015). Development of culturomics is necessary not only to isolate novel bacteria, but also to improve the resolution of 16S rRNA amplicon and metagenomics studies as well as to ameliorate taxonomic classification and avoid misinterpretation of data (Fournier, Lagier et al. 2015, Lawson and Rainey 2015). Moreover, a complementation of public strain collections would facilitate standardization of gnotobiotic experiments, guarantee the availability of bacterial strains to the entire scientific community, enable the design of *in vitro* experiments to optimize the interpretation of “omics” datasets in combination with genome sequence databases (Bleich and Hansen 2012, Kim, Cho et al. 2012). Strain collections based on human isolates were readily implemented (*e.g.* to address clinically relevant questions). However, very few mouse-derived bacterial strains are currently available and fully sequenced. However, as explained before, the use of mouse-strains to colonize mouse gut is particularly important to study molecular and host-specific interactions between the commensals and their host. Therefore, efforts must also be made to isolate more mouse-derived strains, submit their genomes to sequencing and generate public genome databases and strain collections. Moreover, contrary to human pathogens, which have been extensively studied in the past, commensals have been poorly characterized. Thus, it appears essential to generate more commensal reference strains. In our study, we aimed at isolating and establishing culture methods of intestinal mouse-derived bacteria under anaerobic conditions. Our research lead us to isolate and characterize new genera such as KB18 (Ruminococcaceae; *Incertae Sedis*) and YL45 (*Parasutterella* spp.), which were taxonomically assigned using Silva database (**Table 35**). However, it is known that the Silva database contains sequences of unequal quality that can come from misidentified organisms and largely reflects uncultured taxa (Fodor, DeSantis et al. 2012, Ricker, Qian et al. 2012, Fournier, Lagier et al. 2015). Therefore, in order to better assign novel strains, we used another well-curated database, EzTaxon, which only contains sequences of type strains (*i.e.* cultured described species that are deposited in at least two recognized collections in two different countries) (Kim, Cho et al. 2012). All sequences of this database were also subjected to phylogenetic analysis which leads to a complete hierarchical classification system. Therefore, we used 16S rRNA gene sequence alignment against EzTaxon database to identify novel species among Oligo-MM strains (*i.e.* with a match ≤ 97 % sequence identity to a type strain) (**Table 37**). This analysis revealed that the Oligo-MM¹² consortium contains one novel species *Bacteroides* sp. nov. (I48), two members of a novel genus Clostridiales gen. nov. (KB18) and *Sutterella*_f gen. nov. (YL45), and one member of a novel family *Barnesiella*-like fam. nov. (YL27). Therefore, new names were proposed for these strains: *Bacteroides caecimuris* (I48), *Acutalibacter muris* (KB18), *Turicimonas muris* (YL45) and *Muribaculum intestinalis* (YL27)

(Lagkouvardos *et al.*, submitted). By isolating novel strains, we aimed at exploring the potential of the so far uncultured majority of mouse intestinal bacteria. Up-to-date, we focused on members of the superkingdom Bacteria. However, it is known that members of the superkingdom Archaea such as *Methanobrevibacter smithii* and *Methanosphaera stadtmanae* can influence host immune homeostasis (Bang, Weidenbach *et al.* 2014). They have also been shown to interact with Bacteria members such as *Bacteroides thetaiotaomicron* which can modulate the metabolic landscape of the host (Samuel and Gordon 2006). In future experiments, it would be interesting to test whether Archaea representatives, alone or together with the Oligo-MM¹², are also involved in CR. To my knowledge, it remains unknown.

Table 37. Taxonomic assignment of the Oligo-MM strains using EzTaxon database

| Taxonomic classification | Strain ID | Taxonomic Identity | Eztaxon besthit |
|---------------------------------|------------------|------------------------------------|---|
| phylum Actinobacteria | | | |
| class Actinobacteria | | | |
| order Bifidobacteriales | | | |
| family Bifidobacteriaceae | YL2 | <i>Bifidobacterium animalis</i> | |
| phylum Bacteroidetes | | | |
| class Bacteroidia | | | |
| order Bacteroidales | YL27 | <i>Barnesiella</i> -like fam. nov. | 86.16 % <i>Barnesiella intestinihominis</i> |
| family Bacteroidaceae | I48 | <i>Bacteroides sp. nov.</i> | 96.86 % <i>Bacteroides xylanisolvens</i> |
| phylum Proteobacteria | | | |
| class Betaproteobacteria | | | |
| order Burkholderiales | | | |
| family Sutterellaceae | YL45 | <i>Sutterella_f gen. nov.</i> | 93.92 % <i>Parasutterella excrementihominis</i> |
| phylum Verrucomicrobia | | | |
| class Verrucomicrobiae | | | |
| order Verrucomicrobiales | | | |
| family Verrucomicrobiaceae | YL44 | <i>Akkermansia muciniphila</i> | |
| phylum Firmicutes | | | |
| class Bacilli | | | |
| order Lactobacillales | | | |
| family Enterococcaceae | KB1 | <i>Enterococcus sp.</i> | |
| family Lactobacillaceae | I49 | <i>Lactobacillus reuteri</i> | |
| class Clostridia | | | |
| order Clostridiales | | | |
| family Lachnospiraceae | YL32 | <i>Clostridium clostridioforme</i> | |
| | YL58 | <i>Blautia sp.</i> | |
| family Ruminococcaceae | YL31 | <i>Flavonifractor plautii</i> | |
| | KB18 | Clostridiales <i>gen. nov.</i> | 92.09 % <i>C. leptum</i> |
| class Erysipelotrichia | | | |
| order Erysipelotrichales | | | |
| family Erysipelotrichaceae | I46 | <i>Clostridium innocuum</i> | |

Full length 16S rRNA gene sequences were aligned against the EzTaxon database.

6.2. The AGR2^{ko} mice: A mouse model to study the role of the mucus layer and the microbiota during *S. Tm* infection

6.2.1. Does mutation of AGR2 gene only affect the cecal mucus layer?

6.2.1.1. AGR2^{ko} mice do not develop spontaneous colitis in contrast to other mucin-deficient mouse models

In this study, the AGR2^{ko} mouse model was used to study the role of the mucus layer during *S. Tm* infection as AGR2^{ko} mice lack a functional intestinal mucus layer (Park, Zhen et al. 2009). Previous studies used other mucin-deficient mouse models to analyze the role of the mucus layer such as MUC2-deficient, *Winnie* and *Eeyore* mice (Velcich, Yang et al. 2002, Heazlewood, Cook et al. 2008). Lack of an intestinal mucus layer allows the bacteria to come in direct contact with epithelial cells, penetrate into the normally sterile crypts and even into epithelial cells (Johansson, Phillipson et al. 2008). Therefore, these mice are known to develop spontaneous colitis and to be more susceptible to enteric infections and chemically induced colitis, although the colitis phenotype was also shown to vary depending on the mouse genetic background as well as housing hygiene conditions (Velcich, Yang et al. 2002, Van der Sluis, De Koning et al. 2006, Heazlewood, Cook et al. 2008, Bergstrom, Kisson-Singh et al. 2010, Bao, Guo et al. 2014). To my knowledge, AGR2^{ko} mice have never been used to study the role of mucus layer during enteropathogen infection. In our study, AGR2^{ko} mice did not develop spontaneous colitis when housed under SPF conditions. Surprisingly, they showed high mortality once rederived germfree. This is contradictory with other observations reporting that mucin-deficient mice generally do not develop colitis or high mortality when housed under germfree conditions (Sellon, Tonkonogy et al. 1998). The underlying reasons for this remain currently unknown.

6.2.1.2. AGR2^{ko} and AGR2^{het} mice exhibit differential phenotype and gene expression

It has been reported that AGR2^{ko} mice exhibit other differences besides the absent mucus layer as compared to AGR2^{wt} mice. In fact, mutation of AGR2 gene is also associated with body weight loss, premature death, intestinal morphologic abnormalities, dysregulation of immune responses, increased neutrophil infiltration in the intestinal epithelium and increased ER stress response (Gupta, Wodziak et al. 2013). Moreover, dysregulation of AGR2 gene expression has also been associated with tumor growth and metastasis (Ramachandran, Arumugam et al. 2008, Hong, Wang et al. 2013, Sung, Choi et al. 2014). In this study, we focused on the mucus layer deficiency. However, we cannot exclude the possibility that

AGR2 gene mutation could also influence *S. Tm* infection by other mechanisms besides the mucus layer deficiency.

First, this is supported by the fact that AGR2 protein has been localized intracellularly and extracellularly (Bergstrom, Berg et al. 2014). Even though its functions remain unknown, we cannot exclude that AGR2 could exhibit an antimicrobial activity. Second, it is also supported by analyses of gene expression using DNA microarrays either on stomach or cecal tissues. In stomach tissues, 858 genes were found to show at least a 3-fold change in gene expression in AGR2^{ko} vs AGR^{het} mice (Gupta, Wodziak et al. 2013). Among these genes, the authors highlighted the *Reg* family of genes such as RegIII β , which can kill *Salmonella* spp. (Stelter, Kappeli et al. 2011, van Ampting, Loonen et al. 2012). In agreement with this study, we found that gut epithelial gene expression varies for several gene sets between AGR2^{ko} and AGR^{het} mice (**Tables 49 and 50**). Whereas few gene sets were found to be upregulated in AGR2^{ko} mice (e.g. cholesterol biosynthesis), several gene sets were significantly downregulated in AGR2^{ko} mice, as compared to AGR2^{het} mice. Among them, we found genes involved in cell cycle, metabolism, damage response, cancer pathways and immune response (e.g. interleukin-2 signaling and immunoregulatory interactions between a lymphoid and a non-lymphoid cells). This suggests that AGR2^{ko} mice exhibit decelerated epithelial turnover. In this thesis, we also showed that sm-treated AGR2^{ko} mice exhibit attenuated susceptibility to *S. Tm* infection at d1 p.i. and decreased *S. Tm* numbers in cecal tissue (**Figures 26 and 27**). Therefore, it would be reasonable to speculate that this protective effect against *S. Tm*-induced inflammation could be due to a global downregulation of inflammatory immune responses or an upregulation of immune responses involved in *S. Tm* killing. Interestingly, several immune-related gene sets were found to be repressed in ileal epithelium of MUC2^{ko} mice as compared to MUC2^{wt} mice (Sovran, Loonen et al. 2015). Among these gene sets were found genes involved in Toll-like receptor-, immune- and chemokine-signaling. Genes involved in adaptive immune responses were also found to be downregulated in MUC2^{ko} mice, although this downregulation depends also on mouse age. Therefore, due to the high complexity of regulation of immune responses, this hypothesis would require further investigation. Thus, the effects of differential gene expression remain unclear with respect to *S. Tm* infection between AGR2^{ko} and AGR^{het} mice.

Furthermore, Sovran *et al.*, also pointed out that MUC2^{het} mice also exhibit differential gene expression as compared to MUC2^{wt} mice. For instance, immune-related gene sets were upregulated in MUC2^{het} mice as compared to MUC2^{wt} mice (Sovran, Loonen et al. 2015). This differential gene expression suggests that heterozygous and wild-type mice may also exhibit different phenotypes. AGR2^{het} and AGR2^{wt} mice show a similar phenotype with respect to morphology of the mucus layer (Bergstrom, Berg et al. 2014). However, we did not investigate further neither the gene expression of AGR2^{wt}

epithelial cells as compared to AGR2^{het} cells, nor the response of AGR2^{wt} mice to *S. Tm* infection. It could be that AGR2^{het} mice exhibit a phenotype which is biased as compared to AGR2^{wt} mice. Therefore, we would not have compared AGR2^{ko} mice to mice harboring “normal” mucus layer and gene expression. This could have hampered the interpretation of the gene expression analysis, for example.

6.2.1.3. AGR2^{ko} and AGR2^{het} mice exhibit differential microbiota composition

In agreement with other studies we showed that mucin-deficient mice harbor different microbiota composition as compared to mice with an intact mucus layer (**Figure 30**) (Bel, Elkis et al. 2014, Sommer, Adam et al. 2014, Sovran, Loonen et al. 2015). This could be due to the fact that the mucus represents a potential ecological niche and nutrient source for bacteria (Li, Limenitakis et al. 2015). In 2014, Bel *et al.* showed that mice with altered mucus layer (*i.e.* mice harboring a thicker and more robust colonic mucus layer) had decreased susceptibility to chemically induced colitis and that this relative protection was transmissible using fecal transplantation (Bel, Elkis et al. 2014). In our study, we concluded that the gut microbiota of sm-treated AGR2^{ko} mice conferred protection against *S. Tm* infection at early time-point (**Figures 26 and 34**). However, we did not analyze the transmissibility of this protection to AGR2^{het} mice by transplantation of cecal content from sm-treated AGR2^{ko} mice into AGR2^{het,GF} mice, for example. Such an experiment would be important to confirm the protective role of the microbiota against *S. Tm* infection in AGR2^{ko} mice.

Additionally, we used differential antibiotic treatment foregoing *S. Tm* infection to show that this protective effect could be due to bacterial taxa that are resistant to sm but not to amp. By applying indicator taxa analysis, we correlated this protective effect to the presence of bacterial members assigned to the phylum *Deferribacteres* (**Figure 36**). Up-to-date, this phylum has not been extensively investigated. On the one hand, some studies question whether it might play a deleterious role in periodontal diseases in humans (Hutter, Schlagenhauf et al. 2003, Kumar, Griffen et al. 2003, Saito, Leonardo Rde et al. 2006), in DSS-induced colitis in mice (Berry, Schwab et al. 2012) and during *Citrobacter rodentium* infection (Hoffmann, Hill et al. 2009) or whether it would be able to translocate from intestinal tract to hepatobiliary system (Robertson, O'Rourke et al. 2005). On the other hand, the phylum *Deferribacteres* has also been associated with beneficial effects against DSS-induced colitis (Ooi, Li et al. 2013). Intriguingly, we had already correlated a bacterial member of this phylum (*i.e.* ASF457 assigned to *Mucispirillum* spp.) to increased CR against *S. Tm* due to a potential role of its T6SS in interfering with *S. Tm* growth (**Figures 19 and 20, block “D”**). However, it remains unclear whether such a protective effect would also depend on the microbiota context. Moreover, bacterial taxa assigned to Ruminococcaceae and Clostridiales were

also found as enriched in sm-treated AGR2^{ko} mice (**Figure 36**). It is reasonable to speculate that these taxa could also play a role in protection, as they have already been associated with recovery of colonization resistance against *C. difficile* and a vancomycin-resistant *Enterococcus* strain (Jump, Polinkovsky et al. 2014). Thus, it would be interesting to test whether bacterial strains which are isolated from sm-treated AGR2^{ko} mice would be protective against *S. Tm*-induced inflammation when inoculated to AGR2^{ko,GF} mice alone or combined with the Oligo-MM¹² consortium.

Finally, we also observed that microbiota of AGR2^{ko} mice was less susceptible to antibiotic treatment than the microbiota of the other experimental groups (**Figure 32B**). It is known that the translocating activity of T3SS-1 is induced upon contact with epithelial cells (Zierler and Galan 1995). Thus, the residual sm-resistant microbiota might physically hamper *S. Tm* to reach the epithelial border. This hypothesis might deserve further investigation.

6.2.2. Which other mechanisms could protect sm-treated AGR2^{ko} mice against *S. Tm* infection?

6.2.2.1. *S. Tm* exhibits reduced T3SS-1 expression in sm-treated AGR2^{ko} mice

In order to invade epithelial cells and to trigger inflammation, *S. Tm* injects numerous effector proteins into the host cell via a T3SS encoded on SPI-1 and named as T3SS-1 (Kaiser, Diard et al. 2012). This T3SS-1 is essential for *S. Tm* internalization and to manipulate host-signaling pathways. Mechanisms involved in these processes have been well characterized (Fabrega and Vila 2013, LaRock, Chaudhary et al. 2015). In mouse gut lumen, it was shown that approximately 15 % of *S. Tm* cells expressed T3SS-1 (Ackermann, Stecher et al. 2008). This was also confirmed *in vitro* (Hautefort, Proenca et al. 2003, Schlumberger, Muller et al. 2005). However, the mechanisms that regulate the bistable expression of T3SS-1 need to be further investigated. Several transcriptional regulators have been reported to modulate SPI-1 expression. For example, Fis is required for full activation of SPI-1 genes (Kelly, Goldberg et al. 2004), whereas HilC and HilD can activate the transcription of HilA, which in turn activates the genes encoding for T3SS-1 as well as effector proteins (Bajaj, Hwang et al. 1995). Low oxygen levels found in the gut can also modulate SPI-1 gene expression as it influences DNA supercoiling topology. For example, relaxed DNA supercoiling can repress *invA*, a regulator encoded on SPI-1 (Galan and Curtiss 1990) or activate *hilC* and *hilD* expression, which consequently can induce T3SS-1 expression (Cameron and Dorman 2012). Other environmental factors were found to repress T3SS-1 expression *in vitro* such as naringenin which is a citrus flavonoid (Vikram, Jesudhasan et al. 2011) and L-arabinose (Lopez-Garrido,

Puerta-Fernandez et al. 2015) as well as products released by the gut microbiota like SCFA (*e.g.* propionate and butyrate) and lactate (Durant, Corrier et al. 2000, Durant, Corrier et al. 2000, Lawhon, Maurer et al. 2002). Interestingly, lactic acid-producing bacteria were also found to alter SPI-1 expression *in vivo* but the mechanism remains unclear (Yang, Brisbin et al. 2014).

In this thesis, we showed that relative expression of T3SS-1 at epithelial border and in lumen of cecum of sm-treated AGR2^{ko} mice was significantly reduced as compared to amp-treated AGR2^{ko} mice (**Figure 38A,B**). Therefore, we reasoned that the gut microbiota might be able to influence T3SS-1 gene expression through mechanisms that remain to be determined. A reasonable approach to investigate these mechanisms in AGR2^{ko} mice would be to test whether the effect is also recapitulated in gnotobiotic AGR2^{ko} and AGR2^{het} mice colonized with the Oligo-MM¹² consortium. If yes, we could narrow down the bacterial isolates responsible for this effect and start deciphering the mechanism of interaction with *S. Tm* genes at a molecular level. If no, we could add different commensal strains isolated from sm-treated AGR2^{ko} mice (*e.g.* bacterial strains assigned to the taxa *Deferribacteres* or Ruminococcaceae) and test their interaction with T3SS-1 expression *in vitro* and *in vivo*. It is tempting to speculate that the gut microbiota might be causal for the reduced T3SS-1 expression in *S. Tm* observed in sm-treated AGR2^{ko} mice although other factors should also be considered.

6.2.2.2. Effects of antibiotic treatments on the host and on *S. Tm*

Not only can antibiotics severely damage the gut microbiota (Reikvam, Erofeev et al. 2011, Schubert, Sinani et al. 2015), but they can also have deleterious effects on the host. Long-term antibiotic-induced dysbiosis has been associated with increased body adiposity, colitis, diarrhea and allergies (Hill, Siracusa et al. 2012, Liou and Turnbaugh 2012, Varughese, Vakil et al. 2013, Satokari, Fuentes et al. 2014). Moreover, mice supplied with an antibiotic mixture (*i.e.* ampicillin, vancomycin, neomycin and metronidazole) can experience increased baseline morbidity and mortality depending on their genotype (Reikvam, Erofeev et al. 2011). Conversely, it was also reported that mice gavaged with a different mixture (*i.e.* vancomycin, neomycin, metronidazole and amphotericin-B) together with drinking water supplemented with ampicillin did not show distress or pain (Reikvam, Erofeev et al. 2011). The reason for this remains unclear. It could be due to the mode of antibiotic administration (*i.e.* continuously in drinking water or every 12 h by gavage), the duration of administration (*i.e.* seventeen days to several weeks) or other reasons such as genetic background, housing conditions, age, presence of opportunistic pathogens within the microbiota or microbiota composition (Ayres, Trinidad et al. 2012, Pham, Clare et al. 2014). The intestinal mucus layer was also shown to influence antibiotic permeation from gut lumen through

epithelial cells (Coghill, Hopwood et al. 1983, Goddard 1998). While ampicillin is known to be moderately well absorbed from the gut lumen, streptomycin is known not to be absorbed (Croswell, Amir et al. 2009). However, the effect of mucus deficiency on the absorption or the interactions of these antibiotics with epithelial cells remain unclear. Additionally, depletion of the gut microbiota by antibiotics can influence host gene expression and consequently, the host gut metabolic landscape (Lange, Buerger et al. 2016). In intestinal epithelial cells, 36 genes presenting at least a two-fold altered expression were upregulated in antibiotic treated mice (*e.g.* RegIII β) and 70 genes were downregulated (*e.g.* caspase 14) (Reikvam, Erofeev et al. 2011). Finally, the antibiotic novobiocin was shown to activate T3SS-1 genes expression by changing DNA topology (Cameron and Dorman 2012). Novobiocin is produced from the same bacterial genus as streptomycin (*i.e.* *Streptomyces* spp.) and belongs to the antibiotic class of aminocoumarins which are known to inhibit the DNA gyrase. Streptomycin is known to enhance susceptibility to infections by *S. Tm* and this effect was reported to be due to the depletion of microbiota by streptomycin (Ng, Ferreyra et al. 2013). However, the effects of sm on *S. Tm* virulence gene expression have never been studied in detail. In this thesis, the use of two antibiotics in AGR2^{ko} mice allowed us to highlight the role of the microbiota in protection against *S. Tm* infection (**Figures 26 & 34**). However, we cannot rule out the possibility that antibiotics may influence *S. Tm* infection by modulating the gene expression and the physiology of AGR2^{ko} mice (*e.g.* increased anti-inflammatory responses) or *S. Tm*. Thus, we could speculate that the protective effect observed against *S. Tm* in sm-treated AGR2^{ko} mice could be due to interactions of sm with epithelial cells, which would be enhanced in AGR2^{ko} due to the absence of a functional mucus layer. Moreover, in humans, the standard posology of sm and amp is 15 mg/kg and 50-200 mg/kg, respectively. In mice, we used 25 mg/mouse, a much higher dose. This represents approximately 1250 mg/kg which is 6 to 83-fold more than in humans. Streptomycin is known to be more toxic (*i.e.* nephrotoxicity and ototoxicity, in humans) than ampicillin (Rybak, Abate et al. 1999). Therefore, effects of sm and amp posology used for mouse experiment cannot be ignored although poorly characterized in mice.

7. Appendix

Table 38. Microbial composition of the Oligo-MM¹⁰ inoculum determined by qPCR

| Strain ID | Isol46 | Isol49 | YL58 | YL31 | YL32 | YL44 | KB1 | YL2 | YL45 | Isol48 |
|----------------|----------|----------|----------|----------|----------|----------|----------|----------|----------|----------|
| Rel. abundance | 0,00E+00 | 5,71E-03 | 3,78E-02 | 2,15E-01 | 1,51E-02 | 1,88E-01 | 9,57E-03 | 7,28E-03 | 2,45E-02 | 4,97E-01 |

Amount of 16S rRNA gene copies per 5 ng fecal DNA are given as relative abundance and corresponding bar plots are presented in **Figure 8B**.

Table 39. Microbial composition in feces determined by amplicon sequencing using the Silva database to assign taxonomy at the family level

| Days post-inoculation (d) | d0 | d0 | d0 | d0 | d10 | d10 | d10 | d10 | d20 | d20 | d20 | d20 |
|---------------------------|------------------|----------|----------|----------|---|----------|----------|----------|----------|----------|----------|----------|
| Mouse number | 222 | 224 | 227 | 228 | 222 | 223 | 227 | 228 | 224 | 225 | 230 | 231 |
| Microbiota | ASF ³ | | | | ASF ³ + Oligo-MM ¹⁰ | | | | | | | |
| Taxon (Family level) | | | | | | | | | | | | |
| Nocardiaceae | 0,00E+00 | 0,00E+00 | 0,00E+00 | 0,00E+00 | 0,00E+00 | 0,00E+00 | 0,00E+00 | 0,00E+00 | 0,00E+00 | 0,00E+00 | 0,00E+00 | 0,00E+00 |
| Microbacteriaceae | 0,00E+00 | 5,50E-05 | 0,00E+00 | 0,00E+00 | 0,00E+00 | 0,00E+00 | 0,00E+00 | 0,00E+00 | 0,00E+00 | 0,00E+00 | 0,00E+00 | 0,00E+00 |
| Promicromonosporaceae | 0,00E+00 | 0,00E+00 | 0,00E+00 | 0,00E+00 | 0,00E+00 | 7,44E-05 | 0,00E+00 | 0,00E+00 | 0,00E+00 | 0,00E+00 | 0,00E+00 | 0,00E+00 |
| Bacteroidales;Other | 0,00E+00 | 0,00E+00 | 0,00E+00 | 0,00E+00 | 0,00E+00 | 0,00E+00 | 0,00E+00 | 0,00E+00 | 0,00E+00 | 0,00E+00 | 0,00E+00 | 0,00E+00 |
| Bacteroidaceae | 1,17E-04 | 2,20E-04 | 5,64E-05 | 2,75E-04 | 1,32E-01 | 1,93E-01 | 1,23E-01 | 1,02E-01 | 1,99E-01 | 1,96E-01 | 2,99E-01 | 2,38E-01 |
| Porphyromonadaceae | 9,09E-01 | 8,18E-01 | 9,14E-01 | 8,50E-01 | 1,81E-01 | 2,00E-01 | 1,72E-01 | 1,95E-01 | 2,41E-01 | 2,76E-01 | 2,23E-01 | 2,56E-01 |
| Prevotellaceae | 0,00E+00 | 0,00E+00 | 0,00E+00 | 0,00E+00 | 0,00E+00 | 0,00E+00 | 0,00E+00 | 0,00E+00 | 0,00E+00 | 0,00E+00 | 0,00E+00 | 0,00E+00 |
| Rikenellaceae | 0,00E+00 | 0,00E+00 | 0,00E+00 | 0,00E+00 | 0,00E+00 | 0,00E+00 | 0,00E+00 | 0,00E+00 | 0,00E+00 | 6,75E-05 | 0,00E+00 | 0,00E+00 |
| S24-7 | 1,76E-04 | 5,50E-05 | 0,00E+00 | 5,50E-05 | 7,31E-05 | 0,00E+00 | 6,54E-05 | 0,00E+00 | 0,00E+00 | 0,00E+00 | 8,56E-05 | 7,48E-05 |
| Deferribacteraceae | 5,69E-03 | 2,44E-02 | 6,10E-03 | 1,14E-02 | 7,31E-05 | 2,23E-04 | 0,00E+00 | 3,30E-04 | 1,42E-04 | 2,03E-04 | 4,28E-04 | 0,00E+00 |
| Lactobacillales;Other | 3,99E-03 | 5,89E-03 | 4,01E-03 | 6,87E-03 | 0,00E+00 | 7,44E-05 | 0,00E+00 | 0,00E+00 | 0,00E+00 | 6,75E-05 | 8,56E-05 | 0,00E+00 |
| Enterococcaceae | 0,00E+00 | 5,50E-05 | 0,00E+00 | 0,00E+00 | 0,00E+00 | 0,00E+00 | 5,88E-04 | 1,98E-04 | 0,00E+00 | 0,00E+00 | 0,00E+00 | 0,00E+00 |
| Lactobacillaceae | 8,06E-02 | 1,51E-01 | 7,59E-02 | 1,31E-01 | 3,66E-04 | 5,95E-04 | 0,00E+00 | 3,30E-04 | 3,54E-04 | 2,03E-04 | 3,42E-04 | 9,72E-04 |
| Lachnospiraceae | 5,87E-05 | 2,75E-04 | 0,00E+00 | 3,85E-04 | 1,21E-01 | 1,48E-01 | 2,00E-01 | 3,13E-01 | 1,48E-01 | 2,01E-01 | 1,51E-01 | 1,65E-01 |
| Ruminococcaceae | 5,87E-05 | 0,00E+00 | 0,00E+00 | 0,00E+00 | 2,34E-03 | 1,79E-03 | 4,57E-04 | 1,38E-03 | 3,19E-03 | 3,58E-03 | 1,11E-03 | 2,77E-03 |
| Clostridiales; uncultured | 0,00E+00 | 0,00E+00 | 0,00E+00 | 0,00E+00 | 0,00E+00 | 0,00E+00 | 0,00E+00 | 0,00E+00 | 0,00E+00 | 0,00E+00 | 0,00E+00 | 0,00E+00 |
| Erysipelotrichaceae | 0,00E+00 | 0,00E+00 | 0,00E+00 | 0,00E+00 | 5,85E-04 | 1,86E-03 | 6,54E-05 | 7,91E-04 | 4,25E-04 | 5,40E-04 | 3,42E-04 | 2,17E-03 |
| Rhizobiaceae | 5,87E-05 | 5,50E-05 | 0,00E+00 | 0,00E+00 | 0,00E+00 | 0,00E+00 | 0,00E+00 | 0,00E+00 | 0,00E+00 | 0,00E+00 | 0,00E+00 | 0,00E+00 |
| Alcaligenaceae | 0,00E+00 | 0,00E+00 | 0,00E+00 | 0,00E+00 | 3,66E-04 | 3,72E-04 | 5,88E-04 | 1,19E-03 | 7,79E-04 | 6,75E-04 | 6,85E-04 | 6,73E-04 |
| Comamonadaceae | 5,87E-05 | 3,30E-04 | 0,00E+00 | 1,65E-04 | 0,00E+00 | 0,00E+00 | 0,00E+00 | 3,30E-04 | 1,42E-04 | 0,00E+00 | 0,00E+00 | 0,00E+00 |
| Desulfovibrionaceae | 0,00E+00 | 0,00E+00 | 0,00E+00 | 0,00E+00 | 0,00E+00 | 0,00E+00 | 0,00E+00 | 0,00E+00 | 0,00E+00 | 0,00E+00 | 0,00E+00 | 0,00E+00 |
| Verrucomicrobiaceae | 5,87E-05 | 5,50E-05 | 5,64E-05 | 1,65E-04 | 5,62E-01 | 4,55E-01 | 5,03E-01 | 3,84E-01 | 4,08E-01 | 3,22E-01 | 3,24E-01 | 3,34E-01 |

| Days post-inoculation (d) | d22 | d22 | d22 | d43 | d43 | d43 | d43 | d43 | d43 |
|---------------------------|---|----------|----------|------------------|----------|----------|---|----------|----------|
| Mouse number | 347 | 348 | 349 | 350 | 351 | 352 | 353 | 354 | 355 |
| Microbiota | ASF ⁵ + Oligo-MM ¹⁰ | | | ASF ⁵ | | | ASF ⁵ + Oligo-MM ¹⁰ | | |
| Taxon (Family level) | | | | | | | | | |
| Nocardiaceae | 0,00E+00 | 0,00E+00 | 0,00E+00 | 5,80E-05 | 0,00E+00 | 0,00E+00 | 0,00E+00 | 0,00E+00 | 0,00E+00 |
| Microbacteriaceae | 0,00E+00 | 0,00E+00 | 0,00E+00 | 5,80E-05 | 0,00E+00 | 0,00E+00 | 0,00E+00 | 0,00E+00 | 0,00E+00 |
| Promicromonosporaceae | 0,00E+00 | 0,00E+00 | 0,00E+00 | 1,16E-04 | 0,00E+00 | 0,00E+00 | 8,39E-05 | 0,00E+00 | 0,00E+00 |
| Bacteroidales;Other | 0,00E+00 | 0,00E+00 | 0,00E+00 | 0,00E+00 | 0,00E+00 | 0,00E+00 | 0,00E+00 | 1,30E-04 | 0,00E+00 |
| Bacteroidaceae | 3,85E-01 | 2,87E-01 | 3,54E-01 | 5,80E-05 | 1,38E-04 | 0,00E+00 | 4,18E-01 | 3,77E-01 | 4,01E-01 |
| Porphyromonadaceae | 2,45E-01 | 2,50E-01 | 2,06E-01 | 9,25E-01 | 8,57E-01 | 8,42E-01 | 2,49E-01 | 2,66E-01 | 1,98E-01 |
| Prevotellaceae | 0,00E+00 | 0,00E+00 | 0,00E+00 | 0,00E+00 | 0,00E+00 | 0,00E+00 | 0,00E+00 | 0,00E+00 | 0,00E+00 |
| Rikenellaceae | 0,00E+00 | 0,00E+00 | 0,00E+00 | 0,00E+00 | 0,00E+00 | 0,00E+00 | 0,00E+00 | 0,00E+00 | 0,00E+00 |
| S24-7 | 7,17E-05 | 4,88E-04 | 0,00E+00 | 5,80E-05 | 0,00E+00 | 0,00E+00 | 8,39E-05 | 0,00E+00 | 0,00E+00 |
| Deferribacteraceae | 0,00E+00 | 1,63E-04 | 9,58E-05 | 1,36E-02 | 1,22E-02 | 1,51E-02 | 2,52E-03 | 3,90E-04 | 2,74E-04 |
| Lactobacillales;Other | 0,00E+00 | 0,00E+00 | 0,00E+00 | 0,00E+00 | 0,00E+00 | 0,00E+00 | 0,00E+00 | 0,00E+00 | 0,00E+00 |
| Enterococcaceae | 1,43E-04 | 0,00E+00 | 0,00E+00 | 0,00E+00 | 6,91E-05 | 0,00E+00 | 0,00E+00 | 0,00E+00 | 2,74E-04 |
| Lactobacillaceae | 5,74E-04 | 1,63E-04 | 9,58E-04 | 6,04E-02 | 1,29E-01 | 1,42E-01 | 5,87E-04 | 5,21E-04 | 1,92E-03 |
| Lachnospiraceae | 6,74E-02 | 1,21E-01 | 1,96E-01 | 0,00E+00 | 2,07E-04 | 0,00E+00 | 1,80E-01 | 2,06E-01 | 1,53E-01 |
| Ruminococcaceae | 3,87E-03 | 4,88E-04 | 1,63E-03 | 0,00E+00 | 0,00E+00 | 0,00E+00 | 4,11E-03 | 9,11E-04 | 1,92E-03 |
| Clostridiales;_uncultured | 0,00E+00 | 0,00E+00 | 0,00E+00 | 0,00E+00 | 0,00E+00 | 0,00E+00 | 0,00E+00 | 0,00E+00 | 0,00E+00 |
| Erysipelotrichaceae | 1,65E-03 | 1,63E-04 | 6,71E-04 | 0,00E+00 | 0,00E+00 | 0,00E+00 | 8,39E-04 | 2,60E-04 | 9,14E-04 |
| Rhizobiaceae | 0,00E+00 | 0,00E+00 | 0,00E+00 | 5,80E-05 | 0,00E+00 | 0,00E+00 | 0,00E+00 | 0,00E+00 | 0,00E+00 |
| Alcaligenaceae | 1,48E-02 | 6,35E-03 | 6,61E-03 | 0,00E+00 | 0,00E+00 | 0,00E+00 | 8,98E-03 | 3,51E-03 | 6,67E-03 |
| Comamonadaceae | 7,17E-05 | 0,00E+00 | 0,00E+00 | 1,16E-04 | 4,14E-04 | 8,44E-05 | 8,39E-05 | 0,00E+00 | 0,00E+00 |
| Desulfovibrionaceae | 0,00E+00 | 0,00E+00 | 0,00E+00 | 0,00E+00 | 0,00E+00 | 0,00E+00 | 0,00E+00 | 0,00E+00 | 0,00E+00 |
| Verrucomicrobiaceae | 2,81E-01 | 3,34E-01 | 2,34E-01 | 5,80E-05 | 9,67E-04 | 9,28E-04 | 1,36E-01 | 1,46E-01 | 2,36E-01 |

Number of 16S amplicon sequencing reads is given as relative abundance and corresponding bar plots are presented in **Figure 8C**.

Table 40. Microbial composition in small intestines determined by amplicon sequencing using the Silva database to assign taxonomy at the family level

| Days post-inoculation (d) | d10 | d10 | d10 | d10 | d10 | d20 | d20 | d20 | d20 |
|---------------------------|---|----------|----------|----------|----------|----------|----------|----------|----------|
| Mouse number | 222 | 223 | 227 | 228 | 229 | 224 | 225 | 230 | 231 |
| Microbiota | ASF ⁵ + Oligo-MM ¹⁰ | | | | | | | | |
| Taxon (Family level) | | | | | | | | | |
| Nocardiaceae | 1,35E-04 | 2,01E-04 | 2,77E-04 | 2,52E-04 | 0,00E+00 | 0,00E+00 | 3,70E-03 | 1,53E-03 | 5,86E-03 |
| Microbacteriaceae | 2,02E-04 | 5,35E-04 | 2,77E-04 | 1,89E-04 | 0,00E+00 | 5,61E-05 | 4,09E-03 | 2,11E-03 | 4,35E-03 |
| Promicromonosporaceae | 0,00E+00 | 6,02E-04 | 2,08E-04 | 1,89E-04 | 6,25E-05 | 0,00E+00 | 1,16E-03 | 1,05E-03 | 2,73E-03 |
| Bacteroidales;Other | 0,00E+00 | 0,00E+00 | 0,00E+00 | 0,00E+00 | 0,00E+00 | 0,00E+00 | 0,00E+00 | 0,00E+00 | 0,00E+00 |
| Bacteroidaceae | 1,35E-03 | 5,16E-02 | 6,24E-04 | 8,20E-04 | 5,62E-04 | 2,81E-04 | 6,79E-03 | 4,79E-04 | 3,34E-03 |
| Porphyromonadaceae | 3,77E-03 | 5,47E-02 | 4,37E-03 | 3,22E-03 | 3,06E-03 | 4,66E-03 | 1,91E-02 | 1,53E-03 | 8,29E-03 |
| Prevotellaceae | 0,00E+00 | 0,00E+00 | 0,00E+00 | 0,00E+00 | 0,00E+00 | 0,00E+00 | 0,00E+00 | 0,00E+00 | 0,00E+00 |
| Rikenellaceae | 0,00E+00 | 0,00E+00 | 0,00E+00 | 0,00E+00 | 0,00E+00 | 5,61E-05 | 0,00E+00 | 0,00E+00 | 0,00E+00 |

| Days post-inoculation (d) | d10 | d10 | d10 | d10 | d10 | d20 | d20 | d20 | d20 |
|---------------------------|---|----------|----------|----------|----------|----------|----------|----------|----------|
| Mouse number | 222 | 223 | 227 | 228 | 229 | 224 | 225 | 230 | 231 |
| Microbiota | ASF ³ + Oligo-MM ¹⁰ | | | | | | | | |
| Taxon (Family level) | | | | | | | | | |
| S24-7 | 0,00E+00 | 0,00E+00 | 0,00E+00 | 0,00E+00 | 0,00E+00 | 0,00E+00 | 0,00E+00 | 0,00E+00 | 0,00E+00 |
| Deferribacteraceae | 0,00E+00 | 6,68E-05 | 0,00E+00 | 0,00E+00 | 0,00E+00 | 0,00E+00 | 1,54E-04 | 0,00E+00 | 0,00E+00 |
| Lactobacillales;Other | 0,00E+00 | 0,00E+00 | 0,00E+00 | 0,00E+00 | 0,00E+00 | 0,00E+00 | 0,00E+00 | 0,00E+00 | 0,00E+00 |
| Enterococcaceae | 6,73E-05 | 3,61E-03 | 5,55E-04 | 4,42E-04 | 2,37E-03 | 0,00E+00 | 7,71E-05 | 9,58E-05 | 2,02E-04 |
| Lactobacillaceae | 3,70E-03 | 5,27E-02 | 2,77E-04 | 8,83E-04 | 2,50E-04 | 1,07E-03 | 4,32E-03 | 9,77E-03 | 1,52E-03 |
| Lachnospiraceae | 9,08E-03 | 1,37E-01 | 1,53E-02 | 1,10E-02 | 2,25E-03 | 1,51E-03 | 2,63E-02 | 1,55E-02 | 2,18E-02 |
| Ruminococcaceae | 0,00E+00 | 2,67E-04 | 1,39E-04 | 3,15E-04 | 6,25E-05 | 4,49E-04 | 8,49E-04 | 1,63E-03 | 5,05E-04 |
| Clostridiales: uncultured | 0,00E+00 | 0,00E+00 | 0,00E+00 | 0,00E+00 | 0,00E+00 | 0,00E+00 | 0,00E+00 | 0,00E+00 | 0,00E+00 |
| Erysipelotrichaceae | 2,22E-03 | 3,74E-03 | 8,32E-04 | 2,14E-03 | 2,81E-03 | 9,54E-04 | 4,40E-03 | 1,15E-03 | 1,37E-02 |
| Rhizobiaceae | 2,69E-04 | 4,68E-04 | 2,77E-04 | 1,89E-04 | 6,25E-05 | 5,61E-05 | 4,55E-03 | 2,87E-03 | 8,19E-03 |
| Alcaligenaceae | 9,70E-02 | 2,43E-02 | 4,10E-02 | 4,98E-02 | 7,14E-02 | 2,91E-02 | 8,66E-02 | 1,15E-01 | 1,22E-01 |
| Comamonadaceae | 2,15E-03 | 3,74E-03 | 2,08E-03 | 2,27E-03 | 3,12E-04 | 8,42E-04 | 3,24E-02 | 2,22E-02 | 5,31E-02 |
| Desulfovibrionaceae | 0,00E+00 | 0,00E+00 | 0,00E+00 | 0,00E+00 | 0,00E+00 | 0,00E+00 | 0,00E+00 | 0,00E+00 | 0,00E+00 |
| Verrucomicrobiaceae | 8,80E-01 | 6,67E-01 | 9,34E-01 | 9,28E-01 | 9,17E-01 | 9,61E-01 | 8,05E-01 | 8,25E-01 | 7,54E-01 |

Number of 16S amplicon sequencing reads are given as relative abundance and corresponding bar plots are presented in **Figure 8D**.

Table 41. Microbial composition in feces determined by amplicon sequencing using a custom sequence collection to assign taxonomy at the genus level

| Days post-inoculation (d) | d0 | d0 | d0 | d0 | d10 | d10 | d10 | d10 | d20 | d20 | d20 | d20 |
|--|------------------|----------|----------|----------|---|----------|----------|----------|----------|----------|----------|----------|
| Mouse number | 222 | 224 | 227 | 228 | 222 | 223 | 227 | 228 | 224 | 225 | 230 | 231 |
| Microbiota | ASF ³ | | | | ASF ³ + Oligo-MM ¹⁰ | | | | | | | |
| Taxon (Genus level) | | | | | | | | | | | | |
| <i>Bifidobacterium</i> | 0,00E+00 | 0,00E+00 | 0,00E+00 | 0,00E+00 | 0,00E+00 | 7,44E-05 | 0,00E+00 | 0,00E+00 | 0,00E+00 | 0,00E+00 | 0,00E+00 | 0,00E+00 |
| <i>Bacteroides</i> | 1,17E-04 | 2,20E-04 | 5,64E-05 | 2,75E-04 | 1,32E-01 | 1,93E-01 | 1,23E-01 | 1,02E-01 | 1,99E-01 | 1,96E-01 | 2,99E-01 | 2,38E-01 |
| Bacteroidales;Other | 0,00E+00 | 0,00E+00 | 0,00E+00 | 0,00E+00 | 0,00E+00 | 0,00E+00 | 0,00E+00 | 0,00E+00 | 0,00E+00 | 6,75E-05 | 0,00E+00 | 0,00E+00 |
| <i>Parabacteroides</i> | 9,09E-01 | 8,18E-01 | 9,14E-01 | 8,50E-01 | 1,81E-01 | 2,00E-01 | 1,72E-01 | 1,95E-01 | 2,41E-01 | 2,76E-01 | 2,23E-01 | 2,56E-01 |
| <i>Barnesiella</i> | 1,76E-04 | 5,50E-05 | 0,00E+00 | 5,50E-05 | 7,31E-05 | 0,00E+00 | 6,54E-05 | 0,00E+00 | 0,00E+00 | 0,00E+00 | 8,56E-05 | 7,48E-05 |
| <i>Mucispirillum</i> | 5,69E-03 | 2,44E-02 | 6,10E-03 | 1,14E-02 | 7,31E-05 | 2,23E-04 | 0,00E+00 | 3,30E-04 | 1,42E-04 | 2,03E-04 | 4,28E-04 | 0,00E+00 |
| <i>Enterococcus</i> | 0,00E+00 | 5,50E-05 | 0,00E+00 | 0,00E+00 | 0,00E+00 | 0,00E+00 | 5,88E-04 | 1,98E-04 | 0,00E+00 | 0,00E+00 | 0,00E+00 | 0,00E+00 |
| <i>Lactobacillus</i> | 8,46E-02 | 1,56E-01 | 7,99E-02 | 1,38E-01 | 3,66E-04 | 6,70E-04 | 0,00E+00 | 3,30E-04 | 3,54E-04 | 2,70E-04 | 4,28E-04 | 9,72E-04 |
| <i>Blautia</i> | 0,00E+00 | 1,10E-04 | 0,00E+00 | 5,50E-05 | 7,31E-04 | 1,79E-03 | 7,84E-04 | 1,91E-03 | 8,50E-04 | 6,75E-04 | 1,37E-03 | 3,67E-03 |
| Lachnospiraceae; <i>Incertae_Sedis</i> | 5,87E-05 | 1,65E-04 | 0,00E+00 | 3,30E-04 | 1,21E-01 | 1,46E-01 | 1,99E-01 | 3,12E-01 | 1,47E-01 | 2,00E-01 | 1,49E-01 | 1,62E-01 |
| Lachnospiraceae;Other | 0,00E+00 | 0,00E+00 | 0,00E+00 | 0,00E+00 | 0,00E+00 | 0,00E+00 | 0,00E+00 | 0,00E+00 | 0,00E+00 | 0,00E+00 | 0,00E+00 | 0,00E+00 |
| Lachnospiraceae;uncultured | 0,00E+00 | 0,00E+00 | 0,00E+00 | 0,00E+00 | 0,00E+00 | 0,00E+00 | 0,00E+00 | 0,00E+00 | 0,00E+00 | 0,00E+00 | 8,56E-05 | 0,00E+00 |
| Clostridiales;Other | 0,00E+00 | 0,00E+00 | 0,00E+00 | 0,00E+00 | 0,00E+00 | 0,00E+00 | 0,00E+00 | 0,00E+00 | 0,00E+00 | 0,00E+00 | 0,00E+00 | 0,00E+00 |
| <i>Flavonifractor</i> | 5,87E-05 | 0,00E+00 | 0,00E+00 | 0,00E+00 | 2,34E-03 | 1,79E-03 | 4,57E-04 | 1,38E-03 | 3,19E-03 | 3,58E-03 | 1,11E-03 | 2,77E-03 |
| Ruminococcaceae; <i>Incertae_Sedis</i> | 0,00E+00 | 0,00E+00 | 0,00E+00 | 0,00E+00 | 0,00E+00 | 0,00E+00 | 0,00E+00 | 0,00E+00 | 0,00E+00 | 0,00E+00 | 0,00E+00 | 0,00E+00 |
| Erysipelotrichaceae; <i>Incertae_Sedis</i> | 0,00E+00 | 0,00E+00 | 0,00E+00 | 0,00E+00 | 5,85E-04 | 1,86E-03 | 6,54E-05 | 7,91E-04 | 4,25E-04 | 5,40E-04 | 3,42E-04 | 2,17E-03 |

| Days post-inoculation (d) | d0 | d0 | d0 | d0 | d10 | d10 | d10 | d10 | d20 | d20 | d20 | d20 |
|---------------------------|------------------|----------|----------|----------|---|----------|----------|----------|----------|----------|----------|----------|
| Mouse number | 222 | 224 | 227 | 228 | 222 | 223 | 227 | 228 | 224 | 225 | 230 | 231 |
| Microbiota | ASF ⁵ | | | | ASF ⁵ + Oligo-MM ¹⁰ | | | | | | | |
| Taxon (Genus level) | | | | | | | | | | | | |
| Bacteria;Other | 5,87E-05 | 1,10E-04 | 0,00E+00 | 0,00E+00 | 0,00E+00 | 0,00E+00 | 0,00E+00 | 0,00E+00 | 0,00E+00 | 0,00E+00 | 0,00E+00 | 0,00E+00 |
| <i>Parasutterella</i> | 5,87E-05 | 3,30E-04 | 0,00E+00 | 1,65E-04 | 3,66E-04 | 3,72E-04 | 5,88E-04 | 1,52E-03 | 9,21E-04 | 6,75E-04 | 6,85E-04 | 6,73E-04 |
| <i>Akkermansia</i> | 5,87E-05 | 5,50E-05 | 5,64E-05 | 1,65E-04 | 5,62E-01 | 4,55E-01 | 5,03E-01 | 3,84E-01 | 4,08E-01 | 3,22E-01 | 3,24E-01 | 3,34E-01 |

| Days post-inoculation (d) | d22 | d22 | d22 | d43 | d43 | d43 | d43 | d43 | d43 |
|--|---|----------|----------|------------------|----------|----------|---|----------|----------|
| Mouse number | 347 | 348 | 349 | 350 | 351 | 352 | 353 | 354 | 355 |
| Microbiota | ASF ⁵ + Oligo-MM ¹⁰ | | | ASF ⁵ | | | ASF ⁵ + Oligo-MM ¹⁰ | | |
| Taxon (Genus level) | | | | | | | | | |
| <i>Bifidobacterium</i> | 0,00E+00 | 0,00E+00 | 0,00E+00 | 1,16E-04 | 0,00E+00 | 0,00E+00 | 8,39E-05 | 0,00E+00 | 0,00E+00 |
| <i>Bacteroides</i> | 3,85E-01 | 2,87E-01 | 3,54E-01 | 5,80E-05 | 1,38E-04 | 0,00E+00 | 4,18E-01 | 3,77E-01 | 4,01E-01 |
| Bacteroidales;Other | 0,00E+00 | 0,00E+00 | 0,00E+00 | 0,00E+00 | 0,00E+00 | 0,00E+00 | 0,00E+00 | 0,00E+00 | 0,00E+00 |
| <i>Parabacteroides</i> | 2,45E-01 | 2,50E-01 | 2,06E-01 | 9,25E-01 | 8,57E-01 | 8,42E-01 | 2,49E-01 | 2,66E-01 | 1,98E-01 |
| <i>Barnesiella</i> | 7,17E-05 | 4,88E-04 | 0,00E+00 | 5,80E-05 | 0,00E+00 | 0,00E+00 | 8,39E-05 | 1,30E-04 | 0,00E+00 |
| <i>Mucispirillum</i> | 0,00E+00 | 1,63E-04 | 9,58E-05 | 1,36E-02 | 1,22E-02 | 1,51E-02 | 2,52E-03 | 3,90E-04 | 2,74E-04 |
| <i>Enterococcus</i> | 1,43E-04 | 0,00E+00 | 0,00E+00 | 0,00E+00 | 6,91E-05 | 0,00E+00 | 0,00E+00 | 0,00E+00 | 2,74E-04 |
| <i>Lactobacillus</i> | 5,74E-04 | 1,63E-04 | 9,58E-04 | 6,04E-02 | 1,29E-01 | 1,42E-01 | 5,87E-04 | 5,21E-04 | 1,92E-03 |
| <i>Blautia</i> | 1,08E-03 | 1,14E-03 | 3,83E-03 | 0,00E+00 | 0,00E+00 | 0,00E+00 | 1,51E-03 | 1,95E-03 | 3,38E-03 |
| Lachnospiraceae; <i>Incertae_Sedis</i> | 6,64E-02 | 1,20E-01 | 1,92E-01 | 0,00E+00 | 2,07E-04 | 0,00E+00 | 1,79E-01 | 2,04E-01 | 1,50E-01 |
| Lachnospiraceae;Other | 0,00E+00 | 1,63E-04 | 9,58E-05 | 0,00E+00 | 0,00E+00 | 0,00E+00 | 1,68E-04 | 2,60E-04 | 0,00E+00 |
| Lachnospiraceae;uncultured | 0,00E+00 | 0,00E+00 | 0,00E+00 | 0,00E+00 | 0,00E+00 | 0,00E+00 | 0,00E+00 | 0,00E+00 | 0,00E+00 |
| Clostridiales;Other | 0,00E+00 | 0,00E+00 | 0,00E+00 | 0,00E+00 | 0,00E+00 | 0,00E+00 | 0,00E+00 | 0,00E+00 | 0,00E+00 |
| <i>Flavonifractor</i> | 3,87E-03 | 4,88E-04 | 1,63E-03 | 0,00E+00 | 0,00E+00 | 0,00E+00 | 4,11E-03 | 9,11E-04 | 1,92E-03 |
| Ruminococcaceae; <i>Incertae_Sedis</i> | 0,00E+00 | 0,00E+00 | 0,00E+00 | 0,00E+00 | 0,00E+00 | 0,00E+00 | 0,00E+00 | 0,00E+00 | 0,00E+00 |
| Erysipelotrichaceae; <i>Incertae_Sedis</i> | 1,65E-03 | 1,63E-04 | 6,71E-04 | 0,00E+00 | 0,00E+00 | 0,00E+00 | 8,39E-04 | 2,60E-04 | 9,14E-04 |
| Bacteria;Other | 0,00E+00 | 0,00E+00 | 0,00E+00 | 1,74E-04 | 0,00E+00 | 0,00E+00 | 0,00E+00 | 0,00E+00 | 0,00E+00 |
| <i>Parasutterella</i> | 1,48E-02 | 6,35E-03 | 6,61E-03 | 1,16E-04 | 4,14E-04 | 8,44E-05 | 9,06E-03 | 3,51E-03 | 6,67E-03 |
| <i>Akkermansia</i> | 2,81E-01 | 3,34E-01 | 2,34E-01 | 5,80E-05 | 9,67E-04 | 9,28E-04 | 1,36E-01 | 1,46E-01 | 2,36E-01 |

Number of 16S amplicon sequencing reads are given as relative abundance and corresponding bar plots are presented in **Figure 9A**.

Table 42. Microbial composition in small intestines determined by amplicon sequencing using a custom sequence collection to assign taxonomy at the genus level

| Days post-inoculation (d) | d10 | d10 | d10 | d10 | d10 | d20 | d20 | d20 | d20 |
|------------------------------------|---|----------|----------|----------|----------|----------|----------|----------|----------|
| Mouse number | 222 | 223 | 227 | 228 | 229 | 224 | 225 | 230 | 231 |
| Microbiota | ASF ³ + Oligo-MM ¹⁰ | | | | | | | | |
| Taxon (Genus level) | | | | | | | | | |
| <i>Bifidobacterium</i> | 0,00E+00 | 6,02E-04 | 2,08E-04 | 1,89E-04 | 6,25E-05 | 0,00E+00 | 1,16E-03 | 1,05E-03 | 2,73E-03 |
| <i>Bacteroides</i> | 1,35E-03 | 5,16E-02 | 6,24E-04 | 8,20E-04 | 5,62E-04 | 2,81E-04 | 6,79E-03 | 4,79E-04 | 3,34E-03 |
| Bacteroidales;Other | 0,00E+00 | 0,00E+00 | 0,00E+00 | 0,00E+00 | 0,00E+00 | 5,61E-05 | 0,00E+00 | 0,00E+00 | 0,00E+00 |
| <i>Parabacteroides</i> | 3,77E-03 | 5,47E-02 | 4,37E-03 | 3,22E-03 | 3,06E-03 | 4,66E-03 | 1,91E-02 | 1,53E-03 | 8,29E-03 |
| <i>Barnesiella</i> | 0,00E+00 | 0,00E+00 | 0,00E+00 | 0,00E+00 | 0,00E+00 | 0,00E+00 | 0,00E+00 | 0,00E+00 | 0,00E+00 |
| <i>Mucispirillum</i> | 0,00E+00 | 6,68E-05 | 0,00E+00 | 0,00E+00 | 0,00E+00 | 0,00E+00 | 1,54E-04 | 0,00E+00 | 0,00E+00 |
| <i>Enterococcus</i> | 6,73E-05 | 3,61E-03 | 5,55E-04 | 4,42E-04 | 2,37E-03 | 0,00E+00 | 7,71E-05 | 9,58E-05 | 2,02E-04 |
| <i>Lactobacillus</i> | 3,70E-03 | 5,27E-02 | 2,77E-04 | 8,83E-04 | 2,50E-04 | 1,07E-03 | 4,32E-03 | 9,77E-03 | 1,52E-03 |
| <i>Blautia</i> | 2,22E-03 | 5,62E-03 | 2,50E-03 | 2,40E-03 | 6,87E-04 | 7,29E-04 | 6,09E-03 | 4,69E-03 | 8,29E-03 |
| Lachnospiraceae;Incertae_Sedis | 6,86E-03 | 1,31E-01 | 1,28E-02 | 8,58E-03 | 1,56E-03 | 7,86E-04 | 2,02E-02 | 1,08E-02 | 1,35E-02 |
| Lachnospiraceae;Other | 0,00E+00 | 6,68E-05 | 0,00E+00 | 0,00E+00 | 0,00E+00 | 0,00E+00 | 0,00E+00 | 0,00E+00 | 0,00E+00 |
| Lachnospiraceae;uncultured | 0,00E+00 | 0,00E+00 | 0,00E+00 | 0,00E+00 | 0,00E+00 | 0,00E+00 | 0,00E+00 | 0,00E+00 | 0,00E+00 |
| Clostridiales;Other | 0,00E+00 | 0,00E+00 | 0,00E+00 | 0,00E+00 | 0,00E+00 | 0,00E+00 | 0,00E+00 | 0,00E+00 | 0,00E+00 |
| <i>Flavonifractor</i> | 0,00E+00 | 2,67E-04 | 1,39E-04 | 3,15E-04 | 6,25E-05 | 4,49E-04 | 8,49E-04 | 1,63E-03 | 5,05E-04 |
| Ruminococcaceae;Incertae_Sedis | 0,00E+00 | 0,00E+00 | 0,00E+00 | 0,00E+00 | 0,00E+00 | 0,00E+00 | 0,00E+00 | 0,00E+00 | 0,00E+00 |
| Erysipelotrichaceae;Incertae_Sedis | 2,22E-03 | 3,74E-03 | 8,32E-04 | 2,14E-03 | 2,81E-03 | 9,54E-04 | 4,40E-03 | 1,15E-03 | 1,37E-02 |
| Bacteria;Other | 6,05E-04 | 1,20E-03 | 8,32E-04 | 6,31E-04 | 6,25E-05 | 1,12E-04 | 1,23E-02 | 6,51E-03 | 1,84E-02 |
| <i>Parasutterella</i> | 9,91E-02 | 2,81E-02 | 4,31E-02 | 5,21E-02 | 7,17E-02 | 2,99E-02 | 1,19E-01 | 1,37E-01 | 1,75E-01 |
| <i>Akkermansia</i> | 8,80E-01 | 6,67E-01 | 9,34E-01 | 9,28E-01 | 9,17E-01 | 9,61E-01 | 8,05E-01 | 8,25E-01 | 7,54E-01 |

Number of 16S amplicon sequencing reads are given as relative abundance and corresponding bar plots are presented in **Figure 9B**.

Table 43. Microbial composition in the frozen inoculum determined by amplicon sequencing using a custom sequence collection to assign taxonomy at the genus level

| Taxon (Genus level) | Inoculum |
|--------------------------------|----------|
| <i>Bifidobacterium</i> | 0,00E+00 |
| <i>Bacteroides</i> | 4,54E-01 |
| Bacteroidales;Other | 0,00E+00 |
| <i>Parabacteroides</i> | 7,33E-04 |
| <i>Barnesiella</i> | 0,00E+00 |
| <i>Mucispirillum</i> | 0,00E+00 |
| <i>Enterococcus</i> | 4,77E-02 |
| <i>Lactobacillus</i> | 3,27E-03 |
| <i>Blautia</i> | 1,21E-02 |
| Lachnospiraceae;Incertae_Sedis | 9,26E-02 |
| Lachnospiraceae;Other | 0,00E+00 |

| Taxon (Genus level) | Inoculum |
|--|----------|
| Lachnospiraceae;uncultured | 0,00E+00 |
| Clostridiales;Other | 0,00E+00 |
| <i>Flavonifractor</i> | 4,11E-02 |
| Ruminococcaceae; <i>Incertae_Sedis</i> | 0,00E+00 |
| Erysipelotrichaceae; <i>Incertae_Sedis</i> | 3,79E-02 |
| Bacteria;Other | 0,00E+00 |
| <i>Parasutterella</i> | 6,00E-04 |
| <i>Akkermansia</i> | 3,10E-01 |

Number of 16S amplicon sequencing reads are given as relative abundance and corresponding bar plots are presented in **Figure 9C**.

Table 44. Microbial composition in feces and cecal content determined by amplicon sequencing using a custom sequence collection to assign taxonomy at the genus level

| Days post-inoculation (d) | Feces | | | | | | |
|--|---|----------|----------|----------|----------|----------|----------|
| | d10 | d10 | d10 | d20 | d20 | d20 | d20 |
| Mouse number | 222 | 227 | 228 | 224 | 225 | 230 | 231 |
| Microbiota | ASF ⁵ + Oligo-MM ¹⁰ | | | | | | |
| Taxon (Genus level) | | | | | | | |
| <i>Bifidobacterium</i> | 0,00E+00 | 0,00E+00 | 0,00E+00 | 0,00E+00 | 0,00E+00 | 0,00E+00 | 0,00E+00 |
| <i>Bacteroides</i> | 1,32E-01 | 1,23E-01 | 1,02E-01 | 1,99E-01 | 1,96E-01 | 2,99E-01 | 2,38E-01 |
| Bacteroidales;Other | 0,00E+00 | 0,00E+00 | 0,00E+00 | 0,00E+00 | 6,75E-05 | 0,00E+00 | 0,00E+00 |
| <i>Parabacteroides</i> | 1,81E-01 | 1,72E-01 | 1,95E-01 | 2,41E-01 | 2,76E-01 | 2,23E-01 | 2,56E-01 |
| <i>Barnesiella</i> | 7,31E-05 | 6,54E-05 | 0,00E+00 | 0,00E+00 | 0,00E+00 | 8,56E-05 | 7,48E-05 |
| <i>Mucispirillum</i> | 7,31E-05 | 0,00E+00 | 3,30E-04 | 1,42E-04 | 2,03E-04 | 4,28E-04 | 0,00E+00 |
| <i>Enterococcus</i> | 0,00E+00 | 5,88E-04 | 1,98E-04 | 0,00E+00 | 0,00E+00 | 0,00E+00 | 0,00E+00 |
| <i>Lactobacillus</i> | 3,66E-04 | 0,00E+00 | 3,30E-04 | 3,54E-04 | 2,70E-04 | 4,28E-04 | 9,72E-04 |
| <i>Blautia</i> | 7,31E-04 | 7,84E-04 | 1,91E-03 | 8,50E-04 | 6,75E-04 | 1,37E-03 | 3,67E-03 |
| Lachnospiraceae; <i>Incertae_Sedis</i> | 1,21E-01 | 1,99E-01 | 3,12E-01 | 1,47E-01 | 2,00E-01 | 1,49E-01 | 1,62E-01 |
| Lachnospiraceae;Other | 0,00E+00 | 0,00E+00 | 0,00E+00 | 0,00E+00 | 0,00E+00 | 0,00E+00 | 0,00E+00 |
| Lachnospiraceae;uncultured | 0,00E+00 | 0,00E+00 | 0,00E+00 | 0,00E+00 | 0,00E+00 | 8,56E-05 | 0,00E+00 |
| Clostridiales;Other | 0,00E+00 | 0,00E+00 | 0,00E+00 | 0,00E+00 | 0,00E+00 | 0,00E+00 | 0,00E+00 |
| <i>Flavonifractor</i> | 2,34E-03 | 4,57E-04 | 1,38E-03 | 3,19E-03 | 3,58E-03 | 1,11E-03 | 2,77E-03 |
| Ruminococcaceae; <i>Incertae_Sedis</i> | 0,00E+00 | 0,00E+00 | 0,00E+00 | 0,00E+00 | 0,00E+00 | 0,00E+00 | 0,00E+00 |
| Erysipelotrichaceae; <i>Incertae_Sedis</i> | 5,85E-04 | 6,54E-05 | 7,91E-04 | 4,25E-04 | 5,40E-04 | 3,42E-04 | 2,17E-03 |
| Bacteria;Other | 0,00E+00 | 0,00E+00 | 0,00E+00 | 0,00E+00 | 0,00E+00 | 0,00E+00 | 0,00E+00 |
| <i>Parasutterella</i> | 3,66E-04 | 5,88E-04 | 1,52E-03 | 9,21E-04 | 6,75E-04 | 6,85E-04 | 6,73E-04 |
| <i>Akkermansia</i> | 5,62E-01 | 5,03E-01 | 3,84E-01 | 4,08E-01 | 3,22E-01 | 3,24E-01 | 3,34E-01 |

| Cecal content | | | | | | | |
|---|---|----------|----------|----------|----------|----------|----------|
| Days post-inoculation (d) | d10 | d10 | d10 | d20 | d20 | d20 | d20 |
| Mouse number | 222 | 227 | 228 | 224 | 225 | 230 | 231 |
| Microbiota | ASF ⁵ + Oligo-MM ¹⁰ | | | | | | |
| Taxon (Genus level) | | | | | | | |
| <i>Bifidobacterium</i> | 0,00E+00 | 0,00E+00 | 0,00E+00 | 0,00E+00 | 0,00E+00 | 0,00E+00 | 0,00E+00 |
| <i>Bacteroides</i> | 1,87E-01 | 1,42E-01 | 1,84E-01 | 2,29E-01 | 1,88E-01 | 2,23E-01 | 2,11E-01 |
| Bacteroidales;Other | 0,00E+00 | 0,00E+00 | 0,00E+00 | 0,00E+00 | 0,00E+00 | 0,00E+00 | 0,00E+00 |
| Cecal content | | | | | | | |
| Days post-inoculation (d) | d10 | d10 | d10 | d20 | d20 | d20 | d20 |
| Mouse number | 222 | 227 | 228 | 224 | 225 | 230 | 231 |
| Microbiota | ASF ⁵ + Oligo-MM ¹⁰ | | | | | | |
| Taxon (Genus level) | | | | | | | |
| <i>Parabacteroides</i> | 3,26E-01 | 3,09E-01 | 2,97E-01 | 2,88E-01 | 2,94E-01 | 2,80E-01 | 3,26E-01 |
| <i>Barnesiella</i> | 6,77E-05 | 0,00E+00 | 9,53E-05 | 1,38E-04 | 5,77E-05 | 0,00E+00 | 0,00E+00 |
| <i>Mucispirillum</i> | 4,74E-04 | 4,40E-04 | 1,24E-03 | 2,77E-04 | 2,31E-04 | 6,42E-04 | 7,15E-04 |
| <i>Enterococcus</i> | 0,00E+00 | 3,52E-04 | 9,53E-05 | 0,00E+00 | 0,00E+00 | 0,00E+00 | 0,00E+00 |
| <i>Lactobacillus</i> | 4,74E-04 | 5,28E-04 | 9,53E-05 | 8,99E-04 | 3,46E-04 | 3,42E-04 | 1,02E-04 |
| <i>Blautia</i> | 1,56E-03 | 1,41E-03 | 4,77E-04 | 1,04E-03 | 1,15E-03 | 1,80E-03 | 1,53E-03 |
| Lachnospiraceae;Incertae_Sedis | 2,39E-01 | 3,79E-01 | 3,11E-01 | 2,30E-01 | 2,84E-01 | 3,13E-01 | 3,12E-01 |
| Lachnospiraceae;Other | 6,77E-05 | 0,00E+00 | 0,00E+00 | 0,00E+00 | 0,00E+00 | 0,00E+00 | 1,02E-04 |
| Lachnospiraceae;uncultured | 0,00E+00 | 0,00E+00 | 0,00E+00 | 0,00E+00 | 0,00E+00 | 0,00E+00 | 0,00E+00 |
| Clostridiales;Other | 0,00E+00 | 0,00E+00 | 0,00E+00 | 0,00E+00 | 0,00E+00 | 0,00E+00 | 0,00E+00 |
| <i>Flavonifractor</i> | 2,71E-03 | 7,04E-04 | 1,72E-03 | 3,25E-03 | 2,83E-03 | 2,35E-03 | 3,06E-03 |
| Ruminococcaceae;Incertae_Sedis | 0,00E+00 | 0,00E+00 | 0,00E+00 | 0,00E+00 | 0,00E+00 | 0,00E+00 | 0,00E+00 |
| <i>Erysipelotrichaceae;Incertae_Sedis</i> | 5,41E-04 | 8,81E-05 | 8,58E-04 | 1,11E-03 | 6,35E-04 | 2,99E-04 | 8,17E-04 |
| Bacteria;Other | 0,00E+00 | 0,00E+00 | 0,00E+00 | 0,00E+00 | 0,00E+00 | 0,00E+00 | 1,02E-04 |
| <i>Parasutterella</i> | 1,22E-03 | 4,40E-04 | 9,53E-04 | 8,30E-04 | 1,21E-03 | 7,70E-04 | 1,43E-03 |
| <i>Akkermansia</i> | 2,41E-01 | 1,66E-01 | 2,03E-01 | 2,45E-01 | 2,27E-01 | 1,78E-01 | 1,43E-01 |

Number of 16S amplicon sequencing reads are given as relative abundance and corresponding bar plots are presented in **Figure 10**.

Table 45. Oligo-MM¹² fecal composition over generations analyzed by qPCR

| Mouse generation | Strain ID | | | | | | | | | | | |
|------------------|-----------|----------|----------|----------|----------|----------|----------|----------|----------|----------|----------|----------|
| | I46 | I49 | YL58 | YL27 | YL31 | YL32 | KB18 | YL44 | KB1 | YL2 | YL45 | I48 |
| F0 | 0,00E+00 | 4,24E-04 | 9,56E-03 | 1,19E-01 | 1,82E-02 | 9,01E-03 | 0,00E+00 | 3,70E-01 | 9,88E-04 | 0,00E+00 | 5,92E-02 | 4,14E-01 |
| F0 | 0,00E+00 | 4,52E-04 | 1,10E-02 | 1,33E-01 | 2,29E-02 | 9,83E-03 | 1,86E-03 | 2,03E-01 | 6,22E-04 | 0,00E+00 | 4,74E-02 | 5,70E-01 |
| F1 | 0,00E+00 | 0,00E+00 | 6,49E-03 | 1,16E-01 | 2,40E-02 | 7,83E-03 | 0,00E+00 | 3,61E-01 | 3,92E-04 | 4,37E-06 | 4,35E-02 | 4,41E-01 |
| F1 | 0,00E+00 | 0,00E+00 | 7,01E-03 | 1,16E-01 | 1,45E-02 | 2,48E-02 | 0,00E+00 | 2,96E-01 | 5,52E-04 | 6,47E-06 | 4,49E-02 | 4,96E-01 |
| F1 | 0,00E+00 | 3,04E-04 | 8,82E-03 | 1,12E-01 | 2,29E-02 | 1,10E-02 | 3,19E-05 | 2,47E-01 | 8,53E-04 | 0,00E+00 | 4,18E-02 | 5,55E-01 |
| Mouse | Strain ID | | | | | | | | | | | |

| generation | I46 | I49 | YL58 | YL27 | YL31 | YL32 | KB18 | YL44 | KB1 | YL2 | YL45 | I48 |
|------------|----------|----------|----------|----------|----------|----------|----------|----------|----------|----------|----------|----------|
| F1 | 0,00E+00 | 1,90E-04 | 7,22E-03 | 1,11E-01 | 1,96E-02 | 6,99E-03 | 6,42E-04 | 2,58E-01 | 8,88E-04 | 0,00E+00 | 5,65E-02 | 5,38E-01 |
| F1 | 0,00E+00 | 1,04E-03 | 8,77E-03 | 8,91E-02 | 2,88E-02 | 1,28E-02 | 0,00E+00 | 2,57E-01 | 1,42E-03 | 0,00E+00 | 6,17E-02 | 5,40E-01 |
| F2 | 0,00E+00 | 6,39E-04 | 2,32E-03 | 9,96E-02 | 1,90E-02 | 1,41E-02 | 0,00E+00 | 1,97E-01 | 0,00E+00 | 0,00E+00 | 2,95E-02 | 6,37E-01 |
| F2 | 0,00E+00 | 9,36E-04 | 4,31E-03 | 9,28E-02 | 2,43E-02 | 2,08E-02 | 9,65E-07 | 1,86E-01 | 6,45E-05 | 0,00E+00 | 3,01E-02 | 6,41E-01 |
| F2 | 0,00E+00 | 7,79E-04 | 5,05E-03 | 1,02E-01 | 2,17E-02 | 1,84E-02 | 0,00E+00 | 2,56E-01 | 5,17E-05 | 0,00E+00 | 3,42E-02 | 5,62E-01 |
| F2 | 0,00E+00 | 2,55E-03 | 8,85E-03 | 1,02E-01 | 2,40E-02 | 1,19E-02 | 0,00E+00 | 1,70E-01 | 5,51E-05 | 0,00E+00 | 3,62E-02 | 6,45E-01 |
| F2 | 0,00E+00 | 1,99E-03 | 4,19E-03 | 1,05E-01 | 2,11E-02 | 1,83E-02 | 1,04E-06 | 2,25E-01 | 4,29E-05 | 0,00E+00 | 3,80E-02 | 5,87E-01 |
| | I46 | I49 | YL58 | YL27 | YL31 | YL32 | KB18 | YL44 | KB1 | YL2 | YL45 | I48 |
| F2 | 0,00E+00 | 1,04E-03 | 4,06E-03 | 7,92E-02 | 1,98E-02 | 1,73E-02 | 0,00E+00 | 2,32E-01 | 0,00E+00 | 0,00E+00 | 3,56E-02 | 6,11E-01 |
| F2 | 0,00E+00 | 8,02E-04 | 4,56E-03 | 9,01E-02 | 2,08E-02 | 2,34E-02 | 0,00E+00 | 2,53E-01 | 1,41E-04 | 0,00E+00 | 3,00E-02 | 5,78E-01 |
| F2 | 0,00E+00 | 9,07E-04 | 3,97E-03 | 7,99E-02 | 1,70E-02 | 1,21E-02 | 0,00E+00 | 1,51E-01 | 1,01E-04 | 0,00E+00 | 3,29E-02 | 7,02E-01 |
| F2 | 0,00E+00 | 6,64E-04 | 4,07E-03 | 8,08E-02 | 1,86E-02 | 1,95E-02 | 0,00E+00 | 2,33E-01 | 1,17E-04 | 0,00E+00 | 3,72E-02 | 6,06E-01 |
| F2 | 0,00E+00 | 6,76E-04 | 4,33E-03 | 8,79E-02 | 1,88E-02 | 1,36E-02 | 0,00E+00 | 2,27E-01 | 1,12E-04 | 0,00E+00 | 3,45E-02 | 6,13E-01 |
| F2 | 0,00E+00 | 9,04E-04 | 3,82E-03 | 8,82E-02 | 1,75E-02 | 1,41E-02 | 0,00E+00 | 2,00E-01 | 4,79E-05 | 0,00E+00 | 3,63E-02 | 6,39E-01 |
| F3 | 0,00E+00 | 1,86E-03 | 9,68E-03 | 9,98E-02 | 2,19E-02 | 1,94E-02 | 0,00E+00 | 2,27E-01 | 3,11E-04 | 0,00E+00 | 2,37E-02 | 5,96E-01 |
| F3 | 0,00E+00 | 8,94E-04 | 1,28E-02 | 1,07E-01 | 2,45E-02 | 3,41E-02 | 0,00E+00 | 2,55E-01 | 6,37E-04 | 0,00E+00 | 2,77E-02 | 5,38E-01 |
| F3 | 0,00E+00 | 2,52E-03 | 7,98E-03 | 1,02E-01 | 2,04E-02 | 1,99E-02 | 0,00E+00 | 2,66E-01 | 4,98E-04 | 0,00E+00 | 2,74E-02 | 5,54E-01 |
| F3 | 0,00E+00 | 1,90E-03 | 8,22E-03 | 1,00E-01 | 2,35E-02 | 2,00E-02 | 0,00E+00 | 2,02E-01 | 3,11E-04 | 0,00E+00 | 2,38E-02 | 6,20E-01 |
| F3 | 0,00E+00 | 2,36E-03 | 7,55E-03 | 1,06E-01 | 2,26E-02 | 2,54E-02 | 0,00E+00 | 2,22E-01 | 4,91E-04 | 0,00E+00 | 3,40E-02 | 5,80E-01 |
| F3 | 0,00E+00 | 2,77E-03 | 5,62E-03 | 9,89E-02 | 2,22E-02 | 1,56E-02 | 0,00E+00 | 2,64E-01 | 6,73E-04 | 0,00E+00 | 3,33E-02 | 5,57E-01 |
| F4 | 0,00E+00 | 0,00E+00 | 8,41E-03 | 1,25E-01 | 1,96E-02 | 1,03E-02 | 0,00E+00 | 1,71E-01 | 1,66E-04 | 8,12E-06 | 1,83E-02 | 6,47E-01 |
| F4 | 0,00E+00 | 6,16E-04 | 7,11E-03 | 1,08E-01 | 1,74E-02 | 1,07E-02 | 0,00E+00 | 2,11E-01 | 7,34E-05 | 0,00E+00 | 2,18E-02 | 6,23E-01 |
| F4 | 0,00E+00 | 1,04E-03 | 8,44E-03 | 9,69E-02 | 1,72E-02 | 7,39E-03 | 0,00E+00 | 1,50E-01 | 2,57E-04 | 3,80E-06 | 2,30E-02 | 6,96E-01 |
| F4 | 0,00E+00 | 6,89E-04 | 7,22E-03 | 9,43E-02 | 1,71E-02 | 1,16E-02 | 0,00E+00 | 1,55E-01 | 1,45E-04 | 4,49E-06 | 1,89E-02 | 6,95E-01 |
| F4 | 0,00E+00 | 5,59E-04 | 5,48E-03 | 9,82E-02 | 1,63E-02 | 9,75E-03 | 0,00E+00 | 1,43E-01 | 7,52E-05 | 0,00E+00 | 2,38E-02 | 7,03E-01 |
| F4 | 0,00E+00 | 7,48E-04 | 7,06E-03 | 8,79E-02 | 1,88E-02 | 9,40E-03 | 0,00E+00 | 1,75E-01 | 1,17E-04 | 0,00E+00 | 3,21E-02 | 6,69E-01 |

Amount of 16S rRNA gene copies per 5 ng fecal DNA are given as relative abundance of total bacteria. Refer to **Figure 12** for the corresponding bar plots.

Table 46. Microbial composition in feces determined by amplicon sequencing using the Silva database to assign taxonomy at the family level

| Days post-inoculation (d) | d41 | | | | | | | | |
|---------------------------|------------------|----------|----------|----------|---|----------|----------|----------|----------|
| Mouse number | 381 | 382 | 383 | 384 | 385 | 386 | 387 | 388 | 390 |
| Microbiota | ASF ⁵ | | | | ASF ⁵ + Oligo-MM ¹² | | | | |
| Taxon (Family level) | | | | | | | | | |
| Nocardiaceae | 0,00E+00 | 0,00E+00 | 6,63E-05 | 0,00E+00 | 0,00E+00 | 0,00E+00 | 0,00E+00 | 0,00E+00 | 0,00E+00 |
| Microbacteriaceae | 1,09E-04 | 0,00E+00 | 0,00E+00 | 0,00E+00 | 0,00E+00 | 0,00E+00 | 0,00E+00 | 0,00E+00 | 0,00E+00 |
| Promicromonosporaceae | 0,00E+00 | 0,00E+00 | 0,00E+00 | 0,00E+00 | 0,00E+00 | 0,00E+00 | 0,00E+00 | 0,00E+00 | 0,00E+00 |
| Bacteroidales;Other | 0,00E+00 | 0,00E+00 | 0,00E+00 | 0,00E+00 | 0,00E+00 | 2,41E-03 | 2,60E-03 | 2,93E-03 | 3,04E-03 |
| Bacteroidaceae | 5,47E-04 | 0,00E+00 | 6,63E-05 | 1,60E-04 | 2,54E-03 | 4,04E-01 | 3,54E-01 | 3,83E-01 | 3,71E-01 |
| Porphyromonadaceae | 9,45E-01 | 9,72E-01 | 9,11E-01 | 9,43E-01 | 9,55E-01 | 2,32E-01 | 2,33E-01 | 2,82E-01 | 2,28E-01 |
| Prevotellaceae | 0,00E+00 | 0,00E+00 | 0,00E+00 | 0,00E+00 | 0,00E+00 | 7,77E-05 | 0,00E+00 | 0,00E+00 | 4,47E-04 |
| Rikenellaceae | 1,09E-04 | 0,00E+00 | 0,00E+00 | 5,32E-05 | 0,00E+00 | 0,00E+00 | 0,00E+00 | 8,37E-05 | 0,00E+00 |
| S24-7 | 0,00E+00 | 3,17E-04 | 0,00E+00 | 1,06E-04 | 2,95E-04 | 1,95E-02 | 2,24E-02 | 2,25E-02 | 1,32E-02 |
| Deferribacteraceae | 5,14E-03 | 7,93E-04 | 5,63E-03 | 1,07E-02 | 9,10E-03 | 1,55E-04 | 4,88E-04 | 3,35E-04 | 1,07E-03 |
| Lactobacillales;Other | 0,00E+00 | 0,00E+00 | 0,00E+00 | 0,00E+00 | 0,00E+00 | 0,00E+00 | 0,00E+00 | 0,00E+00 | 0,00E+00 |
| Enterococcaceae | 0,00E+00 | 0,00E+00 | 1,33E-04 | 0,00E+00 | 1,18E-04 | 0,00E+00 | 0,00E+00 | 0,00E+00 | 8,95E-05 |
| Lactobacillaceae | 4,34E-02 | 1,46E-02 | 7,47E-02 | 4,62E-02 | 3,15E-02 | 2,64E-03 | 4,88E-04 | 3,35E-04 | 7,16E-04 |
| Lachnospiraceae | 5,14E-03 | 1,05E-02 | 7,55E-03 | 5,32E-05 | 1,77E-04 | 6,93E-02 | 2,12E-01 | 9,06E-02 | 2,62E-01 |
| Ruminococcaceae | 0,00E+00 | 0,00E+00 | 0,00E+00 | 0,00E+00 | 0,00E+00 | 2,41E-03 | 1,46E-03 | 3,93E-03 | 2,51E-03 |
| Clostridiales;_uncultured | 0,00E+00 | 0,00E+00 | 0,00E+00 | 0,00E+00 | 0,00E+00 | 0,00E+00 | 0,00E+00 | 0,00E+00 | 0,00E+00 |
| Erysipelotrichaceae | 1,09E-04 | 0,00E+00 | 0,00E+00 | 0,00E+00 | 0,00E+00 | 1,32E-03 | 2,44E-04 | 1,17E-03 | 6,26E-04 |
| Rhizobiaceae | 0,00E+00 | 3,17E-04 | 6,63E-05 | 0,00E+00 | 5,91E-05 | 7,77E-05 | 0,00E+00 | 0,00E+00 | 0,00E+00 |
| Alcaligenaceae | 0,00E+00 | 0,00E+00 | 0,00E+00 | 0,00E+00 | 5,91E-05 | 8,55E-03 | 8,79E-03 | 8,03E-03 | 6,98E-03 |
| Comamonadaceae | 0,00E+00 | 6,34E-04 | 2,65E-04 | 1,06E-04 | 5,91E-05 | 2,33E-04 | 0,00E+00 | 0,00E+00 | 8,95E-05 |
| Desulfobivriaceae | 0,00E+00 | 0,00E+00 | 6,63E-05 | 0,00E+00 | 0,00E+00 | 0,00E+00 | 0,00E+00 | 0,00E+00 | 0,00E+00 |
| Verrucomicrobiaceae | 5,47E-04 | 6,34E-04 | 0,00E+00 | 0,00E+00 | 1,18E-03 | 2,57E-01 | 1,65E-01 | 2,05E-01 | 1,10E-01 |

| Days post-inoculation (d) | d41 | | | | |
|---------------------------|------------------------|----------|----------|----------|----------|
| Mouse number | 391 | 392 | 393 | 394 | 395 |
| Microbiota | ASF ⁵ + CON | | | | |
| Taxon (Family level) | | | | | |
| Nocardiaceae | 1,12E-04 | 9,85E-05 | 0,00E+00 | 0,00E+00 | 2,30E-04 |
| Microbacteriaceae | 1,12E-04 | 0,00E+00 | 2,11E-04 | 0,00E+00 | 0,00E+00 |
| Promicromonosporaceae | 0,00E+00 | 0,00E+00 | 0,00E+00 | 4,63E-04 | 1,15E-04 |
| Bacteroidales;Other | 4,49E-04 | 6,90E-04 | 2,32E-03 | 6,95E-04 | 8,05E-04 |
| Bacteroidaceae | 5,37E-02 | 2,89E-02 | 4,60E-02 | 2,61E-02 | 2,31E-02 |
| Porphyromonadaceae | 2,28E-02 | 1,57E-02 | 2,22E-02 | 1,57E-02 | 1,93E-02 |
| Prevotellaceae | 9,67E-02 | 5,57E-02 | 1,27E-01 | 1,84E-02 | 1,91E-02 |
| Rikenellaceae | 5,43E-02 | 4,62E-02 | 9,47E-02 | 6,07E-02 | 6,90E-02 |
| S24-7 | 6,06E-01 | 7,18E-01 | 4,84E-01 | 5,79E-01 | 6,39E-01 |
| Deferribacteraceae | 4,49E-04 | 5,91E-04 | 2,11E-03 | 1,85E-03 | 8,05E-04 |
| Lactobacillales;Other | 0,00E+00 | 0,00E+00 | 0,00E+00 | 0,00E+00 | 0,00E+00 |

| Days post-inoculation (d) | d41 | | | | |
|---------------------------|------------------------|----------|----------|----------|----------|
| Mouse number | 391 | 392 | 393 | 394 | 395 |
| Microbiota | ASF ⁵ + CON | | | | |
| Taxon (Family level) | | | | | |
| Enterococcaceae | 0,00E+00 | 1,97E-04 | 0,00E+00 | 1,16E-04 | 0,00E+00 |
| Lactobacillaceae | 1,76E-02 | 2,72E-02 | 2,42E-02 | 2,44E-02 | 5,20E-02 |
| Lachnospiraceae | 1,16E-01 | 7,94E-02 | 1,61E-01 | 2,44E-01 | 1,33E-01 |
| Ruminococcaceae | 1,82E-02 | 1,22E-02 | 2,41E-02 | 1,25E-02 | 1,79E-02 |
| Clostridiales: uncultured | 2,02E-03 | 1,77E-03 | 2,74E-03 | 3,36E-03 | 5,98E-03 |
| Erysipelotrichaceae | 7,85E-04 | 1,87E-03 | 4,22E-04 | 1,97E-03 | 4,26E-03 |
| Rhizobiaceae | 0,00E+00 | 0,00E+00 | 0,00E+00 | 1,16E-04 | 0,00E+00 |
| Alcaligenaceae | 6,62E-03 | 7,68E-03 | 5,17E-03 | 4,98E-03 | 7,25E-03 |
| Comamonadaceae | 8,97E-04 | 1,97E-04 | 6,33E-04 | 1,16E-03 | 1,15E-04 |
| Desulfovibrionaceae | 3,59E-03 | 4,04E-03 | 3,27E-03 | 5,33E-03 | 7,94E-03 |
| Verrucomicrobiaceae | 0,00E+00 | 9,85E-05 | 1,06E-04 | 0,00E+00 | 0,00E+00 |

Number of 16S amplicon sequencing reads are given as relative abundance and corresponding bar plots are presented in **Figure 13C**.

Table 47. Microbial composition in feces of ASF and Oligo-MM strains before infection determined by qPCR

| Mouse number | 381 | 382 | 383 | 384 | 385 | 386 | 387 | 388 | 389 | 390 |
|--------------|------------------|------------------|------------------|------------------|------------------|---|---|---|---|---|
| Microbiota | ASF ⁵ | ASF ⁵ | ASF ⁵ | ASF ⁵ | ASF ⁵ | ASF ⁵ + Oligo-MM ¹² | ASF ⁵ + Oligo-MM ¹² | ASF ⁵ + Oligo-MM ¹² | ASF ⁵ + Oligo-MM ¹² | ASF ⁵ + Oligo-MM ¹² |
| I46 | 0,00E+00 | 0,00E+00 | 0,00E+00 | | | 0,00E+00 | 0,00E+00 | 0,00E+00 | NA | 0,00E+00 |
| I49 | 0,00E+00 | 0,00E+00 | 0,00E+00 | | | 0,00E+00 | 0,00E+00 | 5,12E-05 | NA | 0,00E+00 |
| YL58 | 0,00E+00 | 0,00E+00 | 0,00E+00 | | | 5,31E-03 | 3,63E-03 | 4,04E-03 | NA | 1,79E-03 |
| YL27 | 0,00E+00 | 0,00E+00 | 0,00E+00 | | | 4,20E-02 | 4,01E-02 | 4,03E-02 | NA | 4,25E-02 |
| YL31 | 7,92E-06 | 8,30E-05 | 1,76E-05 | | | 1,81E-02 | 1,35E-02 | 2,05E-02 | NA | 1,23E-02 |
| YL32 | 0,00E+00 | 0,00E+00 | 0,00E+00 | | | 8,94E-03 | 2,46E-02 | 1,11E-02 | NA | 1,90E-02 |
| KB18 | 0,00E+00 | 0,00E+00 | 0,00E+00 | | | 0,00E+00 | 0,00E+00 | 0,00E+00 | NA | 0,00E+00 |
| YL44 | 0,00E+00 | 0,00E+00 | 0,00E+00 | | | 2,36E-01 | 2,22E-01 | 2,15E-01 | NA | 2,70E-01 |
| KB1 | 0,00E+00 | 0,00E+00 | 0,00E+00 | | | 0,00E+00 | 0,00E+00 | 2,55E-06 | NA | 4,06E-05 |
| YL2 | 0,00E+00 | 0,00E+00 | 0,00E+00 | | | 0,00E+00 | 0,00E+00 | 0,00E+00 | NA | 0,00E+00 |
| YL45 | 0,00E+00 | 0,00E+00 | 0,00E+00 | | | 2,66E-02 | 3,43E-02 | 3,01E-02 | NA | 4,23E-02 |
| I48 | 0,00E+00 | 0,00E+00 | 0,00E+00 | | | 4,85E-01 | 4,60E-01 | 4,83E-01 | NA | 3,57E-01 |
| ASF356 | 0,00E+00 | 0,00E+00 | 0,00E+00 | 0,00E+00 | 0,00E+00 | 0,00E+00 | 0,00E+00 | 0,00E+00 | NA | 0,00E+00 |
| ASF361 | 7,24E-02 | 2,55E-02 | 7,28E-02 | 4,26E-02 | 3,58E-02 | 1,37E-03 | 6,68E-04 | 8,96E-04 | NA | 5,66E-04 |
| ASF457 | 7,31E-02 | 3,28E-02 | 7,79E-02 | 7,64E-02 | 7,16E-02 | 9,06E-04 | 7,66E-04 | 3,56E-04 | NA | 4,67E-03 |
| ASF519 | 8,54E-01 | 9,42E-01 | 8,49E-01 | 8,81E-01 | 8,93E-01 | 1,75E-01 | 2,01E-01 | 1,95E-01 | NA | 2,50E-01 |
| ASF360 | 0,00E+00 | 0,00E+00 | 0,00E+00 | | | 0,00E+00 | 0,00E+00 | 0,00E+00 | NA | 0,00E+00 |
| ASF502(SB2) | 0,00E+00 | 0,00E+00 | 0,00E+00 | | | 0,00E+00 | 0,00E+00 | 0,00E+00 | NA | 0,00E+00 |
| ASF500 | 0,00E+00 | 0,00E+00 | 0,00E+00 | 0,00E+00 | 0,00E+00 | 0,00E+00 | 0,00E+00 | 0,00E+00 | NA | 0,00E+00 |

| Mouse number | 381 | 382 | 383 | 384 | 385 | 386 | 387 | 388 | 389 | 390 |
|------------------------------|------------------|------------------|------------------|------------------|------------------|--|--|--|--|--|
| Microbiota | ASF ⁵ | ASF ⁵ | ASF ⁵ | ASF ⁵ | ASF ⁵ | ASF ⁵ + Oligo- MM ¹² | ASF ⁵ + Oligo- MM ¹² | ASF ⁵ + Oligo- MM ¹² | ASF ⁵ + Oligo- MM ¹² | ASF ⁵ + Oligo- MM ¹² |
| <i>S. Tm</i> ^{avir} | 0,00E+00 | 0,00E+00 | 0,00E+00 | | | 0,00E+00 | 0,00E+00 | 0,00E+00 | NA | |

Amount of 16S rRNA gene copies per 5 ng fecal DNA are given as relative abundance and corresponding bar plots are presented in **Figure 14**. Grey filling stays for values below detection limit.

Table 48. Microbial composition in feces of ASF- and Oligo-MM-colonized mice before infection determined by qPCR

| Mouse number | 996 | 997 | 998 | 999 | 1000 | 1001 | 1002 | 1003 |
|------------------------------|------------------|------------------|------------------|--|--|--|--|--|
| Microbiota | ASF ⁴ | ASF ⁴ | ASF ⁴ | ASF ⁴ + ASF ⁷ | ASF ⁴ + ASF ⁷ | ASF ⁴ + ASF ⁷ | ASF ⁴ + ASF ⁷ | ASF ⁴ + ASF ⁷ |
| I46 | 0,00E+00 | 0,00E+00 | 0,00E+00 | 0,00E+00 | 0,00E+00 | 0,00E+00 | | |
| I49 | 0,00E+00 | 0,00E+00 | 0,00E+00 | 0,00E+00 | 0,00E+00 | 0,00E+00 | | |
| YL58 | 0,00E+00 | 0,00E+00 | 0,00E+00 | 0,00E+00 | 0,00E+00 | 0,00E+00 | | |
| YL27 | 0,00E+00 | 0,00E+00 | 0,00E+00 | 0,00E+00 | 0,00E+00 | 0,00E+00 | | |
| YL31 | 0,00E+00 | 0,00E+00 | 0,00E+00 | 0,00E+00 | 0,00E+00 | 0,00E+00 | | |
| YL32 | 0,00E+00 | 0,00E+00 | 0,00E+00 | 0,00E+00 | 0,00E+00 | 0,00E+00 | | |
| KB18 | 0,00E+00 | 0,00E+00 | 0,00E+00 | 0,00E+00 | 0,00E+00 | 0,00E+00 | | |
| YL44 | 0,00E+00 | 0,00E+00 | 0,00E+00 | 0,00E+00 | 0,00E+00 | 0,00E+00 | | |
| KB1 | 0,00E+00 | 0,00E+00 | 0,00E+00 | 0,00E+00 | 0,00E+00 | 0,00E+00 | | |
| YL2 | 0,00E+00 | 0,00E+00 | 0,00E+00 | 0,00E+00 | 0,00E+00 | 0,00E+00 | | |
| YL45 | 0,00E+00 | 0,00E+00 | 0,00E+00 | 0,00E+00 | 0,00E+00 | 0,00E+00 | | |
| I48 | 0,00E+00 | 0,00E+00 | 0,00E+00 | 0,00E+00 | 0,00E+00 | 0,00E+00 | | |
| ASF356 | 2,91E-02 | 2,18E-02 | 2,59E-02 | 1,12E-02 | 1,68E-02 | 1,77E-02 | 2,42E-02 | 2,35E-02 |
| ASF361 | 1,95E-01 | 1,21E-01 | 1,74E-01 | 2,00E-01 | 1,52E-01 | 1,43E-01 | 2,08E-01 | 2,14E-01 |
| ASF457 | 0,00E+00 | 0,00E+00 | 0,00E+00 | 8,74E-03 | 1,57E-02 | 1,22E-02 | 1,11E-02 | 1,35E-02 |
| ASF519 | 7,76E-01 | 8,57E-01 | 8,00E-01 | 7,80E-01 | 8,15E-01 | 8,27E-01 | 7,56E-01 | 7,49E-01 |
| ASF360 | 0,00E+00 | 0,00E+00 | 0,00E+00 | 0,00E+00 | 0,00E+00 | 3,90E-05 | 0,00E+00 | 0,00E+00 |
| ASF502(SB2) | 0,00E+00 | 0,00E+00 | 0,00E+00 | 0,00E+00 | 0,00E+00 | 2,99E-06 | 0,00E+00 | 0,00E+00 |
| ASF500 | 0,00E+00 | 0,00E+00 | 0,00E+00 | 0,00E+00 | 0,00E+00 | 2,42E-05 | 0,00E+00 | 1,26E-05 |
| <i>S. Tm</i> ^{avir} | 0,00E+00 | 0,00E+00 | 0,00E+00 | 0,00E+00 | 0,00E+00 | 0,00E+00 | | |

| Mouse number | 942 | 943 | 944 | 945 | 946 | 947 | 948 | 949 | 950 | 951 | 952 | 953 |
|-----------------------|------------------------|------------------------|------------------------|------------------------|------------------------|------------------------|---|---|---|---|---|---|
| Microbiota | Oligo-MM ¹² | Oligo-MM ¹² | Oligo-MM ¹² | Oligo-MM ¹² | Oligo-MM ¹² | Oligo-MM ¹² | Oligo-MM ¹² + ASF ⁷ | Oligo-MM ¹² + ASF ⁷ | Oligo-MM ¹² + ASF ⁷ | Oligo-MM ¹² + ASF ⁷ | Oligo-MM ¹² + ASF ⁷ | Oligo-MM ¹² + ASF ⁷ |
| I46 | 0,00E+00 | 0,00E+00 | 0,00E+00 | 0,00E+00 | 0,00E+00 | 0,00E+00 | 0,00E+00 | 0,00E+00 | 0,00E+00 | 0,00E+00 | 0,00E+00 | 0,00E+00 |
| I49 | 1,76E-03 | 8,15E-04 | 5,12E-04 | 4,49E-04 | 5,97E-04 | 3,25E-04 | 5,99E-04 | 1,48E-03 | 1,22E-03 | 2,15E-03 | 1,28E-03 | 3,48E-04 |
| YL58 | 1,49E-02 | 1,50E-02 | 1,78E-02 | 7,21E-03 | 5,31E-03 | 1,16E-02 | 1,14E-02 | 1,19E-02 | 1,50E-02 | 1,44E-02 | 1,33E-02 | 1,56E-02 |
| YL27 | 1,45E-01 | 1,33E-01 | 1,39E-01 | 1,80E-01 | 1,96E-01 | 2,22E-01 | 7,57E-02 | 9,79E-02 | 7,56E-02 | 6,45E-02 | 6,36E-02 | 5,00E-02 |
| YL31 | 2,20E-02 | 1,59E-02 | 1,44E-02 | 9,40E-03 | 1,03E-02 | 7,15E-03 | 1,87E-02 | 1,69E-02 | 1,17E-02 | 1,95E-02 | 2,25E-02 | 1,75E-02 |
| YL32 | 3,06E-02 | 3,07E-02 | 3,98E-02 | 4,58E-02 | 1,55E-02 | 4,43E-02 | 8,92E-02 | 3,89E-02 | 7,76E-02 | 4,21E-02 | 9,55E-02 | 1,09E-01 |
| KB18 | 0,00E+00 | 0,00E+00 | 0,00E+00 | 0,00E+00 | 0,00E+00 | 0,00E+00 | 0,00E+00 | 0,00E+00 | 0,00E+00 | 0,00E+00 | 0,00E+00 | 0,00E+00 |
| YL44 | 2,90E-01 | 2,69E-01 | 1,91E-01 | 3,35E-01 | 2,70E-01 | 1,91E-01 | 1,86E-01 | 1,52E-01 | 1,31E-01 | 2,64E-01 | 1,78E-01 | 1,53E-01 |
| KB1 | 4,45E-05 | 5,35E-05 | 8,75E-05 | 6,72E-05 | 2,66E-05 | 4,30E-05 | 8,52E-05 | 7,96E-05 | 5,52E-05 | 4,32E-05 | 2,90E-05 | 8,16E-05 |
| YL2 | 0,00E+00 | 6,57E-06 | 0,00E+00 | 0,00E+00 | 0,00E+00 | 0,00E+00 | 0,00E+00 | 0,00E+00 | 0,00E+00 | 0,00E+00 | 0,00E+00 | 4,57E-06 |
| YL45 | 3,63E-02 | 3,80E-02 | 4,77E-02 | 4,55E-02 | 3,89E-02 | 4,76E-02 | 3,12E-02 | 3,35E-02 | 3,59E-02 | 3,16E-02 | 3,04E-02 | 4,29E-02 |
| I48 | 4,60E-01 | 4,98E-01 | 5,49E-01 | 3,77E-01 | 4,64E-01 | 4,76E-01 | 4,65E-01 | 5,33E-01 | 5,20E-01 | 4,63E-01 | 4,43E-01 | 4,42E-01 |
| ASF356 | 0,00E+00 | 0,00E+00 | 0,00E+00 | | | | 0,00E+00 | 0,00E+00 | 5,80E-03 | 7,63E-03 | 0,00E+00 | 0,00E+00 |
| ASF361 | 0,00E+00 | 0,00E+00 | 0,00E+00 | | | | 4,79E-03 | 3,08E-03 | 1,16E-05 | 0,00E+00 | 1,49E-03 | 1,96E-03 |
| ASF457 | 0,00E+00 | 0,00E+00 | 0,00E+00 | | | | 1,62E-02 | 7,93E-03 | 1,76E-02 | 5,66E-03 | 1,19E-02 | 1,16E-02 |
| ASF519 | 0,00E+00 | 0,00E+00 | 0,00E+00 | | | | 1,01E-01 | 1,03E-01 | 1,08E-01 | 8,56E-02 | 1,39E-01 | 1,57E-01 |
| ASF360 | 0,00E+00 | 0,00E+00 | 0,00E+00 | | | | 0,00E+00 | 0,00E+00 | 0,00E+00 | 0,00E+00 | 0,00E+00 | 0,00E+00 |
| ASF502(SB2) | 0,00E+00 | 0,00E+00 | 0,00E+00 | | | | 0,00E+00 | 0,00E+00 | 0,00E+00 | 0,00E+00 | 0,00E+00 | 0,00E+00 |
| ASF500 | 0,00E+00 | 0,00E+00 | 0,00E+00 | | | | 0,00E+00 | 0,00E+00 | 0,00E+00 | 0,00E+00 | 0,00E+00 | 0,00E+00 |
| S. Tm ^{avir} | 0,00E+00 | 0,00E+00 | 0,00E+00 | | | | 0,00E+00 | 0,00E+00 | 0,00E+00 | 0,00E+00 | 0,00E+00 | 0,00E+00 |

Amount of 16S rRNA gene copies per 5 ng fecal DNA are given as relative abundance and corresponding bar plots are presented in **Figure 18B**. Grey filling stays for analysis not performed.

Table 49. Gene sets upregulated in cecal epithelium of AGR2^{ko} mice as compared to AGR2^{het} littermates

| NAME | SIZE | NES | FDR q-val |
|--------------------------------|------|----------|-----------|
| REACT_CHOLESTEROL BIOSYNTHESIS | 16 | 2,109206 | 0,025354 |
| NCL_ANTHRAXPATHWAY | 17 | 1,882678 | 0,155662 |
| BIOC_HIVNEFPATHWAY | 50 | 1,898674 | 0,19743 |

Only the significant upregulated gene sets are shown here (FDR<0.25).

Table 50. Gene sets downregulated in cecal epithelium of AGR2^{ko} mice as compared to AGR2^{het} littermates

| NAME | SIZE | NES | FDR q-val |
|---|------|----------|-----------|
| REACT_MITOTIC M-M_G1 PHASES | 132 | -2,63888 | 0 |
| REACT_DNA REPLICATION | 145 | -2,61878 | 0 |
| WIP_MM_DNA_REPLICATION | 39 | -2,50171 | 0 |
| REACT_G1_S TRANSITION | 70 | -2,49978 | 0 |
| REACT_MITOTIC G1-G1_S PHASES | 78 | -2,49747 | 0 |
| REACT_S PHASE | 82 | -2,49701 | 0 |
| REACT_CELL CYCLE, MITOTIC | 224 | -2,46865 | 0 |
| REACT_SYNTHESIS OF DNA | 69 | -2,4529 | 0 |
| REACT_DNA STRAND ELONGATION | 22 | -2,44621 | 0 |
| NCL_AURORA_B_PATHWAY | 34 | -2,25125 | 4,89E-05 |
| REACT_ACTIVATION OF THE PRE-REPLICATIVE COMPLEX | 21 | -2,26184 | 5,12E-05 |
| REACT_ASSEMBLY OF THE PRE-REPLICATIVE COMPLEX | 50 | -2,26748 | 5,38E-05 |
| REACT_G2_M CHECKPOINTS | 30 | -2,26886 | 5,66E-05 |
| REACT_M PHASE | 73 | -2,27245 | 5,97E-05 |
| REACT_MITOTIC PROMETAPHASE | 70 | -2,28769 | 6,33E-05 |
| REACT_TELOMERE MAINTENANCE | 25 | -2,36994 | 6,72E-05 |
| REACT_CHROMOSOME MAINTENANCE | 25 | -2,3835 | 7,17E-05 |
| REACT_MEIOTIC RECOMBINATION (MOUSE) | 58 | -2,40668 | 7,68E-05 |
| KEGG_DNA REPLICATION | 34 | -2,4071 | 8,27E-05 |
| REACT_CELL CYCLE CHECKPOINTS | 85 | -2,41208 | 8,96E-05 |
| REACT_REGULATION OF DNA REPLICATION | 55 | -2,23133 | 9,09E-05 |
| REACT_M_G1 TRANSITION | 59 | -2,43479 | 9,78E-05 |
| REACT_DNA REPLICATION PRE-INITIATION | 59 | -2,44487 | 1,08E-04 |
| REACT_ORC1 REMOVAL FROM CHROMATIN | 53 | -2,18705 | 2,94E-04 |
| REACT_REMOVAL OF LICENSING FACTORS FROM ORIGINS | 55 | -2,19737 | 3,06E-04 |
| REACT_SWITCHING OF ORIGINS TO A POST-REPLICATIVE STATE | 53 | -2,17222 | 3,52E-04 |
| NCL_FANCONI_PATHWAY | 44 | -2,17796 | 3,66E-04 |
| KEGG_SYSTEMIC LUPUS ERYTHEMATOSUS | 98 | -2,14963 | 6,09E-04 |
| REACT_ACTIVATION OF ATR IN RESPONSE TO REPLICATION STRESS | 27 | -2,12349 | 8,25E-04 |
| WIP_MM_G1_TO_S_CELL_CYCLE_CONTROL | 60 | -2,12509 | 8,53E-04 |
| REACT_MEIOTIC SYNAPSIS (MOUSE) | 66 | -2,11112 | 8,66E-04 |
| NCL_PLK1_PATHWAY | 40 | -2,12808 | 8,82E-04 |
| REACT_SCF(SKP2)-MEDIATED DEGRADATION OF P27_P21 | 43 | -2,10127 | 0,001001 |
| REACT_MRNA SPLICING | 72 | -2,08338 | 0,001223 |
| REACT_G1_S DNA DAMAGE CHECKPOINTS | 45 | -2,07715 | 0,001311 |
| REACT_REGULATION OF INSULIN-LIKE GROWTH FACTOR (IGF) ACTIVITY BY INSULIN-LIKE GROWTH FACTOR BINDING PROTEINS (IGFBPS) | 25 | -2,06927 | 0,001394 |
| REACT_CYCLIN E ASSOCIATED EVENTS DURING G1_S TRANSITION | 47 | -2,05732 | 0,0015 |
| REACT_PROCESSING OF CAPPED INTRON-CONTAINING PRE-MRNA | 75 | -2,05544 | 0,001516 |
| KEGG_HOMOLOGOUS RECOMBINATION | 25 | -2,05037 | 0,001537 |
| KEGG_NUCLEOTIDE EXCISION REPAIR | 43 | -2,05189 | 0,001548 |
| REACT_P53-DEPENDENT G1_S DNA DAMAGE CHECKPOINT | 43 | -2,05356 | 0,00156 |
| REACT_CDT1 ASSOCIATION WITH THE CDC6_ORC_ORIGIN COMPLEX | 44 | -2,03157 | 0,001958 |
| REACT_AUTODEGRADATION OF THE E3 UBIQUITIN LIGASE COPI | 39 | -2,02304 | 0,001997 |
| NCL_ATR_PATHWAY | 37 | -2,02674 | 0,002014 |
| REACT_MRNA SPLICING - MAJOR PATHWAY | 72 | -2,02518 | 0,002015 |
| REACT_P53-DEPENDENT G1 DNA DAMAGE RESPONSE | 43 | -2,02889 | 0,002037 |
| REACT_MRNA PROCESSING | 90 | -2,02392 | 0,002041 |
| WIP_MM_PROTEASOME_DEGRADATION | 55 | -2,01205 | 0,002272 |
| REACT_STABILIZATION OF P53 | 39 | -2,00003 | 0,002515 |
| KEGG_CELL CYCLE | 121 | -2,00028 | 0,002566 |
| REACT_CYCLIN A_CDK2-ASSOCIATED EVENTS AT S PHASE ENTRY | 48 | -2,00287 | 0,002573 |
| REACT_MRNA SPLICING - MINOR PATHWAY | 28 | -1,97545 | 0,002993 |

| NAME | SIZE | NES | FDR q-val |
|--|------|----------|-----------|
| REACT_FORMATION OF A POOL OF FREE 40S SUBUNITS | 54 | -1,97385 | 0,003015 |
| REACT_UBIQUITIN-DEPENDENT DEGRADATION OF CYCLIN D1 | 40 | -1,97948 | 0,003048 |
| REACT_UBIQUITIN MEDIATED DEGRADATION OF PHOSPHORYLATED CDC25A | 39 | -1,97548 | 0,003048 |
| REACT_APC_C-MEDIATED DEGRADATION OF CELL CYCLE PROTEINS | 62 | -1,98028 | 0,003107 |
| WIP_MM_CELL_CYCLE | 84 | -1,96911 | 0,003184 |
| REACT_ACTIVATION OF APC_C AND APC_C_CDC20 MEDIATED DEGRADATION OF MITOTIC PROTEINS | 52 | -1,96525 | 0,00322 |
| REACT_DNA REPAIR | 68 | -1,96541 | 0,003276 |
| REACT_CDC20_PHOSPHO-APC_C MEDIATED DEGRADATION OF CYCLIN A | 51 | -1,95604 | 0,0034 |
| REACT_REGULATION OF MITOTIC CELL CYCLE | 62 | -1,9504 | 0,003544 |
| KEGG_PROTEASOME | 43 | -1,95087 | 0,00355 |
| KEGG_RNA TRANSPORT | 144 | -1,95232 | 0,003555 |
| REACT_P53-INDEPENDENT DNA DAMAGE RESPONSE | 39 | -1,94757 | 0,003606 |
| REACT_APC_C_CDHI MEDIATED DEGRADATION OF CDC20 AND OTHER APC_C_CDHI TARGETED PROTEINS IN LATE MITOSIS_EARLY G1 | 53 | -1,94627 | 0,003633 |
| NCI_BARD1PATHWAY | 27 | -1,94294 | 0,003692 |
| REACT_APC_C_CDC20 MEDIATED DEGRADATION OF MITOTIC PROTEINS | 51 | -1,93892 | 0,003862 |
| REACT_UBIQUITIN-DEPENDENT DEGRADATION OF CYCLIN D | 40 | -1,93831 | 0,003885 |
| REACT_P53-INDEPENDENT G1_S DNA DAMAGE CHECKPOINT | 39 | -1,92998 | 0,004108 |
| REACT_CDK-MEDIATED PHOSPHORYLATION AND REMOVAL OF CDC6 | 39 | -1,90627 | 0,005406 |
| KEGG_PYRIMIDINE METABOLISM | 93 | -1,88722 | 0,006725 |
| REACT_EUKARYOTIC TRANSLATION ELONGATION | 50 | -1,88791 | 0,006789 |
| REACT_REGULATION OF APC_C ACTIVATORS BETWEEN G1_S AND EARLY ANAPHASE | 58 | -1,88209 | 0,006994 |
| REACT_FORMATION AND MATURATION OF MRNA TRANSCRIPT | 105 | -1,88091 | 0,006999 |
| KEGG_SPLICEOSOME | 112 | -1,88231 | 0,00709 |
| REACT_SCF-BETA-TRCP MEDIATED DEGRADATION OF EMI1 | 43 | -1,8763 | 0,007257 |
| REACT_APC_C_CDC20 MEDIATED DEGRADATION OF SECURIN | 49 | -1,87253 | 0,0074 |
| REACT_AUTODEGRADATION OF CDHI BY CDHI_APC_C | 45 | -1,86714 | 0,007507 |
| REACT_METABOLISM OF RNA | 52 | -1,86747 | 0,007589 |
| REACT_EUKARYOTIC TRANSLATION TERMINATION | 47 | -1,86815 | 0,00766 |
| REACT_METABOLISM OF PROTEINS | 155 | -1,85895 | 0,007742 |
| REACT_CLEAVAGE OF GROWING TRANSCRIPT IN THE TERMINATION REGION | 29 | -1,85472 | 0,00778 |
| REACT_PROCESSING OF CAPPED INTRONLESS PRE-MRNA | 19 | -1,85761 | 0,007788 |
| REACT_POST-ELONGATION PROCESSING OF INTRONLESS PRE-MRNA | 19 | -1,85622 | 0,007821 |
| REACT_RNA POLYMERASE II TRANSCRIPTION TERMINATION | 29 | -1,85931 | 0,007823 |
| REACT_POST-ELONGATION PROCESSING OF THE TRANSCRIPT | 29 | -1,8522 | 0,007874 |
| KEGG_FANCONI ANEMIA PATHWAY | 48 | -1,85938 | 0,007905 |
| REACT_FORMATION OF THE TERNARY COMPLEX, AND SUBSEQUENTLY, THE 43S COMPLEX | 26 | -1,85979 | 0,007936 |
| REACT_TRANSLATION | 74 | -1,84872 | 0,00805 |
| WIP_MM_NUCLEOTIDE_METABOLISM | 20 | -1,84193 | 0,008685 |
| BIOC_AMIPATHWAY | 18 | -1,82941 | 0,009952 |
| REACT_REGULATION OF APOPTOSIS | 47 | -1,822 | 0,010711 |
| BIOC_CSKPATHWAY | 18 | -1,80562 | 0,012272 |
| KEGG_BASE EXCISION REPAIR | 30 | -1,80648 | 0,012324 |
| REACT_DEGRADATION OF BETA-CATENIN BY THE DESTRUCTION COMPLEX | 48 | -1,79582 | 0,013463 |
| REACT_REGULATION OF ORNITHINE DECARBOXYLASE (ODC) | 39 | -1,78143 | 0,014823 |
| NCI_FOXM1PATHWAY | 38 | -1,78206 | 0,014931 |
| REACT_L13A-MEDIATED TRANSLATIONAL SILENCING OF CERULOPLASMIN EXPRESSION | 61 | -1,78235 | 0,015087 |
| REACT_3'-UTR-MEDIATED TRANSLATIONAL REGULATION | 61 | -1,77266 | 0,016238 |
| REACT_GLOBAL GENOMIC NER (GG-NER) | 21 | -1,76667 | 0,016675 |
| REACT_GENE EXPRESSION | 269 | -1,76684 | 0,016819 |
| REACT_SIGNALING BY WNT | 48 | -1,76776 | 0,016868 |
| REACT_REGULATION OF ACTIVATED PAK-2P34 BY PROTEASOME MEDIATED DEGRADATION | 38 | -1,76081 | 0,017423 |
| KEGG_MISMATCH REPAIR | 21 | -1,75292 | 0,018473 |
| BIOC_MPRPATHWAY | 19 | -1,73406 | 0,022334 |
| REACT_PEPTIDE CHAIN ELONGATION | 47 | -1,70942 | 0,028406 |
| KEGG_MUCIN TYPE O-GLYCAN BIOSYNTHESIS | 25 | -1,70517 | 0,029303 |
| WIP_MM_CYTOPLASMIC_RIBOSOMAL_PROTEINS | 40 | -1,70072 | 0,030245 |
| REACT_TRANSCRIPTION | 94 | -1,69578 | 0,031367 |
| REACT_GTP HYDROLYSIS AND JOINING OF THE 60S RIBOSOMAL SUBUNIT | 63 | -1,69164 | 0,032061 |
| REACT_CAP-DEPENDENT TRANSLATION INITIATION | 67 | -1,68201 | 0,034675 |
| REACT_GLYCOLYSIS | 20 | -1,67923 | 0,035188 |
| BIOC_PROTEASOME PATHWAY | 19 | -1,67813 | 0,035245 |
| KEGG_RNA DEGRADATION | 69 | -1,6728 | 0,036675 |

| NAME | SIZE | NES | FDR q-val |
|---|------|----------|-----------|
| NCI_MYC_ACTIVPATHWAY | 69 | -1,66482 | 0,038683 |
| REACT_REGULATION OF GLUCOKINASE BY GLUCOKINASE REGULATORY PROTEIN | 19 | -1,65724 | 0,040658 |
| REACT_DIABETES PATHWAYS | 242 | -1,6536 | 0,041503 |
| REACT_EUKARYOTIC TRANSLATION INITIATION | 67 | -1,64831 | 0,043037 |
| NCI_E2F_PATHWAY | 70 | -1,64553 | 0,043589 |
| REACT_RNA POLYMERASE II TRANSCRIPTION | 66 | -1,64173 | 0,044596 |
| BIOC_ATRBRCAPATHWAY | 17 | -1,63304 | 0,046842 |
| REACT_POST-TRANSLATIONAL PROTEIN MODIFICATION | 46 | -1,63401 | 0,046909 |
| REACT_POST-ELONGATION PROCESSING OF INTRON-CONTAINING PRE-MRNA | 22 | -1,62063 | 0,051481 |
| REACT_MRNA 3-END PROCESSING | 22 | -1,60823 | 0,056542 |
| NCI_IL2_STAT5PATHWAY | 30 | -1,60723 | 0,056543 |
| REACT_INSULIN SYNTHESIS AND PROCESSING | 79 | -1,60349 | 0,057755 |
| KEGG_RIBOSOME | 52 | -1,59794 | 0,059719 |
| WIP_MM_UREA_CYCLE_AND_METABOLISM_OF_AMINO_GROUPS | 20 | -1,58851 | 0,063692 |
| REACT_DEADENYLATION-DEPENDENT MRNA DECAY | 38 | -1,58351 | 0,065925 |
| KEGG_RIBOSOME BIOGENESIS IN EUKARYOTES | 75 | -1,5795 | 0,067435 |
| NCI_BETACATENIN_NUC_PATHWAY | 75 | -1,575 | 0,068098 |
| REACT_NUCLEOTIDE EXCISION REPAIR | 33 | -1,57644 | 0,068487 |
| REACT_GLUCOSE TRANSPORT | 25 | -1,57508 | 0,068566 |
| REACT_LOSS OF PROTEINS REQUIRED FOR INTERPHASE MICROTUBULE ORGANIZATION FROM THE CENTROSOME | 47 | -1,57293 | 0,068769 |
| REACT_HEXOSE TRANSPORT | 25 | -1,56983 | 0,068919 |
| REACT_METABOLISM OF MRNA | 38 | -1,56994 | 0,069386 |
| WIP_MM_PROSTAGLANDIN_SYNTHESIS_AND_REGULATION | 31 | -1,57075 | 0,069465 |
| REACT_METABOLISM OF AMINO ACIDS AND DERIVATIVES | 143 | -1,56706 | 0,069801 |
| NCI_IL2_P13KPATHWAY | 33 | -1,56514 | 0,069807 |
| REACT_TRANSCRIPTION-COUPLED NER (TC-NER) | 29 | -1,56594 | 0,069856 |
| KEGG_PURINE METABOLISM | 160 | -1,56318 | 0,06992 |
| REACT_LOSS OF NLP FROM MITOTIC CENTROSOMES | 47 | -1,56399 | 0,069938 |
| REACT_METABOLISM OF CARBOHYDRATES | 80 | -1,55989 | 0,071042 |
| REACT_METABOLISM OF NUCLEOTIDES | 48 | -1,5477 | 0,076841 |
| NCI_AR_NONGENOMIC_PATHWAY | 28 | -1,54844 | 0,076942 |
| NCI_HIFI1PATHWAY | 16 | -1,54586 | 0,077463 |
| NCI_TELOMERASEPATHWAY | 62 | -1,53903 | 0,080609 |
| REACT_RNA POLYMERASE I TRANSCRIPTION | 19 | -1,53105 | 0,084866 |
| BIOC_G2PATHWAY | 20 | -1,52354 | 0,088981 |
| REACT_INTERACTIONS OF THE IMMUNOGLOBULIN SUPERFAMILY (IGSF) MEMBER PROTEINS | 22 | -1,52007 | 0,090334 |
| REACT_SIGNALLING TO RAS | 19 | -1,51885 | 0,090515 |
| BIOC_G1PATHWAY | 23 | -1,52031 | 0,090774 |
| BIOC_CELLCYCLEPATHWAY | 21 | -1,51508 | 0,092355 |
| REACT_TRANSLATION INITIATION COMPLEX FORMATION | 31 | -1,50473 | 0,098421 |
| NCI_LKB1_PATHWAY | 44 | -1,50246 | 0,099352 |
| NCI_AURORA_A_PATHWAY | 30 | -1,50117 | 0,099488 |
| NCI_ATM_PATHWAY | 32 | -1,48536 | 0,110575 |
| REACT_RIBOSOMAL SCANNING AND START CODON RECOGNITION | 32 | -1,4811 | 0,113222 |
| KEGG_N-GLYCAN BIOSYNTHESIS | 50 | -1,4726 | 0,117979 |
| REACT_TRANSPORT OF MATURE TRANSCRIPT TO CYTOPLASM | 16 | -1,47305 | 0,118412 |
| REACT_RNA POLYMERASE I, RNA POLYMERASE III, AND MITOCHONDRIAL TRANSCRIPTION | 40 | -1,47309 | 0,11913 |
| REACT_RNA POLYMERASE I PROMOTER CLEARANCE | 17 | -1,46947 | 0,119743 |
| REACT_RNA POLYMERASE I TRANSCRIPTION INITIATION | 16 | -1,46426 | 0,123388 |
| REACT_GLUONEOGENESIS | 26 | -1,45628 | 0,129265 |
| REACT_PYRIMIDINE METABOLISM | 20 | -1,44924 | 0,134292 |
| KEGG_THYROID CANCER | 28 | -1,44971 | 0,13471 |
| KEGG_COMPLEMENT AND COAGULATION CASCADES | 75 | -1,44683 | 0,135605 |
| REACT_MITOTIC G2-G2_M PHASES | 64 | -1,43883 | 0,142173 |
| REACT_G2_M TRANSITION | 61 | -1,43666 | 0,142694 |
| REACT_POST-TRANSLATIONAL MODIFICATION_ SYNTHESIS OF GPI-ANCHORED PROTEINS | 22 | -1,4369 | 0,143316 |
| REACT_INTERLEUKIN-2 SIGNALING | 15 | -1,43147 | 0,147157 |
| REACT_CENTROSOME MATURATION | 54 | -1,41709 | 0,160883 |
| REACT_IMMUNOREGULATORY INTERACTIONS BETWEEN A LYMPHOID AND A NON-LYMPHOID CELL | 35 | -1,4148 | 0,162398 |
| REACT_GLUCOSE METABOLISM | 45 | -1,41358 | 0,162611 |
| REACT_RECRUITMENT OF MITOTIC CENTROSOME PROTEINS AND COMPLEXES | 54 | -1,40779 | 0,168082 |

| NAME | SIZE | NES | FDR q-val |
|--|------|----------|-----------|
| REACT_ASSOCIATION OF TRIC_CCT WITH TARGET PROTEINS DURING BIOSYNTHESIS | 17 | -1,40679 | 0,1682 |
| BIOC_CKIPATHWAY | 15 | -1,39683 | 0,178182 |
| REACT_LYSOSOME VESICLE BIOGENESIS | 20 | -1,39552 | 0,178755 |
| REACT_LIPID DIGESTION, MOBILIZATION, AND TRANSPORT | 24 | -1,39208 | 0,181467 |
| NCL_SIP_META_PATHWAY | 21 | -1,38572 | 0,187576 |
| WIP_MM_TNF-ALPHA_NF-KB_SIGNALING_PATHWAY | 176 | -1,38332 | 0,189235 |
| BIOC_GSK3PATHWAY | 26 | -1,37926 | 0,192819 |
| REACT_CHAPERONIN-MEDIATED PROTEIN FOLDING | 31 | -1,37413 | 0,198061 |
| KEGG_P53 SIGNALING PATHWAY | 66 | -1,36862 | 0,201454 |
| REACT_ACTIVATION OF THE MRNA UPON BINDING OF THE CAP-BINDING COMPLEX AND EIFS, AND SUBSEQUENT BINDING TO 43S | 32 | -1,36879 | 0,202359 |
| KEGG_BASAL TRANSCRIPTION FACTORS | 42 | -1,36913 | 0,203069 |
| KEGG_PENTOSE PHOSPHATE PATHWAY | 30 | -1,36495 | 0,204813 |
| KEGG_ENDOCRINE AND OTHER FACTOR-REGULATED CALCIUM REABSORPTION | 55 | -1,36413 | 0,204835 |
| REACT_CA-DEPENDENT EVENTS | 21 | -1,35546 | 0,214695 |
| REACT_MRNA CAPPING | 21 | -1,34927 | 0,221686 |
| NCL_MYC_PATHWAY | 20 | -1,34382 | 0,227491 |
| NCL_ILK_PATHWAY | 39 | -1,34218 | 0,228471 |
| BIOC_NO2IL12PATHWAY | 15 | -1,3403 | 0,229787 |
| NCL_PI3KPLCTRKPATWAY | 32 | -1,33914 | 0,23023 |
| REACT_FORMATION OF THE EARLY ELONGATION COMPLEX | 21 | -1,3278 | 0,244622 |
| REACT_COOPERATION OF PREFOLDIN AND TRIC_CCT IN ACTIN AND TUBULIN FOLDING | 21 | -1,32529 | 0,247185 |

Only the significant downregulated gene sets are shown here (FDR<0.25).

8. Literature

Aagaard, K., J. Ma, K. M. Antony, R. Ganu, J. Petrosino and J. Versalovic (2014). "The placenta harbors a unique microbiome." Sci Transl Med **6**(237): 237ra265.

Aagaard, K. M. (2014). "Author response to comment on "the placenta harbors a unique microbiome"." Sci Transl Med **6**(254): 254lr253.

Ackermann, M., B. Stecher, N. E. Freed, P. Songhet, W. D. Hardt and M. Doebeli (2008). "Self-destructive cooperation mediated by phenotypic noise." Nature **454**(7207): 987-990.

Adak, A., C. Maity, K. Ghosh and K. C. Mondal (2014). "Alteration of predominant gastrointestinal flora and oxidative damage of large intestine under simulated hypobaric hypoxia." Z Gastroenterol **52**(2): 180-186.

Aguirre, M., A. Eck, P. H. Savelkoul, A. E. Budding and K. Venema (2015). "Diet drives quick changes in the metabolic activity and composition of human gut microbiota in a validated in vitro gut model." Res Microbiol.

Alemka, A., M. Clyne, F. Shanahan, T. Tompkins, N. Corcionivoschi and B. Bourke (2010). "Probiotic colonization of the adherent mucus layer of HT29MTXE12 cells attenuates *Campylobacter jejuni* virulence properties." Infect Immun **78**(6): 2812-2822.

Allen, R. G., W. P. Lafuse, J. D. Galley, M. M. Ali, B. M. Ahmer and M. T. Bailey (2012). "The intestinal microbiota are necessary for stressor-induced enhancement of splenic macrophage microbicidal activity." Brain Behav Immun **26**(3): 371-382.

Allison, G. E., C. Fremaux and T. R. Klaenhammer (1994). "Expansion of bacteriocin activity and host range upon complementation of two peptides encoded within the lactacin F operon." J Bacteriol **176**(8): 2235-2241.

Altschul, S. F., W. Gish, W. Miller, E. W. Myers and D. J. Lipman (1990). "Basic local alignment search tool." J Mol Biol **215**(3): 403-410.

Amann, R. I., B. J. Binder, R. J. Olson, S. W. Chisholm, R. Devereux and D. A. Stahl (1990). "Combination of 16S rRNA-targeted oligonucleotide probes with flow cytometry for analyzing mixed microbial populations." Appl Environ Microbiol **56**(6): 1919-1925.

Aranki, A. and R. Freter (1972). "Use of anaerobic glove boxes for the cultivation of strictly anaerobic bacteria." Am J Clin Nutr **25**(12): 1329-1334.

Aranki, A., S. A. Syed, E. B. Kenney and R. Freter (1969). "Isolation of anaerobic bacteria from human gingiva and mouse cecum by means of a simplified glove box procedure." Appl Microbiol **17**(4): 568-576.

Asker, N., M. A. Axelsson, S. O. Olofsson and G. C. Hansson (1998). "Dimerization of the human MUC2 mucin in the endoplasmic reticulum is followed by a N-glycosylation-dependent transfer of the mono- and dimers to the Golgi apparatus." J Biol Chem **273**(30): 18857-18863.

Atarashi, K., J. Nishimura, T. Shima, Y. Umesaki, M. Yamamoto, M. Onoue, H. Yagita, N. Ishii, R. Evans, K. Honda and K. Takeda (2008). "ATP drives lamina propria T(H)17 cell differentiation." Nature **455**(7214): 808-812.

Atarashi, K., T. Tanoue, K. Oshima, W. Suda, Y. Nagano, H. Nishikawa, S. Fukuda, T. Saito, S. Narushima, K. Hase, S. Kim, J. V. Fritz, P. Wilmes, S. Ueha, K. Matsushima, H. Ohno, B. Olle, S. Sakaguchi, T. Taniguchi, H. Morita, M. Hattori and K. Honda (2013). "Treg induction by a rationally selected mixture of Clostridia strains from the human microbiota." Nature **500**(7461): 232-236.

Atarashi, K., T. Tanoue, T. Shima, A. Imaoka, T. Kuwahara, Y. Momose, G. Cheng, S. Yamasaki, T. Saito, Y. Ohba, T. Taniguchi, K. Takeda, S. Hori, Ivanov, II, Y. Umesaki, K. Itoh and K. Honda (2011). "Induction of colonic regulatory T cells by indigenous Clostridium species." Science **331**(6015): 337-341.

Ayres, J. S., N. J. Trinidad and R. E. Vance (2012). "Lethal inflammasome activation by a multidrug-resistant pathobiont upon antibiotic disruption of the microbiota." Nat Med.

Aziz, R. K., D. Bartels, A. A. Best, M. DeJongh, T. Disz, R. A. Edwards, K. Formsma, S. Gerdes, E. M. Glass, M. Kubal, F. Meyer, G. J. Olsen, R. Olson, A. L. Osterman, R. A. Overbeek, L. K. McNeil, D. Paarmann, T. Paczian, B. Parrello, G. D. Pusch, C. Reich, R. Stevens, O. Vassieva, V. Vonstein, A. Wilke and O. Zagnitko (2008). "The RAST Server: rapid annotations using subsystems technology." BMC Genomics **9**: 75.

Backhed, F. (2012). "Host responses to the human microbiome." Nutr Rev **70 Suppl 1**: S14-17.

Backhed, F., H. Ding, T. Wang, L. V. Hooper, G. Y. Koh, A. Nagy, C. F. Semenkovich and J. I. Gordon (2004). "The gut microbiota as an environmental factor that regulates fat storage." Proc Natl Acad Sci U S A **101**(44): 15718-15723.

Bajaj, V., C. Hwang and C. A. Lee (1995). "hilA is a novel ompR/toxR family member that activates the expression of Salmonella typhimurium invasion genes." Mol Microbiol **18**(4): 715-727.

Bang, C., K. Weidenbach, T. Gutschmann, H. Heine and R. A. Schmitz (2014). "The intestinal archaea Methanosphaera stadtmanae and Methanobrevibacter smithii activate human dendritic cells." PLoS One **9**(6): e99411.

Bankevich, A., S. Nurk, D. Antipov, A. A. Gurevich, M. Dvorkin, A. S. Kulikov, V. M. Lesin, S. I. Nikolenko, S. Pham, A. D. Prjibelski, A. V. Pyshkin, A. V. Sirotkin, N. Vyahhi, G. Tesler, M. A. Alekseyev and P. A. Pevzner (2012). "SPAdes: a new genome assembly algorithm and its applications to single-cell sequencing." J Comput Biol **19**(5): 455-477.

Bao, Y., Y. Guo, Z. Li, W. Fang, Y. Yang, X. Li, Z. Li, B. Xiong, Z. Chen, J. Wang, K. Kang, D. Gou and W. Yang (2014). "MicroRNA profiling in Muc2 knockout mice of colitis-associated cancer model reveals epigenetic alterations during chronic colitis malignant transformation." PLoS One **9**(6): e99132.

Barthel, M., S. Hapfelmeier, L. Quintanilla-Martinez, M. Kremer, M. Rohde, M. Hogardt, K. Pfeffer, H. Russmann and W. D. Hardt (2003). "Pretreatment of mice with streptomycin provides a *Salmonella enterica* serovar Typhimurium colitis model that allows analysis of both pathogen and host." Infect Immun **71**(5): 2839-2858.

Becker, N., J. Kunath, G. Loh and M. Blaut (2011). "Human intestinal microbiota: characterization of a simplified and stable gnotobiotic rat model." Gut Microbes **2**(1): 25-33.

Bel, S., Y. Elkis, H. Elifantz, O. Koren, R. Ben-Hamo, T. Lerer-Goldshtein, R. Rahimi, S. Ben Horin, A. Nyska, S. Shpungin and U. Nir (2014). "Reprogrammed and transmissible intestinal microbiota confer diminished susceptibility to induced colitis in TMF^{-/-} mice." Proc Natl Acad Sci U S A **111**(13): 4964-4969.

Belzer, C., G. K. Gerber, G. Roeselers, M. Delaney, A. DuBois, Q. Liu, V. Belavusava, V. Yeliseyev, A. Houseman, A. Onderdonk, C. Cavanaugh and L. Bry (2014). "Dynamics of the microbiota in response to host infection." PLoS One **9**(7): e95534.

Berer, K., M. Mues, M. Koutrolos, Z. A. Rasbi, M. Boziki, C. Johner, H. Wekerle and G. Krishnamoorthy (2011). "Commensal microbiota and myelin autoantigen cooperate to trigger autoimmune demyelination." Nature.

Berg, R. D. (1996). "The indigenous gastrointestinal microflora." Trends Microbiol **4**(11): 430-435.

Bergstrom, J. H., K. A. Berg, A. M. Rodriguez-Pineiro, B. Stecher, M. E. Johansson and G. C. Hansson (2014). "AGR2, an endoplasmic reticulum protein, is secreted into the gastrointestinal mucus." PLoS One **9**(8): e104186.

Bergstrom, K. S., V. Kisson-Singh, D. L. Gibson, C. Ma, M. Montero, H. P. Sham, N. Ryz, T. Huang, A. Velcich, B. B. Finlay, K. Chadee and B. A. Vallance (2010). "Muc2 protects against lethal infectious colitis by disassociating pathogenic and commensal bacteria from the colonic mucosa." PLoS Pathog **6**(5): e1000902.

Berry, D., C. Schwab, G. Milinovich, J. Reichert, K. Ben Mahfoudh, T. Decker, M. Engel, B. Hai, E. Hainzl, S. Heider, L. Kenner, M. Muller, I. Rauch, B. Strobl, M. Wagner, C. Schleper, T. Urich and A. Loy (2012). "Phylotype-level 16S rRNA analysis reveals new bacterial indicators of health state in acute murine colitis." ISME J **6**(11): 2091-2106.

Berry, D., B. Stecher, A. Schintlmeister, J. Reichert, S. Brugiroux, B. Wild, W. Wanek, A. Richter, I. Rauch, T. Decker, A. Loy and M. Wagner (2013). "Host-compound foraging by intestinal microbiota revealed by single-cell stable isotope probing." Proc Natl Acad Sci U S A **110**(12): 4720-4725.

- Bibiloni, R. (2012). "Rodent models to study the relationships between mammals and their bacterial inhabitants." Gut Microbes **3**(6): 536-543.
- Bleich, A. and A. K. Hansen (2012). "Time to include the gut microbiota in the hygienic standardisation of laboratory rodents." Comp Immunol Microbiol Infect Dis **35**(2): 81-92.
- Boisvert, S., F. Raymond, E. Godzaridis, F. Laviolette and J. Corbeil (2012). "Ray Meta: scalable de novo metagenome assembly and profiling." Genome Biol **13**(12): R122.
- Bouskra, D., C. Brezillon, M. Berard, C. Werts, R. Varona, I. G. Boneca and G. Eberl (2008). "Lymphoid tissue genesis induced by commensals through NOD1 regulates intestinal homeostasis." Nature **456**(7221): 507-510.
- Brandl, K., G. Plitas, C. N. Mihu, C. Ubeda, T. Jia, M. Fleisher, B. Schnabl, R. P. DeMatteo and E. G. Pamer (2008). "Vancomycin-resistant enterococci exploit antibiotic-induced innate immune deficits." Nature **455**(7214): 804-807.
- Brown, J., W. M. de Vos, P. S. DiStefano, J. Dore, C. Huttenhower, R. Knight, T. D. Lawley, J. Raes and P. Turnbaugh (2013). "Translating the human microbiome." Nat Biotechnol **31**(4): 304-308.
- Buffie, C. G., V. Bucci, R. R. Stein, P. T. McKenney, L. Ling, A. Gobourne, D. No, H. Liu, M. Kinnebrew, A. Viale, E. Littmann, M. R. van den Brink, R. R. Jenq, Y. Taur, C. Sander, J. R. Cross, N. C. Toussaint, J. B. Xavier and E. G. Pamer (2015). "Precision microbiome reconstitution restores bile acid mediated resistance to *Clostridium difficile*." Nature **517**(7533): 205-208.
- Bultman, S. J. and C. Jobin (2014). "Microbial-derived butyrate: an oncometabolite or tumor-suppressive metabolite?" Cell Host Microbe **16**(2): 143-145.
- Cameron, A. D. and C. J. Dorman (2012). "A fundamental regulatory mechanism operating through OmpR and DNA topology controls expression of *Salmonella* pathogenicity islands SPI-1 and SPI-2." PLoS Genet **8**(3): e1002615.
- Caporaso, J. G., J. Kuczynski, J. Stombaugh, K. Bittinger, F. D. Bushman, E. K. Costello, N. Fierer, A. G. Pena, J. K. Goodrich, J. I. Gordon, G. A. Huttley, S. T. Kelley, D. Knights, J. E. Koenig, R. E. Ley, C. A. Lozupone, D. McDonald, B. D. Muegge, M. Pirrung, J. Reeder, J. R. Sevinsky, P. J. Turnbaugh, W. A. Walters, J. Widmann, T. Yatsunenko, J. Zaneveld and R. Knight (2010). "QIIME allows analysis of high-throughput community sequencing data." Nat Methods **7**(5): 335-336.
- Carmody, R. N., G. K. Gerber, J. M. Luevano, Jr., D. M. Gatti, L. Somes, K. L. Svenson and P. J. Turnbaugh (2015). "Diet dominates host genotype in shaping the murine gut microbiota." Cell Host Microbe **17**(1): 72-84.
- Cash, H. L., C. V. Whitham, C. L. Behrendt and L. V. Hooper (2006). "Symbiotic bacteria direct expression of an intestinal bactericidal lectin." Science **313**(5790): 1126-1130.

Caspari, D. and J. M. Macy (1983). "The role of carbon dioxide in glucose metabolism of *Bacteroides fragilis*." Arch Microbiol **135**(1): 16-24.

Cha, H. R., S. Y. Chang, J. H. Chang, J. O. Kim, J. Y. Yang, C. H. Kim and M. N. Kweon (2010). "Downregulation of Th17 cells in the small intestine by disruption of gut flora in the absence of retinoic acid." J Immunol **184**(12): 6799-6806.

Chakravorty, S., D. Helb, M. Burday, N. Connell and D. Alland (2007). "A detailed analysis of 16S ribosomal RNA gene segments for the diagnosis of pathogenic bacteria." J Microbiol Methods **69**(2): 330-339.

Cheng, H. and M. Bjerknes (1983). "Cell production in mouse intestinal epithelium measured by stathmokinetic flow cytometry and Coulter particle counting." Anat Rec **207**(3): 427-434.

Chung, H., S. J. Pamp, J. A. Hill, N. K. Surana, S. M. Edelman, E. B. Troy, N. C. Reading, E. J. Villablanca, S. Wang, J. R. Mora, Y. Umesaki, D. Mathis, C. Benoist, D. A. Relman and D. L. Kasper (2012). "Gut immune maturation depends on colonization with a host-specific microbiota." Cell **149**(7): 1578-1593.

Clavel, T., G. Henderson, W. Engst, J. Dore and M. Blaut (2006). "Phylogeny of human intestinal bacteria that activate the dietary lignan secoisolariciresinol diglucoside." FEMS Microbiol Ecol **55**(3): 471-478.

Coghill, S. B., D. Hopwood, S. McPherson and S. Hislop (1983). "The ultrastructural localisation of De-Nol (colloidal tripotassium dicitrato-bismuthate--TDB) in the upper gastrointestinal tract of man and rodents following oral and instrumental administration." J Pathol **139**(2): 105-114.

Connon, S. A. and S. J. Giovannoni (2002). "High-throughput methods for culturing microorganisms in very-low-nutrient media yield diverse new marine isolates." Appl Environ Microbiol **68**(8): 3878-3885.

Cordonnier, C., G. Le Bihan, J. G. Emond-Rheault, A. Garrivier, J. Harel and G. Jubelin (2016). "Vitamin B12 Uptake by the Gut Commensal Bacteria *Bacteroides thetaiotaomicron* Limits the Production of Shiga Toxin by Enterohemorrhagic *Escherichia coli*." Toxins (Basel) **8**(1).

Croswell, A., E. Amir, P. Tegatz, M. Barman and N. H. Salzman (2009). "Prolonged impact of antibiotics on intestinal microbial ecology and susceptibility to enteric *Salmonella* infection." Infect Immun **77**(7): 2741-2753.

Daims, H., A. Bruhl, R. Amann, K. H. Schleifer and M. Wagner (1999). "The domain-specific probe EUB338 is insufficient for the detection of all Bacteria: development and evaluation of a more comprehensive probe set." Syst Appl Microbiol **22**(3): 434-444.

Daims, H., S. Lucker and M. Wagner (2006). "daime, a novel image analysis program for microbial ecology and biofilm research." Environ Microbiol **8**(2): 200-213.

Daims, H., K. Stoecker and M. Wagner (2005). Advanced Methods in Molecular Microbial Ecology, eds Osborn A, Smith C: 213-239.

Day, D. W., B. K. Mandal and B. C. Morson (1978). "The rectal biopsy appearances in Salmonella colitis." Histopathology **2**(2): 117-131.

Degnan, P. H., N. A. Barry, K. C. Mok, M. E. Taga and A. L. Goodman (2014). "Human gut microbes use multiple transporters to distinguish vitamin B(1)(2) analogs and compete in the gut." Cell Host Microbe **15**(1): 47-57.

Demaneche, S., H. Sanguin, J. Pote, E. Navarro, D. Bernillon, P. Mavingui, W. Wildi, T. M. Vogel and P. Simonet (2008). "Antibiotic-resistant soil bacteria in transgenic plant fields." Proc Natl Acad Sci U S A **105**(10): 3957-3962.

Deriu, E., J. Z. Liu, M. Pezeshki, R. A. Edwards, R. J. Ochoa, H. Contreras, S. J. Libby, F. C. Fang and M. Raffatellu (2013). "Probiotic bacteria reduce salmonella typhimurium intestinal colonization by competing for iron." Cell Host Microbe **14**(1): 26-37.

Derrien, M., M. C. Collado, K. Ben-Amor, S. Salminen and W. M. de Vos (2008). "The Mucin degrader *Akkermansia muciniphila* is an abundant resident of the human intestinal tract." Appl Environ Microbiol **74**(5): 1646-1648.

Derrien, M., E. E. Vaughan, C. M. Plugge and W. M. de Vos (2004). "*Akkermansia muciniphila* gen. nov., sp. nov., a human intestinal mucin-degrading bacterium." Int J Syst Evol Microbiol **54**(Pt 5): 1469-1476.

DeSantis, T. Z., I. Dubosarskiy, S. R. Murray and G. L. Andersen (2003). "Comprehensive aligned sequence construction for automated design of effective probes (CASCADE-P) using 16S rDNA." Bioinformatics **19**(12): 1461-1468.

Dewhurst, F. E., C. C. Chien, B. J. Paster, R. L. Ericson, R. P. Orcutt, D. B. Schauer and J. G. Fox (1999). "Phylogeny of the defined murine microbiota: altered Schaedler flora." Appl Environ Microbiol **65**(8): 3287-3292.

Dominguez-Bello, M. G., E. K. Costello, M. Contreras, M. Magris, G. Hidalgo, N. Fierer and R. Knight (2010). "Delivery mode shapes the acquisition and structure of the initial microbiota across multiple body habitats in newborns." Proc Natl Acad Sci U S A **107**(26): 11971-11975.

Donohoe, D. R., L. B. Collins, A. Wali, R. Bigler, W. Sun and S. J. Bultman (2012). "The Warburg effect dictates the mechanism of butyrate-mediated histone acetylation and cell proliferation." Mol Cell **48**(4): 612-626.

Donohoe, D. R., D. Holley, L. B. Collins, S. A. Montgomery, A. C. Whitmore, A. Hillhouse, K. P. Curry, S. W. Renner, A. Greenwalt, E. P. Ryan, V. Godfrey, M. T. Heise, D. S. Threadgill, A. Han, J. A. Swenberg, D. W. Threadgill and S. J. Bultman (2014). "A gnotobiotic mouse model demonstrates that dietary fiber protects against colorectal tumorigenesis in a microbiota- and butyrate-dependent manner." Cancer Discov **4**(12): 1387-1397.

Durant, J. A., D. E. Corrier and S. C. Ricke (2000). "Short-chain volatile fatty acids modulate the expression of the hilA and invF genes of Salmonella typhimurium." J Food Prot **63**(5): 573-578.

Durant, J. A., D. E. Corrier, L. H. Stanker and S. C. Ricke (2000). "Expression of the hilA Salmonella typhimurium gene in a poultry Salm. enteritidis isolate in response to lactate and nutrients." J Appl Microbiol **89**(1): 63-69.

Earle, K. A., G. Billings, M. Sigal, J. S. Lichtman, G. C. Hansson, J. E. Elias, M. R. Amieva, K. C. Huang and J. L. Sonnenburg (2015). "Quantitative Imaging of Gut Microbiota Spatial Organization." Cell Host Microbe **18**(4): 478-488.

Eckburg, P. B., E. M. Bik, C. N. Bernstein, E. Purdom, L. Dethlefsen, M. Sargent, S. R. Gill, K. E. Nelson and D. A. Relman (2005). "Diversity of the human intestinal microbial flora." Science **308**(5728): 1635-1638.

Edgar, R. C., B. J. Haas, J. C. Clemente, C. Quince and R. Knight (2011). "UCHIME improves sensitivity and speed of chimera detection." Bioinformatics **27**(16): 2194-2200.

Endt, K., B. Stecher, S. Chaffron, E. Slack, N. Tchitchek, A. Benecke, L. Van Maele, J. C. Sirard, A. J. Mueller, M. Heikenwalder, A. J. Macpherson, R. Strugnell, C. von Mering and W. D. Hardt (2010). "The microbiota mediates pathogen clearance from the gut lumen after non-typhoidal Salmonella diarrhea." PLoS Pathog **6**(9).

Eri, R. D., R. J. Adams, T. V. Tran, H. Tong, I. Das, D. K. Roche, I. Oancea, C. W. Png, P. L. Jeffery, G. L. Radford-Smith, M. C. Cook, T. H. Florin and M. A. McGuckin (2011). "An intestinal epithelial defect conferring ER stress results in inflammation involving both innate and adaptive immunity." Mucosal Immunol **4**(3): 354-364.

Fabrega, A. and J. Vila (2013). "Salmonella enterica serovar Typhimurium skills to succeed in the host: virulence and regulation." Clin Microbiol Rev **26**(2): 308-341.

Faith, J. J., P. P. Ahern, V. K. Ridaura, J. Cheng and J. I. Gordon (2014). "Identifying gut microbe-host phenotype relationships using combinatorial communities in gnotobiotic mice." Sci Transl Med **6**(220): 220ra211.

Faith, J. J., N. P. McNulty, F. E. Rey and J. I. Gordon (2011). "Predicting a human gut microbiota's response to diet in gnotobiotic mice." Science **333**(6038): 101-104.

Falk, P. G., L. V. Hooper, T. Midtvedt and J. I. Gordon (1998). "Creating and maintaining the gastrointestinal ecosystem: what we know and need to know from gnotobiology." Microbiol Mol Biol Rev **62**(4): 1157-1170.

Ferrand, J., K. Patron, C. Legrand-Frossi, J. P. Fripiat, C. Merlin, C. Alauzet and A. Lozniewski (2014). "Comparison of seven methods for extraction of bacterial DNA from fecal and cecal samples of mice." J Microbiol Methods **105C**: 180-185.

- Figueira, R. and D. W. Holden (2012). "Functions of the Salmonella pathogenicity island 2 (SPI-2) type III secretion system effectors." Microbiology **158**(Pt 5): 1147-1161.
- Flint, H. J. (2012). "Microbiology: Antibiotics and adiposity." Nature **488**(7413): 601-602.
- Flint, H. J., K. P. Scott, S. H. Duncan, P. Louis and E. Forano (2012). "Microbial degradation of complex carbohydrates in the gut." Gut Microbes **3**(4): 289-306.
- Fodor, A. A., T. Z. DeSantis, K. M. Wylie, J. H. Badger, Y. Ye, T. Hepburn, P. Hu, E. Sodergren, K. Liolios, H. Huot-Creasy, B. W. Birren and A. M. Earl (2012). "The "most wanted" taxa from the human microbiome for whole genome sequencing." PLoS One **7**(7): e41294.
- Fournier, P. E., J. C. Lagier, G. Dubourg and D. Raoult (2015). "From culturomics to taxonomogenomics: A need to change the taxonomy of prokaryotes in clinical microbiology." Anaerobe **36**: 73-78.
- Franzosa, E. A., X. C. Morgan, N. Segata, L. Waldron, J. Reyes, A. M. Earl, G. Giannoukos, M. R. Boylan, D. Ciulla, D. Gevers, J. Izard, W. S. Garrett, A. T. Chan and C. Huttenhower (2014). "Relating the metatranscriptome and metagenome of the human gut." Proc Natl Acad Sci U S A **111**(22): E2329-2338.
- Frese, S. A., A. K. Benson, G. W. Tannock, D. M. Loach, J. Kim, M. Zhang, P. L. Oh, N. C. Heng, P. B. Patil, N. Juge, D. A. Mackenzie, B. M. Pearson, A. Lapidus, E. Dalin, H. Tice, E. Goltsman, M. Land, L. Hauser, N. Ivanova, N. C. Kyrpides and J. Walter (2011). "The evolution of host specialization in the vertebrate gut symbiont *Lactobacillus reuteri*." PLoS Genet **7**(2): e1001314.
- Freter, R., H. Brickner, J. Fekete, M. M. Vickerman and K. E. Carey (1983). "Survival and implantation of *Escherichia coli* in the intestinal tract." Infect Immun **39**(2): 686-703.
- Fukuda, S., H. Toh, K. Hase, K. Oshima, Y. Nakanishi, K. Yoshimura, T. Tobe, J. M. Clarke, D. L. Topping, T. Suzuki, T. D. Taylor, K. Itoh, J. Kikuchi, H. Morita, M. Hattori and H. Ohno (2011). "Bifidobacteria can protect from enteropathogenic infection through production of acetate." Nature **469**(7331): 543-547.
- Gagnon, M., P. Savard, A. Riviere, G. LaPointe and D. Roy (2015). "Bioaccessible antioxidants in milk fermented by *Bifidobacterium longum* subsp. *longum* strains." Biomed Res Int **2015**: 169381.
- Galan, J. E. and R. Curtiss, 3rd (1990). "Expression of *Salmonella typhimurium* genes required for invasion is regulated by changes in DNA supercoiling." Infect Immun **58**(6): 1879-1885.
- Ganesh, B. P., R. Klopffleisch, G. Loh and M. Blaut (2013). "Commensal *Akkermansia muciniphila* exacerbates gut inflammation in *Salmonella Typhimurium*-infected gnotobiotic mice." PLoS One **8**(9): e74963.
- Garcia-del Portillo, F., J. W. Foster, M. E. Maguire and B. B. Finlay (1992). "Characterization of the micro-environment of *Salmonella typhimurium*-containing vacuoles within MDCK epithelial cells." Mol Microbiol **6**(22): 3289-3297.

Garcia-del Portillo, F., M. B. Zwick, K. Y. Leung and B. B. Finlay (1993). "Salmonella induces the formation of filamentous structures containing lysosomal membrane glycoproteins in epithelial cells." Proc Natl Acad Sci U S A **90**(22): 10544-10548.

Garvis, S. G., C. R. Beuzon and D. W. Holden (2001). "A role for the PhoP/Q regulon in inhibition of fusion between lysosomes and Salmonella-containing vacuoles in macrophages." Cell Microbiol **3**(11): 731-744.

Gaudier, E., A. Jarry, H. M. Blottiere, P. de Coppet, M. P. Buisine, J. P. Aubert, C. Laboisse, C. Cherbut and C. Hoebler (2004). "Butyrate specifically modulates MUC gene expression in intestinal epithelial goblet cells deprived of glucose." Am J Physiol Gastrointest Liver Physiol **287**(6): G1168-1174.

Gaudier, E., M. Rival, M. P. Buisine, I. Robineau and C. Hoebler (2009). "Butyrate enemas upregulate Muc genes expression but decrease adherent mucus thickness in mice colon." Physiol Res **58**(1): 111-119.

Ge, Z., Y. Feng, N. S. Taylor, M. Ohtani, M. F. Polz, D. B. Schauer and J. G. Fox (2006). "Colonization dynamics of altered Schaedler flora is influenced by gender, aging, and Helicobacter hepaticus infection in the intestines of Swiss Webster mice." Appl Environ Microbiol **72**(7): 5100-5103.

Gerlach, R. G., D. Jackel, N. Geymeier and M. Hensel (2007). "Salmonella pathogenicity island 4-mediated adhesion is coregulated with invasion genes in Salmonella enterica." Infect Immun **75**(10): 4697-4709.

Geuking, M. B., J. Cahenzli, M. A. Lawson, D. C. Ng, E. Slack, S. Hapfelmeier, K. D. McCoy and A. J. Macpherson (2011). "Intestinal bacterial colonization induces mutualistic regulatory T cell responses." Immunity **34**(5): 794-806.

Gill, S. R., M. Pop, R. T. Deboy, P. B. Eckburg, P. J. Turnbaugh, B. S. Samuel, J. I. Gordon, D. A. Relman, C. M. Fraser-Liggett and K. E. Nelson (2006). "Metagenomic analysis of the human distal gut microbiome." Science **312**(5778): 1355-1359.

Goddard, A. F. (1998). "Review article: factors influencing antibiotic transfer across the gastric mucosa." Aliment Pharmacol Ther **12**(12): 1175-1184.

Godl, K., M. E. Johansson, M. E. Lidell, M. Morgelin, H. Karlsson, F. J. Olson, J. R. Gum, Jr., Y. S. Kim and G. C. Hansson (2002). "The N terminus of the MUC2 mucin forms trimers that are held together within a trypsin-resistant core fragment." J Biol Chem **277**(49): 47248-47256.

Goodman, A. L., G. Kallstrom, J. J. Faith, A. Reyes, A. Moore, G. Dantas and J. I. Gordon (2011). "From the Cover: Extensive personal human gut microbiota culture collections characterized and manipulated in gnotobiotic mice." Proc Natl Acad Sci U S A **108**(15): 6252-6257.

Goodman, A. L., N. P. McNulty, Y. Zhao, D. Leip, R. D. Mitra, C. A. Lozupone, R. Knight and J. I. Gordon (2009). "Identifying genetic determinants needed to establish a human gut symbiont in its habitat." Cell Host Microbe **6**(3): 279-289.

Goodrich, J. K., J. L. Waters, A. C. Poole, J. L. Sutter, O. Koren, R. Blekhman, M. Beaumont, W. Van Treuren, R. Knight, J. T. Bell, T. D. Spector, A. G. Clark and R. E. Ley (2014). "Human genetics shape the gut microbiome." Cell **159**(4): 789-799.

Gradel, K. O., H. L. Nielsen, H. C. Schonheyder, T. Ejlersen, B. Kristensen and H. Nielsen (2009). "Increased short- and long-term risk of inflammatory bowel disease after salmonella or campylobacter gastroenteritis." Gastroenterology **137**(2): 495-501.

Greene, J. D. and T. R. Klaenhammer (1994). "Factors involved in adherence of lactobacilli to human Caco-2 cells." Appl Environ Microbiol **60**(12): 4487-4494.

Gronbach, K., I. Flade, O. Holst, B. Lindner, H. J. Ruscheweyh, A. Wittmann, S. Menz, A. Schwartz, P. Adam, B. Stecher, C. Josenhans, S. Suerbaum, A. D. Gruber, A. Kulik, D. Huson, I. B. Autenrieth and J. S. Frick (2014). "Endotoxicity of lipopolysaccharide as a determinant of T-cell-mediated colitis induction in mice." Gastroenterology **146**(3): 765-775.

Gum, J. R., Jr., J. W. Hicks, N. W. Toribara, B. Siddiki and Y. S. Kim (1994). "Molecular cloning of human intestinal mucin (MUC2) cDNA. Identification of the amino terminus and overall sequence similarity to prepro-von Willebrand factor." J Biol Chem **269**(4): 2440-2446.

Gupta, A., D. Wodziak, M. Tun, D. M. Bouley and A. W. Lowe (2013). "Loss of anterior gradient 2 (Agr2) expression results in hyperplasia and defective lineage maturation in the murine stomach." J Biol Chem **288**(6): 4321-4333.

Gurevich, A., V. Saveliev, N. Vyahhi and G. Tesler (2013). "QUAST: quality assessment tool for genome assemblies." Bioinformatics **29**(8): 1072-1075.

Hagesaether, E., E. Christiansen, M. E. Due-Hansen and T. Ulven (2013). "Mucus can change the permeation rank order of drug candidates." Int J Pharm **452**(1-2): 276-282.

Hamer, H. M., D. M. Jonkers, I. B. Renes, S. A. Vanhoutvin, A. Kodde, F. J. Troost, K. Venema and R. J. Brummer (2010). "Butyrate enemas do not affect human colonic MUC2 and TFF3 expression." Eur J Gastroenterol Hepatol **22**(9): 1134-1140.

Hansson, G. C. (2012). "Role of mucus layers in gut infection and inflammation." Curr Opin Microbiol **15**(1): 57-62.

Hapfelmeier, S., K. Ehrbar, B. Stecher, M. Barthel, M. Kremer and W. D. Hardt (2004). "Role of the Salmonella pathogenicity island 1 effector proteins SipA, SopB, SopE, and SopE2 in Salmonella enterica subspecies I serovar Typhimurium colitis in streptomycin-pretreated mice." Infect Immun **72**(2): 795-809.

Hapfelmeier, S. and W. D. Hardt (2005). "A mouse model for S. typhimurium-induced enterocolitis." Trends Microbiol **13**(10): 497-503.

Hapfelmeier, S., M. A. Lawson, E. Slack, J. K. Kirundi, M. Stoel, M. Heikenwalder, J. Cahenzli, Y. Velykoredko, M. L. Balmer, K. Endt, M. B. Geuking, R. Curtiss, 3rd, K. D. McCoy and A. J. Macpherson

(2010). "Reversible microbial colonization of germ-free mice reveals the dynamics of IgA immune responses." Science **328**(5986): 1705-1709.

Hapfelmeier, S., B. Stecher, M. Barthel, M. Kremer, A. J. Muller, M. Heikenwalder, T. Stallmach, M. Hensel, K. Pfeffer, S. Akira and W. D. Hardt (2005). "The Salmonella pathogenicity island (SPI)-2 and SPI-1 type III secretion systems allow Salmonella serovar typhimurium to trigger colitis via MyD88-dependent and MyD88-independent mechanisms." J Immunol **174**(3): 1675-1685.

Harmsen, H. J., G. R. Gibson, P. Elfferich, G. C. Raangs, A. C. Wildeboer-Veloo, A. Argaiz, M. B. Roberfroid and G. W. Welling (2000). "Comparison of viable cell counts and fluorescence in situ hybridization using specific rRNA-based probes for the quantification of human fecal bacteria." FEMS Microbiol Lett **183**(1): 125-129.

Harris, N. R., P. R. Carter, A. S. Yadav, M. N. Watts, S. Zhang, M. Kosloski-Davidson and M. B. Grisham (2011). "Relationship between inflammation and tissue hypoxia in a mouse model of chronic colitis." Inflamm Bowel Dis **17**(3): 742-746.

Hasegawa, M., N. Kamada, Y. Jiao, M. Z. Liu, G. Nunez and N. Inohara (2012). "Protective role of commensals against Clostridium difficile infection via an IL-1beta-mediated positive-feedback loop." J Immunol **189**(6): 3085-3091.

Hautefort, I., M. J. Proenca and J. C. Hinton (2003). "Single-copy green fluorescent protein gene fusions allow accurate measurement of Salmonella gene expression in vitro and during infection of mammalian cells." Appl Environ Microbiol **69**(12): 7480-7491.

Hayashi, H., M. Sakamoto and Y. Benno (2002). "Phylogenetic analysis of the human gut microbiota using 16S rDNA clone libraries and strictly anaerobic culture-based methods." Microbiol Immunol **46**(8): 535-548.

Heazlewood, C. K., M. C. Cook, R. Eri, G. R. Price, S. B. Tauro, D. Taupin, D. J. Thornton, C. W. Png, T. L. Crockford, R. J. Cornall, R. Adams, M. Kato, K. A. Nelms, N. A. Hong, T. H. Florin, C. C. Goodnow and M. A. McGuckin (2008). "Aberrant mucin assembly in mice causes endoplasmic reticulum stress and spontaneous inflammation resembling ulcerative colitis." PLoS Med **5**(3): e54.

Helaine, S., A. M. Cheverton, K. G. Watson, L. M. Faure, S. A. Matthews and D. W. Holden (2014). "Internalization of Salmonella by macrophages induces formation of nonreplicating persisters." Science **343**(6167): 204-208.

Higa, A., A. Mulot, F. Delom, M. Bouhcareilh, D. T. Nguyen, D. Boismenu, M. J. Wise and E. Chevet (2011). "Role of pro-oncogenic protein disulfide isomerase (PDI) family member anterior gradient 2 (AGR2) in the control of endoplasmic reticulum homeostasis." J Biol Chem **286**(52): 44855-44868.

Hill, D. A., M. C. Siracusa, M. C. Abt, B. S. Kim, D. Kobuley, M. Kubo, T. Kambayashi, D. F. Larosa, E. D. Renner, J. S. Orange, F. D. Bushman and D. Artis (2012). "Commensal bacteria-derived signals regulate basophil hematopoiesis and allergic inflammation." Nat Med **18**(4): 538-546.

- Hoffmann, C., D. A. Hill, N. Minkah, T. Kirn, A. Troy, D. Artis and F. Bushman (2009). "Community-wide response of the gut microbiota to enteropathogenic *Citrobacter rodentium* infection revealed by deep sequencing." *Infect Immun* **77**(10): 4668-4678.
- Hoiseh, S. K. and B. A. Stocker (1981). "Aromatic-dependent *Salmonella typhimurium* are non-virulent and effective as live vaccines." *Nature* **291**(5812): 238-239.
- Hong, X. Y., J. Wang and Z. Li (2013). "AGR2 expression is regulated by HIF-1 and contributes to growth and angiogenesis of glioblastoma." *Cell Biochem Biophys* **67**(3): 1487-1495.
- Hooper, L. V., J. Xu, P. G. Falk, T. Midtvedt and J. I. Gordon (1999). "A molecular sensor that allows a gut commensal to control its nutrient foundation in a competitive ecosystem." *Proc Natl Acad Sci U S A* **96**(17): 9833-9838.
- Hoskins, L. C., M. Agustines, W. B. McKee, E. T. Boulding, M. Kriaris and G. Niedermeyer (1985). "Mucin degradation in human colon ecosystems. Isolation and properties of fecal strains that degrade ABH blood group antigens and oligosaccharides from mucin glycoproteins." *J Clin Invest* **75**(3): 944-953.
- Hsiao, A., A. M. Ahmed, S. Subramanian, N. W. Griffin, L. L. Drewry, W. A. Petri, R. Haque, T. Ahmed and J. I. Gordon (2014). "Members of the human gut microbiota involved in recovery from *Vibrio cholerae* infection." *Nature* **515**(7527): 423-426.
- Huang, J. Y., S. M. Lee and S. K. Mazmanian (2011). "The human commensal *Bacteroides fragilis* binds intestinal mucin." *Anaerobe*.
- Hudault, S., J. Guignot and A. L. Servin (2001). "Escherichia coli strains colonising the gastrointestinal tract protect germfree mice against *Salmonella typhimurium* infection." *Gut* **49**(1): 47-55.
- Hugon, P., J. C. Lagier, C. Robert, C. Lepolard, L. Papazian, D. Musso, B. Vialettes and D. Raoult (2013). "Molecular studies neglect apparently gram-negative populations in the human gut microbiota." *J Clin Microbiol* **51**(10): 3286-3293.
- Hutter, G., U. Schlagenhauf, G. Valenza, M. Horn, S. Burgemeister, H. Claus and U. Vogel (2003). "Molecular analysis of bacteria in periodontitis: evaluation of clone libraries, novel phylotypes and putative pathogens." *Microbiology* **149**(Pt 1): 67-75.
- Hyatt, D., G. L. Chen, P. F. Locascio, M. L. Land, F. W. Larimer and L. J. Hauser (2010). "Prodigal: prokaryotic gene recognition and translation initiation site identification." *BMC Bioinformatics* **11**: 119.
- Hyatt, D., P. F. LoCasio, L. J. Hauser and E. C. Uberbacher (2012). "Gene and translation initiation site prediction in metagenomic sequences." *Bioinformatics* **28**(17): 2223-2230.
- Inagaki, H., T. Suzuki, K. Nomoto and Y. Yoshikai (1996). "Increased susceptibility to primary infection with *Listeria monocytogenes* in germfree mice may be due to lack of accumulation of L-selectin+ CD44+ T cells in sites of inflammation." *Infect Immun* **64**(8): 3280-3287.

Itoh, K. and R. Freter (1989). "Control of *Escherichia coli* populations by a combination of indigenous clostridia and lactobacilli in gnotobiotic mice and continuous-flow cultures." *Infect Immun* **57**(2): 559-565.

Itoh, K. and T. Mitsuoka (1985). "Characterization of clostridia isolated from faeces of limited flora mice and their effect on caecal size when associated with germ-free mice." *Lab Anim* **19**(2): 111-118.

Jakobsson, H. E., A. M. Rodriguez-Pineiro, A. Schutte, A. Ermund, P. Boysen, M. Bemark, F. Sommer, F. Backhed, G. C. Hansson and M. E. Johansson (2015). "The composition of the gut microbiota shapes the colon mucus barrier." *EMBO Rep* **16**(2): 164-177.

JCVI (2013). "ENA: Experiment SRX313003. [Online] Available at: <http://www.ebi.ac.uk/ena/data/view/SRX313003> [Accessed October 2014]."

Johansson, M. E., D. Ambort, T. Pelaseyed, A. Schutte, J. K. Gustafsson, A. Ermund, D. B. Subramani, J. M. Holmen-Larsson, K. A. Thomsson, J. H. Bergstrom, S. van der Post, A. M. Rodriguez-Pineiro, H. Sjovall, M. Backstrom and G. C. Hansson (2011). "Composition and functional role of the mucus layers in the intestine." *Cell Mol Life Sci* **68**(22): 3635-3641.

Johansson, M. E., J. K. Gustafsson, K. E. Sjoberg, J. Petersson, L. Holm, H. Sjovall and G. C. Hansson (2010). "Bacteria penetrate the inner mucus layer before inflammation in the dextran sulfate colitis model." *PLoS One* **5**(8): e12238.

Johansson, M. E. and G. C. Hansson (2012). "Preservation of mucus in histological sections, immunostaining of mucins in fixed tissue, and localization of bacteria with FISH." *Methods Mol Biol* **842**: 229-235.

Johansson, M. E., H. E. Jakobsson, J. Holmen-Larsson, A. Schutte, A. Ermund, A. M. Rodriguez-Pineiro, L. Arike, C. Wising, F. Svensson, F. Backhed and G. C. Hansson (2015). "Normalization of Host Intestinal Mucus Layers Requires Long-Term Microbial Colonization." *Cell Host Microbe* **18**(5): 582-592.

Johansson, M. E., J. M. Larsson and G. C. Hansson (2011). "The two mucus layers of colon are organized by the MUC2 mucin, whereas the outer layer is a legislator of host-microbial interactions." *Proc Natl Acad Sci U S A* **108 Suppl 1**: 4659-4665.

Johansson, M. E., M. Phillipson, J. Petersson, A. Velcich, L. Holm and G. C. Hansson (2008). "The inner of the two Muc2 mucin-dependent mucus layers in colon is devoid of bacteria." *Proc Natl Acad Sci U S A* **105**(39): 15064-15069.

Johansson, M. E., K. A. Thomsson and G. C. Hansson (2009). "Proteomic analyses of the two mucus layers of the colon barrier reveal that their main component, the Muc2 mucin, is strongly bound to the Fcgbp protein." *J Proteome Res* **8**(7): 3549-3557.

Jump, R. L., A. Polinkovsky, K. Hurlless, B. Sitzlar, K. Eckart, M. Tomas, A. Deshpande, M. M. Nerandzic and C. J. Donskey (2014). "Metabolomics analysis identifies intestinal microbiota-derived biomarkers of colonization resistance in clindamycin-treated mice." PLoS One **9**(7): e101267.

Kaeberlein, T., K. Lewis and S. S. Epstein (2002). "Isolating "uncultivable" microorganisms in pure culture in a simulated natural environment." Science **296**(5570): 1127-1129.

Kaiser, P., M. Diard, B. Stecher and W. D. Hardt (2012). "The streptomycin mouse model for Salmonella diarrhea: functional analysis of the microbiota, the pathogen's virulence factors, and the host's mucosal immune response." Immunol Rev **245**(1): 56-83.

Kamada, N., Y. G. Kim, H. P. Sham, B. A. Vallance, J. L. Puente, E. C. Martens and G. Nunez (2012). "Regulated Virulence Controls the Ability of a Pathogen to Compete with the Gut Microbiota." Science.

Kanehisa, M., S. Goto, Y. Sato, M. Kawashima, M. Furumichi and M. Tanabe (2014). "Data, information, knowledge and principle: back to metabolism in KEGG." Nucleic Acids Res **42**(Database issue): D199-205.

Keeney, K. M. and B. B. Finlay (2013). "Microbiology: EHEC Downregulates Virulence in Response to Intestinal Fucose." Curr Biol **23**(3): R108-110.

Kelly, A., M. D. Goldberg, R. K. Carroll, V. Danino, J. C. Hinton and C. J. Dorman (2004). "A global role for Fis in the transcriptional control of metabolism and type III secretion in Salmonella enterica serovar Typhimurium." Microbiology **150**(Pt 7): 2037-2053.

Kero, J., M. Gissler, M. M. Gronlund, P. Kero, P. Koskinen, E. Hemminki and E. Isolauri (2002). "Mode of delivery and asthma -- is there a connection?" Pediatr Res **52**(1): 6-11.

Kim, O. S., Y. J. Cho, K. Lee, S. H. Yoon, M. Kim, H. Na, S. C. Park, Y. S. Jeon, J. H. Lee, H. Yi, S. Won and J. Chun (2012). "Introducing EzTaxon-e: a prokaryotic 16S rRNA gene sequence database with phylotypes that represent uncultured species." Int J Syst Evol Microbiol **62**(Pt 3): 716-721.

Kittler, J., J. Illingworth and J. Föglein (1985). "Threshold selection based on a simple image statistic." Comp. Vis. Graph. Image Proc.(30): 125-147.

Koenig, J. E., A. Spor, N. Scalfone, A. D. Fricker, J. Stombaugh, R. Knight, L. T. Angenent and R. E. Ley (2011). "Succession of microbial consortia in the developing infant gut microbiome." Proc Natl Acad Sci U S A **108 Suppl 1**: 4578-4585.

Konturek, P. C., D. Haziri, T. Brzozowski, T. Hess, S. Heyman, S. Kwiecien, S. J. Konturek and J. Koziel (2015). "Emerging role of fecal microbiota therapy in the treatment of gastrointestinal and extra-gastrointestinal diseases." J Physiol Pharmacol **66**(4): 483-491.

Koopman, J. P., H. M. Kennis, J. W. Mullink, R. A. Prins, A. M. Stadhouders, H. De Boer and M. P. Hectors (1984). "'Normalization' of germfree mice with anaerobically cultured caecal flora of 'normal' mice." Lab Anim **18**(2): 188-194.

Koren, O., J. K. Goodrich, T. C. Cullender, A. Spor, K. Laitinen, H. K. Backhed, A. Gonzalez, J. J. Werner, L. T. Angenent, R. Knight, F. Backhed, E. Isolauri, S. Salminen and R. E. Ley (2012). "Host remodeling of the gut microbiome and metabolic changes during pregnancy." Cell **150**(3): 470-480.

Koren, O., D. Knights, A. Gonzalez, L. Waldron, N. Segata, R. Knight, C. Huttenhower and R. E. Ley (2013). "A guide to enterotypes across the human body: meta-analysis of microbial community structures in human microbiome datasets." PLoS Comput Biol **9**(1): e1002863.

Kovalev, L. I., S. S. Shishkin, P. Z. Khasigov, N. K. Dzeranov, A. V. Kazachenko, I. Toropygin and S. V. Mamykina (2006). "[Identification of AGR2 protein, a novel potential cancer marker, using proteomics technologies]." Prikl Biokhim Mikrobiol **42**(4): 480-484.

Krych, L., C. H. Hansen, A. K. Hansen, F. W. van den Berg and D. S. Nielsen (2013). "Quantitatively different, yet qualitatively alike: a meta-analysis of the mouse core gut microbiome with a view towards the human gut microbiome." PLoS One **8**(5): e62578.

Krzanowski, W. J. (2000). "Principles of multivariate analysis. A user's perspective." Oxford University Press, Oxford, United Kingdom.

Kumar, P. S., A. L. Griffen, J. A. Barton, B. J. Paster, M. L. Moeschberger and E. J. Leys (2003). "New bacterial species associated with chronic periodontitis." J Dent Res **82**(5): 338-344.

Lagier, J. C., P. Hugon, S. Khelaifia, P. E. Fournier, B. La Scola and D. Raoult (2015). "The rebirth of culture in microbiology through the example of culturomics to study human gut microbiota." Clin Microbiol Rev **28**(1): 237-264.

Lam, L. H. and D. M. Monack (2014). "Intraspecies competition for niches in the distal gut dictate transmission during persistent Salmonella infection." PLoS Pathog **10**(12): e1004527.

Lane, D. J., E. Stackebrandt and M. Goodfellow (1991). "16S/23S rRNA sequencing." Nucleic acid techniques in bacterial systematics: 115-175.

Lange, K., M. Buerger, A. Stallmach and T. Bruns (2016). "Effects of Antibiotics on Gut Microbiota." Dig Dis **34**(3): 260-268.

Langendijk, P. S., F. Schut, G. J. Jansen, G. C. Raangs, G. R. Kamphuis, M. H. Wilkinson and G. W. Welling (1995). "Quantitative fluorescence in situ hybridization of Bifidobacterium spp. with genus-specific 16S rRNA-targeted probes and its application in fecal samples." Appl Environ Microbiol **61**(8): 3069-3075.

LaRock, D. L., A. Chaudhary and S. I. Miller (2015). "Salmonellae interactions with host processes." Nat Rev Microbiol **13**(4): 191-205.

Laukens, D., B. M. Brinkman, J. Raes, M. De Vos and P. Vandenabeele (2015). "Heterogeneity of the gut microbiome in mice: guidelines for optimizing experimental design." FEMS Microbiol Rev.

- Lawhon, S. D., R. Maurer, M. Suyemoto and C. Altier (2002). "Intestinal short-chain fatty acids alter *Salmonella typhimurium* invasion gene expression and virulence through BarA/SirA." Mol Microbiol **46**(5): 1451-1464.
- Lawley, T. D., K. Chan, L. J. Thompson, C. C. Kim, G. R. Govoni and D. M. Monack (2006). "Genome-wide screen for *Salmonella* genes required for long-term systemic infection of the mouse." PLoS Pathog **2**(2): e11.
- Lawley, T. D., S. Clare, A. W. Walker, M. D. Stares, T. R. Connor, C. Raisen, D. Goulding, R. Rad, F. Schreiber, C. Brandt, L. J. Deakin, D. J. Pickard, S. H. Duncan, H. J. Flint, T. G. Clark, J. Parkhill and G. Dougan (2012). "Targeted restoration of the intestinal microbiota with a simple, defined bacteriotherapy resolves relapsing *Clostridium difficile* disease in mice." PLoS Pathog **8**(10): e1002995.
- Lawson, P. A. and F. A. Rainey (2015). "Proposal to restrict the genus *Clostridium* (Prazmowski) to *Clostridium butyricum* and related species." Int J Syst Evol Microbiol.
- Lee, S. M., G. P. Donaldson, Z. Mikulski, S. Boyajian, K. Ley and S. K. Mazmanian (2013). "Bacterial colonization factors control specificity and stability of the gut microbiota." Nature **501**(7467): 426-429.
- Ley, R. E., F. Backhed, P. Turnbaugh, C. A. Lozupone, R. D. Knight and J. I. Gordon (2005). "Obesity alters gut microbial ecology." Proc Natl Acad Sci U S A **102**(31): 11070-11075.
- Ley, R. E., M. Hamady, C. Lozupone, P. J. Turnbaugh, R. R. Ramey, J. S. Bircher, M. L. Schlegel, T. A. Tucker, M. D. Schrenzel, R. Knight and J. I. Gordon (2008). "Evolution of mammals and their gut microbes." Science **320**(5883): 1647-1651.
- Ley, R. E., C. A. Lozupone, M. Hamady, R. Knight and J. I. Gordon (2008). "Worlds within worlds: evolution of the vertebrate gut microbiota." Nat Rev Microbiol **6**(10): 776-788.
- Li, H., J. P. Limenitakis, T. Fuhrer, M. B. Geuing, M. A. Lawson, M. Wyss, S. Brugiroux, I. Keller, J. A. Macpherson, S. Rupp, B. Stolp, J. V. Stein, B. Stecher, U. Sauer, K. D. McCoy and A. J. Macpherson (2015). "The outer mucus layer hosts a distinct intestinal microbial niche." Nat Commun **6**: 8292.
- Li, Z., Z. Wu, H. Chen, Q. Zhu, G. Gao, L. Hu, H. Negi, S. Kamle and D. Li (2015). "Induction of anterior gradient 2 (AGR2) plays a key role in insulin-like growth factor-1 (IGF-1)-induced breast cancer cell proliferation and migration." Med Oncol **32**(6): 577.
- Linnenbrink, M., J. Wang, E. A. Hardouin, S. Kunzel, D. Metzler and J. F. Baines (2013). "The role of biogeography in shaping diversity of the intestinal microbiota in house mice." Mol Ecol **22**(7): 1904-1916.
- Liou, A. P. and P. J. Turnbaugh (2012). "Antibiotic exposure promotes fat gain." Cell Metab **16**(4): 408-410.
- Liu, J. Z., S. Jellbauer, A. J. Poe, V. Ton, M. Pesciaroli, T. E. Kehl-Fie, N. A. Restrepo, M. P. Hosking, R. A. Edwards, A. Battistoni, P. Pasquali, T. E. Lane, W. J. Chazin, T. Vogl, J. Roth, E. P. Skaar and M.

Raffatellu (2012). "Zinc sequestration by the neutrophil protein calprotectin enhances salmonella growth in the inflamed gut." Cell Host Microbe **11**(3): 227-239.

Loetscher, Y., A. Wieser, J. Lengefeld, P. Kaiser, S. Schubert, M. Heikenwalder, W. D. Hardt and B. Stecher (2012). "Salmonella transiently reside in luminal neutrophils in the inflamed gut." PLoS One **7**(4): e34812.

Lopez-Garrido, J., E. Puerta-Fernandez, I. Cota and J. Casadesus (2015). "Virulence Gene Regulation by L-Arabinose in Salmonella enterica." Genetics **200**(3): 807-819.

Lotz, M., D. Gutle, S. Walther, S. Menard, C. Bogdan and M. W. Hornef (2006). "Postnatal acquisition of endotoxin tolerance in intestinal epithelial cells." J Exp Med **203**(4): 973-984.

Ma, B. W., N. A. Bokulich, P. A. Castillo, A. Kananurak, M. A. Underwood, D. A. Mills and C. L. Bevens (2012). "Routine habitat change: a source of unrecognized transient alteration of intestinal microbiota in laboratory mice." PLoS One **7**(10): e47416.

MacIntyre, D. L., S. T. Miyata, M. Kitaoka and S. Pukatzki (2010). "The Vibrio cholerae type VI secretion system displays antimicrobial properties." Proc Natl Acad Sci U S A **107**(45): 19520-19524.

Macpherson, A. J. and T. Uhr (2004). "Induction of protective IgA by intestinal dendritic cells carrying commensal bacteria." Science **303**(5664): 1662-1665.

Maier, L., R. Vyas, C. D. Cordova, H. Lindsay, T. S. Schmidt, S. Brugiroux, B. Periaswamy, R. Bauer, A. Sturm, F. Schreiber, C. von Mering, M. D. Robinson, B. Stecher and W. D. Hardt (2013). "Microbiota-derived hydrogen fuels salmonella typhimurium invasion of the gut ecosystem." Cell Host Microbe **14**(6): 641-651.

Marchesi, J. and F. Shanahan (2007). "The normal intestinal microbiota." Curr Opin Infect Dis **20**(5): 508-513.

Marcobal, A., A. M. Southwick, K. A. Earle and J. L. Sonnenburg (2013). "A refined palate: Bacterial consumption of host glycans in the gut." Glycobiology **23**(9): 1038-1046.

Maukonen, J., C. Simoes and M. Saarela (2012). "The currently used commercial DNA-extraction methods give different results of clostridial and actinobacterial populations derived from human fecal samples." FEMS Microbiol Ecol **79**(3): 697-708.

Maurice, C. F., H. J. Haiser and P. J. Turnbaugh (2013). "Xenobiotics shape the physiology and gene expression of the active human gut microbiome." Cell **152**(1-2): 39-50.

Milani, C., A. Hevia, E. Foroni, S. Duranti, F. Turrone, G. A. Lugli, B. Sanchez, R. Martin, M. Gueimonde, D. van Sinderen, A. Margolles and M. Ventura (2013). "Assessing the fecal microbiota: an optimized ion torrent 16S rRNA gene-based analysis protocol." PLoS One **8**(7): e68739.

Milk, K. (2014). "ENA: Experiment DRX013306. [Online] Available at: <http://www.ebi.ac.uk/ena/data/view/DRX013306> [Accessed October 2014].".

Miller, C. P., M. Bohnhoff and D. Rifkind (1956). "The effect of an antibiotic on the susceptibility of the mouse's intestinal tract to Salmonella infection." Trans Am Clin Climatol Assoc **68**: 51-55; discussion 55-58.

Monack, D. M., D. M. Bouley and S. Falkow (2004). "Salmonella typhimurium persists within macrophages in the mesenteric lymph nodes of chronically infected Nramp1^{+/+} mice and can be reactivated by IFN γ neutralization." J Exp Med **199**(2): 231-241.

Monack, D. M., B. Raupach, A. E. Hromockyj and S. Falkow (1996). "Salmonella typhimurium invasion induces apoptosis in infected macrophages." Proc Natl Acad Sci U S A **93**(18): 9833-9838.

Morgan, X. C., T. L. Tickle, H. Sokol, D. Gevers, K. L. Devaney, D. V. Ward, J. A. Reyes, S. A. Shah, N. LeLeiko, S. B. Snapper, A. Bousvaros, J. Korzenik, B. E. Sands, R. J. Xavier and C. Huttenhower (2012). "Dysfunction of the intestinal microbiome in inflammatory bowel disease and treatment." Genome Biol **13**(9): R79.

Muller, A. J., C. Hoffmann, M. Galle, A. Van Den Broeke, M. Heikenwalder, L. Falter, B. Misselwitz, M. Kremer, R. Beyaert and W. D. Hardt (2009). "The S. Typhimurium effector SopE induces caspase-1 activation in stromal cells to initiate gut inflammation." Cell Host Microbe **6**(2): 125-136.

Nanjing University, C. (2013). "ENA: Experiment ERX166941. [Online] Available at: <http://www.ebi.ac.uk/ena/data/view/ERX166941> [Accessed October 2014].".

Nedialkova, L. P., R. Denzler, M. B. Koeppel, M. Diehl, D. Ring, T. Wille, R. G. Gerlach and B. Stecher (2014). "Inflammation fuels colicin Ib-dependent competition of Salmonella serovar Typhimurium and E. coli in enterobacterial blooms." PLoS Pathog **10**(1): e1003844.

Ng, K. M., J. A. Ferreyra, S. K. Higginbottom, J. B. Lynch, P. C. Kashyap, S. Gopinath, N. Naidu, B. Choudhury, B. C. Weimer, D. M. Monack and J. L. Sonnenburg (2013). "Microbiota-liberated host sugars facilitate post-antibiotic expansion of enteric pathogens." Nature.

Nguyen, T. L., S. Vieira-Silva, A. Liston and J. Raes (2015). "How informative is the mouse for human gut microbiota research?" Dis Model Mech **8**(1): 1-16.

Nicholson, J. K., E. Holmes, J. Kinross, R. Burcelin, G. Gibson, W. Jia and S. Pettersson (2012). "Host-gut microbiota metabolic interactions." Science **336**(6086): 1262-1267.

Nicholson, J. K., E. Holmes and I. D. Wilson (2005). "Gut microorganisms, mammalian metabolism and personalized health care." Nat Rev Microbiol **3**(5): 431-438.

Norin, E. and T. Midtvedt (2010). "Intestinal microflora functions in laboratory mice claimed to harbor a "normal" intestinal microflora. Is the SPF concept running out of date?" Anaerobe **16**(3): 311-313.

- Ogata, H., S. Goto, K. Sato, W. Fujibuchi, H. Bono and M. Kanehisa (1999). "KEGG: Kyoto Encyclopedia of Genes and Genomes." Nucleic Acids Res **27**(1): 29-34.
- Ohland, C. L. and C. Jobin (2015). "Microbial activities and intestinal Homeostasis: A delicate balance between health and disease." Cell Mol Gastroenterol Hepatol **1**(1): 28-40.
- Ooi, J. H., Y. Li, C. J. Rogers and M. T. Cantorna (2013). "Vitamin D regulates the gut microbiome and protects mice from dextran sodium sulfate-induced colitis." J Nutr **143**(10): 1679-1686.
- Orcutt, R. P., F. J. Giannim and R. J. Judge (1987). "Development of an "altered Schaedler flora" for NCI gnotobiotic rodents." Microecol Ther **17**: 59.
- Pacheco, A. R., M. M. Curtis, J. M. Ritchie, D. Munera, M. K. Waldor, C. G. Moreira and V. Sperandio (2012). "Fucose sensing regulates bacterial intestinal colonization." Nature.
- Paesold, G., D. G. Guiney, L. Eckmann and M. F. Kagnoff (2002). "Genes in the Salmonella pathogenicity island 2 and the Salmonella virulence plasmid are essential for Salmonella-induced apoptosis in intestinal epithelial cells." Cell Microbiol **4**(11): 771-781.
- Paliy, O., H. Kenche, F. Abernathy and S. Michail (2009). "High-throughput quantitative analysis of the human intestinal microbiota with a phylogenetic microarray." Appl Environ Microbiol **75**(11): 3572-3579.
- Papavasileiou, K., E. Papavasileiou, A. Tseleni-Kotsovili, S. Bersimis, C. Nicolaou, A. Ioannidis and S. Chatzipanagiotou (2010). "Comparative antimicrobial susceptibility of biofilm versus planktonic forms of Salmonella enterica strains isolated from children with gastroenteritis." Eur J Clin Microbiol Infect Dis **29**(11): 1401-1405.
- Park, S. W., G. Zhen, C. Verhaeghe, Y. Nakagami, L. T. Nguyenvu, A. J. Barczak, N. Killeen and D. J. Erle (2009). "The protein disulfide isomerase AGR2 is essential for production of intestinal mucus." Proc Natl Acad Sci U S A **106**(17): 6950-6955.
- Patel, J. C. and J. E. Galan (2005). "Manipulation of the host actin cytoskeleton by Salmonella--all in the name of entry." Curr Opin Microbiol **8**(1): 10-15.
- Patel, S. and B. A. McCormick (2014). "Mucosal Inflammatory Response to Salmonella typhimurium Infection." Front Immunol **5**: 311.
- Penders, J., C. Thijs, C. Vink, F. F. Stelma, B. Snijders, I. Kummeling, P. A. van den Brandt and E. E. Stobberingh (2006). "Factors influencing the composition of the intestinal microbiota in early infancy." Pediatrics **118**(2): 511-521.
- Pernthaler, A., C. M. Preston, J. Pernthaler, E. F. DeLong and R. Amann (2002). "Comparison of fluorescently labeled oligonucleotide and polynucleotide probes for the detection of pelagic marine bacteria and archaea." Appl Environ Microbiol **68**(2): 661-667.

Persson, S., M. Rosenquist, B. Knoblach, R. Khosravi-Far, M. Sommarin and M. Michalak (2005). "Diversity of the protein disulfide isomerase family: identification of breast tumor induced Hag2 and Hag3 as novel members of the protein family." Mol Phylogenet Evol **36**(3): 734-740.

Pfleiderer, A., J. C. Lagier, F. Armougom, C. Robert, B. Vialettes and D. Raoult (2013). "Culturomics identified 11 new bacterial species from a single anorexia nervosa stool sample." Eur J Clin Microbiol Infect Dis.

Pham, T. A., S. Clare, D. Goulding, J. M. Arasteh, M. D. Stares, H. P. Browne, J. A. Keane, A. J. Page, N. Kumasaka, L. Kane, L. Mottram, K. Harcourt, C. Hale, M. J. Arends, D. J. Gaffney, P. Sanger Mouse Genetics, G. Dougan and T. D. Lawley (2014). "Epithelial IL-22RA1-Mediated Fucosylation Promotes Intestinal Colonization Resistance to an Opportunistic Pathogen." Cell Host Microbe **16**(4): 504-516.

Ploger, S., F. Stumpff, G. B. Penner, J. D. Schulzke, G. Gabel, H. Martens, Z. Shen, D. Gunzel and J. R. Aschenbach (2012). "Microbial butyrate and its role for barrier function in the gastrointestinal tract." Ann N Y Acad Sci **1258**: 52-59.

Png, C. W., S. K. Linden, K. S. Gilshenan, E. G. Zoetendal, C. S. McSweeney, L. I. Sly, M. A. McGuckin and T. H. Florin (2010). "Mucolytic bacteria with increased prevalence in IBD mucosa augment in vitro utilization of mucin by other bacteria." Am J Gastroenterol **105**(11): 2420-2428.

Pongpech, P., D. J. Hentges, W. W. Marsh and M. E. Eberle (1989). "Effect of streptomycin administration on association of enteric pathogens with cecal tissue of mice." Infect Immun **57**(7): 2092-2097.

Price, M. N., P. S. Dehal and A. P. Arkin (2009). "FastTree: computing large minimum evolution trees with profiles instead of a distance matrix." Mol Biol Evol **26**(7): 1641-1650.

Quast, C., E. Pruesse, P. Yilmaz, J. Gerken, T. Schweer, P. Yarza, J. Peplies and F. O. Glockner (2013). "The SILVA ribosomal RNA gene database project: improved data processing and web-based tools." Nucleic Acids Res **41**(Database issue): D590-596.

Raffatellu, M., M. D. George, Y. Akiyama, M. J. Hornsby, S. P. Nuccio, T. A. Paixao, B. P. Butler, H. Chu, R. L. Santos, T. Berger, T. W. Mak, R. M. Tsolis, C. L. Bevins, J. V. Solnick, S. Dandekar and A. J. Baumler (2009). "Lipocalin-2 resistance confers an advantage to Salmonella enterica serotype Typhimurium for growth and survival in the inflamed intestine." Cell Host Microbe **5**(5): 476-486.

Raghunathan, A., J. Reed, S. Shin, B. Palsson and S. Daefler (2009). "Constraint-based analysis of metabolic capacity of Salmonella typhimurium during host-pathogen interaction." BMC Syst Biol **3**: 38.

Ramachandran, V., T. Arumugam, H. Wang and C. D. Logsdon (2008). "Anterior gradient 2 is expressed and secreted during the development of pancreatic cancer and promotes cancer cell survival." Cancer Res **68**(19): 7811-7818.

Rappe, M. S. and S. J. Giovannoni (2003). "The uncultured microbial majority." Annu Rev Microbiol **57**: 369-394.

- Rausch, P., N. Steck, A. Suwandi, J. A. Seidel, S. Kunzel, K. Bhullar, M. Basic, A. Bleich, J. M. Johnsen, B. A. Vallance, J. F. Baines and G. A. Grassl (2015). "Expression of the Blood-Group-Related Gene B4galnt2 Alters Susceptibility to Salmonella Infection." *PLoS Pathog* **11**(7): e1005008.
- Reed, S., H. Neuman, S. Moscovich, R. P. Glahn, O. Koren and E. Tako (2015). "Chronic Zinc Deficiency Alters Chick Gut Microbiota Composition and Function." *Nutrients* **7**(12): 9768-9784.
- Reeves, A. E., M. J. Koenigsnecht, I. L. Bergin and V. B. Young (2012). "Suppression of *Clostridium difficile* in the Gastrointestinal Tract of Germ-Free Mice Inoculated with a Murine Lachnospiraceae Isolate." *Infect Immun*.
- Reikvam, D. H., A. Erofeev, A. Sandvik, V. Grcic, F. L. Jahnsen, P. Gaustad, K. D. McCoy, A. J. Macpherson, L. A. Meza-Zepeda and F. E. Johansen (2011). "Depletion of murine intestinal microbiota: effects on gut mucosa and epithelial gene expression." *PLoS One* **6**(3): e17996.
- Ren, D., C. Li, Y. Qin, R. Yin, X. Li, M. Tian, S. Du, H. Guo, C. Liu, N. Zhu, D. Sun, Y. Li and N. Jin (2012). "Inhibition of *Staphylococcus aureus* adherence to Caco-2 cells by lactobacilli and cell surface properties that influence attachment." *Anaerobe* **18**(5): 508-515.
- Rescigno, M., G. Rotta, B. Valzasina and P. Ricciardi-Castagnoli (2001). "Dendritic cells shuttle microbes across gut epithelial monolayers." *Immunobiology* **204**(5): 572-581.
- Rhee, S. J., W. A. Walker and B. J. Cherayil (2005). "Developmentally regulated intestinal expression of IFN-gamma and its target genes and the age-specific response to enteric *Salmonella* infection." *J Immunol* **175**(2): 1127-1136.
- Ricker, N., H. Qian and R. R. Fulthorpe (2012). "The limitations of draft assemblies for understanding prokaryotic adaptation and evolution." *Genomics* **100**(3): 167-175.
- Rivera-Chavez, F., S. E. Winter, C. A. Lopez, M. N. Xavier, M. G. Winter, S. P. Nuccio, J. M. Russell, R. C. Laughlin, S. D. Lawhon, T. Sterzenbach, C. L. Bevins, R. M. Tsohis, R. Harshey, L. G. Adams and A. J. Baumler (2013). "Salmonella uses energy taxis to benefit from intestinal inflammation." *PLoS Pathog* **9**(4): e1003267.
- Robertson, B. R., J. L. O'Rourke, B. A. Neilan, P. Vandamme, S. L. On, J. G. Fox and A. Lee (2005). "*Mucispirillum schaedleri* gen. nov., sp. nov., a spiral-shaped bacterium colonizing the mucus layer of the gastrointestinal tract of laboratory rodents." *Int J Syst Evol Microbiol* **55**(Pt 3): 1199-1204.
- Rogers, G. B., J. Kozłowska, J. Keeble, K. Metcalfe, M. Fao, S. E. Dowd, A. J. Mason, M. A. McGuckin and K. D. Bruce (2014). "Functional divergence in gastrointestinal microbiota in physically-separated genetically identical mice." *Sci Rep* **4**: 5437.
- Rojo, D., M. J. Gosalbes, R. Ferrari, A. E. Perez-Cobas, E. Hernandez, R. Oltra, J. Buesa, A. Latorre, C. Barbas, M. Ferrer and A. Moya (2015). "*Clostridium difficile* heterogeneously impacts intestinal community architecture but drives stable metabolome responses." *ISME J* **9**(10): 2206-2220.

Round, J. L. and S. K. Mazmanian (2009). "The gut microbiota shapes intestinal immune responses during health and disease." Nat Rev Immunol **9**(5): 313-323.

Russell, A. B., A. G. Wexler, B. N. Harding, J. C. Whitney, A. J. Bohn, Y. A. Goo, B. Q. Tran, N. A. Barry, H. Zheng, S. B. Peterson, S. Chou, T. Gonen, D. R. Goodlett, A. L. Goodman and J. D. Mougous (2014). "A Type VI Secretion-Related Pathway in Bacteroidetes Mediates Interbacterial Antagonism." Cell Host Microbe.

Rybak, M. J., B. J. Abate, S. L. Kang, M. J. Ruffing, S. A. Lerner and G. L. Drusano (1999). "Prospective evaluation of the effect of an aminoglycoside dosing regimen on rates of observed nephrotoxicity and ototoxicity." Antimicrob Agents Chemother **43**(7): 1549-1555.

Rydstrom, A. and M. J. Wick (2007). "Monocyte recruitment, activation, and function in the gut-associated lymphoid tissue during oral Salmonella infection." J Immunol **178**(9): 5789-5801.

Saito, D., T. Leonardo Rde, J. L. Rodrigues, S. M. Tsai, J. F. Hofling and R. B. Goncalves (2006). "Identification of bacteria in endodontic infections by sequence analysis of 16S rDNA clone libraries." J Med Microbiol **55**(Pt 1): 101-107.

Salonen, A., J. Nikkila, J. Jalanka-Tuovinen, O. Immonen, M. Rajilic-Stojanovic, R. A. Kekkonen, A. Palva and W. M. de Vos (2010). "Comparative analysis of fecal DNA extraction methods with phylogenetic microarray: effective recovery of bacterial and archaeal DNA using mechanical cell lysis." J Microbiol Methods **81**(2): 127-134.

Samuel, B. S. and J. I. Gordon (2006). "A humanized gnotobiotic mouse model of host-archaeal-bacterial mutualism." Proc Natl Acad Sci U S A **103**(26): 10011-10016.

Sarma-Rupavtarm, R. B., Z. Ge, D. B. Schauer, J. G. Fox and M. F. Polz (2004). "Spatial distribution and stability of the eight microbial species of the altered schaedler flora in the mouse gastrointestinal tract." Appl Environ Microbiol **70**(5): 2791-2800.

Sassone-Corsi, M. and M. Raffatellu (2015). "No vacancy: how beneficial microbes cooperate with immunity to provide colonization resistance to pathogens." J Immunol **194**(9): 4081-4087.

Satoh-Takayama, N., C. A. Vosshenrich, S. Lesjean-Pottier, S. Sawa, M. Lochner, F. Rattis, J. J. Mention, K. Thiam, N. Cerf-Bensussan, O. Mandelboim, G. Eberl and J. P. Di Santo (2008). "Microbial flora drives interleukin 22 production in intestinal NKp46+ cells that provide innate mucosal immune defense." Immunity **29**(6): 958-970.

Satokari, R., S. Fuentes, E. Mattila, J. Jalanka, W. M. de Vos and P. Arkkila (2014). "Fecal transplantation treatment of antibiotic-induced, noninfectious colitis and long-term microbiota follow-up." Case Rep Med **2014**: 913867.

Schaedler, R. W., R. Dubs and R. Costello (1965). "Association of Germfree Mice with Bacteria Isolated from Normal Mice." J Exp Med **122**: 77-82.

Schillinger, C., A. Petrich, R. Lux, B. Riep, J. Kikhney, A. Friedmann, L. E. Wolinsky, U. B. Gobel, H. Daims and A. Moter (2012). "Co-localized or randomly distributed? Pair cross correlation of in vivo grown subgingival biofilm bacteria quantified by digital image analysis." PLoS One **7**(5): e37583.

Schlumberger, M. C., A. J. Muller, K. Ehrbar, B. Winnen, I. Duss, B. Stecher and W. D. Hardt (2005). "Real-time imaging of type III secretion: Salmonella SipA injection into host cells." Proc Natl Acad Sci U S A **102**(35): 12548-12553.

Schmidt, T. S., J. F. Matias Rodrigues and C. von Mering (2015). "Limits to robustness and reproducibility in the demarcation of operational taxonomic units." Environ Microbiol **17**(5): 1689-1706.

Schubert, A. M., H. Sinani and P. D. Schloss (2015). "Antibiotic-Induced Alterations of the Murine Gut Microbiota and Subsequent Effects on Colonization Resistance against Clostridium difficile." MBio **6**(4): e00974.

Schwab, C., D. Berry, I. Rauch, I. Rennisch, J. Ramesmayer, E. Hainzl, S. Heider, T. Decker, L. Kenner, M. Muller, B. Strobl, M. Wagner, C. Schleper, A. Loy and T. Urich (2014). "Longitudinal study of murine microbiota activity and interactions with the host during acute inflammation and recovery." ISME J.

Seedorf, H., N. W. Griffin, V. K. Ridaura, A. Reyes, J. Cheng, F. E. Rey, M. I. Smith, G. M. Simon, R. H. Scheffrahn, D. Woebken, A. M. Spormann, W. Van Treuren, L. K. Ursell, M. Pirrung, A. Robbins-Pianka, B. L. Cantarel, V. Lombard, B. Henrissat, R. Knight and J. I. Gordon (2014). "Bacteria from diverse habitats colonize and compete in the mouse gut." Cell **159**(2): 253-266.

Segata, N., J. Izard, L. Waldron, D. Gevers, L. Miropolsky, W. S. Garrett and C. Huttenhower (2011). "Metagenomic biomarker discovery and explanation." Genome Biol **12**(6): R60.

Sellin, M. E., A. A. Muller, B. Felmy, T. Dolowschiak, M. Diard, A. Tardivel, K. M. Maslowski and W. D. Hardt (2014). "Epithelium-Intrinsic NAIP/NLRC4 Inflammasome Drives Infected Enterocyte Expulsion to Restrict Salmonella Replication in the Intestinal Mucosa." Cell Host Microbe **16**(2): 237-248.

Sellon, R. K., S. Tonkonogy, M. Schultz, L. A. Dieleman, W. Grenther, E. Balish, D. M. Rennick and R. B. Sartor (1998). "Resident enteric bacteria are necessary for development of spontaneous colitis and immune system activation in interleukin-10-deficient mice." Infect Immun **66**(11): 5224-5231.

Shankar, V., M. J. Hamilton, A. Khoruts, A. Kilburn, T. Unno, O. Paliy and M. J. Sadowsky (2014). "Species and genus level resolution analysis of gut microbiota in Clostridium difficile patients following fecal microbiota transplantation." Microbiome **2**: 13.

Shimotoyodome, A., S. Meguro, T. Hase, I. Tokimitsu and T. Sakata (2000). "Short chain fatty acids but not lactate or succinate stimulate mucus release in the rat colon." Comp Biochem Physiol A Mol Integr Physiol **125**(4): 525-531.

Slezak, K., Z. Krupova, S. Rabot, G. Loh, F. Levenez, A. Descamps, P. Lepage, J. Dore, S. Bellier and M. Blaut (2014). "Association of germ-free mice with a simplified human intestinal microbiota results in a shortened intestine." Gut Microbes **5**(2): 176-182.

Smith, P. M., M. R. Howitt, N. Panikov, M. Michaud, C. A. Gallini, Y. M. Bohlooly, J. N. Glickman and W. S. Garrett (2013). "The microbial metabolites, short-chain fatty acids, regulate colonic Treg cell homeostasis." Science **341**(6145): 569-573.

Sogin, M. L., H. G. Morrison, J. A. Huber, D. Mark Welch, S. M. Huse, P. R. Neal, J. M. Arrieta and G. J. Herndl (2006). "Microbial diversity in the deep sea and the underexplored "rare biosphere"." Proc Natl Acad Sci U S A **103**(32): 12115-12120.

Sommer, F., N. Adam, M. E. Johansson, L. Xia, G. C. Hansson and F. Backhed (2014). "Altered mucus glycosylation in core 1 O-glycan-deficient mice affects microbiota composition and intestinal architecture." PLoS One **9**(1): e85254.

Sommer, M. O., G. Dantas and G. M. Church (2009). "Functional characterization of the antibiotic resistance reservoir in the human microflora." Science **325**(5944): 1128-1131.

Sovran, B., L. M. Loonen, P. Lu, F. Hugenholtz, C. Belzer, E. H. Stolte, M. V. Boekschoten, P. van Baarlen, M. Kleerebezem, P. de Vos, J. Dekker, I. B. Renes and J. M. Wells (2015). "IL-22-STAT3 pathway plays a key role in the maintenance of ileal homeostasis in mice lacking secreted mucus barrier." Inflamm Bowel Dis **21**(3): 531-542.

Stecher, B., M. Barthel, M. C. Schlumberger, L. Haberli, W. Rabsch, M. Kremer and W. D. Hardt (2008). "Motility allows *S. Typhimurium* to benefit from the mucosal defence." Cell Microbiol **10**(5): 1166-1180.

Stecher, B., S. Chaffron, R. Kappeli, S. Hapfelmeier, S. Friedrich, T. C. Weber, J. Kirundi, M. Suar, K. D. McCoy, C. von Mering, A. J. Macpherson and W. D. Hardt (2010). "Like will to like: abundances of closely related species can predict susceptibility to intestinal colonization by pathogenic and commensal bacteria." PLoS Pathog **6**(1): e1000711.

Stecher, B., R. Denzler, L. Maier, F. Bernet, M. J. Sanders, D. J. Pickard, M. Barthel, A. M. Westendorf, K. A. Krogfelt, A. W. Walker, M. Ackermann, U. Dobrindt, N. R. Thomson and W. D. Hardt (2012). "Gut inflammation can boost horizontal gene transfer between pathogenic and commensal Enterobacteriaceae." Proc Natl Acad Sci U S A **109**(4): 1269-1274.

Stecher, B., S. Hapfelmeier, C. Muller, M. Kremer, T. Stallmach and W. D. Hardt (2004). "Flagella and chemotaxis are required for efficient induction of *Salmonella enterica* serovar *Typhimurium* colitis in streptomycin-pretreated mice." Infect Immun **72**(7): 4138-4150.

Stecher, B., A. J. Macpherson, S. Hapfelmeier, M. Kremer, T. Stallmach and W. D. Hardt (2005). "Comparison of *Salmonella enterica* serovar *Typhimurium* colitis in germfree mice and mice pretreated with streptomycin." Infect Immun **73**(6): 3228-3241.

Stecher, B., R. Robbiani, A. W. Walker, A. M. Westendorf, M. Barthel, M. Kremer, S. Chaffron, A. J. Macpherson, J. Buer, J. Parkhill, G. Dougan, C. von Mering and W. D. Hardt (2007). "Salmonella enterica serovar typhimurium exploits inflammation to compete with the intestinal microbiota." PLoS Biol **5**(10): 2177-2189.

Stefka, A. T., T. Feehley, P. Tripathi, J. Qiu, K. McCoy, S. K. Mazmanian, M. Y. Tjota, G. Y. Seo, S. Cao, B. R. Theriault, D. A. Antonopoulos, L. Zhou, E. B. Chang, Y. X. Fu and C. R. Nagler (2014). "Commensal bacteria protect against food allergen sensitization." Proc Natl Acad Sci U S A **111**(36): 13145-13150.

Stelzer, C., R. Kappeli, C. Konig, A. Krahl, W. D. Hardt, B. Stecher and D. Bumann (2011). "Salmonella-Induced Mucosal Lectin RegIIIbeta Kills Competing Gut Microbiota." PLoS One **6**(6): e20749.

Struss, A. K., P. Pasini, D. Flomenhoft, H. Shashidhar and S. Daunert (2012). "Investigating the effect of antibiotics on quorum sensing with whole-cell biosensing systems." Anal Bioanal Chem **402**(10): 3227-3236.

Subramani, D. B., M. E. Johansson, G. Dahlen and G. C. Hansson (2010). "Lactobacillus and Bifidobacterium species do not secrete protease that cleaves the MUC2 mucin which organises the colon mucus." Benef Microbes **1**(4): 343-350.

Subramanian, A., P. Tamayo, V. K. Mootha, S. Mukherjee, B. L. Ebert, M. A. Gillette, A. Paulovich, S. L. Pomeroy, T. R. Golub, E. S. Lander and J. P. Mesirov (2005). "Gene set enrichment analysis: a knowledge-based approach for interpreting genome-wide expression profiles." Proc Natl Acad Sci U S A **102**(43): 15545-15550.

Suez, J., T. Korem, D. Zeevi, G. Zilberman-Schapira, C. A. Thaiss, O. Maza, D. Israeli, N. Zmora, S. Gilad, A. Weinberger, Y. Kuperman, A. Harmelin, I. Kolodkin-Gal, H. Shapiro, Z. Halpern, E. Segal and E. Elinav (2014). "Artificial sweeteners induce glucose intolerance by altering the gut microbiota." Nature **514**(7521): 181-186.

Sung, H. Y., E. N. Choi, D. Lyu, A. K. Park, W. Ju and J. H. Ahn (2014). "Aberrant hypomethylation-mediated AGR2 overexpression induces an aggressive phenotype in ovarian cancer cells." Oncol Rep **32**(2): 815-820.

Thiel, R. and M. Blaut (2005). "An improved method for the automated enumeration of fluorescently labelled bacteria in human faeces." J Microbiol Methods **61**(3): 369-379.

Thiennimitr, P., S. E. Winter and A. J. Baumler (2012). "Salmonella, the host and its microbiota." Curr Opin Microbiol **15**(1): 108-114.

Thijm, H. A. and D. van der Waaij (1979). "The effect of three frequently applied antibiotics on the colonization resistance of the digestive tract of mice." J Hyg (Lond) **82**(3): 397-405.

Ubeda, C., V. Bucci, S. Caballero, A. Djukovic, N. C. Toussaint, M. Equinda, L. Lipuma, L. Ling, A. Gobourne, D. No, Y. Taur, R. R. Jenq, M. R. van den Brink, J. B. Xavier and E. G. Pamer (2013).

"Intestinal Microbiota Containing *Barnesiella* Species Cures Vancomycin-Resistant *Enterococcus faecium* Colonization." Infect Immun **81**(3): 965-973.

Uchiya, K., M. A. Barbieri, K. Funato, A. H. Shah, P. D. Stahl and E. A. Groisman (1999). "A *Salmonella* virulence protein that inhibits cellular trafficking." EMBO J **18**(14): 3924-3933.

Vaishnava, S., C. L. Behrendt, A. S. Ismail, L. Eckmann and L. V. Hooper (2008). "Paneth cells directly sense gut commensals and maintain homeostasis at the intestinal host-microbial interface." Proc Natl Acad Sci U S A **105**(52): 20858-20863.

van Ampting, M. T., L. M. Loonen, A. J. Schonewille, I. Konings, C. Vink, J. Iovanna, M. Chamaillard, J. Dekker, R. van der Meer, J. M. Wells and I. M. Bovee-Oudenhoven (2012). "Intestinally secreted C-type lectin Reg3b attenuates salmonellosis but not listeriosis in mice." Infect Immun **80**(3): 1115-1120.

Van der Sluis, M., B. A. De Koning, A. C. De Bruijn, A. Velcich, J. P. Meijerink, J. B. Van Goudoever, H. A. Buller, J. Dekker, I. Van Seuningen, I. B. Renes and A. W. Einerhand (2006). "Muc2-deficient mice spontaneously develop colitis, indicating that MUC2 is critical for colonic protection." Gastroenterology **131**(1): 117-129.

van der Waaij, D., J. M. Berghuis-de Vries and L.-v. Lekkerkerk (1971). "Colonization resistance of the digestive tract in conventional and antibiotic-treated mice." J Hyg (Lond) **69**(3): 405-411.

van Meer, G., D. R. Voelker and G. W. Feigenson (2008). "Membrane lipids: where they are and how they behave." Nat Rev Mol Cell Biol **9**(2): 112-124.

Vanhoutvin, S. A., F. J. Troost, H. M. Hamer, P. J. Lindsey, G. H. Koek, D. M. Jonkers, A. Kodde, K. Venema and R. J. Brummer (2009). "Butyrate-induced transcriptional changes in human colonic mucosa." PLoS One **4**(8): e6759.

Varughese, C. A., N. H. Vakil and K. M. Phillips (2013). "Antibiotic-associated diarrhea: a refresher on causes and possible prevention with probiotics--continuing education article." J Pharm Pract **26**(5): 476-482.

Velcich, A., W. Yang, J. Heyer, A. Fragale, C. Nicholas, S. Viani, R. Kucherlapati, M. Lipkin, K. Yang and L. Augenlicht (2002). "Colorectal cancer in mice genetically deficient in the mucin Muc2." Science **295**(5560): 1726-1729.

Velge, P., A. Wiedemann, M. Rosselin, N. Abed, Z. Boumart, A. M. Chausse, O. Grepinet, F. Namdari, S. M. Roche, A. Rossignol and I. Virlogeux-Payant (2012). "Multiplicity of *Salmonella* entry mechanisms, a new paradigm for *Salmonella* pathogenesis." Microbiologyopen **1**(3): 243-258.

Verberkmoes, N. C., A. L. Russell, M. Shah, A. Godzik, M. Rosenquist, J. Halfvarson, M. G. Lefsrud, J. Apajalahti, C. Tysk, R. L. Hettich and J. K. Jansson (2009). "Shotgun metaproteomics of the human distal gut microbiota." ISME J **3**(2): 179-189.

Vieira-Pinto, M. O., M., F. Bernardo and C. Martins (2007). "Rapid detection of Salmonella sp. in pork samples using fluorescent in situ hybridization: a comparison with VIDAS-SLM system and ISO 6579 cultural method." Arq. Bras. Med. Vet. Zootec. **59**(6): 1388-1393.

Vikram, A., P. R. Jesudhasan, G. K. Jayaprakasha, S. D. Pillai, A. Jayaraman and B. S. Patil (2011). "Citrus flavonoid represses Salmonella pathogenicity island 1 and motility in *S. Typhimurium* LT2." Int J Food Microbiol **145**(1): 28-36.

Wang, J., M. Linnenbrink, S. Kunzel, R. Fernandes, M. J. Nadeau, P. Rosenstiel and J. F. Baines (2014). "Dietary history contributes to enterotype-like clustering and functional metagenomic content in the intestinal microbiome of wild mice." Proc Natl Acad Sci U S A **111**(26): E2703-2710.

Wang, Q., G. M. Garrity, J. M. Tiedje and J. R. Cole (2007). "Naive Bayesian classifier for rapid assignment of rRNA sequences into the new bacterial taxonomy." Appl Environ Microbiol **73**(16): 5261-5267.

Wang, R. F. and S. R. Kushner (1991). "Construction of versatile low-copy-number vectors for cloning, sequencing and gene expression in *Escherichia coli*." Gene **100**: 195-199.

Wang, Z., Y. Hao and A. W. Lowe (2008). "The adenocarcinoma-associated antigen, AGR2, promotes tumor growth, cell migration, and cellular transformation." Cancer Res **68**(2): 492-497.

Wannemuehler, M. J., A. M. Overstreet, D. V. Ward and G. J. Phillips (2014). "Draft genome sequences of the altered schaedler flora, a defined bacterial community from gnotobiotic mice." Genome Announc **2**(2).

Watanabe, M., H. Kojima and M. Fukui (2013). "Desulfotomaculum intricatum sp. nov., a sulfate reducer isolated from freshwater lake sediment." Int J Syst Evol Microbiol **63**(Pt 10): 3574-3578.

Wei, Y., J. Gong, W. Zhu, D. Guo, L. Gu, N. Li and J. Li (2015). "Fecal microbiota transplantation restores dysbiosis in patients with methicillin resistant *Staphylococcus aureus* enterocolitis." BMC Infect Dis **15**: 265.

Weisburg, W. G., S. M. Barns, D. A. Pelletier and D. J. Lane (1991). "16S ribosomal DNA amplification for phylogenetic study." J Bacteriol **173**(2): 697-703.

Wenzel, U. A., M. K. Magnusson, A. Rydstrom, C. Jonstrand, J. Hengst, M. E. Johansson, A. Velcich, L. Ohman, H. Strid, H. Sjovall, G. C. Hansson and M. J. Wick (2014). "Spontaneous colitis in muc2-deficient mice reflects clinical and cellular features of active ulcerative colitis." PLoS One **9**(6): e100217.

Wichmann, A., A. Allahyar, T. U. Greiner, H. Plovier, G. O. Lunden, T. Larsson, D. J. Drucker, N. M. Delzenne, P. D. Cani and F. Backhed (2013). "Microbial modulation of energy availability in the colon regulates intestinal transit." Cell Host Microbe **14**(5): 582-590.

Willing, B. P., A. Vacharaksa, M. Croxen, T. Thanachayanont and B. B. Finlay (2011). "Altering Host Resistance to Infections through Microbial Transplantation." PLoS One **6**(10): e26988.

Wilson, K. H. and R. B. Blitchington (1996). "Human colonic biota studied by ribosomal DNA sequence analysis." *Appl Environ Microbiol* **62**(7): 2273-2278.

Winter, S. E., P. Thiennimitr, M. G. Winter, B. P. Butler, D. L. Huseby, R. W. Crawford, J. M. Russell, C. L. Bevins, L. G. Adams, R. M. Tsois, J. R. Roth and A. J. Baumler (2010). "Gut inflammation provides a respiratory electron acceptor for Salmonella." *Nature* **467**(7314): 426-429.

Wlodarska, M., B. Willing, K. M. Keeney, A. Menendez, K. S. Bergstrom, N. Gill, S. L. Russell, B. A. Vallance and B. B. Finlay (2011). "Antibiotic treatment alters the colonic mucus layer and predisposes the host to exacerbated *Citrobacter rodentium*-induced colitis." *Infect Immun* **79**(4): 1536-1545.

Woting, A., N. Pfeiffer, L. Hanske, G. Loh, S. Klaus and M. Blaut (2015). "Alleviation of high fat diet-induced obesity by oligofructose in gnotobiotic mice is independent of presence of *Bifidobacterium longum*." *Mol Nutr Food Res* **59**(11): 2267-2278.

Woting, A., N. Pfeiffer, G. Loh, S. Klaus and M. Blaut (2014). "Clostridium ramosum promotes high-fat diet-induced obesity in gnotobiotic mouse models." *MBio* **5**(5): e01530-01514.

Wrzosek, L., S. Miquel, M. L. Noordine, S. Bouet, M. Joncquel Chevalier-Curt, V. Robert, C. Philippe, C. Bridonneau, C. Cherbuy, C. Robbe-Masselot, P. Langella and M. Thomas (2013). "Bacteroides thetaiotaomicron and Faecalibacterium prausnitzii influence the production of mucus glycans and the development of goblet cells in the colonic epithelium of a gnotobiotic model rodent." *BMC Biol* **11**: 61.

Wymore Brand, M., M. J. Wannemuehler, G. J. Phillips, A. Proctor, A. M. Overstreet, A. E. Jergens, R. P. Orcutt and J. G. Fox (2015). "The Altered Schaedler Flora: Continued Applications of a Defined Murine Microbial Community." *ILAR J* **56**(2): 169-178.

Xiong, X., D. N. Frank, C. E. Robertson, S. S. Hung, J. Markle, A. J. Canty, K. D. McCoy, A. J. Macpherson, P. Poussier, J. S. Danska and J. Parkinson (2012). "Generation and analysis of a mouse intestinal metatranscriptome through Illumina based RNA-sequencing." *PLoS One* **7**(4): e36009.

Xue, Y., H. Zhang, H. Wang, J. Hu, M. Du and M. J. Zhu (2014). "Host inflammatory response inhibits *Escherichia coli* O157:H7 adhesion to gut epithelium through augmentation of mucin expression." *Infect Immun* **82**(5): 1921-1930.

Yang, X., J. Brisbin, H. Yu, Q. Wang, F. Yin, Y. Zhang, P. Sabour, S. Sharif and J. Gong (2014). "Selected lactic acid-producing bacterial isolates with the capacity to reduce *Salmonella* translocation and virulence gene expression in chickens." *PLoS One* **9**(4): e93022.

Yatsunencko, T., F. E. Rey, M. J. Manary, I. Trehan, M. G. Dominguez-Bello, M. Contreras, M. Magris, G. Hidalgo, R. N. Baldassano, A. P. Anokhin, A. C. Heath, B. Warner, J. Reeder, J. Kuczynski, J. G. Caporaso, C. A. Lozupone, C. Lauber, J. C. Clemente, D. Knights, R. Knight and J. I. Gordon (2012). "Human gut microbiome viewed across age and geography." *Nature* **486**(7402): 222-227.

Ye, Y., J. H. Choi and H. Tang (2011). "RAPSearch: a fast protein similarity search tool for short reads." *BMC Bioinformatics* **12**: 159.

Zarepour, M., K. Bhullar, M. Montero, C. Ma, T. Huang, A. Velcich, L. Xia and B. A. Vallance (2013). "The Mucin Muc2 Limits Pathogen Burdens and Epithelial Barrier Dysfunction during Salmonella enterica Serovar Typhimurium Colitis." Infect Immun **81**(10): 3672-3683.

Zengler, K., G. Toledo, M. Rappe, J. Elkins, E. J. Mathur, J. M. Short and M. Keller (2002). "Cultivating the uncultured." Proc Natl Acad Sci U S A **99**(24): 15681-15686.

Zhang, Z., J. Geng, X. Tang, H. Fan, J. Xu, X. Wen, Z. S. Ma and P. Shi (2014). "Spatial heterogeneity and co-occurrence patterns of human mucosal-associated intestinal microbiota." ISME J **8**(4): 881-893.

Zhao, F., R. Edwards, D. Dizon, K. Afrasiabi, J. R. Mastroianni, M. Geyfman, A. J. Ouellette, B. Andersen and S. M. Lipkin (2010). "Disruption of Paneth and goblet cell homeostasis and increased endoplasmic reticulum stress in Agr2^{-/-} mice." Dev Biol **338**(2): 270-279.

Zhao, Y., H. Tang and Y. Ye (2012). "RAPSearch2: a fast and memory-efficient protein similarity search tool for next-generation sequencing data." Bioinformatics **28**(1): 125-126.

Zheng, X., G. Xie, A. Zhao, L. Zhao, C. Yao, N. H. Chiu, Z. Zhou, Y. Bao, W. Jia, J. K. Nicholson and W. Jia (2011). "The footprints of gut microbial-mammalian co-metabolism." J Proteome Res **10**(12): 5512-5522.

Zierler, M. K. and J. E. Galan (1995). "Contact with cultured epithelial cells stimulates secretion of Salmonella typhimurium invasion protein InvJ." Infect Immun **63**(10): 4024-4028.

9. Acknowledgments

There is an enormous amount of people I would like to thank for their help, support, understanding and contribution. From active scientific discussions to more personal support, passing by technical help, specific teaching or even general conversation, each of the following persons has contributed, in its way, to the achievements of this PhD thesis.

Supervisors.

First of all, I would like to thank the people without whom this adventure will not have been possible starting with Prof. Dr. Dr. Jürgen Heesemann, Prof. Dr. Bärbel Stecher. Prof. Heesemann, thank you so much for your support and brilliant scientific discussions, you are definitely an inexhaustible source of ideas and exiting theories. You made the Max-von-Pettenkofer (MvP) Institute a place with an inspiring and friendly atmosphere, where personal and professional success can meet. I guess this is one of your secrets, which makes you being such a great leader! And talking about great leadership, a wonderful and devoted supervisor: Prof. Bärbel Stecher. Bärbel, I remember the first time I met Yvonne and Lisa, they both told me how “lucky I was” and, not that I doubted it, but I realized pretty quickly how right they were. These five years spent by your side are just unforgettable. You have definitely been one of my strongest driving forces and an amazing mentor not only for the work-related questions but also at a private life level. On the first evening of my interview, you have asked me to think overnight about my decision to join you in your freshly starting group. My choice was in fact made the morning we had met and, even though I am having a hard time writing everything up ;-), I have never regretted it! Thank you so much for being so devoted, kind, fair, enthusiastic, eternal optimistic, trustful, ..., well, for being who you are. You changed my life, sharpened my scientific skills and helped me being (I hope) a better researcher.

Family.

Secondly, I would like to thank my family who, even though being really happy for me, are quite impatient to have me back. Alain & Mathilde, alias papa & maman, un immense merci pour votre inestimable soutien, nos nombreuses discussions, vos efforts pour comprendre mes projets de thèse et votre confiance même lorsque je n’ai cessé de répéter “je suis sur la fin” durant des mois! Avec un peu de chance, il y aura bientôt un second docteur dans la famille sauf que le nouveau aura tué des souris au lieu

de sauver des humains. Merci aussi à vous deux pour l'éducation que vous m'avez apporté, la confiance que vous m'avez toujours témoignée, l'équilibre et l'amour que j'ai reçu et dont un enfant pourrait rêver. Jérémie & Audrey, malgré la distance nous avons su rester une fratrie. Un grand merci pour l'intérêt que vous avez témoigné à ce travail doctoral ainsi que pour votre soutien. J'ai enfin fini...à nous les vacances et les folies!! Mamie Elfriede, mamie Marie & papy Salomon, je souhaiterais vous remercier du fond du cœur pour m'avoir soutenu et encourager dans cette aventure un peu folle. Ne vous en faites pas, je reviendrai...un jour peut-être ! ;-)

Mentors.

In the third part, I would like to thank my mentors who supported me during this PhD work, most of the time without even noticing it. Dr. Robert Zumbihl, alias Robert, you were definitely the one who guided me into the wonderful MvP Institute journey. I cannot find the right words to express how grateful I am. You have been an inspiration (yes, I mean it!) during three years of microbiological classes and I will always remember the day you introduced me to the MvP Institute and how supportive you have been in many ways. As you have seen, I signed in for the Munich "adventure" and have not regretted it a single day. Dr. Ombeline Rossier and Dr. David Berry, thank you so much for our rewarding discussions, your technical assistance and great support. You have been a priceless help to me.

Friends.

The fourth part is dedicated to my friends who, for most of them, still do not realize how much they mean to me. I am sure I will forget some people and I do hope they won't be too upset about it. Let's say, it is because of work! Mickaël, alias Mikado Borracho, I know that you have improved your English enough to understand the few following words. Thank you for being such a devoted and close friend. I know that I should call you more often but it is not my fault; phones are not allowed in the mouse house ;-). I also know I should visit Montpellier more often too but how could I when I am such a work-alcoholic...and there are no regular direct flights from Munich to Montpellier. However, I do know that despite the distance, I can count on you and you, on me. Thanks for standing by me in the good moments and even more in the bad ones! Lubov, thanks a lot for being such an amazing friend. I cannot believe five years are already gone since we met. Starting the entire lab and doing our PhD thesis together have been the craziest things I have ever done; dancing in the lab over the weekend (sorry boss...and thanks for the radio-CD post! ;-)), having lunch ...diners together in front of our computers, co-organizing the Christmas

party (ok, you have done most of it by yourself but I have had a lot of fun watching you dealing with western blots and Christmas tree decorations), helping each other to translate German formularies, winning despite of all expectations the MvP kicker tournament, nicely explaining to the new colleagues how bad it is not to participate in the common lab-work, , and I should probably thank you in advance for the time you are going to spend on my thesis corrections. I wish you all the best you do deserve in the career path you will chose. Audrey V., my dear Audrey, we met quite roughly eight years ago and to my surprise, and probably yours too, we coped so well together! I am sure one day, we will find a way to work in the same lab and that day is going to be legen ... wait for it ... dary! Thanks a lot Copine for being such a close and good friend. I promise to do my best to come back to France ... if Flamby promises to resign! Debora & Lukas, my two favorite kicker players, thanks a lot for the good mood you spread around as an Ebola pandemic. And Lukas, thank you so much for having introduced me to the “Whatever” American philosophy, you changed my life that day! P.S. Sorry for the salt into the coffee ... but it was really meant to help you smile! Debora, your Italian enthusiasm and optimism is just awesome. You are able to light up a rainy day in a heartbeat, do not change anything!! Halina, thank you for sharing your research experience so often, for supporting me so many times during tough moments and providing advices such as “stop over-working!”. I should have listened to you more carefully. Louise, you were definitely one of the triggering events, who brought me where I am today. I will always be grateful to you for your unconditional support and unwavering optimism from the BCPST-prepa in Versailles to the final step of this PhD work.

Jérôme Lafare, alias mon homme. Certes tu n’as pas connu l’intégralité des cinq années de thèse mais tu es entré dans ma vie au meilleur moment. Le moment où j’étais physiquement et mentalement épuisée. Je te remercie du fond du cœur de m’avoir encouragé, soutenu de toutes tes forces et donné l’énergie nécessaire dont j’avais besoin pour clore ce chapitre. Ce ne sont ici que des mots, et j’espère un jour pouvoir te le montrer, mais je te suis à jamais reconnaissante d’avoir été à mes côtés pour la dernière ligne droite, l’ultime sprint, d’un certain 3 octobre 2014 jusqu’au bout du tunnel.

Colleagues.

This fifth part is dedicated to my colleagues whom I have had the pleasure to get to know and to work with. Dear colleagues, I thank you for all the moments we have shared during these last years. All the discussions we have had, all the candies and cakes we have shared, the good mood spread in the offices as well as in the lab, the cocktail evenings, ... Thank you very much. All of you contributed to change these five years into an amazing journey, full of enriching human and professional experiences.

Diana Kaiser, thank you so much for your very professional help and German lessons, I do use “Schnäppchen” in daily life. Steffi Spriewald, talking about German lessons, sorry that I will never be able to pronounce “Eichhörnchen” properly and thank you very much for your support, especially during the writing process. Markus Beutler, thank you so much for your high contribution to this work. You are definitely doing an amazing work with developing further the Oligo-MM stories and I am sure that you will be even more successful than I am now! Have a lot of fun with the mouse models and keep your enthusiasm, it is awesome! Simone Herp, we still do not know each other so well, but I am sure you are already having a lot of fun working with the ASF mice and *Mucispirillum*! Manuel Diehl, thanks a lot for your great help during the establishment of the gnotobiotic facilities...and the famous MvP kicker tournaments! Jana Glaser, thank you so much for your very helpful advices starting with “you should more take care of you”. I swear I have been working on this one a lot! I would also like to thank Aline Kessler, Christopher Harrison, Lisa Maier, Luisa Fernanda Jimenez Soto, Maximilian Frömberg, Ute Breithaupt, Carina Pfann and Eva Rath. Many thanks for your great conversations, your support and your enthusiasm, sometimes awesomely funny!

I would also like to thank the animal care-takers who made an awesome work and were always free to talk and help. Without such a good team, this work would have been like hell. You made my days, especially you, Saib Hussain. Saib, you cannot imagine how grateful I am that we got to know each other so well. Thousand thanks for your incredible help within the mouse facilities, our amazing “point of views” sharing sessions and your endless support in every case for me.

The last but not the least!

Finally, I would like to thank the germfree, ASF, Oligo-MM, AGR2 and MUC2 mice without whom none of this work would have been possible. I hope your sacrifice have not been fully useless and that, somehow, the scientific community will use the data and models, you and I have been working on so hard in order to better understand the interactions between “us”, our gut microbiota and our pathogens.

10. Curriculum Vitae

Brugiroux Sandrine

French, English, German (*read, written, spoken*)

Date of birth: 14.05.1986

Place of birth: Firminy, France

sandrine.bugiroux@yahoo.fr



Skills

Work with gnotobiotic mice

Performed animal infections

Anaerobic bacterial cultures

Fluorescence *in situ* hybridization

Molecular biology (*clonings, Western blottings, qPCR, RT-PCR, 454 amplicon-sequencing*)

Softwares: statistical analysis (*GraphPad Prism 5*); **sequence analysis** (*CLC DNA Workbench 6, MaGe*); **image analysis** (*DAIME, EndNote*) **and figure processing** (*Adobe Illustrator CS5*)

Immunofluorescence staining

Confocal & epifluorescence microscopy

Cell tissue culture

RNA extraction for microarray analysis

Education

Ph.D. student in **Microbiology**, Max von Pettenkofer Institute (Ludwig Maximilian University of Munich, Germany). Advisor: Prof. B. Stecher Oct. 2010-now
Thesis Research: *Establishment of a gnotobiotic mouse model to study colonization resistance against Salmonella enterica serovar Typhimurium and its first applications.*

M.Sc.2. in **Biology & Health Research: Host-pathogen Interactions & Mechanisms of Defense**, University of Montpellier 2 (France). Advisor: Prof. C. Braun-Breton 2010
Thesis Research: *Studies on the role of multigene families PfEFP-1, -3 and -4 during invasion of red blood cells by Plasmodium falciparum, causative agent of malaria.* (8 months)

M.Sc.1. student in **Biology & Health Research**, University of Montpellier 2 (France) 2009
Advisors: Dr. J.P. Leonetti & Dr. M. Gualtieri
Thesis Research: *Identification and phylogenic characterization of UV-resistant*

environmental bacterial strains and studies of their antimicrobial potential. (6 months)

B.Sc. student in **Microbiology**, University of Montpellier 2 (France). Advisor: Dr. A. Givaudan 2008

Research topic: *Study of the haemolytic activity of a Photorhabdus asymbiotica toxin.* (2 months)

BCPST1. Preparatory school in Biology, Chemistry, Physics & Geology, Lycée Hoche June 2005
(Versailles, France)

Publications

Brugiroux S, Beutler M, Pfann C, Garzetti D, Ruscheweyh HJ, Ring D, Diehl M, Herp S, Lötscher Y, Hussain S, Bunk B, Pukall R, Huson DH, Münch PC, McHardy AC, McCoy KD, Macpherson AJ, Loy A, Clavel T, Berry D, Stecher B. (2016) Genome-guided modular design of a novel defined mouse microbiota that confers colonization resistance against *Salmonella enterica* serovar Typhimurium. **Nat Microbiol.** (Accepted for publication)

Loy A, Pfann C, Steinberger M, Hanson B, Herp S, **Brugiroux S**, Gomes Neto JC, Boekschoten MV, Schwab C, Urich T, Ramer-Tait AE, Rattai T, Stecher B, Berry D. The putative gut pathobiont *Mucispirillum schaedleri* - Intestinal lifestyle and genome evolution by extensive horizontal gene transfer. **ISME.** (Submitted)

Studer N, Desharnais L, Beutler M, **Brugiroux S**, Terrazos M, Menin L, McCoy KD, Kuehne S, Minton N, Stecher B, Bernier-Latmani R, Hapfelmeier S. Functional intestinal microbial secondary bile acid production by 7-alpha-dehydroxylating *Clostridium scindens* in a gnotobiotic mouse model. **Front Cell Infect Microbiol.** (Submitted)

Uchimura Y, Wyss M, **Brugiroux S**, Limenitakis J, Stecher B, McCoy KD, and Macpherson AJ. (2016) Complete Genome Sequences of Twelve Species of a Stable Defined Moderately Diverse Mouse Microbiota 2 (sDMDMm2). **Genome Announc.** 4(5): e00951-16.

Lagkouvardos I, Pukall R, Abt B, Fösel BU, Meier-Kolthoff JP, Kumar Neeraj, Bresciani A, Martinez I, Just S, Ziegler Caroline, **Brugiroux S**, Wenning M, Bui TP, Hugenholtz F, Plugge CM, Peterson DA, Hornef MW, Baines JF, Smidt H, Walter J, Kristiansen K, Nielsen HB, Haller D, Overmann J, Stecher B, Clavel T. (2016) The mouse intestinal bacterial collection (miBC): Host-specific insight into cultivable diversity and genomic novelty of the mouse gut microbiome. **Nat Microbiol.** 1:16131.

Li H, Limenitakis JP, Fuhrer T, Geuking MB, Lawson MA, Wyss M, **Brugiroux S**, Keller I, Macpherson JA, Rupp S, Stolp B, Stein JV, Stecher B, Sauer U, McCoy KD, Macpherson AJ. (2015) The outer mucus layer hosts a distinct intestinal microbial niche. **Nat Commun.** 6:8292.

Berry D, Stecher B, Schintlmeister A, Reichert J, **Brugiroux S**, Wild B, Wanek W, Richter A, Rauch I, Decker T, Loy A, Wagner M. (2013) Host-compound foraging by intestinal microbiota revealed by single-cell stable isotope probing. **Proc Natl Acad Sci U S A.** 110(12):4720-5.

Maier L, Vyas R, Cordova CD, Lindsay H, Schmidt TS, **Brugiroux S**, Periaswamy B, Bauer R, Sturm A, Schreiber F, von Mering C, Robinson MD, Stecher B, Hardt WD. (2013) Microbiota-derived hydrogen fuels *Salmonella* Typhimurium invasion of the gut ecosystem. **Cell Host Microbe.** 14(6):641-51.

Main Academic Conferences

| | |
|--|---------------|
| VAAM. Annual Conference of the Association for General and Applied Microbiology, Marburg, Germany. Poster | March 2015 |
| 7th Seeon Conference “Microbiota, Probiota and Host”, Chiemsee, Germany. Poster | July 2014 |
| FEMS. 5 th Congress of European Microbiologists, Leipzig, Germany. Poster | July 2013 |
| 6th Seeon Conference “Microbiota, Probiota and Host”, Chiemsee, Germany. Poster and oral presentation (two different projects presented) | June 2013 |
| International Yakult Symposium , London, England. Poster | April 2013 |
| DGHM. 64 th Annual meeting of German Society for Hygiene and Microbiology, Hamburg, Germany. Poster | Sept-Oct 2012 |
| 5th Seeon Conference “Microbiota, Probiota and Host”, Chiemsee, Germany. Oral presentation | June 2012 |
| 4th Seeon Conference “Microbiota, Probiota and Host”, Chiemsee, Germany. Poster | April 2011 |

Poster prizes

“Generation of gnotobiotic mice to investigate the role of the intestinal microbiota in *Salmonella enterica* spp. I serovar Typhimurium colitis in AGR2-deficient mice”

(8th Seeon Conference, July 2015), Chiemsee, Germany.

“Why are Agr2-deficient mice resistant against *Salmonella*-induced colitis?”

(6th Seeon Conference, June 2013), Chiemsee, Germany.

“An Oligo-mouse microbiota protective against *Salmonella* Typhimurium infection”

(DGHM, Sept-Oct 2012), Hamburg, Germany.

Teaching activities

“Cultivating obligate anaerobic bacteria: from the bench to the anaerobic chamber”

“Using fluorescence *in situ* hybridization to detect and quantify single cells”

Private teachings from 1-3 days with 1-6 participants depending on the needs.
